GLACIO-LIMNOLOGICAL INTERACTIONS AT LAKE-CALVING GLACIERS

Eleanor C. Haresign

A Thesis Submitted for the Degree of PhD
at the
University of St. Andrews

2004

GLACIO-LIMNOLOGICAL INTERACTIONS AT LAKE-CALVING GLACIERS

Eleanor C. Haresign

A thesis submitted for the degree of Doctor of Philosophy

July 2004

University of St Andrews

ABSTRACT

Iceberg calving is an efficient ablation process which introduces mechanical instability to glacier systems and can cause non-linear climatic response. This thesis uses glaciological and limnological data to examine the relative contributions of calving and melting to mass loss at glacier termini, and the interplay between glaciological and limnological processes. Calving dynamics are investigated at two lake-terminating glaciers; Glaciar León in Chile and Fjallsjökull in Iceland. Glaciar León, a temperate, grounded outlet of the North Patagonian Icefield, terminates at an active but stable calving margin in Lago Leones. The calving rate of 880 m a^{-1} in a mean water depth of 65 m is high for lake-calving glaciers. Detailed survey of the physical limnology of Lago Leones, important for considering heat transfer to the subaqueous ice face, revealed thermocline development towards the terminus between spring and summer. Melting at the waterline along the glacier terminus facilitates calving by undercutting the subaerial calving cliff, and accounts for around a quarter of mass loss at the terminus. Waterline melting is also an important rate-controlling process for calving at Fjallsjökull. Precise quantification of melt rates (subaerial, waterline and subaqueous) at the termini of calving glaciers is difficult and hazardous, but this study has demonstrated the value of two techniques: (1) detailed survey of melt notch growth, and (2) use of a radio-controlled boat to record water temperatures at the ice-water interface. Continuous automated monitoring showed that lake-level fluctuations are integral to calving behaviour, influencing calving event timing and size over diurnal and hourly timescales. Fjallsjökull is sensitive to climatic forcing whereas Glaciar León, which exhibits larger seasonal than annual fluctuations, is less sensitive. Additional controls on calving at both sites are (1) buoyancy, (2) longitudinal stretching, and (3) the force balance at the ice-water interface. Calving operates along a continuum defined by the relative importance of interacting calving mechanisms, to which the climatic response of calving glaciers is sensitive

DECLARATIONS

(i) I, Eleanor Haresign, hereby certify that this thesis, which is approximately 67 500 words in length, has been written by me, that it is the record of work carried out by me and that it has not been submitted in any previous application for a higher degree.

Date 20/12/04 Signature of candidate [redacted]

(ii) I was admitted as a research student in October, 2000 and as a candidate for the degree of Doctor of Philosophy in October 2001; the higher study for which this is a record was carried out in the University of St Andrews between 2000 and 2004.

Date 20/12/04 Signature of candidate [redacted]

(iii) I hereby certify that the candidate has fulfilled the conditions of the Resolution and Regulations appropriate for the degree of Doctor of Philosophy in the University of St Andrews and that the candidate is qualified to submit this thesis in application for that degree.

Date 22.12.04 Signature of supervisor [redacted]

In submitting this thesis to the University of St Andrews I understand that I am giving permission for it to be made available for use in accordance with the regulations of the University Library for the time being in force, subject to any copyright vested in the work not being affected thereby. I also understand that the title and abstract will be published, and that a copy of the work may be made and supplied to any *bona fide* library or research worker.

Date 20/12/04 Signature of candidate [redacted]

ACKNOWLEDGEMENTS

This research was funded by the University of St Andrews, the School of Geography and Geosciences, the Ernest Kleinwort Charitable Trust and by my parents. In addition, funding for fieldwork to Patagonia and Iceland was generously provided by the American Alpine Club, the British Geomorphological Research Group, the Dudley Stamp Memorial Trust, the Royal Scottish Geographical Society, the Quaternary Research Association and the University of St. Andrews.

Many thanks go to the staff and Venturers of Raleigh International, without whose logistical support and enthusiasm the fieldwork in Patagonia would not have been possible. Rob Schindler provided valuable field assistance at Fjallsjökull, innovative equipment maintenance and much needed motivation when the research was not going according to plan. Other fieldwork assistance was given by Andy Casely and others at Edinburgh University, who kindly transported my field equipment to and around Iceland. Jack Jarvis, Andy Mackie and the other technicians in the School also warrant thanks for building field equipment, including the radio-controlled boat and the pressure sensor, which were integral to this research.

Particular thanks are due to my supervisor, Charles Warren, whose enthusiasm, practical advice and encouragement has maintained my fascination for glaciers throughout the course of this research. Doug Benn instigated many constructive discussion groups about calving dynamics, and many of his ideas form the basis of material in this thesis. The helpful suggestions of Stephan Harrison and the detailed reviewing of Brice Rea substantially improved both the thesis and the resultant publication. I have had many hours of fruitful discussion about my work with Lindsey Nicholson, and she is amongst the many people that have assisted me in my research during my time in St Andrews. Thanks to my family and friends for their immeasurable support during the writing of the thesis. Finally, there are countless individuals not listed above who have made significant contributions to my work. My thanks to them all.

CONTENTS

List of Figures

LIST OF TABLES

CHAPTER 1
Introduction

1.1 THESIS AIMS

This study investigates freshwater calving glaciers, which are glaciers terminating in a freshwater lake, from which icebergs are discharged. The thesis explores the dynamics of calving of freshwater-terminating glaciers using empirical data gathered from Glaciar León, Chilean Patagonia, and Fjallsjökull, south-east Iceland, to examine the factors influencing calving processes at freshwater-terminating glaciers and, in particular, the significance of subaqueous melting for calving behaviour. The overall research aims are:

- To investigate the rates, controls and mechanisms of lacustrine calving.
- To explore the interactions between glaciological and limnological processes at freshwater-terminating glaciers.
- To evaluate the influence of calving on glacier response to climatic change.
- To develop novel field techniques for monitoring calving activity and examining the rate-controlling processes.

The remainder of this chapter introduces calving glaciers, defining the phenomenon of calving and the ways in which calving may occur, describing the locations and characteristics of calving glaciers, and identifying some of the process and rate-controlling factors. This is followed by an outline of the significance of calving dynamics, both at a global scale and for individual glaciers, and over different timescales. Finally, the structure of this thesis is described.

1.2 INTRODUCTION TO CALVING GLACIERS

1.2.1. What is calving?

Mass is lost from glaciers by supraglacial, englacial and subglacial melting, by sublimation, and by iceberg calving at marine and freshwater termini. Calving is the process by which ice detaches from a parent glacier to produce icebergs, involving the propagation of a fracture. Calving occurs when tensile stresses at the ice margin exceed the tensile strength of the ice. The calving rate, u_c (unit: m d^{-1} or m a^{-1}) is usually defined as the difference between glacier speed, u_i, and the rate of terminus retreat, u_t.

$$u_c = u_i - u_r \qquad \text{(Eq. 1.1)}$$

1.2.2 Calving margins

Glaciers with calving termini exist throughout the polar regions and in most of the world's glacierized mountain ranges. Calving margins occur in temperate, polar and polythermal ice masses, and may be floating or grounded. A further distinction can be made between glaciers ending in freshwater lakes and those terminating in a marine setting, as well as between those with or without a debris cover, and between glaciers which are and are not topographically constrained. Clearly, there are many possible combinations of these variables, but not all of these exist. Extensively floating temperate glaciers do not occur and flotation is only ever reached transiently e.g. Glaciar Nef, Patagonia and Breiðamerkurjökull, Iceland (Powell & Domack, 1995; Warren *et al.*, 2001). Floating ice shelves offer an entirely different calving environment to grounded margins, and different calving mechanisms operate here, e.g. Antarctic ice shelves (Reeh, 1968; Reeh, in press). These mechanisms receive no consideration in this thesis, as they are not applicable to calving at lake-terminating glaciers. This thesis focuses solely on calving from grounded ice margins.

1.2.3 Modes of calving

There are four main ways in which ice calves from a glacier terminus (Syvtiski, 1989; Warren & Kirkbride, 1997): (1) spalling of thin lamellae of ice from the subaerial cliff, (2) the launch of subaerial seracs undercut at the waterline, or around ice caves, (3) detachment of large tabular bergs where transverse crevassing has propagated through the full thickness of the ice, and (4) subaqueous calving of submarine ice blocks, usually the largest witnessed (Warren *et al.*, 1995a; Motyka, 1997), as illustrated in Figure 1.1. The resultant icebergs occur in a myriad of shapes and sizes (Figure 1.2). At most ice margins several types of iceberg are present, but the dominance of one type over another varies from site to site. It has been considered that greater terminus stability at freshwater calving glaciers produces larger, less frequent bergs, with brash ice being more typical at tidewater glaciers (Qamar, 1988; Warren, 1991; Kirkbride, 1993; Warren, 1994; Warren *et al.*, 1995a; Smith & Ashley, 1996; Pfeffer *et al.*, 2000). However, there are many exceptions to this general rule. For example, whilst at lake-terminating Glaciar Moreno, Patagonia, subaerial seracs are frequently calved, varying in size with the largest bergs the height of the subaerial cliff (Skvarca & Naruse, 1997), Glaciar Nef, on the same eastern side of the Patagonian icefields, produces less frequent tabular bergs of much larger dimensions (Warren *et al.*, 2001). Conversely, spalling of lamellae is known to occur at both the freshwater-calving Miage glacier, Italy (Eijpen, unpublished data; Benn, *pers. comm.*) and at polar tidewater Hansbreen, Svalbard (Vieli *et al.*, 2002). The question is whether the differences in the style of calving events reflect separate mechanisms, or whether a set of controlling factors operates at all glaciers, varying in balance from site to site.

1.2.4 Characteristics of grounded calving termini

Glaciers calving into water bodies are highly active, typically flowing much faster than glaciers terminating on land, with ice velocities sometimes up to 10-20 m day^{-1} (Clarke, 1987). They often have a concave long profile, so that a small change in the equilibrium line altitude (ELA) may result in a large change in glacier mass balance. They are inherently more unstable than land-terminating glaciers, and they may operate under positive feedback conditions, with the potential for rapid disintegration (Meier & Post, 1987). Grounded tidewater glaciers are known to exhibit a cycle of a very slow advance followed by a rapid disintegration and retreat, as illustrated in Figure 1.3 (Meier & Post, 1987).

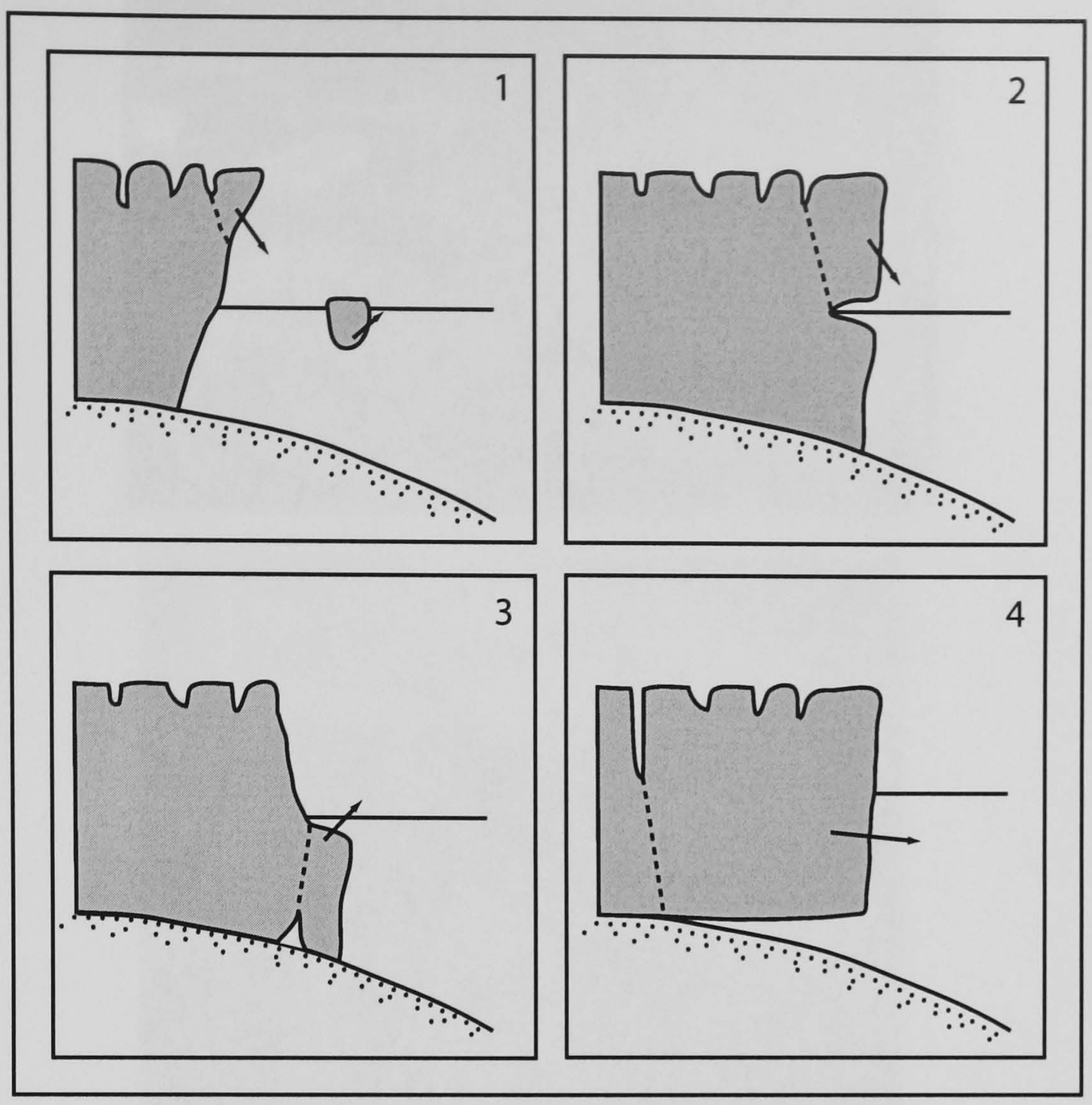

Figure 1.1 Types of calving from a glacier terminus: (1) subaerial launch of a serac; (2) separation of a berg along a joint intersecting a thermoerosional notch; (3) subaqueous launch from an ice foot; (4) separation along a deeply incised crevasse. (Adapted from Benn & Evans, 1998).

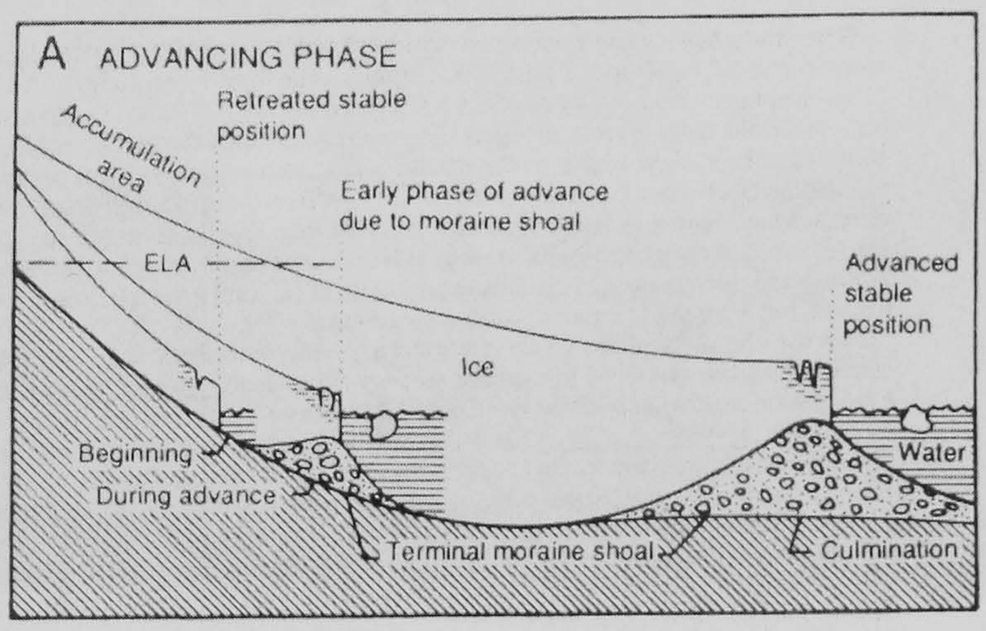

Figure 1.3 Patterns of glacier advance and retreat in association with grounding-line shoals. (A) Slow advance behind a mobile shoal which protects the margin from calving losses. (B) Rapid retreat into deep water, leaving the shoal abandoned at the maximum position. (From Warren, 1992, after Mayo, 1988).

a

b

c

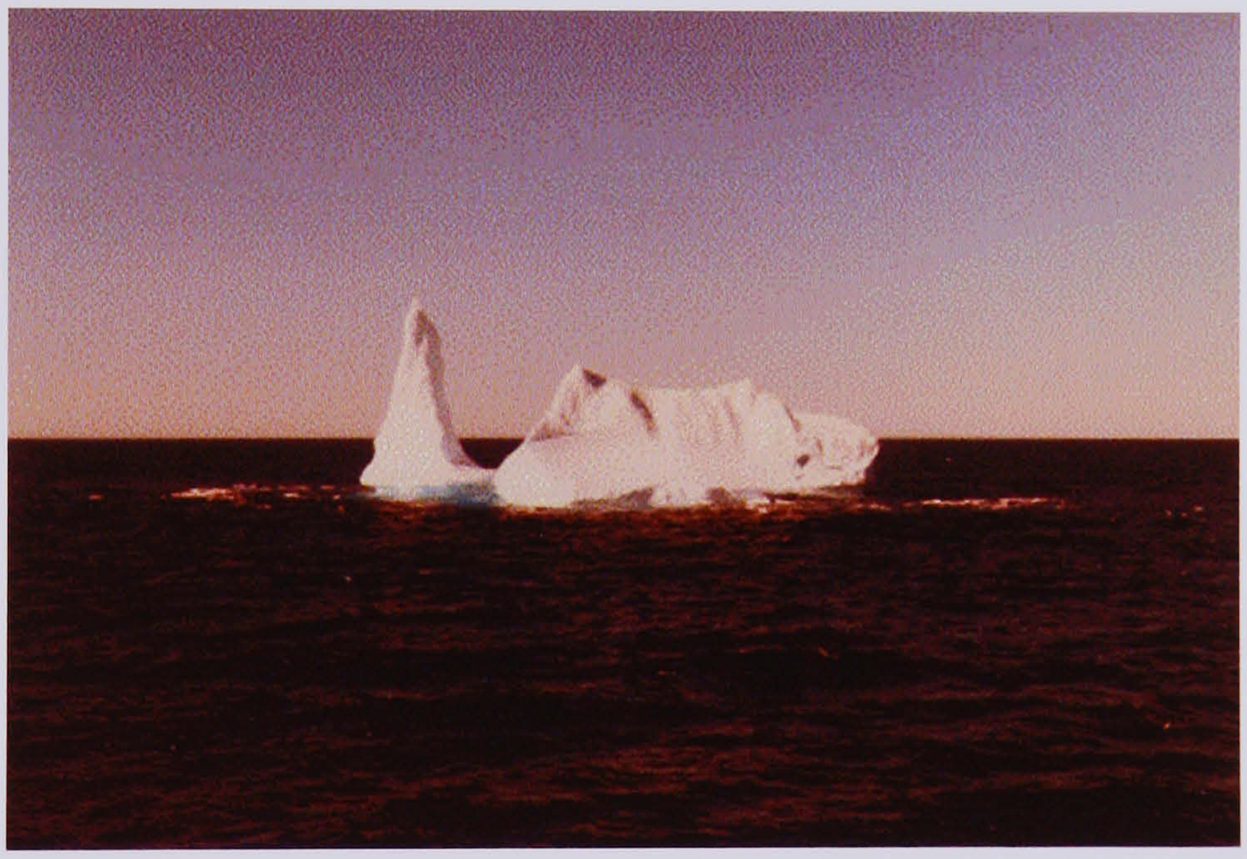

d

Figure 1.2 Examples of iceberg geometries. (a) 'Tabular' icebergs at Glaciar Nef, Patagonia (Warren *et al.*, 2001) (b) Berg at Glaciar León (c) Antarctic iceberg (Provincial Airlines Ltd.) (d) Large tabular berg in Antarctic waters (Canadian ice service).

Slow, stable advancing glaciers tend to terminate in shallow water, generally < 30 m deep, whilst those that are retreating rapidly stand in water > 80 m deep (Meier *et al.*, 1980). Advance of the proglacial moraine shoal causes a slow, stable advance of the terminus. However, overdeepening behind the shoal means that a small recession of the margin, perhaps triggered by a change in mass balance, can initiate catastrophic calving retreat into deepening water (Björnsson, 1996), and quasi-stability of the terminus during retreat depends on other factors, such as bedrock pinning-points or a decrease in the ablation area.

Variables influencing calving glacier dynamics and controlling the terminus position include water depth at the ice margin; bed and valley topography; proglacial sedimentation rate and backpressure; basal sliding; basal water pressure; longitudinal strain rate; buoyancy of ice in the terminal water body; crevasse propagation; tidal fluctuations; the thermal structure of the water body; and meteorological factors. These are reviewed in detail in Chapter 2.1.

1.3 THE SIGNIFICANCE OF CALVING

Antarctica and Greenland, plus other small ice caps and glaciers, contain 87% of Earth's supply of freshwater (Van der Veen, 2002a). Of a surface accumulation of 2880 Gton per year, calving may account for about 2400 Gton water equivalent of ice loss from the cryosphere (Van der Veen, 2002b), illustrating the importance of calving for mass transfer of ice to the oceans. Calving is an extremely efficient mechanism of mass loss compared to surface ablation (Van der Veen, 1996), and can have a profound effect on glacier dynamics. Given the high percentage of present-day glacier margins which are in contact with a body of water (Benn & Evans, 1998), calving is therefore integral to the dynamics of the cryosphere.

Whilst the initial trigger for changes in the behaviour and trends of calving glaciers may be external, such as long-term interactions between climate, glacier activity and landscape evolution (Benn & Evans, 1998), calving dynamics allow glaciers to become partially decoupled from climatic influences, on timescales of up to 1000 years (Meier & Post, 1987; Warren & Hulton, 1990; Warren, 1992). Large moraines may therefore represent glacio-

dynamic thresholds, not climatic halts (Warren, 1991). Icefields with calving glaciers may respond particularly rapidly to climatic warming (Rignot *et al.*, 2003), or may be insensitive, and it is therefore important to understand calving dynamics to predict the response of glaciers to environmental changes, and for understanding past glacier fluctuations.

In the past, glaciologists paid little attention to the dynamics of calving, partly due to the difficulties and dangers of obtaining direct measurements at calving fronts, and partly because calved ice was not considered to be of interest once it had detached from the glacier and was, therefore, no longer part of the glaciological system in question. However, calving losses from ice sheets are now understood to be a dynamic component of the Earth's climatic system, even being able to restrict production of the North Atlantic Deep Water by reducing the salinity and temperature of the marine waters (Broecker, 1994). During the deglaciation of the Northern Hemisphere ice sheets of the last glacial period, calving permitted their rapid disintegration (Pollard, 1984; Licciardi *et al.*, 1999; Mangerud *et al.*, 2001a, 2001b). In the marine environment, evidence for calving is recorded in deep-ocean sediments and ice cores. Outbursts of iceberg production were associated with periodic surges of the Laurentide ice sheet during the last deglaciation, called Heinrich events, and deposited ice-rafted debris, seen in deep sea sediments (Heinrich, 1988; Bond *et al.*, 1992; Alley & MacAyeal, 1994; Bond & Lotti, 1995). By affecting large-scale oceanic thermohaline circulation in the North Atlantic, these outbursts may have been a key cause of the climate regressing temporarily to ice-age conditions during its deglaciation (Broecker, 1994). An improved understanding of calving is therefore required to comprehend better the glaciology of Heinrich events (Clarke *et al.*, 1999).

Whilst most research into ice sheet collapse has focused on the dramatic consequences of iceberg discharge into the North Atlantic Ocean, calving into proglacial lakes has also promoted accelerated retreat. The Laurentide and Scandinavian Ice Sheets were in contact with both the ocean and vast proglacial lakes (Teller, 1987; Barber *et al.*, 1999; Licciardi *et al.*, 1999; Clark *et al.*, 2001; Clarke *et al.*, 2004), and an ice sheet over the Barents and Kara Seas blocked rivers, which resulted in the evolution of ice-contact lakes (Mangerud *et al.*, 2001a, 2001b; Mangerud *et al.*, 2004), yet the significance of freshwater calving along these extensive margins has largely been overlooked. Furthermore, the thermal regime of the proglacial lakes in Eurasia was important in providing a summer

cooling mechanism over large parts of Russia, by reducing melting of the southern margin of the Barents-Kara ice sheet (Krinner *et al.*, 2004). By affecting the surface mass balance of the ice sheet, the lakes caused accelerated ice sheet growth and delayed ice sheet decay ~ 90 000 years ago. Studies of lake-calving glacier dynamics are crucial for understanding the role these proglacial lakes played during the retreat of these ice sheets along their continental margins.

At the present time, calving accounts for 90 % of ice sheet ablation in Antarctica, where calving from ice shelves on the Antarctic Peninsula, may be causing their rapid disintegration (Warren, 1992; Vaughan & Doake, 1996). Over 90 % of the Antarctic Ice Sheet margin is in contact with the ocean (Drewry *et al.*, 1982). The Wordie Ice Shelf and the northern part of the Larsen Ice Shelf, amongst others, have been collapsing, and the total area of ice shelves lost since the mid-1960s is about 10 000 km^2 (Doake & Vaughan, 1991; Skvarca *et al.*, 1999). In Greenland, ice losses are more equally partitioned into those from calving and melting (Oerlemans, 1993), with calving accounting for 55-60 %. Fast-flowing ice streams constitute major drainage outlets, such as Jakobshavn Isbrae, where flow rates of up to 7 km a^{-1} at the calving margin are recorded (Abdalati & Krabill, 1999).

On a smaller scale, increased calving may contribute to accelerated retreat of valley glaciers fed by small ice fields, such as the tidewater glaciers of Alaska. Early observations of valley glaciers in Alaska showed that fluctuations may bear little or no relation to the climatic record (Post, 1975; Mann, 1986; Meier & Post, 1987; Trabant *et al.*, 1991). Glaciers terminating in the mouth of a fjord were noted to be insensitive to climate, also reaching stillstand positions where the fjord narrowed into a 'pinning point' (Field, 1937; Mercer, 1961; Mann, 1986; Warren, 1992). The anomalous responses to climate change were attributed to instabilities inherent in a calving terminus, highlighting the need to consider the influence of calving ice for the subsequent dynamics of the glacier. In particular, the Columbia Glacier, Alaska, the most thoroughly documented calving glacier, became unstable in the 1980s, and has retreated over 13 km since then, at rates sometimes exceeding several kilometres per year (Pfeffer *et al.*, 2000).

Prompted by the threat of drifting icebergs to oil tankers, researchers turned their attention to studying the factors affecting iceberg production (Brown *et al.*, 1982; Meier & Post, 1987; Krimmel, 1992). Columbia Glacier, Alaska, is extensively documented in terms of its calving behaviour (Krimmel & Vaughn, 1987; Walters & Dunlap, 1987; Meier, 1989;

Van der Veen, 1996; Krimmel, 1997; Venteris *et al.*, 1997; Whillans & Venteris, 1997; Venteris *et al.*, 1997; Pfeffer *et al.*, 2000). The study of Brown *et al.* (1982) was key in identifying a linear relationship between calving rate and water depth at the terminus, and gained widespread acceptance for describing calving processes at grounded tidewater glaciers (Pelto & Warren, 1991; Meier, 1994, 1997; Hanson & Hooke, 2000). However, it does not provide a physical explanation for the processes involved in iceberg calving in itself, and this prompted others to seek a 'universal calving law' (Pelto & Warren, 1991). Most explanations at this time were based on empirical observations, making correlations between measured variables, although some question whether a such a calving law exists to explain calving dynamics in all settings; both polar and temperate, grounded and floating (Van der Veen, 2002a). Given the variety of settings in which calving glaciers may occur (1.2.2), it is unsurprising that a large variety of glacier behaviours may result, making a 'universal calving law' unattainable.

Other valley glaciers which may experience rapid retreat by calving include those terminating in freshwater lakes, formed as glaciers retreat into overdeepened basins, such as those of the Patagonian Icefields, the Southern Alps of New Zealand and Iceland's Vatnajökull Ice Cap. Many Patagonian outlet glaciers calve into lakes, making calving dynamics an integral part of the overall stability of the icefields (Chapter 3). However, whilst the trigger for retreat of calving glaciers is thought to be climatic, the indirect and unstable response of these glaciers emphasizes the need for improved knowledge of calving dynamics.

Economic implications of iceberg calving relate to the threat posed to shipping as well as the hazards associated with glacier lake outburst floods (GLOFs) (Kennett *et al.*, 1997; Yamada, 1998). Predicting glacier response to an increase in water level in an ice-dammed lake requires an understanding of calving behaviour in order to implement careful mitigation measures. Hubbard Glacier, Alaska, has advanced in recent times, blocking Russell Fjord, causing damage to wildlife adjusting to freshening conditions in the water and threatening to spill over into a neighbouring catchment with severe impacts on the fishing-based local economy (Trabant *et al.*, 2003). During such events, water level increases until a threshold is reached and the water bursts through the ice dam, as it did in the summer of 2002. Glaciar Moreno, Patagonia, similarly repeatedly blocks part of Lago Argentino, the most recent outburst occurring in March 2004 (Hennigan, 2004; Chinni & Warren, submitted). Ice-marginal lakes in Iceland regularly undergo periodic

drainage, sometimes more than once a year, and GLOFs also pose a serious threat to the economic stability of Nepal, which depends primarily on the tourism trade in the Himalayas. Supraglacial and ice-marginal lakes form on the debris-covered valley glaciers above the resorts, and drain catastrophically at times (Yamada, 1998; Benn *et al.*, 2000; Richardson & Reynolds, 2000; Reynolds, 2000; Wiseman, 2004; Hands, 2004).

The understanding of calving processes by empirical studies alone is restricted by dangerous access. It is frequently difficult to identify the full range of controlling variables, and to separate the contribution of each. It is therefore no surprise that many theoretical ideas based on empirical evidence have produced a variety of conflicting theories (Hughes, 1992; Meier *et al.*, 1987; Van der Veen, 1996; Kirkbride & Warren, 1997). Furthermore, most are limited in their applicability to other glacial settings and, despite the quantity of high-resolution data from Columbia Glacier which has permitted detailed investigation of the relationships between longitudinal stretching, ice velocity and subglacial hydrology (Meier *et al.*, 1994; Kamb *et al.*, 1994), there is an inherent limit in the usefulness of these data for solving the calving debate. Van der Veen (1997) stresses the need to build regional databases in order to understand fully calving dynamics in all settings.

Empirical studies have provided a basis for the development of calving models that use a theoretical approach, overcoming the difficulties of gaining access to the necessary field data. Models have been constructed in different ways. Some have tackled ice fracture (Iken, 1977; Fastook & Schmidt, 1982; Hughes, 1992; Van der Veen, 1998a, 1998b), whilst others have examined the ice flow regime behind the ice terminus (Vieli *et al.*, 2000), the effect of changes in ice thickness on terminus position (Vieli *et al.*, 2001), buoyancy of the glacier terminus in the proglacial water body (Hughes, 2002) and subaqueous melt rates (Motyka *et al.*, 2003a), and these are reviewed in Chapter 2.1.

Despite the neat appearance of a theoretical model, its value depends on its applicability to the diversity of calving margin settings that exist. Beyond the detailed knowledge of Columbia Glacier, empirical datasets from a range of glaciers are required with which to test these theoretical approaches. In particular, lake-calving glaciers have received considerably less attention than tidewater margins, though a limited number of studies exist for glaciers in New Zealand (Kirkbride, 1993; Kirkbride & Warren, 1997; Hochstein *et al.*, 1995, 1998; Purdie & Fitzharris, 1999; Roehl, 2003), Patagonia (Warren, 1992, 1993,

1994, 1999; Warren & Rivera, 1994; Warren *et al.*, 1995a, 1995b; 1997, 2001; Winchester & Harrison, 1996; Skvarca & Naruse, 1997; Rivera *et al.*, 1997a, 1997b; Rott *et al.*, 1998; Skvarca *et al.*, 2002, 2003), the European Alps (Funk & Röthlisberger, 1989; Funk & Müller, unpublished) and Iceland (Björnsson *et al.*, 2001; Landl *et al.*, 2003). A clear trend has emerged of a strong contrast in calving rates between tidewater and freshwater settings. Calving rates at lacustrine margins are an order of magnitude lower than those at tidewater termini. It is suggested that the dominant process at freshwater margins is the undercutting of the subaerial cliff at the waterline (Warren & Kirkbride, 2003) but, at present, the data are too limited to confirm whether or not calving operates by a separate mechanism to that at tidewater glaciers. Given the importance of lake-calving margins for past ice sheet deglaciation, it is somewhat surprising how little research has been carried out on lake-calving glacier dynamics. The physics of calving processes remain poorly understood, and it is clear that there are many factors which interact to control the calving rate and terminus position. These are outlined in more detail in Chapter 2.1.2.

1.4 THESIS STRUCTURE

This thesis first reviews the process of calving, in Chapter 2, at marine and freshwater environments, evaluating the many controls on calving rates and mechanisms, both in terms of empirical observations and theoretical approaches. The glacio-lacustrine environment and processes of physical limnology in ice-contact lakes are also discussed before examining the literature pertaining to the process of subaqueous melting of ice. In light of the current understanding of calving behaviour, the specific objectives of the research are defined.

The research first focuses on calving in Patagonia. A regional background to the Patagonian Icefields is provided in Chapter 3, before empirical field data, carried out at the lake-terminating Glaciar León, is presented in Chapter 4. Chapter 5 seeks to interpret these data, in terms of both the insights into calving processes at a lake-calving glacier, and the significance for Patagonian Icefield dynamics.

A further study was conducted at lake-calving Fjallsjökull, south-east Iceland. In this smaller-scale study, novel techniques were developed for gathering data from calving

margins. Chapter 6 commences with a description of the regional context, before presenting the outcomes of the fieldwork. The usefulness of the techniques developed is evaluated in Chapter 7, with regard to the information they yield about calving processes operating at the ice cliff of Fjallsjökull, and their further potential for future research.

Chapter 8 synthesises the findings from both Patagonia and Iceland, within a discussion of the factors influencing calving dynamics. In particular, a critical assessment of the current approaches to calculating melting provides a basis for presenting a conceptual model outline of heat transfer to the ice cliff of a lake-calving glacier, which may be used to evaluate subaqueous melt rates. Recommendations for future field research required to develop such models are provided. Finally, this chapter summarises the outcomes of this thesis, linking process-oriented findings to the regional significance of lake-calving dynamics in Patagonia and Iceland, and considers the implications of these findings for the wider issues of understanding calving dynamics.

CHAPTER 2
Calving Glaciers and Glacio-limnological Interactions

2.1 CALVING GLACIERS

This section describes in detail the range of factors contributing to the calving process and discusses the debate regarding calving mechanisms at grounded calving margins that has arisen from empirical and theoretical modelling approaches. Most of this understanding comes from studies at tidewater glaciers. The applicability of these calving controls for calving into a freshwater setting is addressed in section 2.1.2.

2.1.1 Factors affecting calving dynamics

2.1.1.i Topographic geometry and water depth

Early observations of tidewater calving glaciers in Alaska revealed a non-linear response to climate, whereby the fluctuations of these valley glaciers may bear little or no relation to climatic changes (Mercer, 1961; Post, 1975; Mann, 1986; Trabant *et al.*, 1991). The most anomalous responses occur in areas of complex fjord geometry, and those that terminate in fjord mouths adjoining the open sea (Field, 1937; Mercer, 1961; Mann, 1986; Post & Motyka, 1995). Glacier still-stands occur either at the fjord mouth, or where fjord width decreases, providing a 'pinning point' (Mann, 1986). This climatic insensitivity and asynchrony was attributed to the influence of calving ice, and prompted researchers to speculate about the inherent instabilities involved in a calving terminus. In a widening fjord, glacier advance leads to increased calving fluxes, limiting the amount of advance. Conversely, calving fluxes decrease during retreat, prohibiting further retreat. The negative feedback that occurs during both advance and retreat results in a stable terminus. In contrast, terminus advances in a narrowing fjord become self-reinforcing, because the progressive reduction in terminus cross section reduces mass loss. In this case, margin advance occurs rapidly because calving decreases, and the terminus retreats rapidly as calving increases i.e. a situation of positive feedback and an unstable glacier margin (Benn & Evans, 1998). In addition to the influence of valley sides, bottom

topography is important (Thomas, 1979). Glaciers at locations of maximum advance show less climatic sensitivity than at recessional positions, because small terminus advances result in an increase in the calving rate (i.e. negative feedback). An unstable advance occurs over a reverse slope, because a small increase in thickness causes an advance into shallower water, progressively decreasing the calving rate in positive feedback.

The well-established topographic sensitivity of calving glaciers was clarified by Brown *et al.* (1982), who noted that when a calving glacier retreats from a shoal into deeper water, the terminus retreats rapidly, becoming unstable. They ascertained that the calving rate is sensitive to water depth, and derived a relationship between water depth at the ice front, h_w, and the calving rate, u_c (m a^{-1}):

$$u_c = ch_w \qquad \text{(Eq. 2.1)}$$

where the empirically-derived coefficient, c = 27.1 for the set of 12 Alaskan glaciers. Using a larger dataset of 22 tidewater glaciers from Alaska, Greenland and Svalbard, a coefficient of 8.33 was calculated by Pelto & Warren (1991). Values for calving rate and water depth at tidewater glaciers are shown in Table 2.1.

This 'calving law' is widely used to describe calving rates at other glaciers. However, in itself, it does not provide a physically-based explanation for the mechanisms of calving. Neither does it explain the difference in calving rates between tidewater and freshwater calving glaciers where, for any given value of h_w, rates are an order of magnitude lower (2.1.2). First investigated by Funk & Röthlisberger (1989), the coefficient of 1.9 from lake-terminating glaciers has been subsequently revised using expanded datasets (Warren *et al.*, 1995b; Skvarca *et al.*, 2002; Warren & Kirkbride, 2003). Even for those freshwater glaciers calving into deeper water (> 50 m), calving rates in freshwater are many times smaller that those in tidewater (Skvarca *et al.*, 2002). The u_c / h_w relationship cannot be applied to floating margins either, such as those in Greenland, (Reeh, 1968; Warren, 1991). Additionally, the calving law fails over timescales of less than a year (Brown *et al.*, 1982; Meier & Post, 1987; Van der Veen, 1996), or where rapid retreat is occurring (Van der Veen, 1996).

	Water Depth(m)	Calving rate (m a^{-1})	Source
Alaska			
Columbia 1982	134	2185	Meier *et al.* 1985
Grand Pacific	34	220	Brown *et al.* 1982
Harvard	57	1080	Brown *et al.* 1982
Hubbard	100	2630	Brown *et al.* 1982
Johns Hopkins	84	2290	Pelto & Warren 1991
Lituya	70	550	Pelto & Warren 1991
McCarty	14	600	Brown *et al.* 1982
Margerie	34	463	Pelto & Warren 1991
Meares	63	1010	Brown *et al.* 1982
North Crillon	35	640	Pelto & Warren 1991
South Sawyer	220	3200	Brown *et al.* 1982
Tyndall	100	1740	Brown *et al.* 1982
Yale	201	3500	Brown *et al.* 1982
Greenland			
Eqip Sermia	200	850	Carbonell & Bauer 1968
Kangerdluarrsup	300	2600	Carbonell & Bauer 1968
Lille Qarajaq	150	500	Carbonell & Bauer 1968
Umiamako	260	1900	Carbonell & Bauer 1968
Rinks Isbrae	800	4450	Carbonell & Bauer 1968
Jakobshavn Isbrae	900	7700	Pelto *et al.* 1989
Svalbard			
Hansbreen	30	230	Jania 1986
Kollerbreen	50	110	Wilhilm 1963
Kongsbreen	110	1100	Pillewizer 1965
Kongsvegen	30	100	Pillewizer 1965
Mayerbreen	30	240	Wilhilm 1963
Patagonia			
San Rafael	140	4500	Warren *et al.* 1995a; Rignot *et al.* 1996b

Table 2.1 *Water depths and calving rates at tidewater glaciers worldwide. Where more than one study exists only the most recent figures and source are given. Adapted from Pelto & Warren (1991).*

An alternative relationship was postulated by Sikonia (1982), based on the observation of a correlation between meltwater discharge and calving rate.

$$u_c = aD^b h_w^c \qquad \text{(Eq. 2.2)}$$

where D is the meltwater discharge, h_w is the height of the unsupported ice column, and a, b, and c, are empirical constants. However, meltwater discharge data were not available and instead discharge was assumed to be comparable to the runoff of the nearby glacial stream Knik River. Critically, this relationship appeared applicable when the terminus Columbia Glacier was in contact with the moraine. Retreat, however, commenced just prior to 1980, and once the glacier was free on the confining pressure of the moraine, this equation ceased to be applicable (Tangborn, 1997). Subsequently, terminus velocities and calving rates have increased by 500 %, and the glacier is known to be close to flotation at the margin (2.1.1.iii), due to high basal water pressures (2.1.1.ii) (Kamb *et al.*, 1994; Meier *et al.*, 1994). The controls on terminus dynamics clearly altered once the glacier was in retreat, becoming more complex. However, before examining some of these issues, a general appreciation of the significance of the moraine shoal is valuable.

The moraine shoal at the terminus controls the effective water depth in which the glacier stands and from which rapid retreat may occur, indicating that proglacial sedimentation must be important in altering water depths during advancing and retreating cycles of tidewater termini (Powell, 1981; Mayo, 1988; Alley, 1991; Powell, 1991; Hunter *et al.*, 1996a; Hunter *et al.*, 1996b; Fischer & Powell, 1998). Proglacial sedimentation at the cliff margin also provides a restraining force against an advancing terminus (Fischer & Powell, 1998), and can affect the stratification of the water column. Here, the discussion focuses on the ways sedimentation processes may alter water depth and modify backpressure on the ice face The effects of suspended sediment on water column structure are described in section 2.2.3.iii.

Sedimentary processes supplying material to the moraine shoal are well documented (Powell, 1981, 1983, 1990; Dowdeswell, 1987; Hunter *et al.*, 1996a), with glaci-fluvial dumping, mass movements, plume settling, bed deformation, freeze-recycling, iceberg rafting (2.3.1), calve dumping and ice cliff melt-out amongst the common mechanisms, all of which vary in their contribution of sediment to the grounding line (Dowdeswell, 1987; Hunter *et al*, 1996a). Different geomorphologies result from glacier advance and retreat (Powell, 1981, 1990). Controls on the volume of sediment deposited include lithology,

topography, tectonic setting, glacier activity and morphology, number of tributaries and the climatic regime (Hunter *et al.*, 1996b). In general, sedimentation is predominantly from glaci-fluvial activity for temperate glaciers (Powell, 1983; Benn & Evans, 1998), whereas at subpolar glaciers, iceberg rafting is more important (Elverhoi *et al.*, 1983; Dowdeswell & Dowdeswell, 1989). In temperate settings, debris-rich basal ice is rare because basal sediment is quickly flushed out by subglacial streams.

The cyclic nature of advance and retreat seen at calving glaciers was described in Chapter 1.2.4 (Meier & Post, 1987). Glacier advance may occur over centuries to millennia, in comparison to the rapid retreat occurring over periods of decades to a century or more, and relates to topographic morphology, mass balance distribution and the availability of erodible material (Liverman, 1987; Hunter *et al.*, 1996a), rather than climatic fluctuations (Powell, 1991). Once retreat is initiated, the backpressure (due to buttressing of the ice by the moraine shoal) acting on the glacier is released, leading to instability (Meier & Post, 1987) (2.1.1.2).

Models of glacier sensitivity to sediment dynamics may be constrained by data from field studies (Powell, 1981, 1991; Alley, 1991). In a 'conveyor-belt' system of shoal recycling (Alley, 1991), sedimentation rate will decrease rapidly with distance from the terminus at a stable location, where accumulation is mainly controlled by the rate of terminus change (Syvitski, 1989). Building on a model of glacimarine sedimentation at tidewater glaciers (Powell, 1991), Fischer & Powell (1998) examined the role of horizontal normal and shear forces acting on the glacier front as a result of the morainal bank. When glaciers are grounded along substantial morainal banks, the influence of water in restraining the terminus may be insignificant compared to other forces, i.e. bank-related restraining forces are larger than those derived from the buttressing effect of the water column. The increasing restraining forces resulting from moraine shoal growth cause glacier thickening and a decrease in glacier flow, with eventual cessation of terminus advance (Fischer & Powell, 1998). In comparison, retreat is much more rapid due to the increase in flow rates as the restraining forces lessen, allowing thinning and rapid retreat by calving. Rates of advance are slower than for retreat, due to the time required for sediment to accumulate as a bathymetric high (Powell, 1991).

Backstress has been suggested as an explanation for an observed link between seasonal speed and terminus position cycles (Krimmel & Vaughn, 1987). Large ice velocities occur

in autumn when basal water is most abundant. By early winter, restraining forces are at a minimum and a rapid acceleration of flow begins. Gravitational driving stresses are large because the glacier is now at its thickest yearly average, so glacier buoyancy (2.1.1.iii) is greatly reduced and calving decreases. Unless sedimentation rates are very high, short-term advances behind the terminal moraine bank do not produce mechanically significant morainal banks, resulting in a continually decreasing restraint at the terminus at the onset of each new seasonal advance cycle. In this situation, the glacier never slows and thickens appreciably, and enters a period of rapid, sustained retreat. Venteris *et al.* (1997) dispute the seasonal influence of backstress on terminus position. If backstress causes seasonal cycling of terminus position, retreat from the shoal should be concurrent with a decrease in ice velocity and stretching rate. However, the reverse (i.e. an increase in ice velocity and stretching rate) were observed during such seasonally related retreats at Columbia Glacier (Venteris *et al.*, 1997). Furthermore, they found no evidence for the seasonal velocity maxima that should occur progressively later in the year as the glacier retreats off the shoal. The increase in calving rate did not occur until after the terminus had retreated to the foot of the terminal moraine.

It is clear from the dispute above that, as well as not providing a physical explanation for calving, factors other than water depth are also important in controlling rates of ice velocity and calving. Some of these factors are reviewed here, and their implications for calving behaviour discussed.

2.1.1.ii Ice flow, longitudinal stretching and effective basal pressure

Increasing surface flow velocities towards the calving front i.e. longitudinal stretching have been observed on several calving glaciers (Krimmel & Vaughn, 1987; Rott *et al.*, 1998). The fast-flowing nature of calving glaciers is known to relate primarily to basal sliding rather than the internal deformation of ice (Kamb *et al.*, 1994; Meier *et al.*, 1994; Van der Veen, 1996), for which the effective basal pressure is an important controlling factor (Bindschadler, 1983). If the calving rate depends on the flux of ice to the calving cliff, a close correlation between calving rate and ice velocity at the terminus is expected (Van der Veen, 1996). However, calving rates are always calculated from the balance of ice velocity with terminus position change, so a strong correlation between ice velocity and calving rate provides no physical explanation. Nevertheless, high velocities and

acceleration towards the terminus are common characteristics of terminus dynamics at tidewater calving margins, and are inextricably linked to calving behaviour.

The close link between ice velocity and calving rate must be understood in order to develop a physically-based model of calving (Vieli *et al.*, 2000). Modelling of glacier length changes to infer calving rates have been related to sliding velocity and water depth (Bindschadler & Rasmussen, 1983), although this model is limited to only a few hundred meters behind the ice front. The retreat of Columbia Glacier, Alaska, was slower than was predicted by this model, because ice flow velocities increased more than expected, emphasizing the close links between calving and ice speed.

Vieli *et al.* (2000) use a numerical finite-element glacier-flow model at Hansbreen, Svalbard, in an attempt to suggest the important processes controlling flow behind the calving front. In order to implement the basal sliding within the model successfully, a thin viscous layer was added at the base of the glacier, comparable to the deformable sediment modelled in fast-flowing ice streams in Antarctica (Kamb, 1990; MacAyeal, 1992; Tulaczyk *et al.*, 1998). The modelled results replicate the observed ice velocities, indicating the importance of basal processes for flow at Hansbreen terminus. However, further work is required to refine the model, using actual observations of basal sediment to determine a more accurate driving stress for ice sliding. This kind of information is very difficult to obtain directly.

As Vieli *et al.* (2000) have shown, basal conditions are important for ice flow, and may be represented by calculating the effective pressure, p_e, which relates to the balance of ice overburden pressure, p_i, with basal water pressures, p_b (Paterson, 1994), as described in equation 2.3:

$$p_e = p_i - p_b \qquad \text{(Eq. 2.3)}$$

where the overburden pressure is linearly related to ice density, ρ_i, and ice thickness, h_i:

$$p_i = \rho_i g h_i \qquad \text{(Eq. 2.4)}$$

Effective pressure may decrease towards the ice cliff, if the glacier thins towards the terminus and, thus, p_i decreases, permitting faster sliding i.e. extensional flow (Van der Veen, 1997). Empirical data demonstrate a relationship between longitudinal strain rates and calving rates (Meier, 1994; Van der Veen, 1996; Hanson & Hooke, 2000). In particular, calving from surging glaciers often occurs under conditions of extensional flow (Lingle *et*

al., 1993; Pritchard *et al.*, 2003). Accumulated longitudinal strain is an important control on calving rates through the promotion of crevassing and stress weakening of the ice (2.1.1.iv) (Vieli *et al.*, 2001). The reduction in loading may cause ice failure along the glacier base, causing the propagation of bottom crevasses (Hanson & Hooke, 2000). However, the weak correlation between the two indicates that calving does not relate to strain alone, even if high rates are a necessary condition for calving activity.

Changes in effective pressure may also result from alterations to the basal water pressure. An increase in ice velocity with subglacial runoff has been observed at some glaciers (Theakstone & Knudsen, 1986; Meier 1989, Vieli *et al.*, 2001), implying that basal water pressure is important for calving behaviour through its ability to modify sliding velocity. Venteris *et al.* (1997) concluded that processes other than backstress are responsible for the seasonal cycles of ice velocity seen at Columbia Glacier, Alaska (2.1.1.i) and, instead, calving increases in autumn when decreasing basal water volumes increase frictional drag on the bed. Rapid calving then occurs due to the resulting oversteepening of the ice cliff (2.1.1.iv) (Meier *et al.*, 1985). However, it is possible that rapid calving in autumn may also result from warmer water temperatures (Walters *et al.*, 1988). Additionally, reduced calving in winter (Vieli *et al.*, 2001, 2002) may be attributed instead to a decrease in air and water temperature, rather than solely a reflection of increased drag due to reduced subglacial activity, as reduced surface melting results in less water in crevasses, inhibiting crevasse growth (2.1.1.iv).

However, other research has demonstrated the importance of effective basal pressure for ice velocity and calving over seasonal timescales (Walter, 1989; Fahnestock, 1991; Kamb *et al.*, 1994; Meier *et al.*, 1994; Krimmel, 1997; O'Neel *et al.*, 2001). At Columbia Glacier, Alaska, both ice velocity and glacier length vary seasonally. The maximum length occurs in June and minimum in September, lagging the maximum and minimum velocities, respectively, by three months (Krimmel, 1997). The springtime occurrences of maximum ice velocities are likely to relate to increased meltwater pressurizing the subglacial hydraulic system (Pfeffer *et al.*, 2000). Similar seasonal fluctuations are observed at LeConte Glacier, Alaska, retreating from May to October (Motyka *et al.*, 2003a). These seasonal fluctuations, of about 100m, exceed any annual change. They also note that ice velocities during the summer of 1999 remained constant, and argue that seasonal changes in calving and/or melting must account for the seasonal change in terminus position,

perhaps by the combination of heavy rainfall and warm water temperatures triggering terminus destabilisation.

The relationship of calving to basal water pressure has been demonstrated over even shorter timescales, and some suggest that short term variations relate directly to water storage at the bed (Kamb *et al.*, 1994; Meier *et al.*, 1994). Diurnal ice velocity variations are observed at LeConte Glacier, and extend up-glacier, albeit with a decreasing signal, which are thought to be driven by changes in water input from surface ablation (O'Neel *et al.*, 2001). Diurnal changes in elevation are thought to reflect the increase basal water storage resulting from the water fluctuations. At Columbia Glacier, the diurnal peak in ice velocity occurred 7-8 hours after the peak of air temperature or insolation (Meier & Post, 1987), whilst at polar Hansbreen, Spitsbergen, periods of higher velocity, lasting 2-3 days, were attributed to increased basal sliding caused by an increased input of water to the bed (Vieli *et al.*, 2000). Whilst this was thought to be due to higher rates of surface melting, it wasn't considered to change the ice flow significantly over seasonal timescale of months or seasons (Vieli *et al.*, 2002).

Other velocity variations at LeConte Glacier related to rainfall events, although the magnitude of speedup was not directly related to the amount of rainfall, instead relating to the change in water input from the local catchment (O'Neel *et al.*, 2001). At Columbia Glacier, only heavy rainfalls were observed to cause velocity fluctuations (Meier & Post, 1987). Here, the velocity dropped after the rain event, suggesting that subglacial channels were enlarged during the major rainstorm, resulting in a decrease in effective pressure and an increase in basal sliding, which slowed after the rain had ceased.

Early research at tidewater glaciers also highlighted wave and tidal action (Hughes, 1992; Motyka *et al.*, 2003a), although at Columbia Glacier wind-driven wave action cannot be a necessary condition for fast calving as the terminus is protected (2.3.4). The effect of tidal movements on hinge-line migration at floating ice shelves is well documented (Anandakrishnan & Alley, 1997; Rignot, 1998; Rignot *et al.*, 2000; Rabus & Lang, 2002; Shepherd & Peacock, 2003), and tidal influence at grounded tidewater glaciers has become of interest. Tidal action has previously been suggested as being important only if it greatly increases water circulation and heat advection to the front, or significantly weakens calving through the cyclical changes in stress regime (Warren *et al.*, 1995b). However, early studies of tidal influence on calving overlooked the implications of the

water body for calving rates through changes to the effective basal pressure. The same formula used to calculate the overburden pressure at the ice bed (equation 2.4) can be used to calculate water pressure at the fjord or lake bed, using water depth and density values. The maximum water pressure, occurring at the bed, provides a minimum value for the subglacial water pressure, p_b , in order that the basal water always be expelled from the glacier. Thus, basal water pressures will be affected by changes in water level, providing a link between tidal cyclicity and terminus ice velocities.

At fast-flowing LeConte Glacier, Alaska, where ice velocities reach 27 m d^{-1}, multiple short-time-scale forcings relate to semi-diurnal tides as well as the diurnal variations in meltwater input and precipitation events described above (Walters, 1989; O'Neel *et al.*, 2001). On a semi-diurnal timescale, the changes in water column height with tidal motion, which buttress the ice front as a time-varying hydrostatic force imbalance (2.1.1.iv), lead to longitudinal stress gradients that vary with the tide. It has been shown that increased basal water pressure results in higher velocities. However, at LeConte Glacier, minimum speeds occur at high tide, when there is maximum restraint provided by the higher water column. Thus, the restraining force outweighs the increased basal sliding that might otherwise have been expected to occur due to increased water storage at high tide. An increase in surface elevation over the semi-diurnal timescale was observed at the terminus, and O'Neel *et al.* (2001) argue that this provides the key as to why ice velocities do not increase at high tide: at LeConte Glacier, basal drag is low, and most of the drag at the terminus comes from marginal restraints. As a result, the change in basal water pressures has little influence in altering basal sliding. Additionally, the terminus is so close to flotation (2.1.1.iii) that a 1% change in water depth can alter basal water pressures, causing local uplift without a perceptible change in glacier sliding.

This discussion has highlighted the complexity of the factors relating to ice flow dynamics and their relationship to the process of calving at tidewater glaciers. In summary, ice flow at calving glaciers takes place primarily by basal sliding, and is therefore sensitive to changes in effective basal pressure, which depends on changes in ice thickness and basal water pressures. Although water storage at the bed is understood to be a key factor linking ice flow and calving behaviour, situations occur where glacier response appears to be subject to other controls. The ice surface elevation changes at LeConte Glacier in response to semi-diurnal tidal stage variations indicates the importance of the force balance between ice pressure and water pressure at the terminus, which buttresses the ice

cliff. Additionally, the buoyancy of the terminus in the water body is apparent, and its significance is discussed below.

2.1.1.iii Buoyancy

The difference in density between ice and water (values of 0.9 and 1 kg m^{-3}, respectively) means ice is buoyant in water. Using the ratio in equation 2.5, the glacier terminus will be at the point of flotation when the ice thickness to water depth ratio is 0.9, as shown in equation 2.6:

$$h_i \rho_i : h_w \rho_w \qquad \text{(Eq. 2.5)}$$

therefore

$$\frac{h_w}{h_i} = 0.9 \qquad \text{(in uncrevassed ice)} \qquad \text{(Eq. 2.6)}$$

Glacier thinning may occur as a result of accelerated surface melting under a warming climate, or as a result of longitudinal stretching towards the terminus. If h_i falls below the required thickness, and the ratio exceeds 0.9, the glacier terminus becomes buoyant, and a torque is imposed on the terminus which may trigger calving if this force exceeds the tensile strength of the ice. Below this value, buoyancy forces are insufficient to promote large-scale failure by flotation. Whilst temperate calving glaciers are not extensively floating (1.2.2), buoyancy may be a dominant force affecting calving, increasingly so as the terminus approaches flotation thickness (Warren *et al.*, 2001). The torque imposed on the glacier increases as the glacier thickness approaches that required for flotation. This torque stresses the ice, inducing fracture.

From early observations at Breiðamerkurjökull, southeast Iceland, Howarth & Price (1969) suggest that progressive subaerial events caused the ice margin to tilt progressively upward, revealing the subaqueous foot, which eventually broke away. In a more thorough mathematical treatment of buoyant calving, Hughes (2002) attempts to provide a theoretical derivation for the length of the outward protrusion of the subaqueous foot, L, as a function of water depth, as shown in equation 2.7:

$$L = \frac{h_w}{\sqrt{6}} \left(\frac{\rho_w}{\rho_i} \right)^{1/2} \qquad \text{(Eq. 2.7)}$$

The rate of subaerial calving is thought to determine the rate of subsequent subaqueous calving. Whilst buoyancy forces are important here, he assumes that fractures

propagating down from the glacier surface do not extend below the waterline. Whilst this provides a basis for separating processes above and below the waterline in his calculations, it precludes the occurrence of calving events where the whole ice thickness at the terminus is subjected to buoyancy forces, creating the 'tabular' icebergs seen, for example, at Glaciar Nef, Chilean Patagonia (Warren *et al.*, 2001). His model is, therefore, not applicable to all modes of calving.

The significance of the buoyancy of ice in water is well illustrated by the process of subaqueous iceberg calving. A projecting ice foot was first postulated to explain the origin of subaqueous bergs that rise to the surface, sometimes up to 300 m from the glacier margin (Wright, 1892; Warren *et al.*, 1995b; Motyka, 1997). Glaciers where submarine calving is common typically have high calving rates, such as those in Glacier Bay, Alaska (Hunter & Powell, 1998). These feet may extend tens of meters from the ice cliff at the grounding line. Ice that constitutes submarine bergs is deep blue, debris-rich and bubble-free. Ice feet are important for ice-proximal sediment dynamics, as they can push sediment along the sea floor, and calving of subaqueous icebergs is an important way in which glaciers can release debris-rich basal ice by rafting e.g. during Heinrich events (1.3). They may also have implications for understanding the calving process as they indicate that forces of buoyancy are involved in a balance with ice fracture strength (Warren *et al.*, 1995a; Hughes, 2002).

To study submarine calving, Hunter & Powell (1998) used a remotely operated vehicle (ROV) to make direct observations of the geometry of submarine feet, in Glacier Bay, Alaska. Although suspended sediments restricted viewing, close-up images were obtained, illustrating the presence of rills which reflect the upwelling of meltwater along the ice face (2.3.5.ii). They concluded that the formation of ice feet reflects differences in the fracture properties of subglacial and englacial ice, whilst Hunter *et al.* (1996b) interpreted this as resulting from differential melt rates across the glacier terminus, perhaps relating to varying levels of sediment veneer. Submarine bergs calve when the buoyancy of the ice exceeds the critical shear stress, inducing brittle failure. However, the precise nature of submarine calving is even less well understood than subaerial calving.

Despite the documentation of calving in response to buoyant forces, the full range of glacier responses is little understood. It is only when the water depth is 0 m i.e. there is no water body, that buoyancy forces become zero, yet the precise impact of buoyancy

forces at water depths less than the ratio of the threshold of flotation of 0.9 are unknown. It has been suggested that glaciers begin to respond to buoyancy when the ice thickness thins to within a particular fraction of that flotation limit for a given ice thickness (Van der Veen, 1996; Vieli *et al.*, 2001). However, the influence of buoyancy along a continuum of ice thickness-water depth ratios is unknown.

Uncertainties exist in the mechanisms of calving due to buoyancy forces, in terms of the nature of crevasse propagation: whether crevasses can propagate through the entire ice thickness (Hughes, 2002) and whether they can initiate at the glacier bed, extending upwards through the ice (Weertman, 1980; Van der Veen, 1998b). Crevassing is fundamental to calving; understanding its initiation is valuable for calving studies (Van der Veen, 1999), and it is possible to approach calving dynamics from the perspective of ice fracture processes and controls.

2.1.1.iv Calving and crevassing

Higher rates of retreat and associated calving are observed at glaciers with a greater crevasse density (Venteris, 1999). The occurrence of crevasses on glaciers is reviewed by Van der Veen (1999), but no reliable fracture model exists to predict the initiation of crevassing, despite field studies of crevasses since the earliest days of glaciology (Vaughan, 1993; Van der Veen, 1998a, 1998b). A theory of crevasse initiation, relating to critical values of the principal extending strain rate (Vaughan, 1993), is questioned by Van der Veen (1999) who considers that crevassing, in fact, results from tensile stresses reaching a threshold value.

Differential flow in the ice column causes the upper part of the subaerial ice cliff to oversteepen. Where basal flow occurs by sliding (2.1.1.ii), the upper ice column also experiences internal deformation (Figure 2.1). At the terminus, the water body goes some way to confining the oversteepening by buttressing the ice cliff, due to hydrostatic pressure (Figure 2.2). The ice cliff force balance produces a zone of maximum tensile principal stress some distance back from the ice cliff. To consider the role of crack propagation for calving behaviour, Iken (1977) numerically examined the distribution of stresses at the snout of Grubengletscher, using a 2D model.

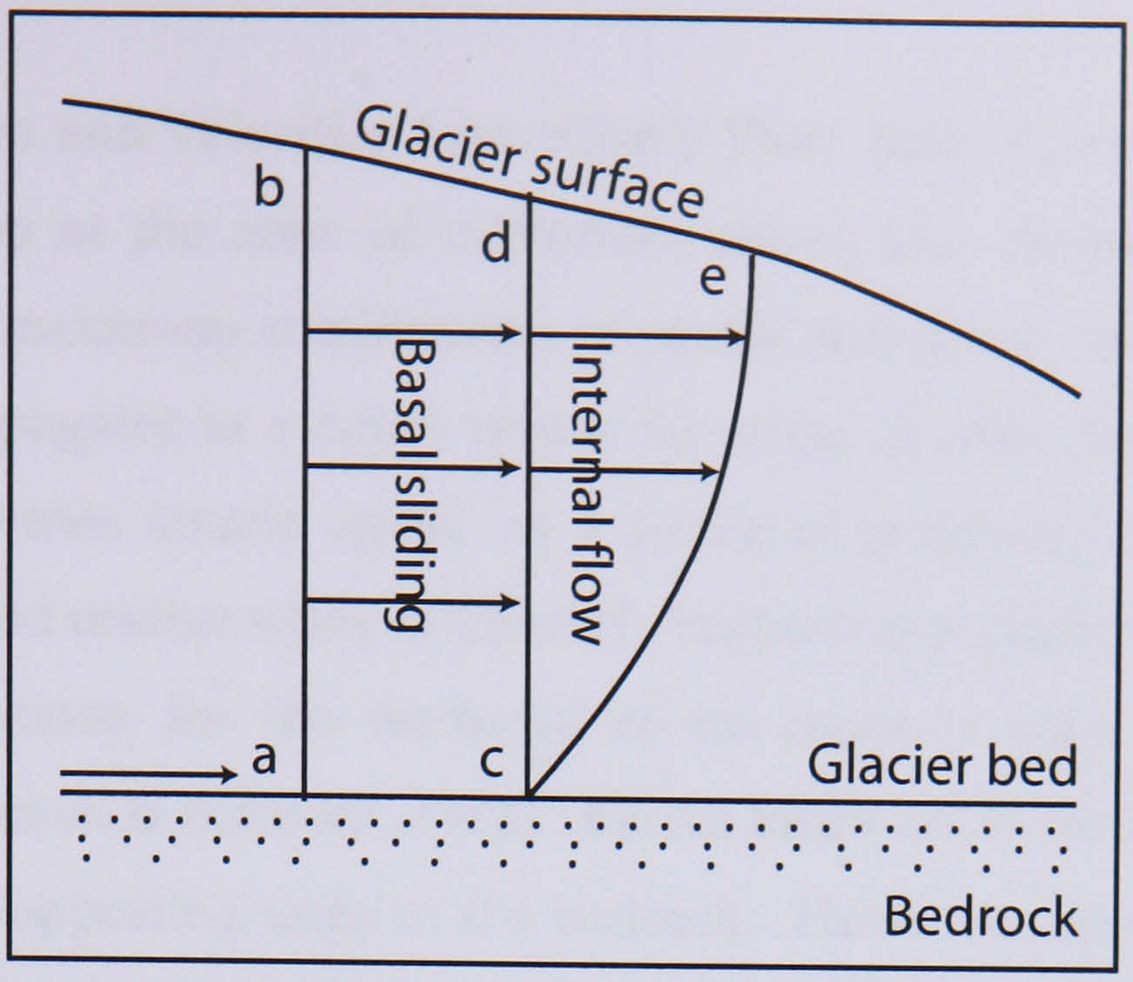

Figure 2.1 At temperate glaciers, ice flow of the line a-b takes place by basal sliding to position c-d, and is also deformed to follow the line c-e by internal deformation. Adapted from Bennett & Glasser (1996), after Boulton (1993).

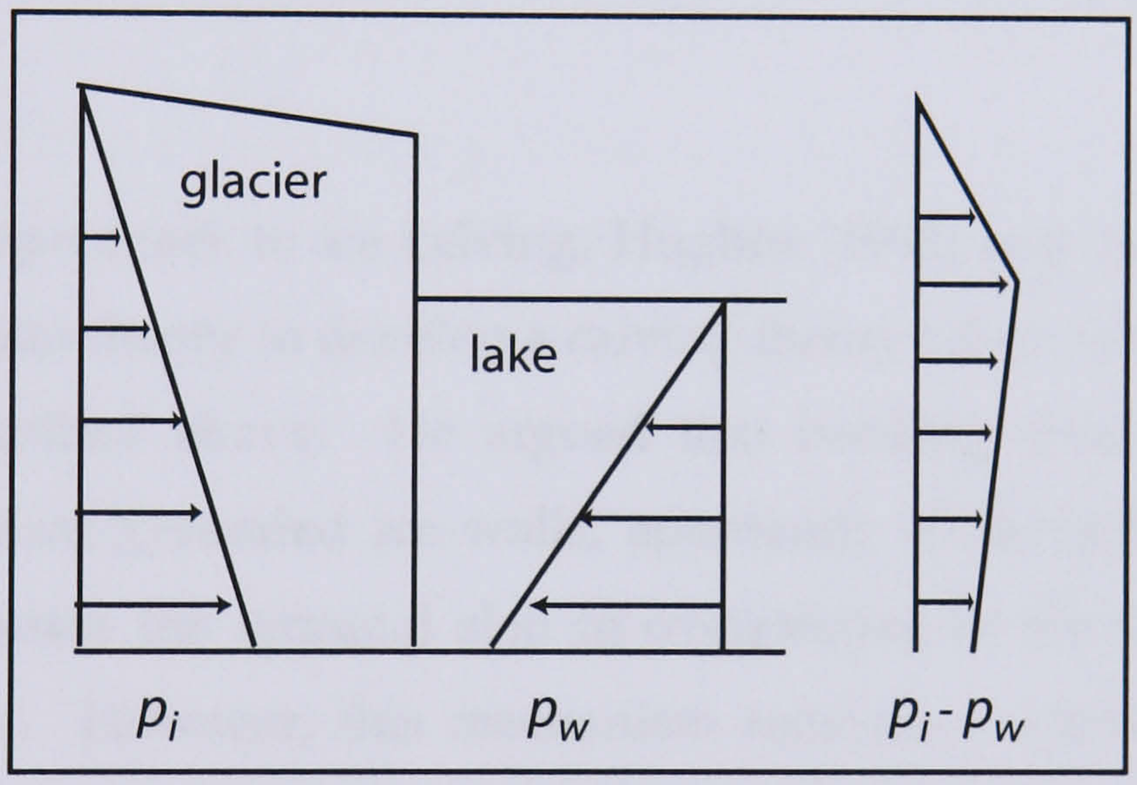

Figure 2.2 The magnitude of horizontal stresses exerted by ice (p_i) and water (p_w) at calving glacier termini.

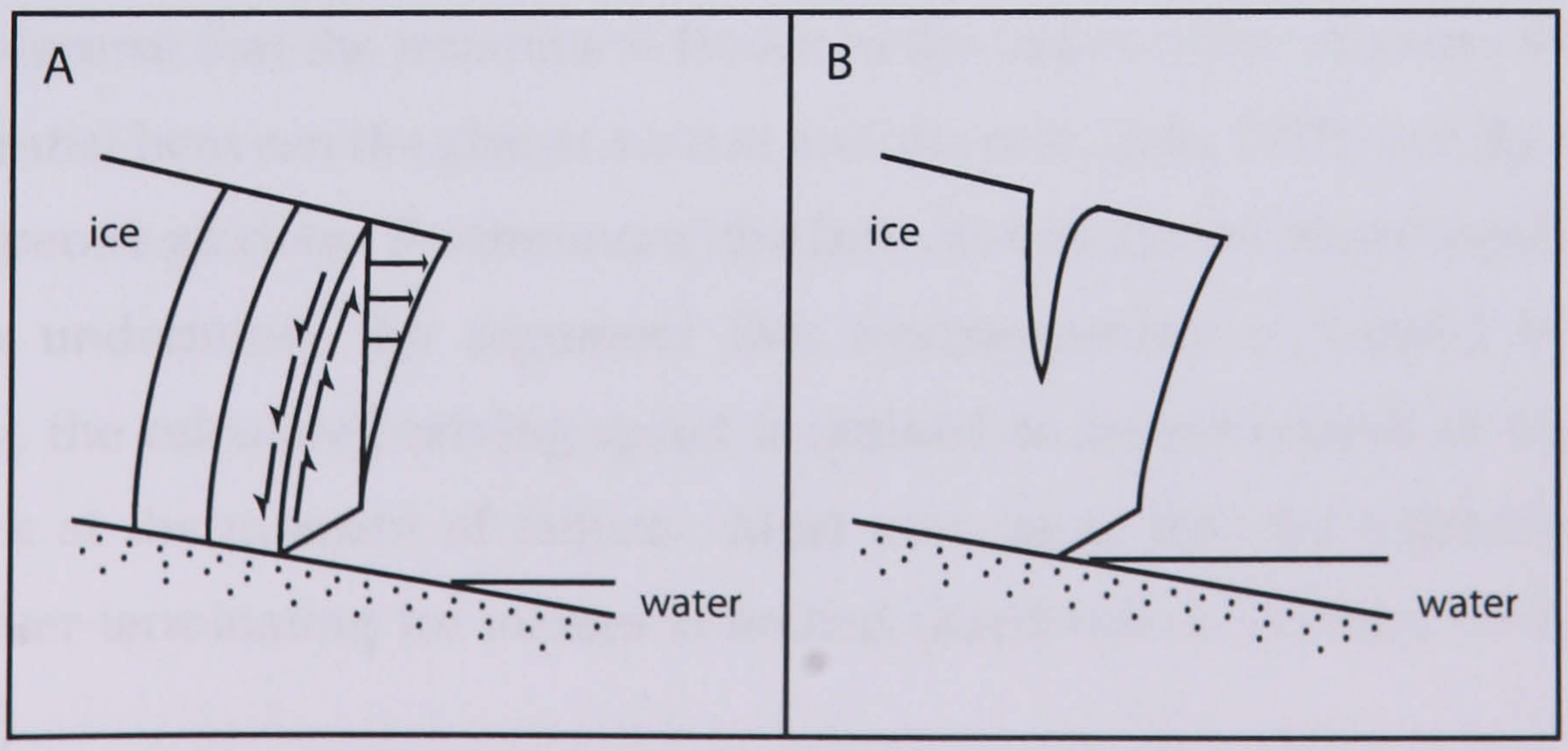

Figure 2.3 (A) The bending creep mechanism for shearing at calving walls. The curving lines are shear bands produced by bending creep. Adapted from Hughes (1992). (B) Crack opening along a plane dipping up-glacier, as modelled by Iken (1997).

By calculating stresses and velocities from Glen's Flow Law, it was demonstrated that cracks would develop at the zone of maximum stress, at a distance equal to the ice thickness, due to the maximum combination of tensile and shear stresses (Benn & Evans, 1998). The crack propagates to a depth where the stress is zero, continuing if the stress below the crack becomes tensile again, as a result of overhang development due to differential ice flow and undercutting of the cliff. Water is recognised to promote crevasse opening by compensating for the tendency of ice creep to lead to crevasse closure (Weertman, 1973; Fastook & Schmidt, 1982). Blocks break off when the centre of gravity has moved past the supporting edge of the bedrock. However, the model assumes that the ice breaks off under its own weight, does not account for water pressure at the base, and assumes that the water pressure acting on the glacier from the shallow, proglacial lake is negligible. Whilst the model provides a sound method for examining the stress evolution of a crack, the presence of a water body at the terminus needs to be accommodated before the model can be directly applied to tidewater or freshwater glaciers.

In later modelling approaches to ice calving, Hughes (1992) and Hughes & Nakagawa (1989) used elastic beam theory to develop a calving theory which reflected flow-induced overhanging, as described above. He argued that bending shear is the mechanism controlling calving from grounded ice walls, apparently evidenced by englacial shear bands. The shear causes the terminal slab to oversteepen in the direction of flow, as shown in Figure 2.3a. However, this mechanism requires a substantial subaerial cliff height above the flotation thickness, and the model is derived from studies on Deception Island, Antarctica, at a cold-based, dry-calving ice cliff, where there is no terminal water body to provide backpressure against the longitudinal stress regime towards the cliff. The model requires that the terminus is frozen to the bed in order to create the necessary stress differential between the glacier surface and the sole (Iken, 1977), not the case at fast-flowing temperate glaciers. Furthermore, the lack of evidence for shear bands disrupting ice foliation undermines the argument that oversteepening is formed in this way. Additionally, the calculated calving speed is defined as the movement of the top of the calving block at the moment of failure. Most now agree that the applicability of this model to water-terminating ice masses is limited (Kirkbride & Warren, 1997; Hanson & Hooke, 2000).

In contrast to the observations made by Hughes (1992), crack opening determined by Iken (1977) occurs along a plane that tilts up to the glacier surface in an up-glacier direction, (Figure 2.3b). Whilst both suggest that the rate controlling process is forward bending along englacial shear bands created by unrelieved tensile stresses, the crevasse orientation of Iken appears a more realistic representation of those seen in nature, and suggests that this study contributes to our understanding of the stress distribution at the terminus with greater success. Fastook & Schmidt (1982) built on these ideas by employing a finite element analysis approach to study crack propagation. The technique allows time evolution of the system to be shown, as it responds to the changing stress configuration. Deformation of the ice shelf leads to increased tension below the crack, and appears to cause the crack to accelerate as it becomes progressively deeper.

An interesting question regarding crevasse propagation is whether calving occurs (1) along pre-existing crevasses that are advected into the ice margin from further up-glacier, or (2) when a new crevasse is formed directly behind the ice cliff. Both cases have been observed. At slow-flowing lake-calving glaciers, such as those in New Zealand, full-height slab calving is thought to occur by the latter mode, due to undercutting of the subaerial cliff by waterline melting and the increasing overhang of the cliff by smaller events (Warren & Kirkbride, 2003). Processes upstream of the ice cliff are therefore thought not to affect, and not be affected by, calving dynamics. Intuitively, it might be expected that calving occurs along advected crevasses at highly crevassed termini e.g. the Alaskan tidewater glaciers, but it is not certain that this is always the case. Additionally, relict crevasse traces, carried passively to the terminus, sometimes provide lines of weakness along which calving occurs (Powell, 1991).

One approach to ice fracture is a linear elastic fracture mechanics (LEFM) model. It relies on small, pre-existing weaknesses at the ice surface, which lead to stress concentrations, propagating a crack. The use of such a model led Van der Veen (1998b) to suggest that bottom crevasses rarely occur on grounded glaciers. This might make it difficult to explain the occurrence of subaqueous calving events (2.1.1.iii). However, he concludes that bottom crevasses occur if the basal water pressure almost equals the ice overburden pressure and, thus, the glacier is close to flotation. The divergence of the velocity field at Columbia Glacier, Alaska, which is close to flotation, suggested a thinning rate in excess of that measured and is attributed to pervasive internal and bottom crevassing (Venteris, 1997).

Sassolas *et al.* (1996) also use an LEFM approach to determine the extent to which individual crack stress fields interact, as it is impractical to model crack-by-crack fracture at a densely crevassed calving terminus. If crevasses are separated by a distance of three to four times the crevasse depth, they have little effect on each other. Thus, at slow-flowing margins with few crevasses, the presence of pre-existing crevasses is unlikely to modify greatly the overall stress regime of the glacier, and perhaps buoyancy forces (2.1.1.iv), or those operating right at the ice cliff, dominate over those relating to ice flow and basal pressure, in determining the propagation of a new crevasse along which a calving event occurs. In comparison, at fast-flowing densely crevassed margins, crevasses are likely to be deep and close together, such that the stress fields will interact, particularly if they are complicated by the presence of water within the crevasse. Crevasses are more likely to be advected to the margin, and calving events may occur along these weaknesses, due to the control exerted by basal sliding and extensional flow.

However, studies using an LEFM approach have limited applicability to real glaciers, as the model assumes an elastic material, whereas polycrystalline glacier ice behaves visco-plastically. Furthermore, intra-granular air bubbles cause grain 'softening', altering the stress regime (Gagnon, & Gammon, 1995). Laboratory experiments provide an alternative setting to examine ice fracture and deformation (Arakawa & Maeno, 1997; Xiao & Jordan, 1996; Wilson *et al.*, 1996; Kim & Sunder, 1997). Integration of such studies to the application of calving behaviour could be a useful approach to understanding crevasse propagation. However, as yet, such laboratory experiments have not yet reproduced the conditions seen in the field.

2.1.1.v Thermal undercutting

In addition to oversteepening caused by differential flow (2.1.1.iv), oversteepening of the ice face may be caused by calving of ice from the lower part of the subaerial ice cliff. Alternatively, it may describe the overhang resulting from melting of the ice face along the water line (Warren & Kirkbride, 2003). Melting may also occur over the subaqueous portion of the ice face (2.3). Both kinds of thermo-erosional activity have been documented (Kirkbride & Warren, 1997, 1999; Purdie & Fitzharris, 1999; Warren, 1999; Vieli *et al.*, 2001; Warren & Kirkbride, 2003). It was previously considered that waterline melt notch development was only important for slow-flowing lake calving glaciers, but

significant melting has been documented more recently at tidewater glaciers (Vieli *et al.*, 2002; Motyka *et al.*, 2003b). Where calving appears to be controlled by waterline melting, cyclic calving behaviour is often exhibited. Calving of small lamellae above the notch leads to oversteepening and progressively larger subaerial events, in the build-up to a large, full-height slab event. A subaqueous calving event sometimes follows. However, calving is sometimes too frequent for an overhang to form (Kirkbride & Warren, 1997).

Where melting primarily governs calving in this way, ice flow speeds are observed to be slow (Kirkbride & Warren, 1997), typically occurring at lake-calving glaciers. However, uncertainties lie in the fact that large melt rates have been calculated at both freshwater and tidewater margins and, despite the correlation between water temperature and calving rate that exists (Warren & Kirkbride, 2003), it does not provide a reliable means to predict calving rates. The characteristics of freshwater calving glaciers, and the differences in calving behaviour that exist between tidewater and freshwater glaciers, are outlined below, considering the significance of factors, including waterline melting, affecting calving there.

2.1.2 Calving into freshwater

In comparison to tidewater glaciers, freshwater calving glaciers are little studied. Interest in freshwater calving was sparked by the responses of Unteraargletscher, Switzerland, and Austdalsbreen and Austerdalsisen, Norway, to damming of the proglacial valley for hydroelectric power production (Theakstone, 1986; Funk & Röthlisberger, 1989; Theakstone & Knudsen, 1989; Hooke *et al.*, 1989; Vischer *et al.*, 1991; Kennett *et al.*, 1997; Funk & Müller, unpublished). For a given water depth, rates of calving are consistently lower (2.1.1.i). Values for calving rate and water depth at lake-calving glaciers are shown in Table 2.2, and the relationship of calving rate to water depth for glaciers at both tidewater and freshwater margins is plotted in Figure 2.4. It clearly shows different slope coefficients for tidewater and freshwater calving glaciers, reflecting the order of magnitude difference in calving rates.

Glacier	Water depth (m)	Calving rate (m a^{-1})	
New Zealand			
Grey (NZ)	12	65	Warren & Kirkbride 2003
Godley	17	65	Warren & Kirkbride 2003
Hooker	20	46	Warren & Kirkbride 2003
Maud	15	106	Warren & Kirkbride 2003
Ruth	4	36	Warren & Kirkbride 2003
Tasman	10	32	Warren & Kirkbride 2003
Patagonia			
Ameghino	153	265	Warren 1999
Grey	165	355	Warren *et al.* 1995b
Moreno	175	510	Rott *et al.* 1998
Nef	325	800	Warren *et al.* 2001
Pio XI	100	413	Rivera *et al.* 1997a
Upsala East	67	85	Skvarca *et al.* 1995b
Upsala West	300	1095	Warren *et al.* 1995b
Iceland			
Breiðamerkurjökull	205	580	Björnsson *et al.* 2001
Norway			
Austdalsbreen			Hooke *et al.* 1989
Alaska			
Mendenhall	70	190	Motyka *et al.* 2003b
Alps			
Sabbione	20	52	Funk & Röthlisberger 1989
Unteraar	12	32	Funk & Röthlisberger 1989
Oberaar	16	50	Funk & Röthlisberger 1989
Gries	13	37	Funk & Röthlisberger 1989

Table 2.2 *Water depths and calving rates at lake-calving glaciers worldwide. Where more than one study exists only the most recent figures and source are given.*

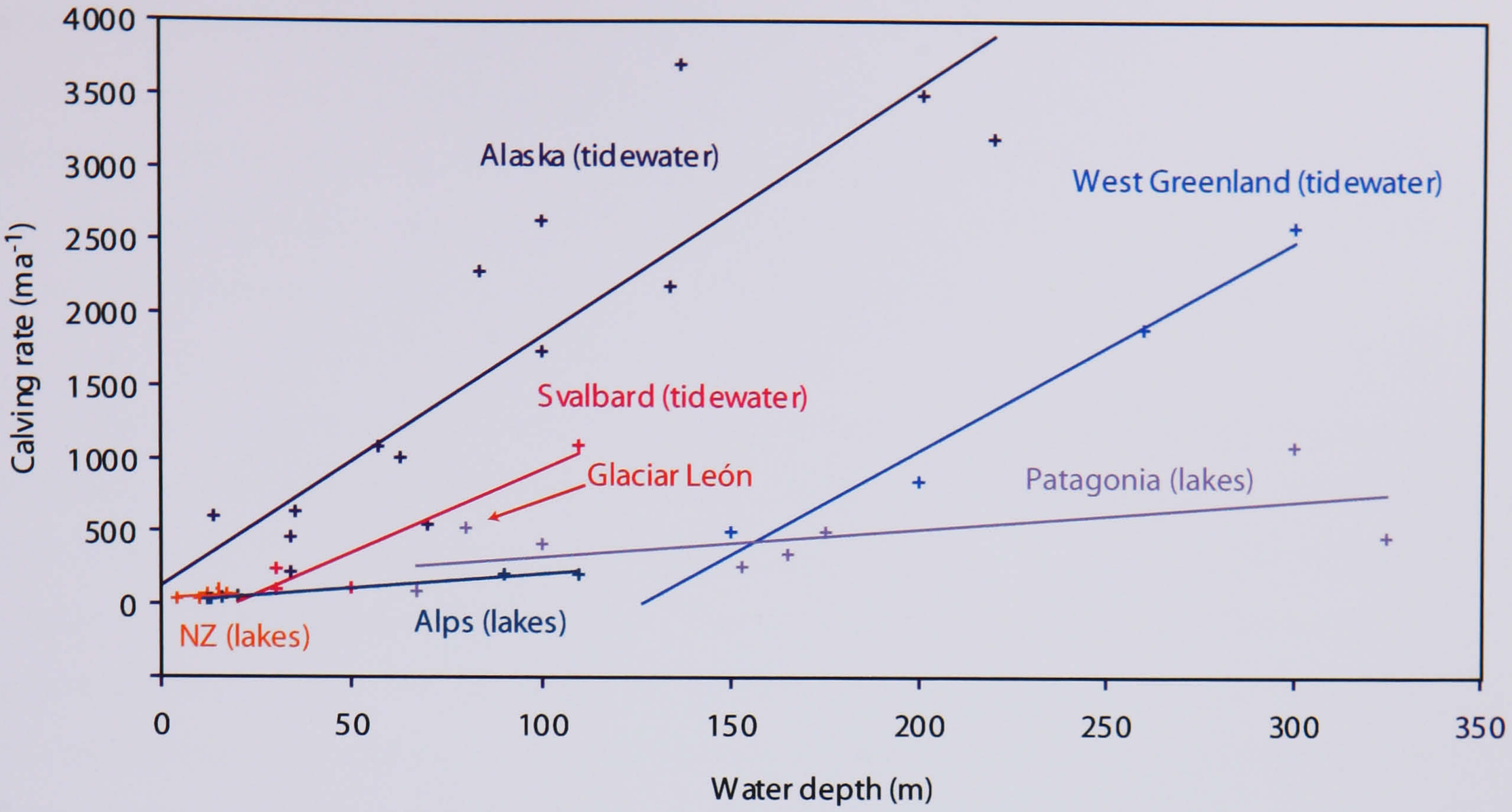

Figure 2.4 The relationship between calving rate and water depth for glaciers in different world regions, illustrating the greater rates of calving which occur at tidewater termini indicated by the steeper gradient of the trendline. Sources: as for Tables 2.1 and 2.2.

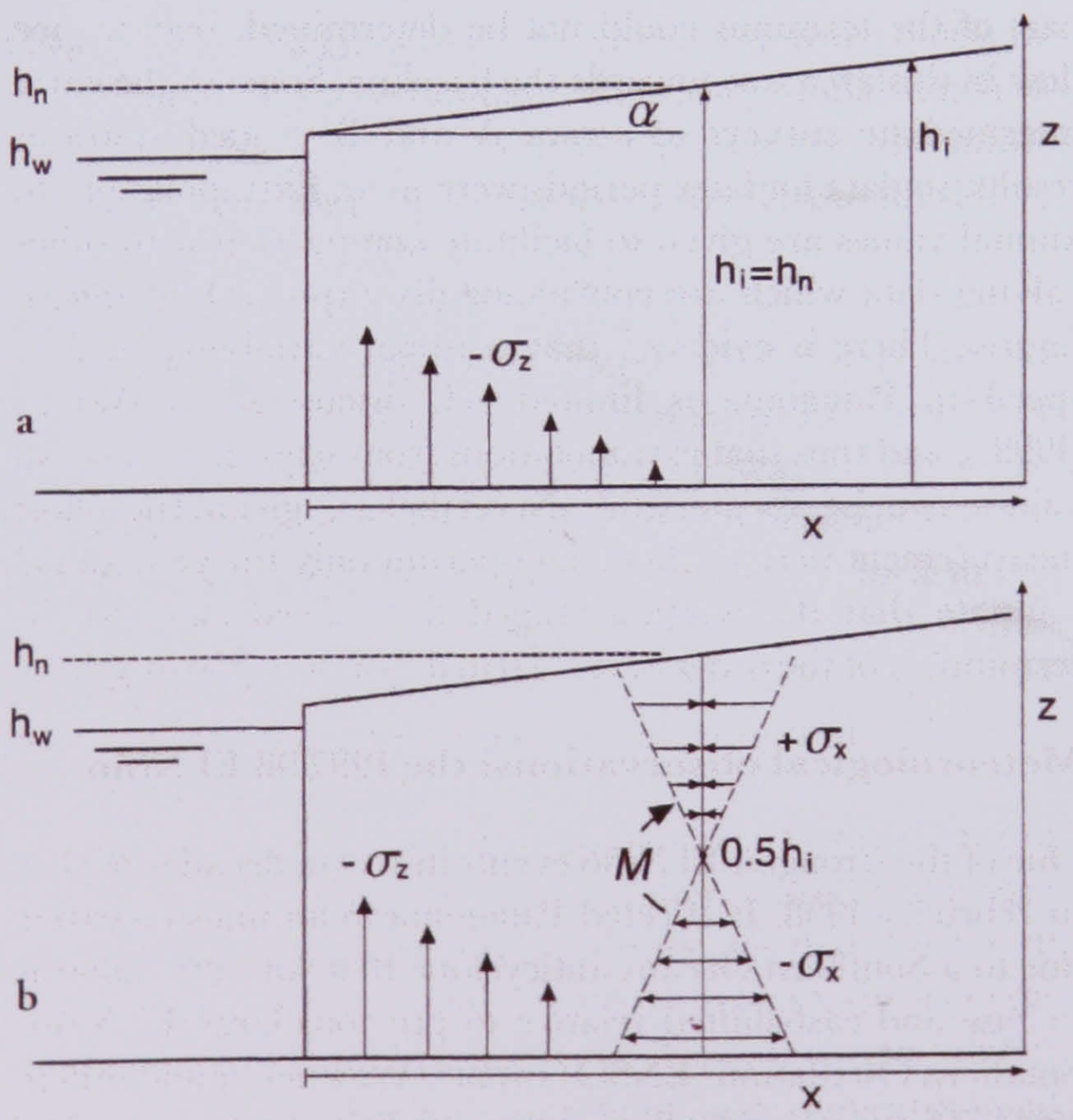

Figure 2.5 Testing the principles of buoyancy-driven calving into water. Further explanation is provided on p. 33. Basal tensile stresses resulting from buoyant forces for a range of terminus ice thicknesses and surface gradients of 5° and 2°. The calculated stresses are based on the assumption that the ice remains in contact with the bed, and that buoyant forces are unresolved by upwarping of the ice. Upwarping rates will increase, and fracture becomes increasingly likely as the length of the buoyant zone increases. Fracture will be encouraged by high ablation rates. Source: Warren *et al.* (2001).

The coefficient of the water depth-calving rate relationship has been revised from 1.9 (Funk & Röthlisberger, 1989) to 1.8 (Warren *et al.*, 1995b), to 3.6 (Skvarca *et al.*, 2002) and most recently, with a global dataset of 21 lake-terminating glaciers, to 2.3 (Warren & Kirkbride, 2003), including deep-water terminating glaciers. In the quest to understand the processes that control calving, it is imperative to understand this large difference in tidewater and freshwater rates. The range of possible factors is discussed below.

Ice velocities are generally slower at freshwater-calving glaciers than tidewater glaciers, resulting in termini with fewer crevasses and a more stable terminus position (Kirkbride & Warren, 1997). Reasons for the difference in calving rate magnitude between freshwater and tidewater glaciers may relate primarily to the contrasting buoyancy of saline and fresh water (2.2.3.i), which are reflected in the slower, more stable termini, as discussed below. Buoyancy contrasts operate in two ways, (1) by affecting the pathways followed by meltwater discharge in the ice-proximal proglacial water body, and (2) by affecting the buoyancy of the glacier ice in the terminal water body. Each is discussed below.

Meltwater is more buoyant than the surrounding water when it enters a saline water body, causing it to upwell close to the ice cliff, inducing greater rates of subaqueous melting (2.3.5.i) (Powell & Molnia, 1989; Motyka *et al.*, 2003a). In comparison, at freshwater glaciers, the smaller buoyancy difference between meltwater and the lake water results in interflows or underflows of meltwater discharge, which implies that meltwater may have less impact on subaqueous melt rates than in the marine setting (cf. Kennett *et al.*, 1997). However, high rates of mass loss are not limited to tidewater termini. Calving in embayments at Austerdalsisen, Norway, appeared to be related to the discharge of such outflows (Theakstone & Knudsen, 1986), and scalloping of subaqueous portions of overturned icebergs is thought to relate to direct melting of the ice surface below the waterline (Theakstone, 1989). Documentation of the rapid retreat of freshwater glaciers such as Glaciar Upsala west, Patagonia, led Venteris (1999) to question whether salinity is important for explaining the difference in calving rates in freshwater and tidewater settings. Laboratory tests also cast doubt over the differences in melt rates between the two settings because melt rates in freshwater may be faster at some temperatures (Eijpen *et al.*, 2003).

The buoyancy difference between the freshwater and saline water bodies also affects the buoyancy of the glacier terminus itself. Low crevasse density, due to lower buoyancy differences, is cited as an explanation for the observation that larger icebergs tend to calve from lake-terminating glaciers (Qamar, 1988; Warren, 1991; Kirkbride, 1993; Warren *et al.*, 1995b). In particular, subaqueous events usually produce the biggest bergs in freshwater settings (Reid & Callender, 1965; Kirkbride & Warren, 1997; Warren & Kirkbride, 1998), perhaps reflecting the 30% lower buoyancy of ice in freshwater than saline water, which may affect the rates at which bergs become detached below the water level (Hanson & Hooke, 2000; Hughes, 2002). However, buoyancy forces are far from insignificant in freshwater, and have long been thought to drive calving from some lake-calving glaciers, from observations in Alaska, Canada, Iceland and Norway (Howarth & Price, 1969; Holdsworth, 1973; Theakstone & Knudsen, 1986; Theakstone, 1989; Lingle *et al.*, 1993). The presence of a reverse surface slope at the terminus of some glaciers is used to infer buoyant forces at the terminus (Theakstone, 1989; Warren *et al.*, 2001), which may respond to a rise in water level. At Generator Lake, Baffin Island, the water level rise in 1987 was so rapid that the glacier was unable to adjust by upward deflection (Holdsworth, 1973). Calving into water 325 m deep (h_w), Glaciar Nef, Patagonia, results from buoyancy forces, as the ice, 475 m thick (h_i), approaches flotation (Warren *et al.*, 2001). Calving of 'tabular' icebergs from a terminus of surface gradient (α) occurs at the point of maximum torque, *M*, some distance up-glacier from the terminus where the tensile stress due to buoyantly-forced upward bending (σ_z) exceeds the tensile strength of the ice (σ_x), as illustrated in Figure 2.5. Although this model was based on observational data over a period of only eight days, this calving mechanism has been interpreted at other lake-calving glaciers. A similar terminus geometry, with a protruding central section into the lake, resulted during the rapid collapse of Austerdalsisen (Theakstone & Knudsen, 1986; Theakstone, 1989). Buoyancy forces must also drive calving at Breiðamerkurjökull, southeast Iceland, and Mendenhall Glacier, Alaska, where the freeboard at the terminus is only a few tens of meters (Derbyshire, 1974; Björnsson *et al.*, 2001; Motyka *et al.*, 2003b). Both glaciers are likely to experience increasing rates of retreat by buoyancy-driven calving, as they recede into still deeper water.

Not all lacustrine calving glaciers calve in response to buoyancy forces. For small, slowly-flowing glaciers, the terminus thickness is often far above the critical height for buoyancy, and calving must be controlled by other factors (Iken, 1977). Warren & Kirkbride (2003) suggest that, where ice velocities and crevasse density are low due to a compressional

stress regime at the terminus, calving occurs due to oversteepening by undercutting of the ice cliff at the waterline. That undercutting of the subaerial cliff by waterline melting is the dominant mechanism at slow-moving glaciers has been suggested for Tasman Glacier, New Zealand, where rates of ice cliff recession are balanced by rates of waterline melt notch development (Warren & Kirkbride, 2003; Roehl, submitted). Only a few years ago, the tip of the terminus was thought to calve in response to buoyancy forces (Purdie & Fitzharris, 1999), and must have since receded to a point where buoyancy is no longer the main control. The notch mechanism describes short-term behaviour, but it cannot be extrapolated to explain the water depth relationship, because notch formation is influenced by lake conditions (2.3.6). Either water depth exerts no control on calving at glaciers which appear to be controlled by waterline melting rate, or another mechanism as yet unidentified must operate on longer timescales. Kirkbride & Warren (1997) identify the need to study short-term processes at lake-calving glaciers, to bridge the gap between short-term processes and statistical correlation at the annual scale.

Over short timescales, studies at tidewater glaciers have demonstrated a link between tidal stage fluctuations and calving (O'Neel *et al.*, 2001), which arises due to the effect of cyclic stage changes on the effective basal pressure by alteration of the basal water pressure (2.1.1.ii). For a given water depth, basal water pressure at lake-calving glaciers is lower than at tidewater glaciers, due to the density difference between the saline and fresh water bodies. Thus, ice velocity is lower. This difference has been suggested to account for the differences in calving rate seen between freshwater and tidewater glaciers, assuming that the correlation between calving and ice speed holds true (Van der Veen, 2002a).

However, the intense crevassing of some lacustrine glaciers e.g. Glaciar Upsala west (Warren *et al.*, 1995b) suggests that freshwater glaciers may respond to longitudinal stretching and basal water pressure in a similar way to tidewater glaciers, in deep water (2.1.1.ii). Glacier flow at Mendenhall Glacier, Alaska, is almost entirely by basal sliding, and the absence of a moraine shoal at the terminus permits extensional flow towards the terminus, evidenced by increased crevasse density (Motyka *et al.*, 2003b). Relatively slow rates of ice velocity and calving here (Table 2.2) (particularly in comparison to its regional tidewater counterparts) suggest that calving due to longitudinal stretching and buoyancy forces is not limited to faster-flowing lacustrine glaciers. Even at slower-flowing glaciers such as Austdalsbreen, Norway, and Maud Glacier, New Zealand, ice velocity increased

with lake stage, as basal water pressures increased from either lake damming or after heavy rain (Hooke *et al.*, 1989; Kirkbride & Warren, 1997).

Although tidal influences are absent from lake-calving glaciers, and the role of greater water depths for permitting high rates of basal sliding are known from studies at tidewater glaciers, the effects of hourly and diurnal fluctuations of lake level on calving have not been examined extensively. Two studies exist, at Glaciar Moreno, Patagonia (Iizuka, *et al.*, 2004), and Mittivakkat Glacier, Greenland (Hasholt, 2002), using a pressure sensor under the water surface to record changes in water level. Abrupt changes in water level are interpreted to result from the waves produced by a calving event, and the wave train provides a means to monitor the timing and size of calving events. Correlations of calving event timing and size were made with diurnal trends in insolation at Glaciar Moreno, whilst calving events in the short dataset from Mittivakkat Glacier were related to changes in water temperature. However, neither of these studies examines the effect of steady changes in lake level for terminus dynamics, in terms of the consequences for effective basal pressure over short-term periods, comparable to the studies of tidal fluctuations at tidewater glaciers (O'Neel *et al.*, 2001).

The influence of sedimentation on water depth at the terminus was described in section 2.1.1.i for tidewater glaciers. The absence of a moraine shoal is confirmed for Mendenhall Glacier, Alaska (Motyka *et al.*, 2003b), and is important for terminus dynamics as it permits accelerating ice flow towards the terminus. It is therefore useful to briefly consider the mechanisms of sedimentation in lacustrine settings, to assess their impact on water depths. Typical sedimentary systems in front of the terminus in ice-contact lakes are similar to a marine moraine shoal (Derbyshire, 1974; Duck & McManus, 1985; Ashley & Warren, 1997). However, there are factors particular to freshwater locations which influence the sedimentation rate and resulting water depths (Johnson, 1997). Sedimentation may not be as concentrated at the terminus, because sediments may be carried further away by underflows or interflows, as well as overflows (2.2.4), evidenced by lamination in the glaci-lacustrine sediments (Liverman, 1987). In the enclosed water body, deposition of ice-rafted debris is sometimes greatest in the distal zone of the lake, near the outflow point, where bergs are carried away by surface currents (McManus & Duck, 1988), before grounding in shallow water at the distal end (Duck & McManus, 1985). In combination, sediment carried by icebergs and glacier meltwater modifies the concentration of sedimentation at the terminus. Therefore, water depth relates more to

lake basin topography than sedimentation rates, as is the case at Mendenhall Glacier, Alaska (Motyka *et al.*, 2003b). Supraglacial sediment may also be significant for calving activity in some cases. The up-glacier spread of supraglacial debris on the Tasman Glacier, New Zealand, has preserved a long ice tongue at a low gradient, preventing terminus retreat from the outwash head and making the glacier vulnerable to calving (Kirkbride & Warren, 1999).

This discussion indicates the wide range of factors controlling calving behaviour. As with tidewater glaciers, the range of lacustrine calving rates is large, and no mechanism at one glacier is identical to that implied by the terminus fluctuations of another. Untangling the signal of calving mechanisms is no more straightforward for lake-calving glaciers than for tidewater margins. 'Chicken-and-egg' type feedback loops make it difficult to clarify the rate-controlling factors i.e. identifying the causal variable from the respondent variable. One particular topic of concern is whether high calving rates cause, or are the result of, fast ice flow. To produce a physically-based model of calving necessitates the resolution of this and other issues, the debates surrounding which are explored below.

2.1.3 The calving debate

The preceding discussion has addressed various factors which influence calving. However, they rarely operate independently, instead affecting calving to varying degrees, their relative importance altering from site to site. It is possible to envisage a continuum of calving glaciers, from fast to slow calving (Warren & Kirkbride, 2003), where the extremes are represented by the slow-moving freshwater glaciers of New Zealand and rapidly calving tidewater glaciers such as Columbia Glacier at the other. However, the wide variety of calving mechanisms which have been described suggests that it is not possible to predict the behaviour of one glacier terminus on the basis of observations from another, if calving mechanisms are indeed particular to individual glacier settings. A summary of calving mechanisms for both freshwater and tidewater glaciers is presented in Table 2.3, and shows that any given calving force or mechanism may operate at both tidewater and freshwater glaciers.

Glacier	Location	Terminus setting	Calving Controls
Columbia	Alaska	Tidewater	Buoyancy, longitudinal stretching, ice flow, shoal backpressure, meteorological variables
LeConte	Alaska	Tidewater	Longitudinal stretching, ice flow, tidal stage fluctuations
Mendenhall	Alaska	Freshwater	Buoyancy & longitudinal stretching
Hansbreen	Svalbard	Tidewater	Longitudinal stretching, ice flow, waterline melting, meteorological variables
Mittivakkat	Greenland	Freshwater	Changes in water temperature
Hooker	New Zealand	Freshwater	Waterline melting
Maud	New Zealand	Freshwater	Waterline melting
Tasman	New Zealand	Freshwater	Waterline melting
San Rafael	Patagonia	Tidewater	Longitudinal stretching, ice flow
Ameghino	Patagonia	Freshwater	Waterline melting
Moreno	Patagonia	Freshwater	Diurnal trends in insolation, water temperature
Pio XI	Patagonia	Freshwater	Sedimentation and shoal backstress
Nef	Patagonia	Freshwater	Buoyancy
Upsala	Patagonia	Freshwater	Longitudinal stretching, shoal backpressure
Austdalsbreen	Norway	Freshwater	Buoyancy
Austerdalsisen	Norway	Freshwater	Waterline melting & buoyancy
Breiðamerkurjökull	Iceland	Freshwater	Buoyancy

Table 2.3 The range of factors controlling calving activity

As well as varying between glaciers, calving mechanisms are known to alter with changes to glacier dynamics: e.g. ice speed, water depth, terminus position, meteorological factors. This ambiguity around the precise controls on calving has led to a two-fold debate about whether calving controls, or is controlled by, terminus position. The u_c / h_w model described in section 2.1.1.i visualizes calving as the 'master' of the terminal dynamics of a glacier (Meier & Post, 1987; Meier, 1994, 1997, 2002, Meier *et al.*, 1994). As calving increases in deeper water, ice velocities increase. This may occur when a glacier retreats off a terminal moraine, releasing backpressure (2.1.1.i). Increased ice flow causes thinning, and the ice thickness is close to flotation, such that it is unstable, and calves rapidly. However, because of the close coupling between calving rate and ice velocity, there is debate over the role of calving in relation to terminus dynamics. The calving rate-water depth model is questioned by Van der Veen (1996, 1997, 2002a) as a 'spurious result' of the seasonal, rather than annual, timescale over which calving rates were measured. Instead, he views calving as the 'slave' of changes to the glacier terminus, as a result of upstream glacier dynamics. He proposes that terminus position is controlled by the ice thickness in excess of flotation. In this model, based on observations of Columbia Glacier, where the terminus thinned to within ~ 50 m of the thickness required for flotation, thinning of the ice causes the glacier to become unstable, responding by calving back to a point where ice thickness again exceeds flotation. Rapid retreat occurs as long as high speeds are maintained. In this case, calving responds to changes in terminus position, which fluctuates due to processes that alter ice thickness and water depth.

Venteris *et al.* (1997) assume that changes in thickness are due to increased stretching by basal sliding towards the terminus. This is the reverse of the water depth model, where changes in calving rate induce terminus fluctuations. Individual calving events leave a progressively higher ice cliff with unbalanced lithostatic stresses, resulting in stretching and further calving (Meier, 1994). Continuity calculations suggest that stretching may have an additional effect on terminus position, as the presence of voids, interpreted as bottom crevasses, could weaken the glacier and contribute to rapid retreat (Venteris, 1999). The importance of thinning on rapid tidewater retreat in Patagonia is further demonstrated with data from both north and south icefields, by comparison with data from the Columbia Glacier, Alaska (Aniya *et al.*, 1997; Venteris, 1999). However, the concept of Van der Veen fails for glaciers which thin past the flotation threshold, or for those which are far from flotation, where other processes, such as waterline melting, must predominate.

Seeking to provide a physical explanation for the water depth-calving rate correlation, Hanson & Hooke (2000) use a numerical model to suggest that oversteepening and bottom crevassing increase with water depth, promoting failure at the top of the ice cliff. This is thought to be due to the distribution of longitudinal stresses and the velocity field at the glacier margin. High longitudinal strain rates result in pervasive fracturing, and the oversteepening initiates calving. Some uncertainty lies in the resulting ice front velocities, because the strain profile resulting from the stress field is not integrated cumulatively to give ice velocities. This results in a maximum ice velocity just above the waterline in the ice cliff. This extruding flow contradicts the overhang development they describe. This study further highlights the difficulty of realistically describing the processes at a calving front.

Furthering the study of Bindschadler & Rasmussen (1983), Vieli *et al.* (2001) investigate the evolution of tidewater glaciers through a basal depression at the terminus. Their model goes some way to reconciling the opposing views of Meier and Van der Veen by demonstrating the relationship of calving rate to water depth in a setting where the glacier will float once a threshold thickness is reached. This occurs as effective pressure decreases towards the terminus, controlled by the decreasing water level in the glacier in relation to sea level. This causes a concurrent increase in sliding and stretching, resulting in thinning of the glacier. This stretching is reflected in the observed increased crevasse density towards the terminus (2.1.1.iv). The model solves the full equations for the stress and velocity fields, and calving is an output of the model, unlike the earlier models. For each time-step, the terminus is moved to the position where ice thickness exceeds flotation forces and, therefore, the model still does not provide a physical explanation for the occurrence of a calving event. It does, however, demonstrate that the water depth relationship only applies to glaciers in a steady state and that, when rapid changes occur, the calving rate increases non-linearly with depth.

Vieli *et al.* (2001) applied the ice flow calculations to retreating and advancing scenarios. The modelled results reproduce the observation of increased calving rates during retreat through the progressively deeper waters of an overdeepening, supporting the water depth model, whilst adjusting to changes in ice thickness, in keeping with the flotation model of Van der Veen. Up-glacier, changes in ice velocity are small, with accelerated sliding occurring only towards the ice cliff. During advance, higher calving rates occur as

the terminus moves into deeper water. Once past the deepest point of the basin, the calving rate decreases rapidly, and the ice velocity less rapidly. Not only is the water depth important but also the direction of slope at the terminus. The model supports observations that rapid changes occurring at tidewater glaciers relate predominantly to bed topography and only indirectly to a mass-balance change (Meier & Post, 1987). Thinning due to a change in climate, and therefore in mass balance, is only a triggering process for a rapid retreat through a basal depression. An abrupt retreat of Hansbreen, Spitsbergen, from 1990-1991, by 280 m, supports this model of retreat through an overdeepened basin, as climatic and mass balance records do not indicate any abrupt change for this period (Vieli *et al.*, 2002). However, a readvance which occurred from 1993 to 1996 was attributed to changes in climatic conditions, though without substantial supporting evidence. Furthermore, the 2D model does not account for the influence of valley sides. These are important for modifying the effective pressure along the centre flow line, but have yet to be incorporated into any numerical modelling effort.

Both the 'slave' and 'master' concepts offer insights into the way in which different factors may influence calving, and show how complex the calving process is. Both approaches are supported by empirical evidence from studies at individual glaciers and, although Vieli *et al.* (2001) go some way to uniting these approaches, there is still the need to reconcile them fully in order to reliably explain glacier fluctuations in the past, and anticipate the near-future behaviour of calving glaciers.

2.1.4 Summary

Calving glaciers are amongst the most dynamic of outlet glaciers. Their anomalous response to climatic forcing signifies that other external or internal factors provide additional controls on terminus fluctuations. The relationship of calving rate with water depth has provided a basis for further investigations of the physics to which this relates. The key factors have been identified as ice flow regime, basal hydrology, the buoyancy of the glacier in the water body, oversteepening of the ice cliff, ice fracture, and the characteristics of the water body influencing waterline melting. However, the relative importance of each factor varies spatially and temporally, and their interactions are complex and, as yet, uncertain. The wide range of calving behaviour seen at different ice margins has limited the applicability of calving relations from one site to the next, raising

the question of whether a universal calving law really exists. In order to understand the physics involved, and accurately predict the future behaviour of such glaciers, it is essential to extend the regional databases of calving statistics (Van der Veen, 1997). Specifically, rate-controlling factors determined from studies of tidewater glaciers need to be tested thoroughly at freshwater margins. Caution is needed when testing models of calving, considering the time-scales over which processes operate, from the duration of a calving event, to the role of calving on long-term glacier fluctuations over tens to thousands of years. Many studies, conducted over time scales of a few weeks or months, are extrapolated to infer annual trends. It is not clear that such extrapolations are justified, as seasonal variations may strongly affect glacier dynamics.

2.2 Ice-contact lakes

2.2.1 Introduction

The dynamics of calving glaciers are intimately related to the water body in which they terminate, both to their geometry and limnology. Knowledge of lake bathymetry and basin geometry is important for interpreting the retreat history of a calving glacier through an overdeepened basin. This is because past water depths, and the location of pinning points in the valley sides, are pertinent to the nature and rates of retreat, and any concurrent downwasting (Vieli *et al.*, 2001). Although the water depth-calving rate relation (Brown *et al.*, 1982) has proved robust and useful, it is also apparent that the water temperature of proglacial water bodies may significantly influence calving rates and processes (Funk & Röthlisberger, 1989; Kennett *et al.*, 1997; Warren, 1999). Thus, whilst the topographic geometry and thermal conditions are both modified by the presence of a glacier (Matthews & Quinlan, 1975), the ice-proximal and distal waters also influence the ice calving rate by affecting melt rates (Kirkbride & Warren, 1997; Purdie & Fitzharris, 1999). This is because lakes represent a large reservoir of heat with the potential to prolong ice melt into the autumn (Kirkbride, 1993). There may be sufficient energy in far-field water to melt ice at rates in the range of observed calving speeds (Gade, 1979; Hanson & Hooke, 2000).

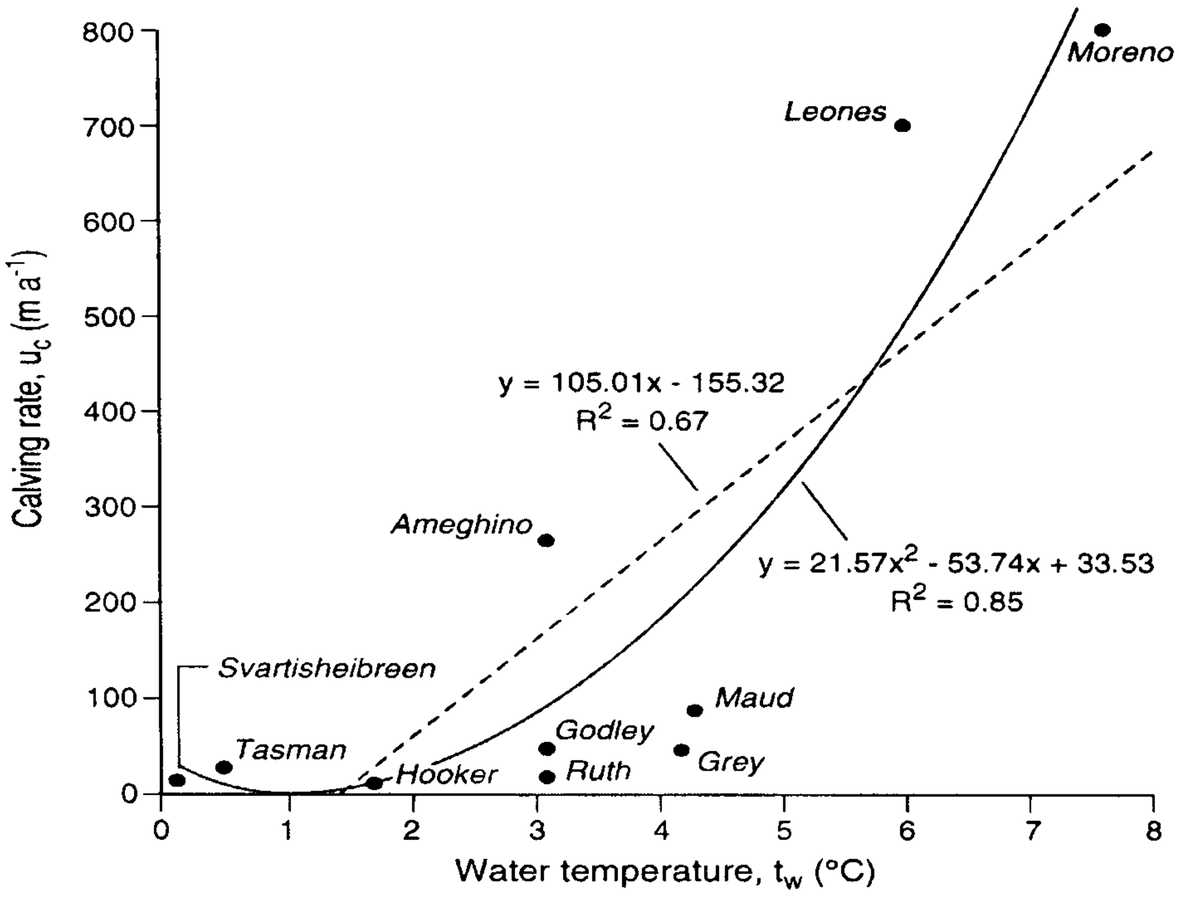

Figure 2.6 Calving rates plotted against water temperature for glaciers in New Zealand, and for the following glaciers: Glaciar Moreno, Argentina, (Rott *et al.*, 1998; Warren, 1999); Glaciar Ameghino, Argentina (Warren, 1999); Glaciar León (Haresign & Warren, in press); and Svartisheibreen, Norway (Kennett *et al.*, 1997). Ice-proximal water temperatures were measured in summer or early autumn at a depth of 10 m. Source: Warren & Kirkbride (2003).

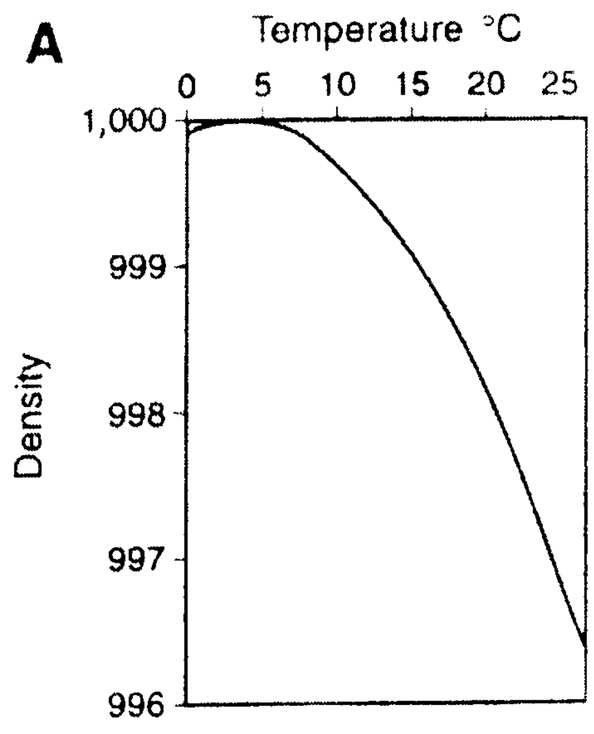

Figure 2.7 The relationship between temperature (°C) and density (kg m^{-3}) for pure water.

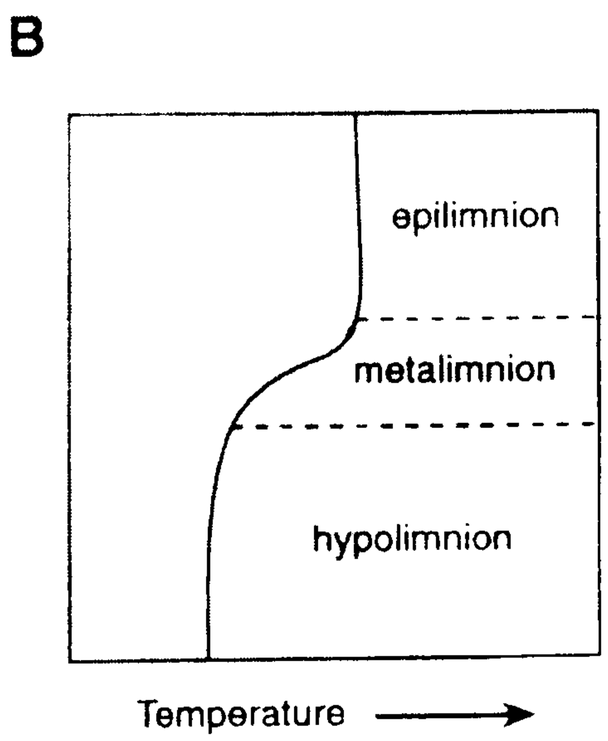

Figure 2.8 Temperature profile in an ice-contact lake resulting from surface heating and wind mixing.

For 10 lake-calving glaciers at which ice-proximal water temperature (t_w) data exist, a positive correlation exists between calving rate, u_c , and *tidewater* , (Figure 2.6) (Warren and Kirkbride, 2003) and the strength of this correlation is similar to that between u_c and water depth, h_w , in freshwater (2.1.2). The presence of the ice-contact water body, and its thermal regime, may therefore be an important factor affecting melt rates and calving processes. In this section, the evolution of ice-contact lakes and their physical limnology are outlined, before discussing the ways in which heat transfer within lakes takes place, important for considering the subaqueous melting potential.

2.2.2 The glacio-lacustrine environment and the evolution of ice-contact lakes

The term glaciolacustrine encompasses both ice-contact lakes and distal lakes, the main difference being the presence or absence of ice. Because few data exist, present understanding rests on a small number of studies, mostly focused on sediment dynamics primarily in distal, ice-fed lakes (Gustavson, 1975; Harris, 1976; Gilbert & Shaw, 1981; Pickrill & Irwin, 1983; Gilbert & Desloges, 1987; McManus & Duck, 1988; Hicks *et al.*, 1990; Ashley, 1995). Available data about the physical limnology and geometry of ice-contact lakes and their influence on calving termini have been reviewed and discussed by Warren & Kirkbride (1998) and Benn and Evans (1998, p. 282ff). Very little attention has been given to the seasonal development of the thermal regime or the interaction between limnological and glaciological processes, the study of Tasman Lake and Tasman Glacier in New Zealand (Roehl, 2003, submitted) being a rare exception. A summary of studies of ice-contact marginal lakes is presented in Table 2.4.

Ice-contact lakes may be supraglacial, englacial, subglacial or ice marginal. Ice marginal lakes may be either ice-dammed (Reid and Callender, 1965; Liverman, 1987; Johnson, 1997) or sediment-dammed (Churski, 1973; Derbyshire, 1974; Björnsson, 1976; Duck & McManus, 1985; Hicks *et al.*, 1990). Ice dammed lakes are usually ephemeral (a year to a few tens of years e.g. Gilbert, 1971) and may drain and refill more than once during the melt season. Those dammed by topography in isostatically-depressed lows enlarge as the glacier recedes (Ashley & Warren, 1997), and tend to be semi-permanent (hundreds to a few thousand years).

Region	Lake	Source	Focus of Research
Canada	Generator	Holdsworth 1973	glacier response to lake level changes
	Hazard	Liverman 1987	sedimentation
	Summit	Gilbert 1971	lake drainage
Himalaya	Imja Cho	Watanabe et al. 1995	supraglacial lake evolution
	Ngozumpa	Benn *et al.* 2000	supraglacial lake evolution
	Tsho Rolpa	Chikita/ Yamada 1998, 1999, Chikita *et al.* 2000a, 2000b; Sakai *et al.* 2000a, 2000b, 2001	ice melting
Iceland	Fjallsárlón	Howarth & Price 1969	bathymetry, lake evolution
	Jökulsárlón	Derbyshire 1974; Harris 1976; Landl *et al.*, 2003	temperature/ salinity/ heat budget
	Skeiðará	Churski 1973	hydrography
New Zealand	Godley	Warren/ Kirkbride 1998; Kirkbride 1993	melting-calving transition
	Hooker	Warren/ Kirkbride 1998; Kirkbride 1993; Hochstein *et al.* 1995	melting-calving transition
	Ivory	Anderton/ Chinn 1978; Hicks *et al.* 1990	sedimentation
	Maud	Kirkbride 1993; Kirkbride/ Warren 1997 Warren/ Kirkbride 1998	ice melting, melting-calving transition
	Tasman	Hochstein *et al.* 1995; Kirkbride 1993; Kirkbride/ Warren 1999 Roehl 2003	ice melting, melting-calving transition
Norway	Austdalsvatnet	Hooke et al. 1989, Laumann/ Wold 1992	glacier response to lake level changes
	Austerdalsvatnet	Theakstone 1989, Theakstone & Knudsen, 1986	glacier response to lake level changes
	Briksdalsvatnet	McManus & Duck 1988	iceberg sedimentation
	Heiavatnet	Kennett *et al.* 1997	outburst tunnel melt
Patagonia	Ameghino	Warren 1999	temperature and calving rate
	Argentino	Skvarca *et al.* 2002	bathymetry, temperature
	Guillermo	Warren *et al.* 1995b	bathymetry, temperature
	Leones	Haresign & Warren (in press)	ice melting
	Moreno	Warren 1994	bathymetry, temperature
	Nef	Warren *et al.* 2001	bathymetry, temperature
USA	Malaspina	Gustavson 1975	sedimentation
	Mendenhall	Motyka *et al.* 2003	bathymetry
	Miller	Reid/ Callendar 1965	iceberg origin
	South Cascade	Campbell 1973	thermal structure

Table 2.4 The range of studies on ice-contact lakes.

Some are actually river-lakes, which discharge slowly but continuously away from the ice, and can be thought of as a low-velocity river or a high-velocity lake. Supraglacial meltwater creates ice-stagnation kettle lakes on inactive portions of the glacier surface, which change continuously as the ice melts. They are short-lived and no studies are documented about their physical limnology. Similarly, no englacial lakes have been studied in detail. Subglacial lakes occur frequently in Iceland, and studies often relate to their interaction with volcanic centres in terms of jökulhlaup events (Geirsdóttir *et al.*, 2000; Björnsson, 2002).

Ice-contact lakes usually form during deglaciation (Howarth & Price, 1969), or during advance and retreat cycles through the same basin (Björnsson, 1996). Many existing ice-contact lakes have formed within the last 60-70 years as glaciers retreated in rapid response to twentieth century warming (Howarth & Price, 1969; Hochstein *et al.*, 1995; Kirkbride & Warren, 1999; Warren, 1999; Motyka *et al.*, 2003b). As glacier termini retreat, water ponds against a moraine, hillslope or rock basin overdeepening faster than it drains by a river or through unlithified sediments (Derbyshire, 1974; Kirkbride, 1993). Drainage in the proglacial area of Breiðamerkurjökull and Fjallsjökull, Iceland, became concentrated into a few major lake and river systems during recent glacier recession, permitting meltwater accumulation between the ice margin and slopes dipping towards the glacier (Howarth & Price, 1969).

Lakes may occur in rock basins resulting from overdeepening due to glacial erosion. Filled with ice during stadials, water takes its place during interstadials. Many examples of this kind can be found in Patagonia, New Zealand and Alaska (Benn & Evans, 1998). The existence of subaqueous moraine ridges identified from bathymetrical studies is useful for understanding the timing of advance and retreat phases (Duck & McManus, 1985; Haresign *et al.*, submitted).

The transition from melting to calving significantly affects glacier mass balance during recession, by altering the efficiency with which the glacier may lose mass i.e. mass loss efficiency by calving and melting is greater than by melting alone (Hillaire-Marcel *et al.*, 1981; Hughes, 1987; Warren, 1992; Kirkbride, 1993). For the large lakes around the Late-Glacial ice sheets, this transition has great glacio-climatic significance (Teller, 1987; Barber *et al.*, 1999; Licciardi *et al.*, 1999; Clark *et al.*, 2001; Mangerud *et al.*, 2001a, 2001b; Clarke *et al.*, 2004; Mangerud *et al.*, 2004). They were so vast that they were able to moderate the

mass balance of the ice sheet, due to local cooling in the summer, which delayed recession (Krinner *et al.*, 2004) (1.3). This sequence, from the establishment of the lake to active glacier calving, has been examined at a smaller scale for glaciers in the central Southern Alps of New Zealand (Kirkbride, 1993). He proposes a three-phase response model of valley glaciers to negative mass balance, based on empirical observations of seven New Zealand glaciers. The model describes how a vertical cliff is obtained by the removal of ice irregularities, due to the development of thermokarst lakes relating to the variations in supraglacial debris. This follows an initial phase of melting and slow downwasting. The time taken to complete the transitions into the third phase of rapid calving varied from 10-25 years. The transition from melting to calving has also been described at Hooker and Tasman glaciers, New Zealand (Hochstein *et al.*, 1998; Kirkbride & Warren, 1999), as well as at Ameghino, Nef and San Quintin glaciers, amongst others, in Patagonia (Warren, 1994; Harrison *et al.*, 2001; Winchester *et al.*, 2001). Decreasing ice thickness and downmelting of the terminus section, under a debris cover, are delayed responses to a long-term mass imbalance. At Hooker Glacier, it was thought that downwasting took place within the aquifer near the margins, inducing the propagation of new fissures through buoyancy, which melted rapidly to form large, coalescing melt channels (Hochstein *et al.*, 1998), although this seems unlikely given that regular calving constitutes the majority of ice loss (Warren & Kirkbride, 1998). In other climatic settings, where significant debris cover is absent, retreat following the onset of calving is rapid, and thought to relate to a threshold in water depth, whereby calving takes over from melting as the dominant mass loss mechanism e.g. Glaciar Ameghino and Glaciar Upsala, Patagonia (Warren, 1994; Warren *et al.*, 1995b).

Proglacial lakes may also develop by the collapse of ice under a supraglacial debris mantle (Benn *et al.*, 2000; Hands, 2004). At Tasman Glacier, where the debris cover is ~ 2 m thick, circular ice-contact lakes grow around the site of englacial conduit collapse, later coalescing (Kirkbride, 1993). Similar processes occur on other large glaciers on the eastern side of the Southern Alps (Purdie & Fitzharris, 1999) and the Nepal Himalaya (Yamada, 1998; Benn *et al.*, 2000; Reynolds, 2000; Richardson & Reynolds, 2000; Wiseman, 2004; Hands, 2004). A different basin expansion mechanism has been described for the ice-floored Tsho Rolpa lake, Nepal Himalaya (Chikita *et al.*, 1998, 2000a). Bottom subsidence from ice melt below the lake occurs in conjunction with retreat of the terminus cliffs by heat transfer from wind-driven currents, counter-currents, and sediment-laden underflows. However, retreat by calving is not observed, although with continued

expansion it seems inevitable in the long term. Any large lake, long-lived enough to initiate calving, is significant for glacier dynamics. Although processes in the immediate ice-proximal area are of greatest importance, the overall size of the lake is also significant through its influence on water temperature and the thermal regime of the lake (Warren, 1994).

2.2.3 Physical limnology

To understand how heat may be transferred to the ice face, it is useful to appreciate the factors affecting the thermal structure of ice-contact lakes. Primary amongst these are water density and stratification, which may depend on temperature-related or sediment-induced density contrasts, and are described below.

2.2.3.i Density

Water density variations govern chemical and physical behaviour in glacier-fed lakes. Changes in density, however small, can have a significant impact on the development of stratification, the movement of influent waters and the subsequent sedimentation patterns, all of which are important for affecting heat transfer to the ice face (Drewry, 1986). Water density is a non-linear function of temperature, with maximum density at 3.98°C (Figure 2.7, p.43). The most important source of density variations in inflow water originates from suspended sediment concentrations (Benn & Evans, 1998), which vary over shorter timescales and over a wider range than temperature. Although dissolved salts, gases and hydrostatic pressure may affect density, they have only a negligible effect in ice-contact lakes.

2.2.3.ii Stratification

Radiation entering the water surface is modified by surface cooling and turbulent mixing by wind. This transfers heat and momentum downwards, dividing the water into upper and lower regions (Hutchinson, 1975). The lower-density layer (epilimnion) typically overlies a cold, higher-density layer at the bottom (hypolimnion) and the two are separated by the metalimnion, a region of rapid temperature change (Figure 2.8, p.43). Density differences between the epilimnion and the hypolimnion increase with increased

surface warming, and decrease due to mixing by wind, which has implications for the seasonal patterns of lake stratification. At its simplest, surface water becomes dense enough to sink as it cools in the autumn, leading to a complete turnover of the water column. The nature of stratification varies between different climatic and environment settings. Lakes may be classified according to stratification trends (Hutchinson, 1975), as presented in Table 2.5.

Classification	Definition	Comments
Amictic	No turnover takes place	Have perennial ice cover, therefore wind-coupling cannot take place
Monomictic	Turnover once a year	Takes place in the summer, and occurs at high altitudes and latitudes. Usually proglacial and ice-contact.
Dimictic	Turnover twice and year	The most common, especially in temperate, distal, glacier-fed lakes. Spring and autumn turnover giving inverse stratification in winter and normal in summer
Polymictic	Turnover several times a year	Occurs because there is no stratification. In cold (< 4 °C) glacial lakes. Common in ice-contact lakes, especially near the margin (Churski, 1973). Warming, water influx and wind-coupling induce (semi-)continuous turnover at ~ 4 °C.

Table 2.5 *Ice-contact lake stratification classification (Hutchinson, 1975).*

Ice-contact lakes are typically polymictic, amictic or monomictic (Reid & Callender, 1965), with water temperatures up to ~ 7 °C (Warren, 1994), although ice-contact lakes in New Zealand and the European Alps are closer to 2 – 4 °C (Funk & Röthlisberger, 1989; Warren & Kirkbride, 1998; Roehl, 2003). Meltwater input close to 0 °C will modify the lake temperature (Warren, 1999), often inhibiting or disrupting the formation of thermal stratification (Warren *et al*, 1995a). Abundant icebergs may also prevent the development of stratification, delivering meltwater to all parts of the lake (Warren 1999; Warren *et al.*, 2001). Disruptions may grade distally into thermal stratification if the water body is large enough (Benn & Evans, 1998). Warmer temperatures are often seen in large lakes, mainly due to the diminished relative impact of meltwater inputs and iceberg melt compared to other smaller lakes nearby, and because the water body is a larger heat reservoir. There may also be a climatic gradient e.g. where a lake extends away from the rain shadow of a

mountain range into a drier, warmer zone (Warren, 1994). Dimictic ice-contact lakes sometimes occur, although the stratification progressively decays during autumn as the thermocline becomes weaker, and may become isothermal during winter (Campbell, 1973). Monitoring of the Tasman Lake, New Zealand, over a whole year revealed a complex thermal regime with pronounced temporal rather than spatial variability, with both isothermal and weakly stratified conditions documented (Roehl, 2003). Many studies of calving dynamics pay little attention to water temperature, making few measurements, which may be misleading when determining the subaqueous melt rate and its role for the overall calving rate (Hochstein *et al.*, 1995; Warren & Kirkbride, 1998; Roehl, 2003).

Lakes may be sediment-stratified rather than thermally-stratified (Gustavson, 1975; Roehl, 2003) if the control exerted by sediments entering the lake overrides the effect of temperature. This can often happen at ice-contact lakes, where glacial meltwater is often sediment-rich e.g. Tsho Rolpa Lake (Chikita *et al*, 2000b). Although chemically-precipitated sediments (e.g. authigenic carbonates and sodic minerals) may control stratification, their minimal presence negates their importance in the ice-contact setting and, in general, thermal and sediment stratification dominate glacier-fed systems. Similarly, glacier-fed lakes are usually ecologically inhospitable and oligotrophic (due to the low levels of irradiance restricting photosynthesis as ice cover exists for a substantial part of the year (Drewry, 1986)), and have little significance for stratification patterns. Although it is difficult to make generalisations about ice-contact lakes, especially given the paucity of studies, most ice-contact lakes appear to be polymictic and sediment stratified (Ashley, 1995).

2.2.3.iii Suspended sediment

In addition to its influence on limnological stratification, sediment may alter the water depth at the calving margin by the deposition of a sediment shoal (Alley, 1991), whose evolution and advance/retreat processes are outlined in section 2.1.1.i. Meltwater inflows of cold water and sediment enter the water column at a variety of water depths, taking up a level of neutral buoyancy in the water column, which is important for understanding their control on the thermal structure of the lake. The vector of the inflow is dictated by the relative densities of lake and meltwater, as well as the nature of existing lake

stratification, and can directly influence melt rates by providing turbulent flow past the ice face (2.3.5.i) (Weeks & Campbell, 1973).

Sediment stratification exhibits a gradual increase of suspended sediment concentration with depth (Gustavson, 1975). It is thought that the density gradient relates to the upward diffusion of sediment from underflows, and the downward settling of sediment from interflows (Benn & Evans, 1998), which is continuously replaced by new inflow, giving a more gradual density profile than that of temperature (Ashley, 1995). Sediment stratification may permit the establishment of a very stable stratification (Sakai *et al.*, 2001), and Chikita *et al.* (2000b) conclude that the sediment stratification at Tsho Rolpa Lake explains why, despite a clear thermocline, the pycnocline (a zone of rapid change in water density with depth) is weak. The mixing of meltwater inflow with the ambient water body is key to considering how heat may be transferred to the ice face.

2.2.4 Mixing and Heat Transfer

Heat transfer within ice-contact lakes is important for determining rates of waterline and subaqueous melting. The question is whether the thermal potential of warm water far from the ice face can be realised through advection of warm waters to the calving front by, for example, convection, turbulent mixing and/or wind. Meltwater and sediment enter the water column at a variety of water depths. Mixing of inflow water with the lake water depends on the inflow characteristics. Density differences between mixing water masses give rise to turbidity exchange and entrainment. Turbulent eddies arise if the velocity shear is greater than the stability due to density stratification (Drewry, 1986). Inflow maintains its integrity as a discrete density current when the ratio of these variables (i.e. the Richardson number) is high (Horne & Goldman, 1994) and homogenisation may occur between the inflow and lake water if there is no stratification.

Meltwater discharge forms several types of inflow, illustrated in Figure 2.9. In the marine environment, meltwater often forms a buoyant overflow plume (Figure 2.9a and b) (Matthews & Quinlan, 1975; Walters *et al.*, 1988; Motyka *et al.*, 2003a), because meltwater at 0 °C is 200 times more buoyant in saltwater than in freshwater.

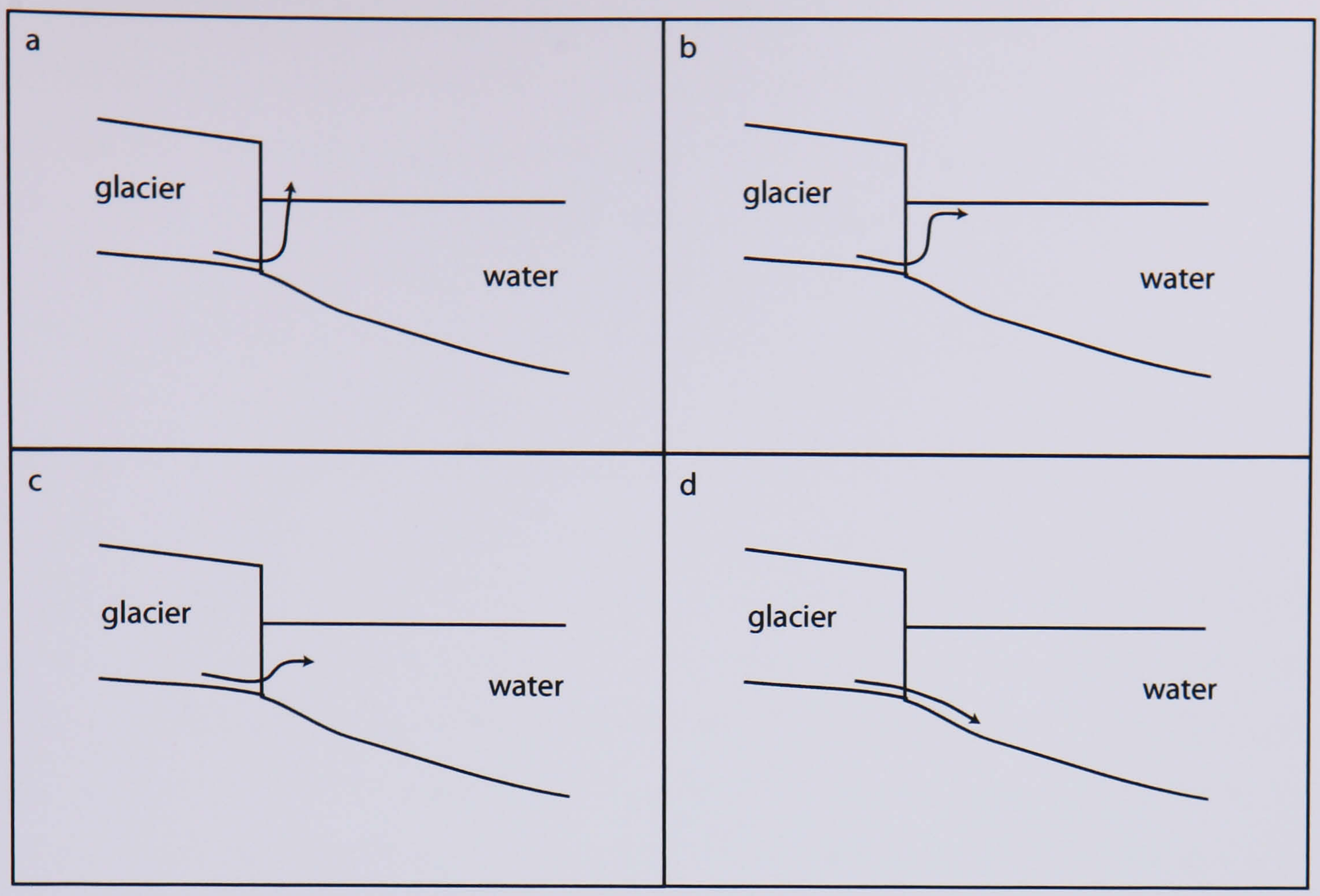

Figure 2.9 The trajectories taken by glacial meltwater entering proglacial water bodies. (a) Buoyant meltwater rises rapidly to the surface, causing superelevation, or boiling, seen in some marine environments (Syvitski, 1989). (b) The common trajectory for buoyant meltwater, forming an overflow plume. (c) Finding a neutral buoyancy in the mid-level of the water column, interflows often occur in stratified lakes. (d) Where levels of sediment in the meltwater are high, the high density dictates the formation of an underflow.

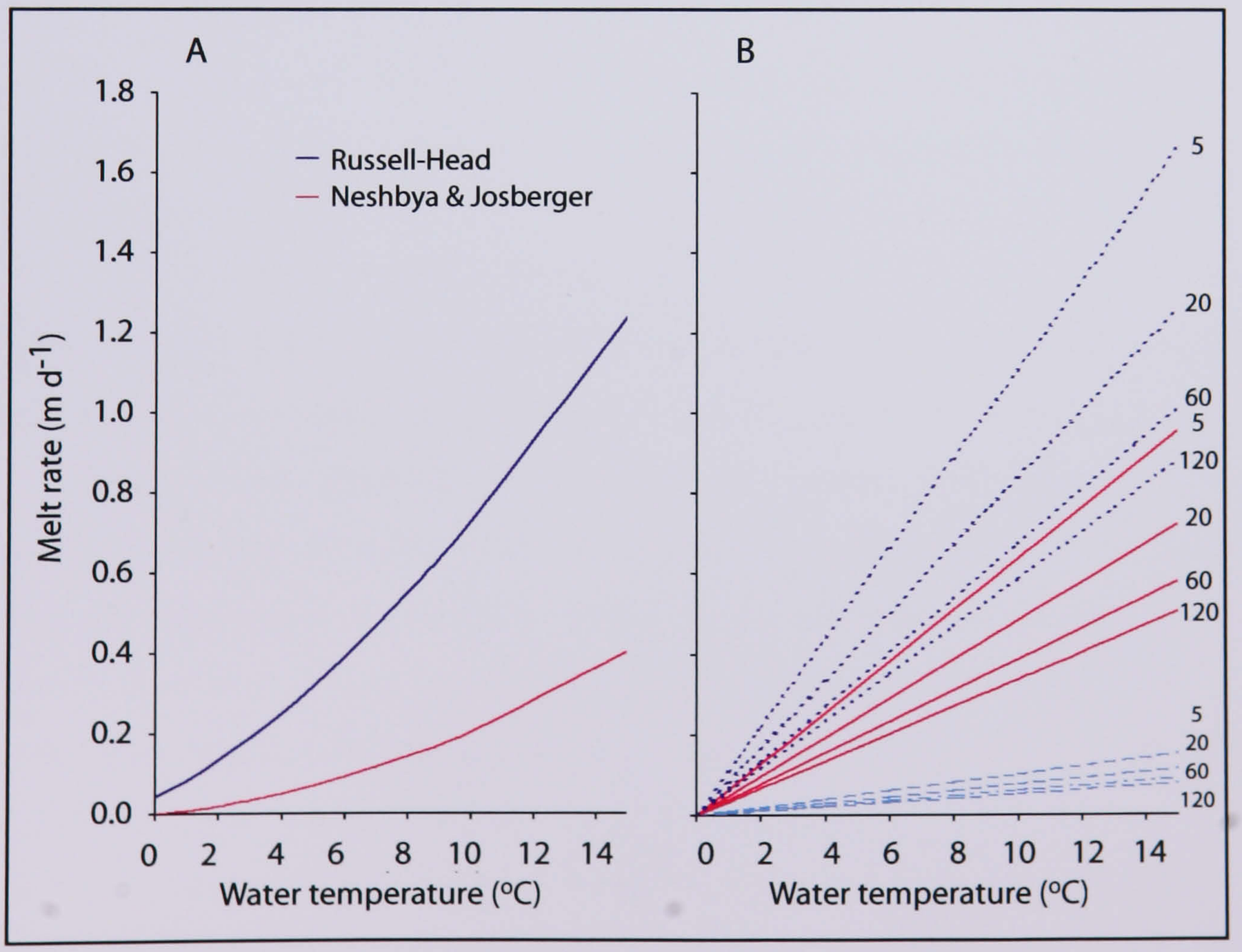

Figure 2.10 Melt curves from iceberg equations of (A) Russell-Head (1980) and Neshyba & Josberger (1979), and (B) Weeks & Campbell (1973). Melt curves with current velocity values of 0.0 (turquoise), 0.1 (pink) and 0.2 (blue) m s^{-1} are plotted with length terms 5, 20, 60 and 120 m, as shown.

However, under certain conditions of high seawater temperature (~ 17 °C), the meltwater sinks because the cooling effect exceeds the freshening effect on the density (Gade, 1979). These overflows cannot carry a large amount of suspended sediment (Benn & Evans, 1998) and there is restricted lateral spreading. If the density difference between the meltwater and the epilimnion is small, then turbulent exchange may occur. (Drewry, 1986). Overflows may also occur in ice-contact lakes, typically between spring and autumn, when suspended sediment discharge is low and non-glacial catchment input is warmer, although it is not the most abundant inflow in glacial lakes (Smith, 1978). Overflows are susceptible to wind stress, so sometimes cannot be differentiated from shallow interflows (Benn & Evans, 1998). Interflows are common in lakes where there is thermal stratification (Figure 2.9c). Underflows are the most common when there are high levels of suspended sediment, especially in the summer months (Figure 2.9d). They behave as turbidity currents, which in lacustrine environments are usually low in density compared to those in a marine setting (Drewry, 1986).

Whilst the greater density contrast of meltwater into saline water inhibits mixing, it results in more powerful, ice-proximal convective cells than may be seen in freshwater, a contrast which is probably part of the explanation for faster calving rates in tidewater (Funk and Röthlisberger, 1989), both due to rapid current velocities past the subaqueous face (Weeks & Campbell, 1973), and as a means to advect distal water to the ice face (Hanson & Hooke, 2000). Melting in freshwater and tidewater settings is described further in section 2.3.

In ice-contact lakes, where convective cells are weaker, and the absence of tides removes this means of heat transfer, waves may be more significant in advecting heat to the ice face. Katabatic winds usually operate in glacial settings, and may encourage water circulation by setting up epilimnial currents (Ashley, 1995) and providing advective diffusion of heat (Chikita & Yamada, 1998). Katabatic winds can also produce seiches (oscillatory waves) by inducing tilting of the lake surface and thermocline due to barometric pressure differences, piling up water downwind (Drewry, 1986). Oscillation occurs about a nodal point when the water tilts back, as the wind abates. The Coriolis effect additionally induces deflection (to the left in the Southern Hemisphere) (Ashley & Smith, 2000). Calving icebergs also generate oscillatory deep-water waves before they come to rest, with wave-lengths of the same order as iceberg diameter (Syvitski, 1989). However, wave action is negligible when large amounts of icebergs, typically brash bergs

(< 2 m) are present in the ice-proximal area, as waves are quickly attenuated (Warren *et al*, 1995a; Warren, 1999; Warren *et al.*, 2001). In addition to its role in advecting heat to the ice face, wave action may cause the development of a waterline notch on the ice face (Martin *et al.*, 1978; El-Tahan *et al.*, 1987; Roehl, submitted), and is discussed further in section 2.3.4.

Although katabatics usually predominate, there are occasions when the wind may blow up the lake towards the ice terminus (Chikita *et al.*, 1998; Haresign & Warren, in press). At Tsho Rolpa Cho, wind-driven waves transport the absorbed radiative heat to the ice cliff because of the long fetch (3km) of the valley wind, resulting in subaqueous melting under water temperatures of > 5 °C (Chikita & Yamada, 1998). Counter-currents in the pycnocline may compensate for the wind-driven currents in the upper layer, and induce the lifting of the lower cold water, establishing a vertical circulation system, accompanied by diurnal oscillations in the thermocline.

2.2.5 Summary

The physical limnology of ice-contact lakes is not well understood, and its influence on calving dynamics has largely been ignored until recently. In particular, the evolution of ice-contact lakes is important for altering glacier mass balance, and seasonal heat storage in the lake along with its thermal regime influences the melting potential at the waterline and subaqueous portion of the ice face. Ice-contact lakes show high spatio-temporal variability in the nature of the stratification that develops, which may depend predominantly on temperature and/or sediment content. Heat transfer may occur by density-driven convection due to meltwater inflow and its interaction with the thermal structure of the water column, along with wind-driven and iceberg-generated waves. Knowledge of ice-contact lake behaviour is fundamental for examining the role of melting on calving dynamics. Consideration of ice melting follows, in section 2.3.

2.3 SUBAQUEOUS MELTING AT CALVING GLACIERS

2.3.1 Introduction

At all calving glaciers, the position of the terminus is controlled by a range of interacting factors, primarily the ice flux to the terminus, the topographic geometry of the lake or fjord, calving rates, sedimentation rates, and melting of the subaerial and subaqueous portions of the terminal ice cliff, as reviewed in section 2.1. Melting has usually been included implicitly in calculated calving rates, because melt rates have been considered to represent an insignificant contribution to mass loss at the terminus compared with mechanical losses by calving (Powell 1991; Dowdeswell and Murray 1990). This conclusion was the result of studies at fast-flowing tidewater glaciers, such as those in Alaska, where ice loss due to melting constitutes only a small fraction of the total ice flux through the terminus into water of typically < 2°C (Syvitski, 1989; Smith & Ashley, 1996; Vieli, 2002). However, the validity of this generalisation is undermined by evidence which suggests that melting is an important process, both at tidewater termini (Walters *et al.*, 1988; Warren *et al.*, 1995b; Warren & Kirkbride, 1997; Vieli *et al.*, 2002) and at lake-calving glaciers (Funk & Röthlisberger, 1989; Warren & Kirkbride 2003; Roehl, submitted). The significance of melting lies not only in its direct contribution to mass losses at calving termini (Motyka *et al.*, 2003a), but also in its role as a trigger for mechanical calving through the creation of thermo-erosional notches at the waterline which undercut the ice cliff and cause ice slabs to break off (Kirkbride & Warren, 1997; Purdie & Fitzharris, 1999). Until recently, it was thought that calving driven by waterline melting was restricted to lake-calving settings, but melt-induced calving also predominates at the tidewater Hansbreen, Svalbard, where seasonal patterns of melting and calving are closely related (Vieli *et al.*, 2002).

Due to the difficulties and dangers of obtaining direct measurements at calving fronts, the interplay between the processes of melting and calving, their relative contributions to overall mass loss, and their seasonal variability remain poorly known. Moreover, there is still no satisfactory melt rate equation that can be reliably applied to temperate calving glaciers. Melt rates of glacier ice in water have been studied in a variety of non-calving settings and a number of temperature-dependent melt relations have been developed from field, experimental and analytical studies. Most of the studies relate to iceberg deterioration, often motivated by an applied interest in their use as a freshwater source

(Weeks & Campbell, 1973) and the hazard that they pose to polar shipping (International Glaciological Society, 1980; Prinsenberg *et al.*, 1991; Smith, 1993; Bigg *et al.*, 1998). The need to calculate sedimentation rates at calving termini has also focused attention on iceberg melt rates (Syvitski, 1989; Dowdeswell & Murray, 1990; Hunter *et al.*, 1996a, 1996b; Ashley & Smith, 2000). The key factors controlling melt rates are temperature, salinity, wave action and current speed, and are described below, followed by a discussion of the application of such melt relations to calving ice cliffs.

2.3.2 Water temperature

Laboratory studies provide a useful environment in which to examine the melting of ice blocks (Martin & Kauffman 1977; Josberger, 1978; Martin *et al.*, 1978; Russell-Head, 1980). As well as overcoming the practical challenges of approaching icebergs prone to overturning, or glacier termini prone to calving, it provides a setting in which the relationship of individual factors with melting can be examined e.g. varying salinity and temperature of the water without the added complexity of incorporating water flow or meteorological components (Eijpen *et al.*, 2003). Power relationships between water temperature and melting in saline waters are thought to be more accurate than a linear relationship (Morgan & Budd, 1978; Budd *et al.*, 1980) and have been developed from such studies by Russell-Head (1980), who proposed equation 2.8:

$$u_m = 0.018(T + 1.8)^{1.5} \qquad (\text{m d}^{-1}) \qquad \text{(Eq. 2.8)}$$

where u_m is the melt rate and T the water temperature. Here, basal and side melt rates were thought to be of a similar value, at around 1.8 m d^{-1} in water of 20 °C, the warm temperatures they anticipated for iceberg harvesting sites. In another experiment by Neshyba & Josberger (1980), the relationship with water temperature applies to simple buoyant convection caused by melting at a vertical ice face in stationary saline water, where

$$u_m = 2.78T + 0.47T^2 \qquad (\text{m a}^{-1}) \qquad \text{(Eq. 2.9)}$$

Experiments have frequently used temperature ranges that exclude the low temperatures typical of ice-proximal environments because they have focused on icebergs in the open ocean, and those intended for freshwater harvesting elsewhere. At a range of water temperatures, the melt rates from equations 2.8 and 2.9 are plotted on Figure 2.10a (p.52). At water temperatures of 2 °C, typical of ice-contact lakes (2.2.3.ii), melt rates from

equation 2.8 are 15 % of those given by equation 2.9, illustrating the huge discrepancy of melt rates with the equation used, emphasizing the lack of understanding of subaqueous melting, and the care that must be taken when inferring melting at calving termini.

2.3.3 Salinity

Salinity has two key implications for melting of ice in water. Firstly, it lowers the freezing point of water, such that the melting potential of a subaqueous ice face in marine water is higher than it would be in freshwater at any given water temperature. Secondly, saline water is denser than freshwater and, thus, incoming glacial meltwater exhibits greater buoyancy in saline water than in a lacustrine setting. Studies of iceberg deterioration in the ocean have focused on the complex circulation resulting from the mixing of the freshwater from the melted ice with the saline water body (Matthews & Quinlan, 1975; Bendall & Gebhart, 1976; Martin & Kauffman, 1978; Gade, 1979; Greisman, 1979; Huppert & Josberger, 1980; Huppert & Turner, 1980; Wilson & Sarma, 1980; Josberger & Martin, 1981; Josberger, 1980, 1983; Sammakia & Gebhart, 1983), and are reviewed by Gade (1993). Of particular interest are the complex turbulent and laminar (Martin & Kauffman, 1978), and double-diffusive (Huppert & Turner, 1980) convections at the boundary layer. However, the laboratory simulations by Eijpen *et al.* (2003) are the only example which measures melt rates in both low-temperature seawater and freshwater, where melting into freshwater will have different characteristics, as salinity is not a factor. Temperature-driven contrasts in varying salinities give rise to the concentration of melting at particular locations along the ice face, as illustrated in Figure 2.11. Free convection produces maximum melt rates of 0.65-0.8 m d^{-1} occurring in water temperatures of 4-6 °C. Melt rates in freshwater were not significantly lower than melt rates in saline water, with rates of 0.6 m d^{-1} below the waterline in temperatures of 8 °C. That melt rates are not considerably slower for freshwater is significant for freshwater calving glaciers. It implies that melting may contribute a large portion of the calving rate for glaciers other than the slow-flowing New Zealand glaciers, which are thought to be driven entirely by waterline melting (Roehl, submitted) e.g. Glaciar Upsala (Skvarca *et al.*, 2003).

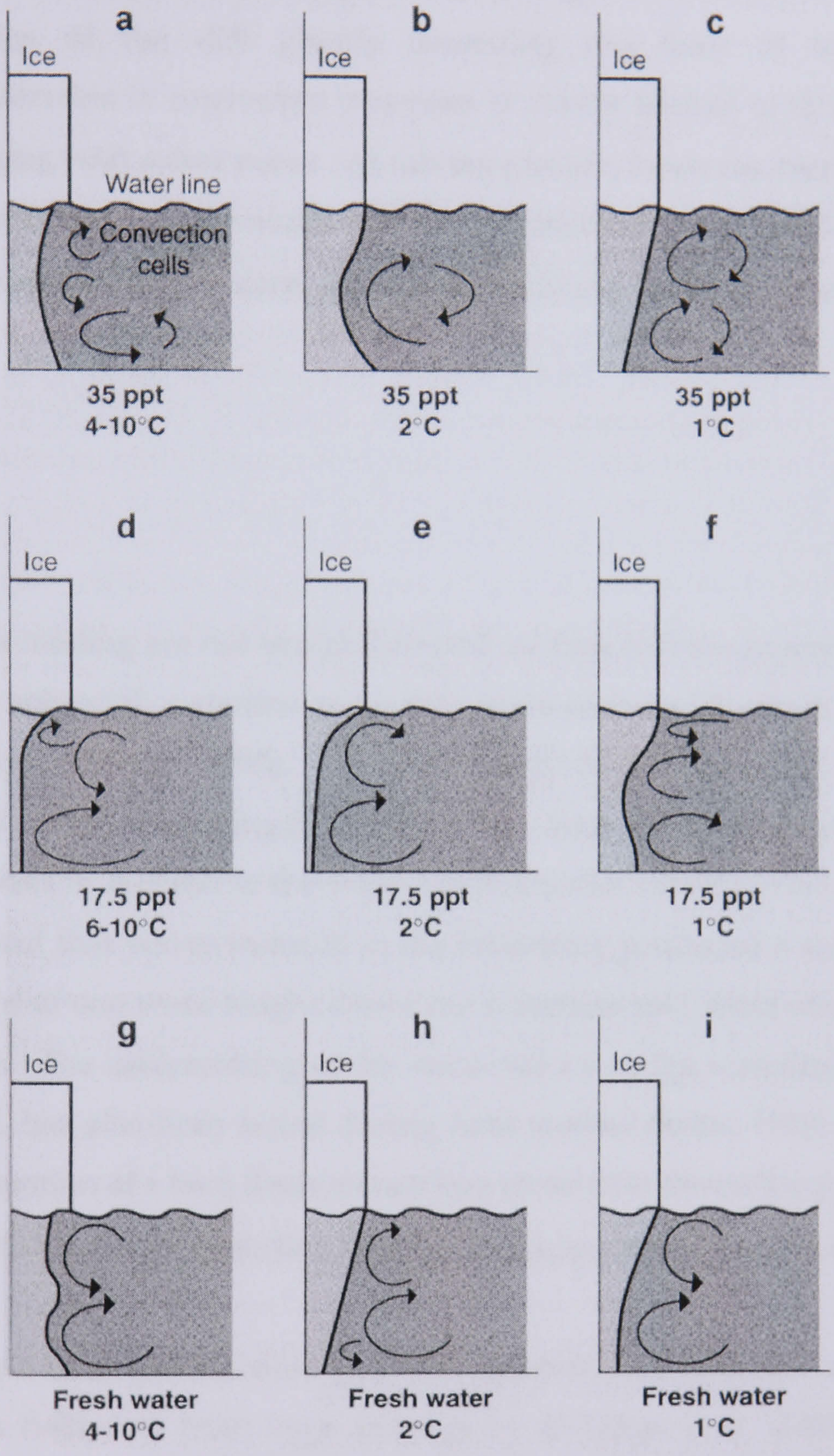

Figure 2.11 Schematic diagrams of circulation arising from the free convection induced by the meltwater produced from the ice face. It shows that for most temperatures and salinities, melting is at a maximum just below the waterline.
Source: Eijpen *et al.* (2003).

Whilst laboratory studies provide a basis for investigating ice melting, their direct applicability to grounded glacier termini is limited. This is because there are uncertainties associated with scaling small blocks of less than 1 m in the laboratory to ice fronts with widths of the order of kilometre (Russell-Head, 1980; Eijpen *et al.*, 2003), and heights of subaqueous portions of the cliff greatly exceeding the draft of most icebergs. Furthermore, consideration of convection processes is mostly limited to that arising from fresh meltwater mixing with saline water. At calving glaciers, however, forced convection from buoyant meltwater may drive much of the turbulence along the ice front, especially during the melt season and particularly at tidewater calving fronts, discussed in section 2.3.5.i.

2.3.4 Wave action

Relationships for ice melting are not straightforward, as they involve processes operating at different rates on subaerial, waterline and subaqueous surfaces (Huppert, 1980; Keys & Williams, 1984; Ventakesh *et al.*, 1985). Laboratory experiments have also been used to monitor the effect of waves on melting (Huppert, 1980). Tank experiments produced melt notches of similar sizes in relation to the wave characteristics (Martin *et al.*, 1978), whilst Josberger (1977) found that waves induced in the laboratory produced a waterline notch with a vertical extent of one wave height above the waterline and about one sixth of that below the waterline. The undercutting of the subaerial ice at the waterline, causing ice chunks to break off, has also been noted during field studies (Robe, 1978; Savage *et al.*, 2000). Such fragmentation of a berg decreases its size more than the melting which causes it, and is indicative of the role of waterline melting for triggering subaerial calving.

A model of melting due to wave action, given in equation 2.10 (White *et al.*, 1980), has been validated with field data from large icebergs by El-Tahan *et al.* (1987). Here, the waterline melt rate per °C of water temperature, is given in terms of a dimensionless relationship for a rough wall:

$$u_m = 0.000146\left(\frac{R}{H}\right)^{0.2}\left(\frac{H}{P}\right) \qquad (\mathrm{m\ s^{-1}\ K^{-1}}) \qquad \text{(Eq. 2.10)}$$

where P and H are the mean period and height of the waves, respectively, and R is the roughness height of the ice surface, taken here as 1 cm (White *et al.*, 1980). Wave erosion

is thought to be the main deterioration mechanism, and waterline melting is one order of magnitude greater than that below the depth of oscillatory wave motion (El-Tahan *et al.*, 1987). However, the temperature-dependent relationships e.g. equations 2.8 and 2.9, which apply to large icebergs (up to several kilometres in length), do not consider wave-induced melting to be important.

Changes in water level at grounded calving faces can modify the effectiveness of wave action for waterline melting. In marine settings, tidal range has been observed to form notches of 0.5 – 2.5 m, and enhance notch height such that it extends 1.5 times the tidal range (Syvitski, 1989). This creates the potential for higher notches than those seen on floating icebergs, which are determined by wave height alone. Although tidal influences are absent in most ice-contact lakes, frequent changes in lake stage can also reduce the rate of melt notch development, with fluctuations of over 0.15 m within 24 hours significantly reducing notch formation at Tasman Glacier (Roehl, submitted). The effectiveness of wave action at calving glaciers is therefore restricted by other water level changes which have no influence on floating ice, and other factors must be important at subaqueous ice faces in order that melting is still a maximum at the waterline. This emphasizes the limited applicability of transferring melt relationships developed for icebergs to grounded calving glaciers.

At some glaciers, brash ice is the main form of iceberg produced (Crocker, 1993; Ashley *et al.*, 1995; Ashley & Smith, 2000). Continued melting of these bergs will cool the surface water in the ice-proximal zone, reducing the temperature of water transferred to the ice face (2.2.4). They also protect the calving front from wind-driven wave activity (Smith & Ashley, 1996). The influence of the calved bergs on the ice cliff in these ways is important for considering whether calving due to thermo-erosional waterline melt notch development or subaqueous melting losses contribute more significantly to overall ice loss at the glacier terminus.

2.3.5 Current speed

The role of upwelling, resulting from glacier discharge and meltwater produced from melting of the ice face, has already been introduced as being a major control on advecting heat and water to the ice face (2.2.4) (Weeks & Campbell, 1973; Keys & Williams, 1994;

Motyka *et al.*, 2003a). Water may upwell along the ice cliff from subglacial or englacial meltwater conduits, direct release at the ice cliff, and wind-induced upwelling as katabatic winds drain cold air (Greisman, 1979). The sources of turbulent flow, and their implications for rates of melting, are outlined below.

2.3.5.i Upwelling from meltwater originating from glacier discharge

Glacier discharge may occur from supraglacial, englacial and subglacial sources. The location of a major discharge outlet may be associated with the position of a calving bay. The number of caves along the waterline of the calving front is a good indicator of the number of outlets that have been functional in the recent past (Theakstone & Knudsen, 1986; Syvitski, 1989). Substantial inputs of conduit meltwater can also sometimes be seen to bubble up to the water surface (Motyka *et al.*, 2003a). In many cases, increased concentrations of suspended sediment indicate the location of a meltwater plume (O'Neel *et al.*, 2001). The exact source of meltwater input to the water body and its subsequent flow path may be difficult to locate. Supraglacial input is unlikely to be significant at typically highly crevassed calving margins.

The trajectory of incoming meltwater, once it exits the glacier, depends on its density and the density of the surrounding water body, as described in section 2.2.4. Underflows and interflows are not as important for melting as overflows. This is because they do not flow against the ice face, and their influence on the forced convection that affects subaqueous melt rates is restricted. The influence of overflows on ice wall melting depends on the Froude number (whether the jet curves upwards or downwards), the diameter of the ice tunnel, the initial jet velocity and the tilt of the ice wall (Syvitski, 1989).

2.3.5.ii Upwelling from meltwater released from the ice face

The flow of melt water produced from the ice face has motivated research into the biological implications for upwelling in the past (Neshyba, 1977). It is important for subaqueous mass loss at calving glaciers as it contributes to the current velocity of the glacier discharge. Free convection resulting from ice melt is either laminar or turbulent, and depends on the temperature, salinity and density structure of the ambient water (Josberger, 1977; Sammakia & Gebhart, 1983). Boundary layer behaviour and the patterns of convection are different for stratified and unstratified water columns. Huppert and

Josberger (1980) showed the influence of a stratified ocean on convection. A thin boundary layer flow exists at the ice face with a thicker, down-flowing layer beyond it, which reaches a level of neutral buoyancy, and then flows out to form a horizontal layer (Huppert, 1980). Significant upwelling is believed to occur near large vertical walls when pre-existing stratification is weak (Josberger & Neshyba, 1980).

Observations of the subaqueous ice face, using a remotely-operated submersible vehicle on the Antarctic Peninsula, revealed a highly fractured ice front with vertical cracks and scalloped features (Ashley & Smith, 2000). Also termed rills (Powell & Molnia, 1989), these scalloped features must reflect local-scale melting of the ice face itself, as no evidence of meltwater inflow was seen, except on two occasions when a surface plume was observed, and have been observed elsewhere e.g. Alaska, Norway (Theakstone, 1989; Hunter & Powell, 1998). This confirms that meltwater produced from the ice face itself may result in subsequent further melting. Currents relating to upwelling from ice cliff melt imply a positive feedback mechanism for melting. Direct melting of the ice face may inhibit melting by cooling of the boundary layer, or promote melting through its contribution to upwelling current velocity. It is uncertain which of these has the greater effect.

2.3.5.iii Upwelling from wind-induced heat advection

Heat advection by wind action was described in section 2.2.4, and affects both wave activity (2.3.4), and heat advection over longer distances. Winds blowing towards the glacier may generate downwelling near the ice margin, and this can either retard the upward-rising melt, thus decreasing the rate of ice melt, or increase the melt rate by bringing warmer surface water to depth (Syvitski, 1989). The temperature difference between the far-field and the meltwater produced from the ice face determines the degree of mixing that occurs (Gade, 1979). However, when there is ice cover, such heat advection is reduced, and waterline melting is inhibited.

2.3.5.iv Incorporating upwelling into melting relationships

The significance of upwelling speed is demonstrated in the melt rate derived by Weeks and Campbell (1973) for icebergs in saline water, based on theoretical considerations. It is of particular interest because of its application in subsequent studies at calving termini

(Powell, 1983; Powell & Molnia 1989; Syvitski, 1989; Dowdeswell & Murray, 1990; Hunter *et al.*, 1996a, 1996b). Their proposed relation is:

$$u_m = 6.74 \times 10^{-6} v^{0.8} \frac{T}{l^{0.2}} \qquad (\mathrm{m\ s^{-1}}) \qquad \text{(eq. 2.11)}$$

where T is temperature (°C), l is ice length and v is water current velocity. The formula is derived in terms of the thermal conductivity relating to flow past the ice face (Reynolds and Prandlt numbers) to find the heat flow, which is rewritten in terms of velocity, temperature and the length of the iceberg side. The specific heat capacity and thermal conductivity vary between saline and fresh water, so this equation is inapplicable to freshwater settings or where the water is not wholly saline e.g. where large volumes of meltwater from the glacier act to freshen the immediate ice-proximal area (Warren *et al.*, 1995b; Eijpen *et al.*, 2003). Typical values ranging from 0.001 to 0.3 m s^{-1} are applied for the flow velocity and are discussed in the next section. In equation 2.11, u_m is sensitive to changes in temperature and current speed (Figure 2.10b, p. 52), and relatively insensitive to length changes, although rates are enhanced for relatively small bergs (Smith & Ashley, 1996). Keys & Williams (1984) also demonstrated the significance of relative (or current) velocity in their detailed field study of seven icebergs in the Southern Ocean. In the lee of the flow, submarine melt rates were estimated to be 0.04 m d^{-1}, compared to double that at the upstream end, in water temperatures of -1 °C. As the berg becomes smaller, waterline melting and calving become relatively more important (Crocker, 1993; Savage *et al.*, 2000). Similar observations were made by Smith & Ashley (1996), comparing 'real' brash icebergs in the lab and the field, whose melt rates were found by repeatedly weighing icebergs. Those in open water conditions melted 12-26 times more rapidly than those protected from currents in densely-packed ice jams.

All these melt equations given here are based on pure ice, and it should be noted that debris content will reduce the rate of melting due to the lower thermal conductivity (Drewry, 1986), although the ice-water interface may be rougher, which would increase melting (Dowdeswell & Murray, 1990). The precise effect of varying percentage debris concentration is unknown.

2.3.6 Applying melt equations at calving termini

Despite the problems described above of applying relationships which have been developed in the laboratory or the open ocean to calving termini, in the absence of alternatives these equations for clean ice have been employed, (though not always accurately (Dowdeswell & Murray, 1990)), to calculate subaqueous melt rates at tidewater glaciers (Dowdeswell & Murray, 1990; Powell, 1983; Powell & Molnia 1989; Syvitski, 1989; Vieli *et al.*, 2001, 2002). At Hansbreen, Svalbard, undercutting at the waterline occurs when sea ice is absent (Vieli *et al.*, 2002), and appears to control the calving rate, causing ice to break off in thin lamellae. Using equation 2.10, a melt rate of 180 m a^{-1} was determined for Hansbreen, at a water temperature of 1 °C (Vieli *et al.*, 2001). However, it is not clear whether the lack of calving by this mechanism during winter is accounted for, as the value otherwise overpredicts annual melt losses. Calculating mass loss in this way is questionable because, even if waterline melting by wave action drives the majority of calving, it is unlikely that currents have no effect on this rate, and a meaningful melt equation must aspire to incorporate all the factors that contribute to melting.

Because of the difficulty in obtaining current data, workers using equation 2.11 have often estimated values for the boundary-layer water velocity. Others have obtained data using an electromagnetic flow probe, calibrated by integrating vessel drift using GPS (Motyka *et al.*, 2003a), or made estimates based on iceberg-drift velocity at the water surface (Hunter *et al.*, 1996a). At LeConte Glacier, Alaska, where meltwater plumes were visible from bubbling of the water surface, velocities ranged from 0.13 to 0.52 m s^{-1} (Motyka *et al.*, 2003a).

Hunter *et al.* (1996a) apply values of 0.03 m s^{-1} (Powell & Molnia, 1989) for buoyant upwelling at Muir and Grand Pacific glaciers, and 0.25 m s^{-1} for longitudinal currents at Margerie Glacier, to yield melt rates of 21-31 m a^{-1}, on the basis that these are the dominant directions of water flow at each location. This seems questionable, in that there are likely to be components of flow in both directions at all the glaciers. Whilst the subaqueous cliff height is used for the length term at Muir and Grand Pacific glaciers, glacier width is employed for Margerie Glacier, adding to the uncertainty in the direct comparability of the results (Hunter *et al.*, 1996b).

Horne (1985) reports the first boundary layer measurements from along the front of the glacier in South Cape Fjord, Ellesmere Island. An upwelling velocity of 0.0017 m s^{-1} was calculated for the boundary layer (3 cm out from the wall) from the buoyancy of the ice wall melt. This is significantly lower than the rates described above and was used to predict a melt rate here of 0.1 m a^{-1} (Syvitski, 1989). When compared to a melt rate of ~ 150 m a^{-1} at Muir Inlet (Powell, 1983) where, instead, horizontal velocity and glacier width were used, it is clear that clarification on the determination of each term is required. Moreover, small differences in upwelling rates greatly affect the calculated value of u_m (Dowdeswell and Murray 1990), yet upwelling rates in the boundary zone at calving fronts are poorly known and highly variable.

At tidewater glaciers, where the water temperature is low (< 2 °C), Dowdeswell & Murray (1990) concluded that ice cliff melt rates were an insignificant influence on calving, regardless of the melt equation applied. However, at higher water temperatures these relations indicate that values of u_m rise to around 40-60 m a^{-1}, and at slower-flowing, freshwater-calving glaciers this may account for the majority of the ice loss at the terminus (Warren & Kirkbride, 2003; Roehl, submitted). Melt rates in freshwater are even less well constrained, as there are very few studies that consider subaqueous melting in an ice-contact lake. Changes in lake volume were used to give a subaqueous melt rate of 25 ± 5 m a^{-1} at Hooker Glacier, New Zealand (Hochstein *et al.*, 1998). Hochstein *et al.* claim that melting is the dominant mode of lake expansion, but it seems unlikely that this can be greater than the observed calving losses triggered by waterline melt notching and those due to subaqueous calving, which is the origin of the majority of the icebergs floating in the lake. Roehl (2003) uses a flow value of 0.1 m s^{-1} to calculate values of melt at Tasman Glacier, New Zealand. Values are found using both equations 2.8 and 2.10, using estimated values of current velocity of 0.1 and 0.2 m s^{-1}. At temperatures of 1.5 °C, a melt rate of 40 m a^{-1} using equation 2.10 is compared to the Hochstein *et al.* (1998) figure, although erroneously confuses this study with one by Hochstein *et al.* (1995), at Tasman Glacier, rather than Hooker Glacier.

2.3.7 Alternative Approaches

Methods using balance equations have also been employed to find melt rates. One way of achieving this is to employ an ice flux balance, using the difference between ice flux into the terminus and iceberg discharge from the terminus, but the uncertainties of calculating the latter from field observations are very large (Warren *et al.* 1995b; Motyka *et al.* 2003a). In an enclosed lake setting, one way to consider energy transfer to the ice face is to define a heat budget for the lake, an approach used by Sakai *et al.* (2000a). The equation for heat storage of the lake, ΔS, is:

$$\Delta S = H_s - H_o + H_i - H_m \qquad \text{(Eq. 2.12)}$$

where

H_s = the net heat input at the water surface

H_i = the net heat input by water inflow

H_o = the heat released at the outlet

H_m = the latent heat available for ice melting

Field data are used to give H_m as the residual value. However, this method is hampered by the difficulty of accurately accounting for all the inputs and outputs. It is somewhat oversimplistic (Figure 2.12) and this small lake (< 2 km^2) expands primarily by melting of the sides and base, and is therefore not directly comparable to the setting of a grounded glacier terminus. At Unteraargletscher, Switzerland, radiation (Q_R), detectable heat (Q_H) and latent heat flux (Q_L) budgets were used to find the energy exchange at the lake surface, Q_T (Funk & Röthlisberger, 1989):

$$Q_T = Q_R + Q_H + Q_L \qquad \text{(Eq. 2.13)}$$

where

$$Q_R = G(1-\alpha) + A - E \qquad \text{(Eq. 2.14)}$$

$$Q_H = fc_p(T_a - T_s) \qquad \text{(Eq. 2.15)}$$

$$Q_L = f' L(e_a - e_s) \qquad \text{(Eq. 2.16)}$$

and

G = global short wave radiation influx

α = albedo

A = incoming long wave radiation

E = outgoing long wave radiation

f = heat transfer coefficient (a function of wind speed)

c_p = specific heat of dry air

T_a = air temperature

T_s = lake surface temperature

f' = heat transfer coefficient

L = latent heat of evaporation

e_a = water vapour pressure of the surrounding air

e_s = water vapour pressure of the air at the lake surface

However, it was assumed that weather conditions were uniform and that there were no surface heat losses. Neither does it incorporate any mode of heat advection within the lake, e.g. along a temperature gradient, or by currents.

Accounting for meteorological heat exchanges and turbulent heat exchanges from the lake surface downwards, Landl *et al.* (2003) described energy fluxes involved in melting floating ice in Jökulsárlón, southeast Iceland where the tidal river Jökulså provides an inflow of seawater at high tide. They consider the transport of thermal energy into the lake from the atmosphere and sea, including turbulent fluxes, using the following relationship:

$$M + \Delta G = R + H_s + H_l + H_p + H_i \qquad (\mathrm{W\ m^{-2}}) \qquad \text{(Eq. 2.17)}$$

where

M = Energy available for melting

ΔG = Rate of gain of heat of a vertical column of water from the surface to the depth at which vertical heat transfer is negligible

R = Net radiation

H_s = Vertical eddy flux of sensible heat

H_l = Vertical eddy flux of latent heat

H_p = Heat supplied by precipitation; at a melting surface the heat supplied by rain is generally negligible, but may be significant if the rain can freeze

H_i = Heat supplied by tidal water inflow from the sea, referred to the lake surface

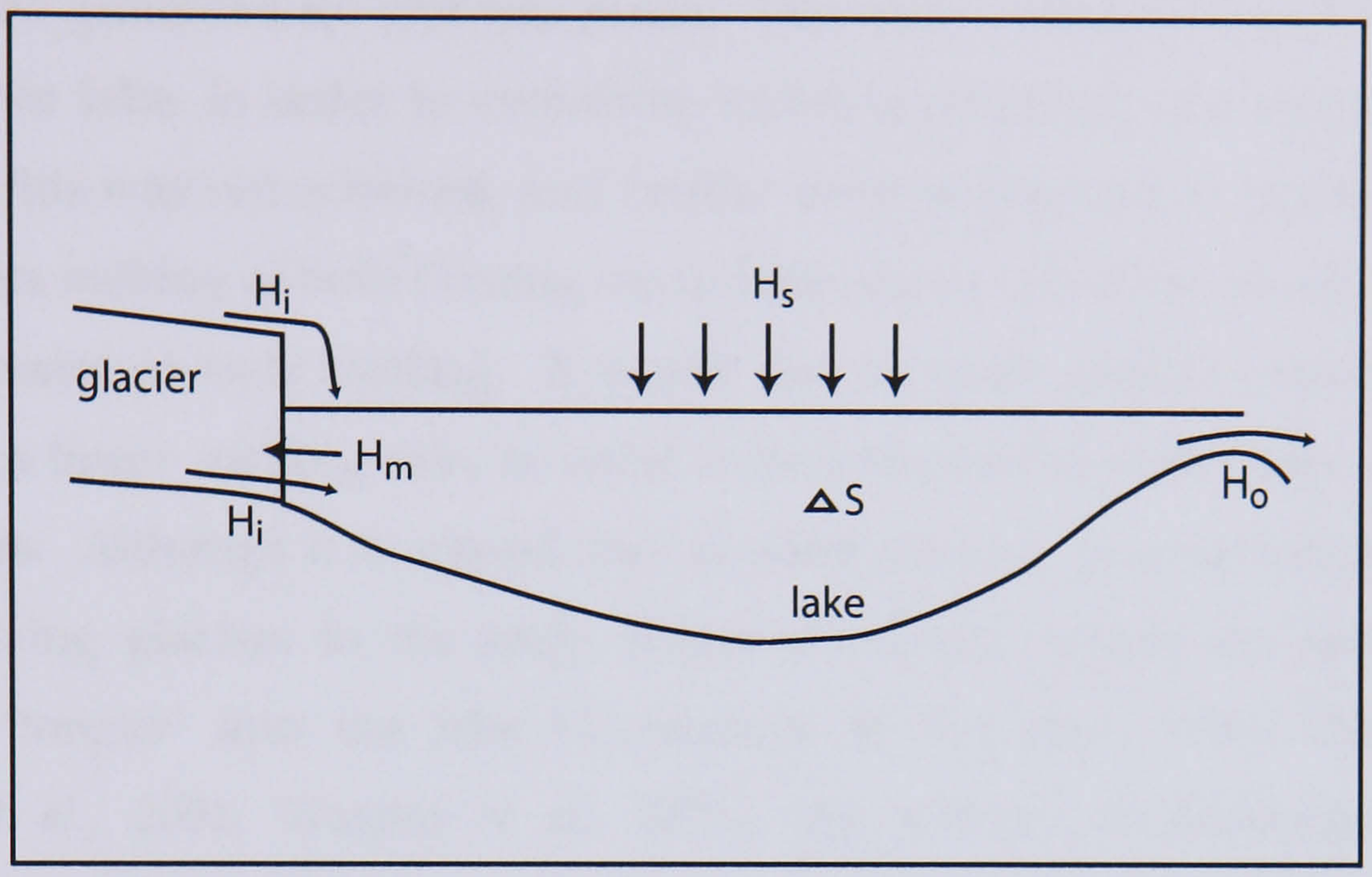

Figure 2.12 Schematic diagram of the heat budget calculated at Tsho Rolpa, an ice-contact lake in Nepal (Sakai *et al.*, 2000). For symbols, refer to Equation 2.12, p.62.

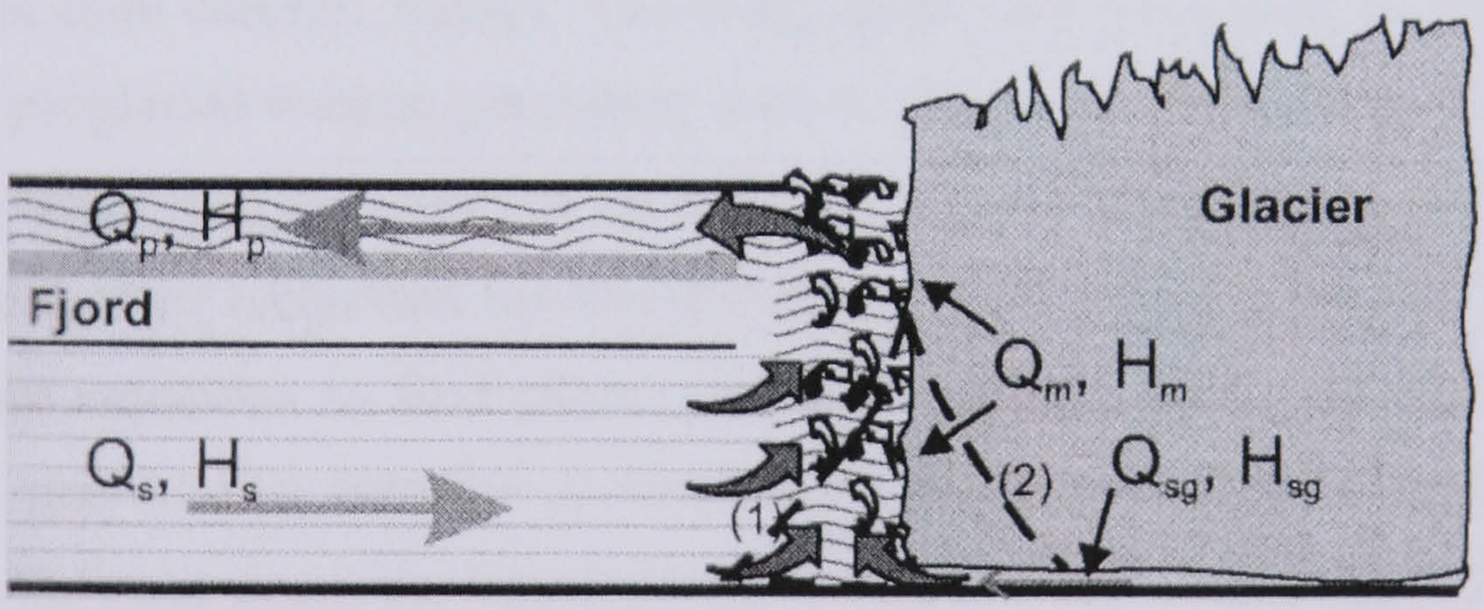

Figure 2.13 Model of forced convective flow in a proglacial fjord. Subglacial discharge, Q_{sg}, carrying heat, H_{sg}, drives convection, drawing deep saline water (Q_s, H_s) towards the terminus where the two components mix and turbulently rise along the ice face. The ascending waters melt ice along the ice face (Q_m, H_m) which adds to the convection. The turbulent plume reaches the water surface then flows away from the terminus in an overflow plume (Q_p, H_p). Dashed lines show possible seasonal geometries of (1) little or no subglacial discharge and melting, and (2) significant submarine melting. Source: Motyka *et al.* (2003a).

However, the values obtained for *M* for each of spring, summer, autumn and winter seasons were used to prescribe the energy, in units of W m^{-2}, required to melt all the ice in the lake. Despite detailed consideration of the calculation of each term, no account for ice melting at the grounded ice cliff was made. The study aimed to understand the energy balance of the lake, in order to contribute towards predicting the future retreat of the glacier, but this was not achieved, and further work is required to develop an approach that considers melting of both floating ice and the glacier terminus, in order to predict the calving response of such melting. It would also be more useful to convert the energy values into a linear melting rate, in order to be comparable with linear calving and ice velocity rates. Although it is argued that, at some glaciers, an areal rate is more suitable for lake-calving glaciers in the early stages of calving, where the terminus forms a prominent 'tongue' into the lake (Theakstone & Knudsen, 1986; Theakstone, 1989; Harrison *et al.*, 2001; Warren *et al.*, 2001), the termini of Breiðamerkurjökull and Fjallsjökull roughly form an approximately straight line, and a linear rate of melting might be more suitable.

Further doubt about the usefulness of the early melt relations is raised by the work of Motyka *et al.* (2003a), working at tidewater LeConte glacier, Alaska. In the most detailed field study to date, they use heat and water balances to study submarine melting at tidewater LeConte Glacier, Alaska. Oceanographic data were used to define convective flow in the proglacial waters, providing data to derive a relationship between the melt rate and the latent heat of fusion for ice and a calculated value for heat lost to melting ice. In their model, they accounted for forced convection by using measured values of near-surface water velocities to find plume discharge (Figure 2.13). From conservation of energy, the heat coming into the system *via* the warm seawater, H_s, and the subglacial water, H_{sg} (=0), must equal the heat leaving the system in the outflow, H_o, plus the latent heat lost to melting the ice, H_m. Therefore,

$$H_m = H_s - H_o \qquad \text{(Eq. 2.18)}$$

Because the ice-proximal water is essentially isothermal, this incoming heat can be determined from

$$H_s = \rho_s Q_s C_s T_s \qquad \text{(Eq. 2.19)}$$

where ρ_s is the density, C_s is the specific heat of seawater, T_s is the temperature of the deep lake water and where, from conservation of water in the fjord, the rate of seawater inflow near the terminus, Q_s, is assumed to be equal to the outflow, Q_o, calculated above. Heat carried away from the terminus by the meltwater is calculated by integrating the following relation for each zone of measured water currents.

$$H_o = W_i \int \rho_i u_i C_i T_o^i dz \qquad \text{(Eq. 2.20)}$$

using the measured values of water temperature within each zone, the velocity of the outflow, and where W_i is the width of the subaqueous ice front. The contributions from both zones were then added to obtain the total outgoing heat flow.

The rate of ice melt, Q_m, is then:

$$Q_m = H_m L^{-1} \qquad (\text{m}^3\ \text{d}^{-1}\ \text{w.e.}) \qquad \text{(Eq. 2.21)}$$

The derived melt rate of 12 m d^{-1} is equivalent to 57 % of the total mass loss at the terminus, and indicates that melting may also strongly undercut the subaerial cliff, triggering calving. This melt rate is greater by a factor of 175 than the rates calculated for comparable settings by Hunter *et al.* (1996a). Additionally, where Vieli *et al.* (2002) expect waterline melt rates at tidewater Hansbreen, Svalbard, to be slower than for icebergs due to open water conditions, salinity and water flow, Motyka *et al.* (2003a) suggest that the reverse is true, given the additional forced convection component in the form of sub or englacial meltwater outflow. Such a gulf of difference between recently published melt rates is remarkable and emphasises how poorly understood these processes are, even in tidewater settings, where work has been focused.

Despite the complexity and detailed field measurements used to calculate melting, the model presented by Motyka *et al.* (2003a) is not without its problems. Whilst the study is useful in highlighting the potential of subaqueous melting to form a significant component of the ablation system, as a result of convective processes, it is inappropriate to neglect energy exchanges with the atmosphere. At most glacier termini, katabatic winds usually prevail, and will be important for delivering turbulent heat fluxes to the water surface. This turbulence, which promotes mixing to greater depths in the water

column (2.2.3.ii), acts to cause mixing of the incoming warm water underneath the outflowing buoyant meltwater. This is likely to reduce the amount of heat coming into the ice face and may, therefore, inhibit the amount of melting that takes place at the ice face. At lake-calving glaciers, in particular, where upwelling currents are weaker, the atmospheric heat exchanges are crucial in determining the surface conditions.

2.3.8 Summary

Melting along the waterline and subaqueous portions of calving ice cliffs contributes to overall mass losses, by direct mass loss and by undercutting the subaerial ice cliff, facilitating calving. Understanding of the precise contribution of such melting to calving rates is inhibited by the lack of a suitable melting relationship that may be reliably applied to calving margins. Existing relationships are developed from laboratory and field studies of floating icebergs, which have limited applicability to grounded calving fronts, where ice dimensions differ, and sources of forced convection vary. The application of these equations requires a full understanding of the derivation of the terms, and the contexts in which they apply. However, they are successful in identifying the likely range of controlling variables i.e. water temperature, salinity, wave action and current speed, from both free and forced convection, providing a basis for further research. Other approaches exist, namely various energy balance calculations, although these rely heavily on accounting fully for all components, to yield an accurate residual value equal to the heat available for melting. Further work is required to calibrate such balances, using measured values of waterline and subaqueous melting. Additionally, given that current velocities are key in influencing melt rates, it is necessary to consider the variability in melt rates across the width of a glacier terminus due to the concentration of melting close to zones of upwelling meltwater discharge. However, obtaining empirical data from the boundary layer is hampered by access, necessitating the use of alternative methods, such as the use of remotely-operated vehicles.

2.4 SPECIFIC THESIS OBJECTIVES

The preceding review of the literature pertaining to (1) the current understanding of the behaviour of calving glaciers, (2) the physical limnology of ice-contact lakes and (3) subaqueous melting of ice faces, has highlighted several key research needs with regard to lake-terminating glacier dynamics, and which are addressed in this thesis under the following objectives:

1. To add to the existing database of lake-calving glaciers. Calving behaviour of lake-terminating glaciers is investigated at Glaciar León, Chilean Patagonia, and Fjallsjökull, southeast Iceland.
2. To clarify the range of rate-controlling factors operating at a calving terminus, and their relative importance for calving dynamics.
3. To test whether waterline melt notch development controls calving at freshwater calving margins.
4. To assess the physical limnology of ice-contact lakes thoroughly, to ascertain ways in which the lake may influence terminus dynamics, and modes of potential heat transfer to the ice face.
5. To develop methods of assessing subaqueous melting rates, which are applicable to grounded calving termini, in order to assess the contribution of such melting to the overall mass loss at the terminus.
6. To examine calving processes over short timescales, permitting an assessment of the immediate triggers for calving events.
7. To evaluate the influence of calving at Glaciar León and Fjallsjökull on their responses to climatic change.

CHAPTER 3

The Patagonian Icefields

3.1 INTRODUCTION

The Patagonian Icefields (46°30′ – 51°30′ S) (Figure 3.1) form one of the largest low-latitude ice masses in the world, and are critically located with respect to Southern Hemisphere atmospheric and oceanic climatic systems (Casassa *et al.*, 2002). The two icefields cover 17200 km^2, and are nourished by precipitation of 6000-8000 mm a^{-1} (Escobar *et al.*, 1992; Warren & Sugden, 1993; Warren & Aniya, 1999). Their presence at such low latitudes means they interact with mid-latitude weather systems and vegetation belts, and terminate in a wide diversity of climatic environments within the belt of the southern westerlies (Warren & Sugden 1993; Moreno 2002). The temperate climate and high snow fall results in rapid throughput of temperate glacier ice and, therefore, a fast response to climatic changes (Rosenblüth *et al.*, 1995). The general trend in Patagonia is for glacier thinning and retreat from a Neoglacial maximum, indicated by vegetation trim lines tens to hundreds of meters above the current ice surface (Casassa, 1995). It has prompted the formation of many ice-contact lakes since the Little Ice Age (LIA) as glaciers have retreated into glacially overdeepened troughs, initiating calving at formerly land-based termini. Calving has therefore become increasingly important to the mass balance and dynamics of the icefield (Warren & Aniya, 1999). The dynamics and climatic sensitivity of the icefields cannot be understood or interpreted without an understanding of calving.

The icefields remained relatively unknown until the 1950s (Shipton, 1959; Casassa & Marangunić, 1987), when the anomalous behaviour of some Patagonian glaciers sparked interest (Nichols & Miller, 1952; Lliboutry, 1953; Mercer, 1964). While most of the early work is based on expedition notes of observations, Lliboutry (1956) was the first to make detailed glaciological studies in Chile and Argentina, and Mercer (1968) later summarized the distribution of glaciers in Patagonia.

Figure 3.1 The location of the main icefields with calving glaciers in southern South America. Source: Warren & Aniya (1999).

Recent work has concentrated on gathering fundamental glaciological data, in particular comprehensive inventory statistics and changes in terminus positions (Aniya, 1988; 1992, 2001; Wada & Aniya, 1995) as well as ice velocities, ablation rates and calving rates (Warren *et al.*, 1995a, 1995b, 2001; Warren, 1999; Warren & Aniya, 1999; Naruse *et* al., 2001; Skvarca *et al.*, 2002) and meteorological, hydrological and geomorphological information (Inoue *et al.*, 1987; Fukami & Naruse, 1987). In addition to aerial photos (Lliboutry, 1956; Naruse *et al.*, 1995b; Aniya, 2001), remotely-sensed satellite data are of increasing use for determining rates of terminus change and ice velocities (Rignot *et al.*, 1996a, 1996b; Rott *et al.*, 1998; Skvarca *et al.*, 1999; Aniya *et al.*, 2000). As well as studies of present-day glacier dynamics, empirical data about both Quaternary and recent fluctuations of the icefields exist for both icefields (Clapperton, 1990, 1993; Heusser, 1993; Marden & Clapperton, 1995; Aniya, 1995, 1996; Winchester & Harrison, 1996, 2000; Aniya *et al.*, 2000). More recently, a range of modelling studies regarding the icefields' growth and decay, and the limits of expansion of ice sheets have focussed on Patagonia, as it provides an ideal site to examine the link between climate and ice sheet behaviour (3.4.2) (Hulton *et al.*, 1994, 2002; Hulton & Sugden, 1997; Purves & Hulton, 2000; Sugden *et al.*, 2002). Glaciological research on the Patagonian Icefields has been previously reviewed by Warren & Sugden (1993) and Warren & Aniya (1999), who focus particularly on calving in southern South America. Here, current icefield characteristics, regional climate and past glacier variations are described, before outlining broader issues concerning icefield changes during the Quaternary, and the importance of calving for icefield dynamics, both past and present.

3.2 The significance of the Patagonian Icefields

In comparison to the Northern Hemisphere, landmass is scarce in the Southern Hemisphere. Glacier variations in South America are therefore important, providing a high-resolution terrestrial record for understanding glacier responses to climatic changes at a global scale (1.3). The tropical Pacific Ocean can drive regional climatic changes by changing upwelling intensity, hemispheric-scale changes by affecting the strength and position of the westerly storm tracks, and can have global scale effects by changing centres of atmospheric convection. This has direct consequences for Patagonia as it covers a broad range of latitudes, and it is therefore one of the few areas in which questions about interhemispheric climate system linkages may be resolved in terms of Quaternary

palaeoenvironments, such as the ongoing debate about the global existence of a Younger Dryas (YD) climatic reversal (3.4.2) (Heusser & Rabassa, 1987; Clapperton, 1990, 1998; Markgraf, 1991, 1993, 2001; Denton *et al.*, 1999; Ivy-Ochs *et al.*, 1999; Bennett *et al.*, 2000; Kim *et al.*, 2002; Hajdas *et al.*, 2003). The icefields are also ideal for examining Quaternary ice sheet dynamics, because the southern mid-latitudes, which lacked large ice sheets during the last glaciation, are far removed from the Northern Hemisphere ice sheets, which may have masked or triggered regional climate changes (Moreno, 2002). The understanding of glacier behaviour in the region is also valuable in approaching applied issues, such as hazards from outburst floods (Nicholls & Miller, 1952; Peña & Escobar, 1985; Skvarca *et al.*, 1999; Depetris & Pasquini, 2000; Harrison & Winchester, 2000) (1.3) and management of water resources (Casassa, 1995). These are dominantly glacial in origin, yet annual mean discharges and water balances are almost unknown.

The current rate of global sea level rise is 1-2 mm a^{-1} (Gornitz, 1995), 0.4 mm a^{-1} of which is believed to originate from the melting of glaciers and small ice caps (Warrick & Oerlemans, 1990). A few authors have related the glacier variations in Patagonia to sea level change (Aniya, 1999; Casassa *et al.*, 2002; Rivera *et al.*, in press). At present, the best estimate implies that general retreat of the South Patagonian Icefield (SPI) has resulted in an contribution of 6% of the global rise in sea level due to melting of small glaciers and ice caps (Casassa *et al.*, 2002). From 1968/75–2000, ice loss from both icefields equated to 0.042 ± 0.002 mm a^{-1} sea level rise, and has more than doubled to 0.105 ± 0.011 mm a^{-1} between 1995-2000. Their contribution to sea level per unit area is larger than that of Alaskan glaciers (Rignot *et al.*, 2003).

3.3 The Patagonian Icefields in the present day

3.3.1 Icefield characteristics

The larger of the two icefields, the South Patagonian Icefield (SPI) covers 13 000 km^2 (Aniya *et al.*, 1996), measuring 370 by 35 km, with maximum and minimum widths of 60 km and 9 km, respectively (Warren & Sugden, 1993; Casassa *et al.*, 2002). It comprises 46 large glaciers, only two of which are not calving, and more than one hundred smaller glaciers. The central part forms a relatively flat icefield with an average elevation of 1600

m (Casassa *et al.*, 2002). The largest glaciers on the SPI are Pío XI (1265 km^2), Viedma (945 km^2), Upsala (902 km^2) and O'Higgins (810 km^2) (Casassa *et al.*, 2002).

The North Patagonian Icefield (NPI), extending 100 by 45 km, covers 4200 km^2 (Figure 3.2). There are 28 glaciers > 5 km^2 (Aniya, 1988), 13 of which calve into proglacial lakes (Aniya, 2001). Most of the icefield lies between altitudes of 1000 m on the west and 1500 m on the east, and includes the highest mountain in Patagonia, Monte San Valentin (3910 m) (Aniya, *et al.*, 1997). The largest outlet glaciers on the NPI are San Rafael, San Quintin (both ~ 760 km^2), Steffen and Colonia (both ~ 450 km^2) (Aniya, 1988). For the icefield's outlet glaciers, accumulation area ratios (AAR) range from 0.4 to 0.8 and the surface elevation of the icefield is at its highest (~ 1500 to 1700 m) between Glaciar León and Glaciar Cachet (Aniya, 1988), from which glaciers descend through icefalls.

Due to the climatic regime (3.3.2), the icefields are thought to consist of temperate ice throughout (Aristarain & Delmas, 1993; Casassa *et al.*, 2002). Ablation data have been obtained at some glaciers for short periods (Fukami & Naruse, 1987; Naruse *et al.*, 1995a; Ohata *et al.*, 1995; Takeuchi *et al.*, 1995a, 1995b, 1996), and a whole year at Glaciar Moreno (Skvarca & Naruse, 1997). Annual ablation and precipitation values of 23.8 $km^3\ a^{-1}$ and 58.4 $km^3\ a^{-1}$ respectively, have been calculated for the SPI from a digital elevation model, where the difference represents the volume lost by calving (Casassa *et al.*, 2002). However, the lack of accumulation data is a limiting factor in developing our understanding of the mass balance of the Patagonian icefields, and remote sensing is required to make a complete assessment of their mass balance (Leiva, 2002). A net accumulation rate of just 1.2 m a^{-1} w.e. was calculated from seasonal deuterium on the SPI at an elevation of 2680 m (Aristarain & Delmas, 1993), low in comparison to other results (13.5 m w.e. at Glaciar Tyndall by Godoi *et al.*, 2002; 5.5 m w.e. at Glaciar Moreno by Rott *et al.*, 1998). Others support this low value (Pohjola, 2002), and it is thought that it reflects snow drift due to the strong winds, evidenced by ice crusts (Aristarain & Delmas, 1993). At Glaciar San Rafael (NPI), mean mass balance is thought to be 3.45 m a^{-1} w.e. (Yamada, 1987).

The divides separating many of the catchments in the accumulation areas consist of ice-sheds defined by subglacial bedrock topography (Warren & Aniya, 1999). Glaciers on the west side are larger than those on the east, due to topographical and meteorological differences (Rignot *et al.*, 2003).

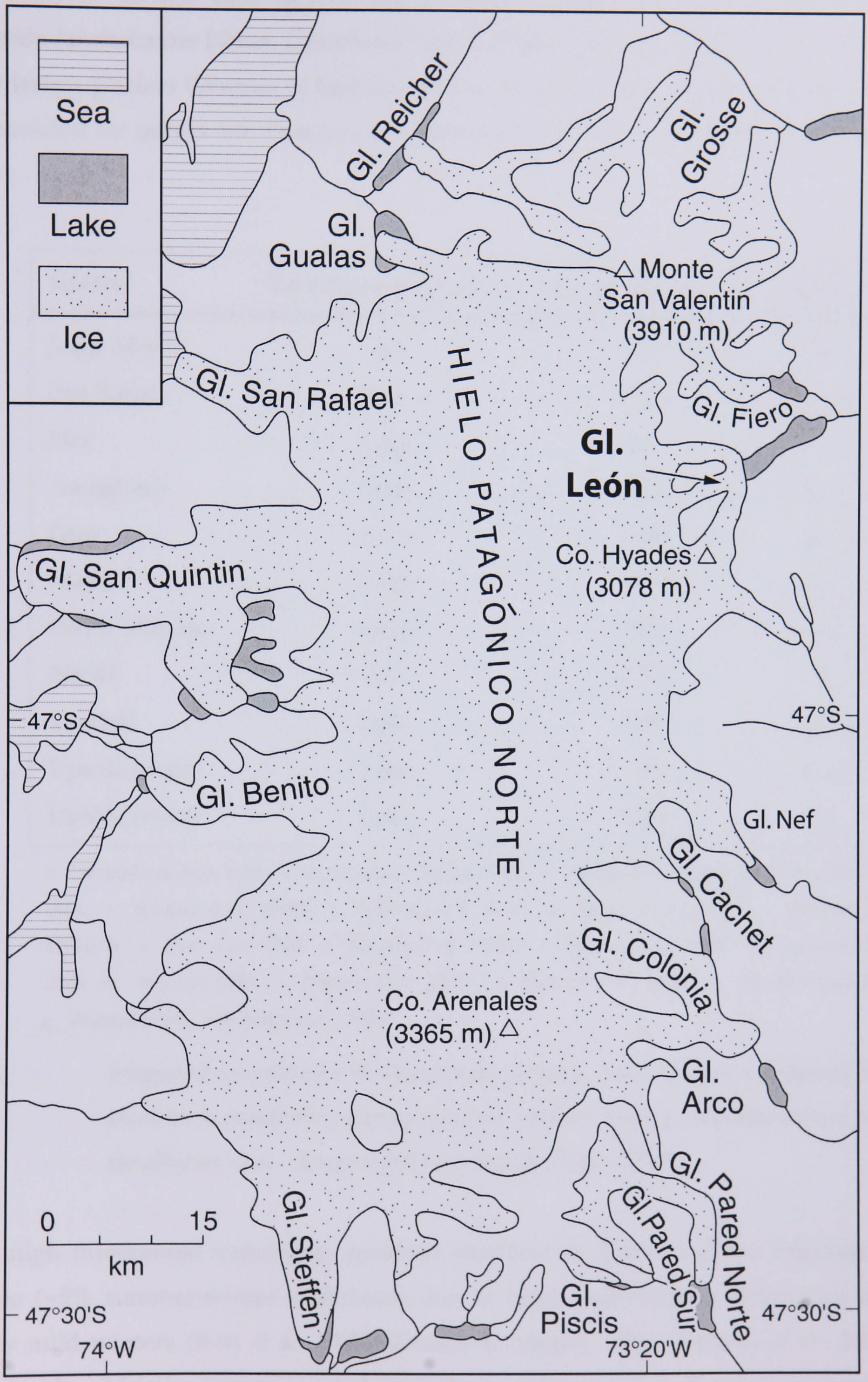

Figure 3.2 Map of the North Patagonian Icefield showing the main outlet glaciers and the location of the study area. Adapted from Glasser *et al.* (in press).

High glacier velocities occur on both icefields. Glaciar San Rafael drains ~18% of the NPI (Aniya, 1988) at ~ 20 m d^{-1} near the terminus in summer (Kondo & Yamada, 1988), placing it alongside Jakobshavns Isbrae, Greenland, and Colombia Glacier, Alaska, as one of the world's fastest glaciers (Warren & Sugden, 1993). However, ice surface velocities have been measured for only a few Patagonian glaciers (Warren & Aniya, 1999), as shown in Table 3.1.

Glacier	Calving environment	Ice velocity (m a^{-1})	Source
Jorge Montt	Sea	240	a
San Rafael	Sea	6205	c, g, n
Nef	Lake	450	r
Ameghino	Lake	310	m, q
Grey	Lake	450	d, o
Mayo	Lake	288	k
Perito Moreno	Lake	650	e, i
Pio XI	Sea	7730	h
Tyndall	Lake	225	b, f
Upsala (east)	Lake	80	o, q
Upsala (west)	Lake	1620	e, j

a. Enomoto & Abe, 1983 *b.* Koizumi & Naruse, 1992 *c.* Kondo & Yamada, 1988 *d.* Lliboutry, 1956 *e.* Naruse *et al.*, 1995b *f.* Nishida *et al.*, 1995 *g.* Rignot *et al.*, 1996b *h.* Rivera *et al.*, 1997a, b *i.* Rott *et* al., 1998 *j.* Skvarca *et al.*, 1995b *k.* Skvarca *et al.*, 1999 *l.* Takeuchi, *et al.*, 1996 *m.* Warren, 1994 *n.* Warren *et al.*, 1995a *o.* Warren *et al.*, 1995b *p.* Warren *et al.*, 1997 *q.* Warren, 1999 *r.* Warren *et al.*, 2001

Table 3.1 *Measured ice velocities for Patagonian glaciers. Most data were obtained from short-term monitoring during summer, and are mostly centreline values from the ablation area. Adapted from Warren & Aniya (1999).*

Despite high interannual variability, seasonal variation in glacier surface velocities is negligible (~5% summer-winter difference) due to high, year-round precipitation and relatively mild winters (Rott *et al.* 1998; Skvarca & Naruse, 1997; Skvarca *et al.*, 2003). Internal and basal friction associated with high flow speeds will also contribute meltwater to the basal hydrological system, facilitating sustained fast flow throughout the year.

In addition to field data, space-borne Synthetic Aperture Radar (SAR) interferometric imagery is often used to gather a range of glaciological data, deriving surface topography, ice velocities and strain rates, with remarkable accuracy, sometimes in combination with Landsat images (Aniya *et al.*, 2000). SAR is particularly useful for the Patagonian Icefields, which are often obscured by cloud cover, and therefore unsuitable for study with visible and infrared sensors. SAR images have been acquired by ERS (European Remote Sensing) and RADARSAT satellites, and by the Space Shuttle Endeavour (Skvarca *et al.*, 1999). Glacier motion and surface topography of the NPI have been mapped to calculate ice discharge (Rignot *et al.*, 1996b), with detail at Glaciar San Rafael permitting an examination of the calving flux and mass balance (Rignot *et al.*, 1996a). Spectacular longitudinal stretching seen in the last few kilometres may be caused by enhanced basal sliding due to high basal water pressure, similar to that seen at Columbia Glacier, Alaska (Meier & Post, 1987). Ice depths and ablation measured at Glaciar Moreno by SAR methods account for the role of lake bottom topography in maintaining a stable terminus position over the last century (Michel & Rignot, 1999; Rott *et al.*, 1998). For rapidly changing glacier positions, such as on the Patagonian Icefields, the fine temporal resolution of remote sensing is invaluable (3.3.3) and a phase correlation method is suitable for fast flow near the terminus. Changes may also be recorded areally rather than linearly, useful for glaciers with small fluctuations, which are rarely parallel to the previous position (Warren & Aniya, 1999).

3.3.2 Regional climate

The year round climate influencing the Patagonian ice sheets is wet, cool and windy with precipitation ~ 4000 mm yr^{-1} at the coast (Inoue *et al.*, 1987), between 6000-10 000 mma^{-1} on the icefield accumulation areas (Escobar *et al.*, 1992; Warren & Aniya, 1999), and falling to 2000 mm to the north and south of the icefields (Hulton & Sugden, 1997). The highest precipitation occurs at ~50°S (Figure 3.3 inset). The seasonal maximum in precipitation varies from north to south, suggesting that the NPI lies at a climatically sensitive position (Winchester & Harrison, 1996; Harrison & Winchester, 1998).

There is a strong west-east precipitation gradient, due to orographic precipitation over the 2000 – 2500 m altitudes of the southern Andes (cf. Figure 9, Winchester & Harrison, 1996). The coastal zone experiences small seasonal variations in precipitation and temperature but high annual variation (Enomoto & Nakajima, 1985). Over the icefields, autumn and winter precipitation maxima are typical, but not universal (Fujiyoshi *et al.*, 1987a, 1987b; Peña & Gutierrez, 1992). In contrast, a very dry continental climate prevails in the rain shadow east of the Andes in Argentine Patagonia, with low rainfall totals of < 1000 mm yr^{-1}, yet is only a few tens of km of the glacier termini in the east (Kerr & Sugden, 1994).

Whilst the maritime glaciers are typically cloud covered, with frequent, intense precipitation (Carrasco *et al.*, 2002), the ablation areas on the east side are often exposed to full sun, resulting in differences in surface melting rates. Constant strong winds are characteristic of the whole region. Near the outlet glaciers these are considerably enhanced by a katabatic element (Ohata *et al.*, 1985), gusting at times to speeds greater than 55 m s^{-1} (Shipton, 1959), and are generally weaker during the winter than in the summer (Carrasco *et al.*, 2002). In combination with high insolation rates, the heat transfer relating to turbulence explains why Soler Glacier experiences 50 % more ablation than Glaciar San Rafael (Ohata *et al.*, 1985).

The maritime climate dictates a low seasonal variation in annual temperatures, with a mean annual temperature ranging from 11.0 °C at 42°S to 5.5°C at 55°S (Miller, 1976). Around the SPI, warming over the last 100 years is 1.3 – 2.0 °C (Rosenblüth *et al.*, 1997; Depetris & Pasquini, 2000). Whilst this warming has nearly doubled in some places in the last three decades, there has been a trend of decreasing precipitation of up to 1400 mm on the western side of the Andes (Rosenblüth *et al.*, 1997; Depetris & Pasquini, 2000), although there is an apparent increase in precipitation at several climate stations since the 1980s (Carrasco *et al*, 2002). Other climatic fluctuations include ENSO variations, although Patagonian Icefield sensitivity to ENSO variations is unclear (Philander, 1990; Villalba *et al.*, 1998; Winchester *et al.*, 1999; Deptris & Pasquini, 2000; Ginot *et al.*, 2002). These studies do, however, indicate the importance of considering interannual variations in climate for glacier dynamics.

3.3.3 Recent glacier variations

Building on the pioneering efforts to inventory SPI glaciers (Lliboutry, 1956; Mercer, 1968), air photos and Landsat data indicate that most Patagonia glacier outlets have retreated around 0.5 – 2 km during the last half century (Naruse *et al.*, 1995b). The complete inventories of the 48 major glaciers of the SPI, including their drainage basin areas (Aniya *et al.*, 1996) and areal frontal variations (Aniya *et al.*, 1997), have been extended by workers at individual glaciers (Warren *et al.*, 1997; Rivera *et al.*, 1997a, 1997b; Skvarca *et al.*, 1999, 2002), and by use of Landsat images (Skvarca & de Angelis, 2002). Exceptions to those retreating at a steady rate (Warren & Aniya, 1999; Aniya *et al.*, 2000) (3.5.2), include the rapid retreat of Glaciar O'Higgins (Casassa *et al.*, 1997), and the net advances of glaciers Pío XI and Moreno (Mercer, 1964; Aniya, 1999; Rivera & Casassa, 1999; Rivera *et al.*, 1997a, b), which approached their Holocene maxima in the early 1990s (Clapperton, 1990; Warren *et al.*, 1997). Glaciar Moreno recently made another readvance, blocking the Canal de los Témpanos before rupturing through into Lago Argentino in March 2004, as it did previously in 1988 (Hennigan, 2004) (3.5.2).

On the NPI, the average annual retreat rate from 1944/45 to 1985/86 was 68 m a^{-1} (Aniya & Enomoto, 1986), during which Glaciar Reicher showed a net advance (Aniya, 1988). Recession slowed from 1990 (0.037 km^2 a^{-1}) (Aniya, 1999), except Glaciar San Rafael, which made a small advance after 1996 (Aniya, 2001), before retreat accelerated from 1999-2000 (0.221 km^2 yr^{-1}). During recession, some glaciers have undergone thinning (Aniya & Wakao, 1997; Rignot *et al.*, 1996b; Warren *et al.*, 2001), triggering rapid short-term retreat (3.5.2). Most recently, substantial retreat has been documented at Glaciar San Rafael, the terminus now some 1000 m further back from its positions in the early 1990s (Glasser & Harrison, *pers comm.*, Amos, 2004).

Rates of retreat and contrasts of glacier behaviour have been greater around the SPI than the NPI in recent decades (Wada & Aniya, 1995; Aniya *et al.*, 1997), the former perhaps reflecting a more marked temperature increase with increasing latitude. Whereas most eastern outlets retreated consistently from the beginning of the century, recession on the west began later, has been interrupted by readvances, and most recently has accelerated markedly, reaching higher mean rates of retreat than those on the east (Warren & Sugden, 1993).

3.4 THE QUATERNARY IN PATAGONIA

3.4.1 Glacial-Interglacial Cycles

Glaciers have existed in Patagonia since the Late Tertiary (Mercer, 1976; Clapperton, 1983; Rabassa & Clapperton, 1990), and in the mid-Quaternary the ice cap covered approximately 300 000 km^2, extending far beyond the Andes to the arid eastern pampas (Clapperton, 1990, 1993). The glacial record of the Quaternary in Patagonia is stratigraphically and morphologically comprehensive, due to the abundance of material for dating as a result of extensive wetlands and active volcanism (Rabassa & Clapperton, 1990; Moreno, 2002). Whilst uplift and stream incision have preserved glacial sediments on interfluves, this instability also acted to remove Early and Mid-Quaternary deposits.

Western Patagonia is a key area for testing hypotheses of global climate change (Moreno, 2002) (3.2), although the extent to which the timing and nature of environmental changes in southern South America have echoed those taking place in the Northern Hemisphere during the Late Glacial remains contentious (Clapperton, 1990, 1998; Markgraf, 1993; Denton *et al.*, 1999; Bennett *et al.*, 2000; Pendall *et al.*, 2001; Markgraf *et al.*, 2002; Hajdas *et al.*, 2003). Seven or eight advances occurred mostly synchronously throughout the Andes from *ca.* 40 000 to 10 000 ^{14}C yr BP (Lowell *et al.*, 1995; Clapperton, 1998; Denton *et al.*, 1999), matching cold intervals seen in Northern Hemisphere ice core and marine sediment records (Broecker, 1994; Bond & Lotti, 1995).

3.4.2 The Late Glacial

During the Last Glacial Maximum (LGM) the extent of the Patagonian Icefields approximated to that shown in Figure 3.3. Deglaciation began at 17 500 – 17 150 cal yr BP in response to stepped warming (Clapperton *et al.*, 1995; McCulloch & Bentley, 1998; Denton *et al.*, 1999), and was rapid, with glaciers retreating to within 10 km of their sources within ~ 2000 years (Lowell *et al.*, 1995). The Rio Baker valley presently separates the two Patagonian Icefields. The icefields have previously been separated in a similar location, between late-glacial readvances (Turner, 2003), dated at 15-14, 13-12 and 11-10 ka BP (Clapperton, 1990; Heusser, 1993).

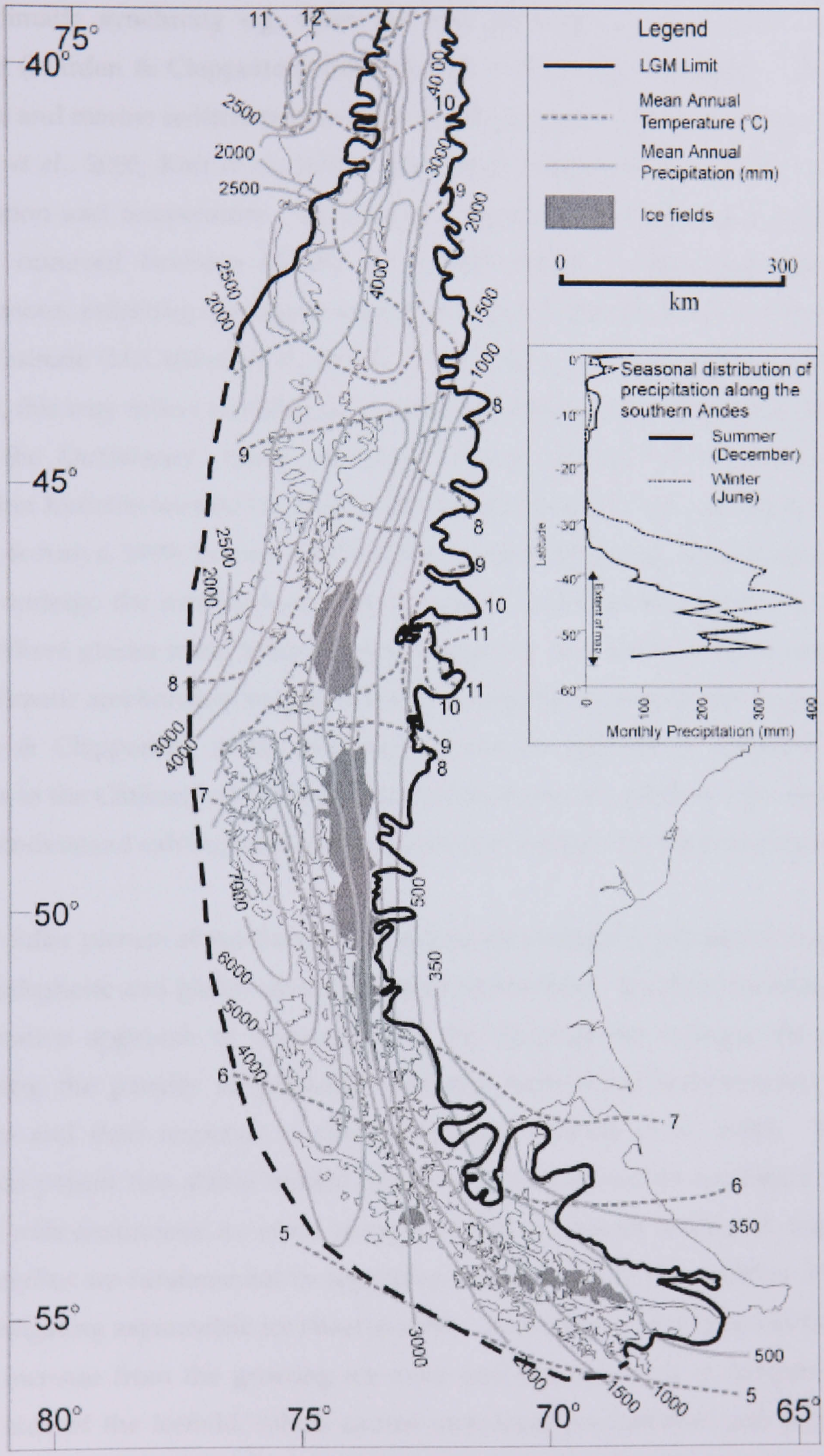

Figure 3.3 The limits of the Last Glacial Maximum in southern South America and the modelled dimensions of the existing Patagonian Icefields (Hulton et al., 2002). All reconstructions of the terrestrial boundaries lean heavily on the mapping of Caldenius (1932). Present day precipitation, the seasonal distribution with latitude, and temperature are also shown.

Some evidence exists for a Younger Dryas (YD) cooling event, supporting theories of global climatic synchrony e.g. from ice core sediments and radiocarbon dating of moraines (Marden & Clapperton, 1995; Hajdas *et al.*, 2003). However, other evidence, from lake and marine sediments in southern Chile, suggests that YD cooling did not occur (Bennett *et al.*, 2000; Kim *et al.*, 2002). Lag times complicate the timing of changes in precipitation and temperature. Synchronous temperature increases in southern South America occurred between 15 and 10 ka BP, whilst precipitation responses were asynchronous, reflecting the lagged migration of the westerlies, by *ca.* 1600 years, to their present latitude (McCulloch *et al.*, 2000). Furthermore, in areas where a YD event is not reported, this may reflect glaciological, instead of climatic, controls such as calving (3.5.2). During the Quaternary, many lacustrine calving glaciers on the east side of the Patagonian Icefields terminated in large lakes extending into the dry Argentinian plains (Warren & Aniya, 1999; Turner, 2003) and the number of calving glaciers has increased as glaciers undergo the melting-to-calving transition, described in section 2.2.1 (Kirkbride, 1993). Where glacier mass balance became negative as a result of such controls, a late-glacial climatic amelioration may have been inadequate to override the deglaciation trend (Marden & Clapperton, 1995), and may explain the absence of extensive late-glacial moraines in the Chilean Lake District and around tidewater glaciers. This emphasizes the need to understand calving mechanisms in order to account for these discrepancies.

A much fuller picture of the Patagonian glacial chronology is required if these regional, inter-hemispheric and global questions are to be resolved. Ice sheet modelling provides an alternative approach to understanding the likely glacier changes since the LGM, overcoming the paucity of empirical data and improving understanding of icefield dynamics and their response to climatic changes (Hulton *et al.*, 2003). Topographic thresholds permit two stable icefield dimensions: one similar to conditions seen today, and one with continuous ice cover along the southern Andes (Hulton & Sugden, 1997). The westerlies are fundamental in supplying precipitation to the icefields (Hulton *et al.*, 1994), instigating asymmetric ice sheet growth. This is due to positive feedback between altitude increase from the growing ice mass and the reduction in temperature on the western side of the icefield, which causes increasing precipitation and further icefield growth (Purves & Hulton, 2000), perhaps accounting for the present asymmetry in ice sheet catchment divides. Fastest icefield growth rates occur at inception between 45–52°S, where the NPI and SPI join (Sugden *et al.*, 2002). Ice builds up rapidly along an intermontane plateau, and rapid discharge of calved ice into fjords on the western side is

indicative of high mass balance. Initial separation of the two icefields occurs, because the plateau is not high enough to sustain such rapid growth until later on. However, Wenzens (2003, 2004) highlights mismatches between modelled icefield boundaries and those mapped from the geomorphological record, particularly on the east side, and presents these as falsifications of the inception and deglaciation models described above. Hulton *et al.* (2003) defend the modelling efforts, which aim to determine the internal and topographic forcing of the growth and decay of the icefields, rather than exactly replicate mapped icefield limits. In other words, they 'bring explanatory power to the particular state of the real world' (Hulton *et al.*, 2003). Moreover, external factors such as sea ice, storm tracks and alterations to albedo or cloud cover have already been recognised as additional parameters which may modify the modelled results, identifying the scope for future work (Purves & Hulton, 2000).

3.4.3 Holocene Neoglacial events

Information about Holocene glacier changes in Patagonia is limited, and only a few sites around the icefields have been studied (Harrison *et al.*, 2004). A scheme of four Neoglacial Holocene advances has been proposed for southern Patagonia, at *c.* 3.6, 2.3 and 1.4 ka BP, and the Little Ice Age (LIA) of the 17th to 19th centuries (Clapperton & Sugden, 1988). This is supported by documentation of other southern Andes glacier advances at ~ 4.5, 3.6, 2.3 and 1.4 ka BP, (Aniya, 1995; Mercer, 1968, 1970, 1976; Wenzens, 1999; Porter, 2000; Haresign *et al.*, submitted), and several since ~ 400 a B.P. (Aniya, 1995, 1996; Marden & Clapperton, 1995; Winchester *et al.*, 2001), implying north-south synchrony. This suggests synchronous icefield response to common climatic forcing, although there are concerns about data reliability since they mostly comprise only minimum radiocarbon dates for moraines, which may disguise local catchment variations. Additionally, topographic effects and glacier dynamics may affect terminus variations, especially at calving margins (Warren & Aniya, 1999; Vieli *et al.*, 2001). Given the large numbers of calving termini around the Patagonian icefields (3.3.1), the glacio-climatic record may have been significantly modulated by glacio-dynamic effects at many sites. As yet, chronological controls are insufficient to establish whether or not periods of glacier advance were synchronous across both icefields or in different sectors of each icefield.

Uncertainty persists about the existence of an east-west gradient in the timing of glacier fluctuations in response to precipitation and temperature gradients (Warren & Sugden, 1993; Hulton *et al.*, 1994; Aniya *et al.*, 1997; Harrison & Winchester, 2000), which were probably steeper at times of icefield expansion in the past, enhancing aridity on the eastern side (Sugden *et al.*, 2002; Turner, 2003). Glaciers flowing westwards attained their maximal Holocene limits at ca. 4.2-4.7 ka BP, whereas those flowing eastwards did not do so until *ca.* 2-2.2 ka BP (Clapperton & Sugden, 1988). However, climate trends have been shown to be similar during the last 21 000 yr BP on both sides of the icefields (Markgraf, 2001; Markgraf *et al.*, 2002).

For periods before the first available aerial photos, dendrochronology and lichenometry remain the only other tools available for the reconstruction of glacier behavior in this region from the late nineteenth century (Winchester & Harrison, 2000; Villalba, 1990). Dendrochronology provides minimum ages for the onset of phases of glacier retreat and surface exposure (Winchester *et al.*, 2001), and has been used to reveal largely synchronous behaviour of glaciers on both sides of the NPI at the end of the LIA (Winchester & Harrison, 1996; Harrison & Winchester, 1998, 2000; Winchester & Harrison, 2000; Winchester *et al.*, 2001; Glasser *et al.*, 2002; Haresign *et al.*, submitted). The similar pattern of glacier recession on both sides of the NPI during the early 1920s, mid-1930s and 1960s (Winchester & Harrison, 1996; Harrison & Winchester, 1998) support the hypothesis that glacier dynamics are principally controlled by changes in precipitation rather than temperature (Warren, 1993). In the late 20th century such synchrony was less apparent due to the increasing influence of calving dynamics and topographic controls as glaciers retreated into overdeepened troughs and experienced rapid calving retreats (Warren and Aniya, 1999; Harrison *et al.*, 2001).

3.5 Climatic Response of Patagonian glaciers

3.5.1 Do Patagonian glaciers respond to changes in precipitation or temperature?

The synchronous fluctuations of some glaciers has been linked to a common climatic forcing (Harrison & Winchester, 2000), although the sharp meteorological boundaries (3.3.2) mean that glacier mass balance response to different climatic parameters varies

over short distances, and the relative importance of temperature and precipitation for glacier mass balance remains unclear. However, whilst meteorological data exist for individual glaciers over short time periods, there is a lack of comprehensive climate data for all areas of the icefields (Burgos *et al.*, 1991), such that regional trends and gradients have to be inferred across large areas. The steepness of the climatic gradients in the region cast doubt over the relevance of remote climate records to the climatic trends around the icefields themselves.

By reflecting changes in the atmospheric pressure system and ocean currents (Kerr & Sugden, 1994), precipitation can alter the equilibrium line altitude (ELA) by tens or hundreds of meters (Warren, 1993). Glacier advance or retreat may be correlated with an increase or reduction in precipitation, respectively (Warren, 1993; Winchester & Harrison, 1996; Harrison & Winchester, 1998) and, over shorter timescales, glacier fluctuations are perhaps driven more specifically by variations in winter precipitation (Warren, 1993). Modelling of ice sheet growth and decay in glacial cycles also suggest that icefield growth and subsequent fluctuations relate primarily to precipitation (Hulton & Sugden, 1997; Purves & Hulton, 2000) (3.4.2). If icefield dynamics respond primarily to precipitation (Warren, 1993) i.e changes in the accumulation area, rather than the ablation area, the steep climatic gradient, whilst creating different climates on either side of the icefield, may be uniform across the icefield divide (Casassa, 1987), and be responsible for synchronous icefield climatic response.

However, glaciers in a wet climate are thought to be especially sensitive to temperature changes (Oerlemans & Fortuin, 1992), and some believe that Patagonia glacier retreat in the last century occured primarily in response to regional warming, rather than a precipitation decrease (Casassa *et al.*, 2002). Greatest icefield sensitivity to temperature has been demonstrated during the LGM (Hulton *et al.*, 2002; Sugden *et al.*, 2002). It is also possible that western outlets respond primarily to precipitation variability while, in the east, temperature is more important (Villalba, 1990; Warren & Sugden, 1993; Aniya *et al.*, 1997).

Other factors include the AAR and the ice surface gradient. Glaciers with a steep gradient and a large AAR (> 0.8) on the SPI have varied little (Aniya *et al.*, 1997). Ohata *et al.* (1985) argued that the strong glacier winds on the east side (Kondo *et al.*, 1985) increase the heat flux to these glacier surfaces, thereby increasing melt rates, compared to those on the

west. However, since a substantial amount of ablation consists of calving, this melting component is not likely to be significant (Harrison & Winchester, 2000).

3.5.2 Calving at Patagonian glaciers

The discussion above has highlighted the effects of climatic forcing on Patagonian glacier variations seen this century. Calving dynamics have a profound effect in controlling terminus position changes (Clapperton & Sugden, 1988) (2.1), and are recognised as being important for icefield dynamics (3.4.3) (Warren, 1993, 1994, 1999; Warren & Sugden, 1993; Warren & Aniya, 1999; Warren *et al.*, 1995, 1995b, 2001; Skvarca *et al.*, 1995, 1999, 2002, 2003). Accelerated glacier retreat occurs following proglacial lake formation (2.2.2) (Kirkbride, 1993), and has occurred at several glaciers on both icefields (Warren, 1994; Warren & Rivera, 1994; Wada & Aniya, 1995; Warren *et al.*, 1995b; Aniya, & Wakao, 1997; Harrison & Winchester, 1998). In general, calving glaciers on the NPI have retreated faster than those that are entirely land-based (Warren & Sugden, 1993). Recent transitions are more common on the NPI, as many of the SPI freshwater-calving glaciers have existed for much longer (3.4.2). For example, the highly active calving of Glaciar Nef (NPI) into Lago Nef only commenced in the 1940s (Aniya & Enomoto, 1986). However, Glaciar Upsala central and east (SPI) has only been calving into Lago Guillermo for the last 40 years or so (Warren *et al.*, 1995b). Melting-calving transitions have occurred in the last ten years on the NPI at Grosse, Exploradores, Reicher and San Quintin glaciers and Glaciar Steffen on the SPI (Aniya & Wakao, 1997; Aniya, 1999; Warren & Aniya, 1999; Harrison *et al.*, 2001). The long-maintained stability and slight readvance of Glaciar León (NPI) may be the result of the glacier's retreat to a position close to the limit of the overdeepening of Lago Leones earlier this century (Aniya & Wakao, 1997; Haresign *et al.*, submitted).

The contrasting recent behaviours of Glaciar Ameghino, Glaciar Moreno and Glaciar Mayo (SPI) exemplify the decoupling of calving glaciers from climatic changes. All three glaciers are situated relatively close together, and show very different recent fluctuations. Glaciar Moreno has been in steady state (Naruse *et al.*, 1995a; Skvarca, & Naruse, 1997) until early in 2004 (3.3.3), whereas both Ameghino (Warren, 1994) and Mayo have retreated asynchronously. Mayo only retreated at its eastern terminus, whilst an advance of the western terminus was most probably a dynamic response to the cessation of calving following the drainage of Laguna Escondida, a former ice-contact lake, in the early 1970s

(Warren, 1999; Skvarca *et al.*, 1999). Although not so closely located, the contrasting behaviour of fast-flowing glaciers San Rafael (NPI, west) and Perito Moreno (SPI, east) (3.3.3) is also unlikely to be directly attributable to climatic influences; the former has made a rapid retreat whilst the latter has advanced with spectacular force (Amos, 2004; Hennigan, 2004). Calving at Moreno takes place into deeper water with smaller calving rates than that at Glaciar San Rafael (Table 2.1, Table 2.2), and internal dynamics must provide an explanation for the contrast in terminus fluctuation behaviour. Observations of thickening at the terminus of Glaciar Moreno in 2002 are akin to those seen in surging glaciers, known to have complex internal dynamics, and a concept that has previously been debated at Glaciar Pio XI (Rivera *et al.*, 1997b).

Research on Patagonian calving glaciers has contributed to the empirical and theoretical understanding of calving, reviewed in section 2.1. Calculated calving speeds support observations from other regions that calving rates in lakes are typically a fraction of those in tidewater (2.1.2). In terms of explaining the contrast between calving rates in freshwater and tidewater, Patagonian studies have revealed some of the important factors affecting calving. For example, the control of sediment budget and fjord topography on calving dynamics has been used to explain the recent behaviour of some glaciers on the SPI. Sediment dynamics influence the effective water depth which, due to its correlation with calving speed, permits climatically independent fluctuations (Alley, 1991) (2.1.1.i). Retreat from a moraine shoal, and the release of terminus-restraining backstress, is thought to be responsible for the rapid recession of Glaciar Upsala (Warren *et al.*, 1995b) since the 1970s. Backstress release is also thought to have also affected Amalia, Upsala, Viedma and O'Higgins glaciers (Aniya, 1999). Glaciers O'Higgins and Amalia retreated from topographic pinning points between 1945 and 1986, despite having high AARs, exemplifying the role of controls other than climate (Aniya, *et al.*, 1996, 1997). The unusual advance of Glaciar Pío XI (Warren *et al.*, 1997) was attributed to increased sedimentation causing a decrease in calving activities. Enhanced retreat then occurred as the release of backstress caused thinning and further retreat by calving (Warren & Rivera, 1999; Aniya, 1999).

The role of buoyancy forces at lake-calving glaciers has already been outlined (2.1.2). The recent behaviour of Glaciar Nef demonstrates the possibility of buoyancy-driven calving at deep-water lacustrine settings. In this case, increasing buoyancy of the terminus in the lake resulted from high rates of surface melting (Naruse *et al.*, 1997; Warren *et al.*, 2001).

Compressional flow towards the terminus, indicated by the lack of substantial transverse crevasses, supports a hypothesis that buoyancy here does not arise from longitudinal stretching and thinning (Warren *et al.*, 2001). At other glaciers, buoyancy forces may occur due to the interaction of fast sliding rates in deep water and longitudinal stretching. This may result in glacier thinning, triggering retreat (Naruse *et al.*, 1995). This may occur as a glacier retreats back from a moraine shoal, as was the case for the rapid retreat at Glaciar Upsala west (Naruse *et al.*, 1997) (2.1.2). From studies of ice flow and calving at Glaciar San Rafael, using SAR-interferometry, Rignot *et al.* (1996a) also suggest that longitudinal stretching at the terminus is fundamental to calving glaciers (3.3.1).

A correlation exists between calving rates and water temperature for lake-calving glaciers (Warren & Kirkbride, 2003). From detailed monitoring of calving at Glaciar San Rafael, Warren *et al.* (1995a) were the first to quantify the significance of subaqueous calving, and suggest that melting may be an important process at calving termini. Both concepts have subsequently been reinforced (2.3.6) (Motyka, 1997; Kirkbride & Warren, 1997; Warren & Kirkbride, 2003; Motyka *et al.*, 2003a; Roehl, 2004). In Patagonia, the much smaller calving rates at Glaciar Ameghino, compared to nearby Glaciar Moreno (Table 2.2, section 2.1.2) may be accounted for by the differences in overall lake temperature. Where Lago Argentino extends 80 km into the dry Patagonian plains, and the cold proximal waters are modified by warm, distal waters, the lack of temperature contrast in Laguna Ameghino relates to the cooling effect of melting icebergs throughout the lake (Warren, 1994, 1999). To some extent, the contrast in calving rates may stem from greater rates of mass loss by waterline melting, undercutting the ice cliff (2.1.1.v).

As for the current global dataset of calving glaciers, a wide range of calving modes and mechanisms exists even within Patagonia. The region is therefore an ideal site for studying calving behaviour, as contrasts between adjacent glaciers under almost identical climatic conditions allows us to better separate the internal and external forcing. That such different calving mechanisms may operate within such close proximity to each other raises the question of whether it is possible to obtain a universal calving law, and whether it is more likely that calving does, in fact, operate along a continuous spectrum, where the dominance of one force over another varies between glaciers.

3.6 A RESEARCH AGENDA FOR THE PATAGONIAN ICEFIELDS

Despite the increasing interest in Patagonian glaciology, and its great relevance to wider issues, much further work is required. There is a need for individual case studies, as neighboring glaciers may have very different relationships with and sensitivity to climate change. Warren & Aniya (1999) outline the value of expanding available climate and mass balance data, and these pointers can be used towards future research, including:

- The identification of climatic boundary zones
- The relative significance of temperature and precipitation variation within the mass balance equation, using micrometeorology and glacier dynamics along transects across the icefields
- Glacier response times
- The climatic sensitivity of the region's calving glaciers for icefield mass balance and its contribution to global sea level rise
- Refinement of models at differing levels of spatial resolution

3.7 SUMMARY

The calving glaciers of Patagonia provide a wealth of information regarding calving mechanisms, and glacier response to climatic changes. It is clear that calving at Patagonian glaciers, like that elsewhere, involves a great number of factors, and that it is not easy to disentangle the catalogue of glacier fluctuations associated with these factors from those relating to climatic forcing. Outlet glaciers from both icefields terminate into both freshwater and tidewater settings, allowing testing of calving relationships into both environments. They also exhibit similar degrees of 'decoupling' from climatic controls and, whilst most glaciers have conformed to the general trend of retreat in response to 20th Century climatic changes, the significant minority of exceptions to this trend cannot be explained by climatic changes alone. This emphasizes the pressing need for detailed studies of individual glaciers, reliable climate data and refined models at appropriate spatial scales.

CHAPTER 4

Glaciar León, Chilean Patagonia: Field Observations

4.1 PHYSICAL SETTING

4.1.1 Location and glacier characteristics

Glaciar León (46°46'S, 73°13'W) is one of eight major outlet glaciers draining the eastern side of the NPI (Figure 3.2), and is ~ 11.4 km long, with an ice surface area of 44.5 km^2 (Aniya, 1988; Rignot 2003). It descends from an icefield accumulation area at a maximum elevation of ~ 3000 m a.s.l. Its three tributaries join below an icefall at ~1500 m a.s.l. to form a single glacier which terminates in Lago Leones at 303 m a.s.l. The equilibrium line lies at 1350 m a.s.l., indicating an accumulation area ratio of 0.67 (Aniya 1988). Glaciers having icefalls between the icefield and the valley outlet are restricted to those on the eastern side, between the Cachet and León glaciers (Aniya, 1988). The entire surface of Glaciar León from the icefall to the terminus is composed of heavily crevassed clean ice, other than the medial moraine which divides the north and central tributaries. The calving front rises 40-50 m above lake level, the southerly third of the ice cliff resting on bedrock, above the water line (Figure 4.1). The steep gradient of the glacier's lower terminus, and the fact that part of the 1.5 km-wide ice cliff has lost contact with the water, indicates that any significant further recession would involve retreat out of the lake and the cessation of calving.

4.1.2 Glacier variations

Although the Leones valley has sometimes been used by climbers as an access route onto the icefield, no scientific observations were made during such expeditions. The only glaciological field measurements prior to this study are samples collected around the lake for lichenometric and dendrochronological dating analysis. Along with optically stimulated luminscence measurements from the terminal moraine on the eastern lakeshore, they were used to investigate the history of glacier retreat from the moraine (Haresign *et al.*, submitted).

Figure 4.1 The terminus of Glaciar León, November 2001, showing the three tributaries converging along lateral moraines, as they descend steeply to Lago Leones. The glacier surface is heavily crevassed. Note also the rock knoll to the left of the glacier terminus. Source: Aniya (*pers. comm.*).

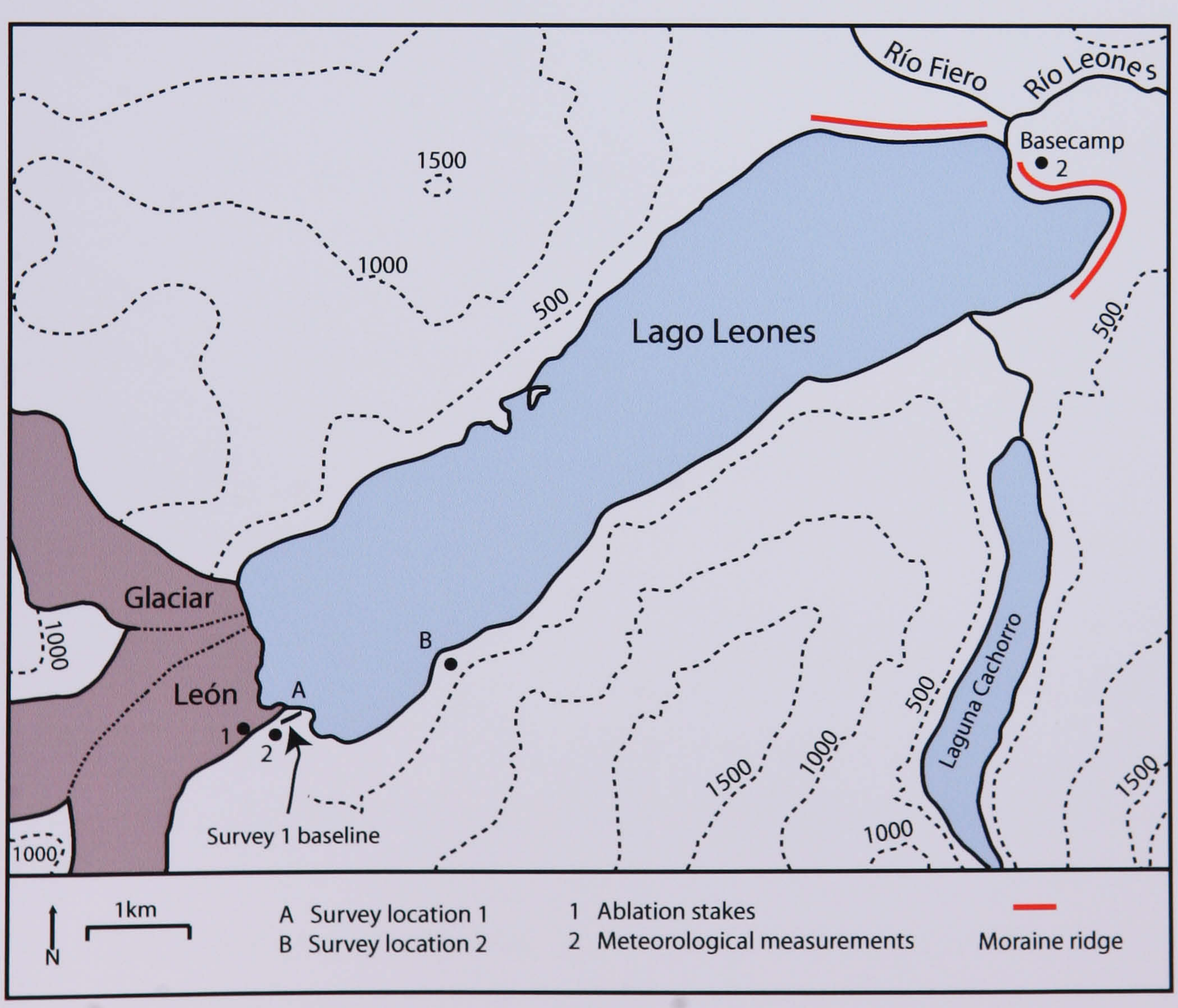

Figure 4.2 Map of Lago Leones and the terminus of Glaciar León, showing the location of the moraine bounding the lake at the north-east end. Also indicated are locations for the baseline used for the two ice velocity surveys, the ablation stakes, the meterological measurements and basecamp. Glaciar Fiero lies to the north (cf. Río Fiero). Map based on the 1:100,000 series of the Chilean Instituto Geográfico Militar, Sheets 162 and 278, and 1974 aerial photographs, updated to show the terminus position in November 2002.

Lago Leones is 10 km long and some 2.5 km wide, and has formed since the glacier margin withdrew from the 135 m-high terminal moraine that now dams the lake at its eastern end (Figure 4.2). However, unlike most other sites around the NPI (Aniya, 1999), the onset of lake formation (and hence calving) did not take place in historic time. The lake formed in the mid Holocene (Haresign *et al.*, submitted) and has been calving throughout the Neoglacial. It is now drained by the fast-flowing Río Leones, dividing the northern side of the terminal moraine from its larger counterpart to the south. Since the first aerial photograph of the glacier in 1944/45 the terminus has fluctuated little (Aniya & Enomoto, 1986; Aniya, 1999), probably because its current position represents a stable pinning point. Slight retreat up to 1991 was followed by a minor, intermittent readvance until 1999, and ~ 100 m retreat occurred between 1999 and 2000 (Aniya, 2001).

4.2 Field Methods

4.2.1 Introduction

At Glaciar León, field data were collected over two month-long periods, on consecutive years. These time periods allow both an appreciation of the interannual variability of the glacier dynamics, as well as sufficient time to collect comprehensive and detailed datasets. Field campaigns took place from October 14 to November 17, 2001, and October 15 to November 15, 2002, during the austral spring, to gather a variety of glaciological, limnological and meteorological data on and around Glaciar León. The following data were collected in the field:

Glaciological observations:	Ice surface velocity, terminus position changes, ice cliff geometry, waterline melt notch development and ablation rates.
Limnological observations:	Lake bathymetry, water temperatures, suspended sediment concentration and salinity
Meteorological observations:	Air temperature, precipitation, wind speed and direction

The glaciological data enable calving rates to be calculated (5.1), as well as providing the means to quantify melting rate of the subaerial ice cliff at the waterline. In combination with the limnological and meteorological parameters, these data are used to assess the range of rate-controlling variables, both for the general behaviour of the glacier and over a short period, of a few weeks. By examining the short-term variations in terminus dynamics, it is possible to evaluate the factors triggering calving, and whether calving controls terminus fluctuations, or occurs as a response to other glaciological variables.

Glaciar León is a good field site at which to address these questions. As the largest lake on the NPI, the significance of calving activity for terminus position is long-standing (Haresign *et al.*, submitted). The glaciology of Glaciar León has not previously been studied, and these data will extend the calving glacier database, both that within Patagonia, and the global database of glaciers terminating in a freshwater setting. This study forms part of a wider regional effort to investigate the dynamics of calving outlets of the NPI, on-going since the early 1990s (Harrison, 1992; Warren, 1993, 1994, 1999; Warren & Aniya, 1999; Warren *et al.*, 1995a, 1995b, 2001). Many of the outlet glaciers of the Patagonian icefields are extremely difficult to access. As Glaciar León is located on the east side, overland access to Lago Leones is relatively simple; a day's walk from the Carretera Austral, the region's primary road link. The glacier can be reached by boat from the east end of the lake (Figure 4.2). Dependence on boat access placed constraints on the timing of data collection because field measurements and observations were only possible when weather conditions permitted, during daylight hours, and as determined by expedition logistics (Table 4.1)

2001	
14-15 Oct	Fieldwork
16-18 Oct	Resupply equipment due to technical failures
19-21 Oct	Fieldwork
22 Oct-5 Nov	Technical problems and change-over of personnel specified by Raleigh International
6-17 Nov	Fieldwork

2002	
15-26 Oct	Fieldwork
27 Oct-3 Nov	Change-over of personnel specified by Raleigh International
4-15 Nov	Fieldwork

Table 4.1 *Overall schedule of fieldwork programme.*

4.2.2 Glaciological Observations

4.2.2.i Triangulation survey method

The intensely crevassed nature of the surface of Glaciar León meant it was not possible to gain access onto the ice, in order to carry out reflector surveys to measure ice surface velocity. This necessitated a triangulation survey. Surveys were carried out from a survey baseline that was located on a rock knoll on the true right side of the glacier (Figure 4.1 and 4.2), using a Leica TC600 total station theodolite. Offering viewing perpendicular to the direction of ice flow, the baseline was 35 m long in 2001 and 69 m in 2002. Longer baseline distances were not possible on the steep, vegetated terrain. Only the central and southerly sections of the ice cliff were visible, as the central promontory concealed the ice cliff to the north. The triangulation method utilises a fixed 'zero' point, from which the horizontal and vertical angles are measured to a number of seracs, surveyed from either end of the baseline, of known coordinates and length. Trigonometrical mathematics can then be used to plot the positions of the seracs, using repeat surveys over known time periods to find the ice surface velocity. Measured seracs can also be used to find the surface gradient of the glacier, and rates of longitudinal stretching. Surveys along the base of the subaerial portion of the cliff were also carried out, to examine terminus changes and measure thermoerosional melt notch sizes.

Standard methods of trigonometry were used to calculate the displacement of each serac or waterline position. The angles from the 'zero' point to the serac, from survey positions S1 and S2 are r_1 and r_2, respectively. The field measurements, providing values of g, r_1, r_2, s_1, s_2, are used to find t_1, t_2 and b, as shown below, and in Figure 4.3a.

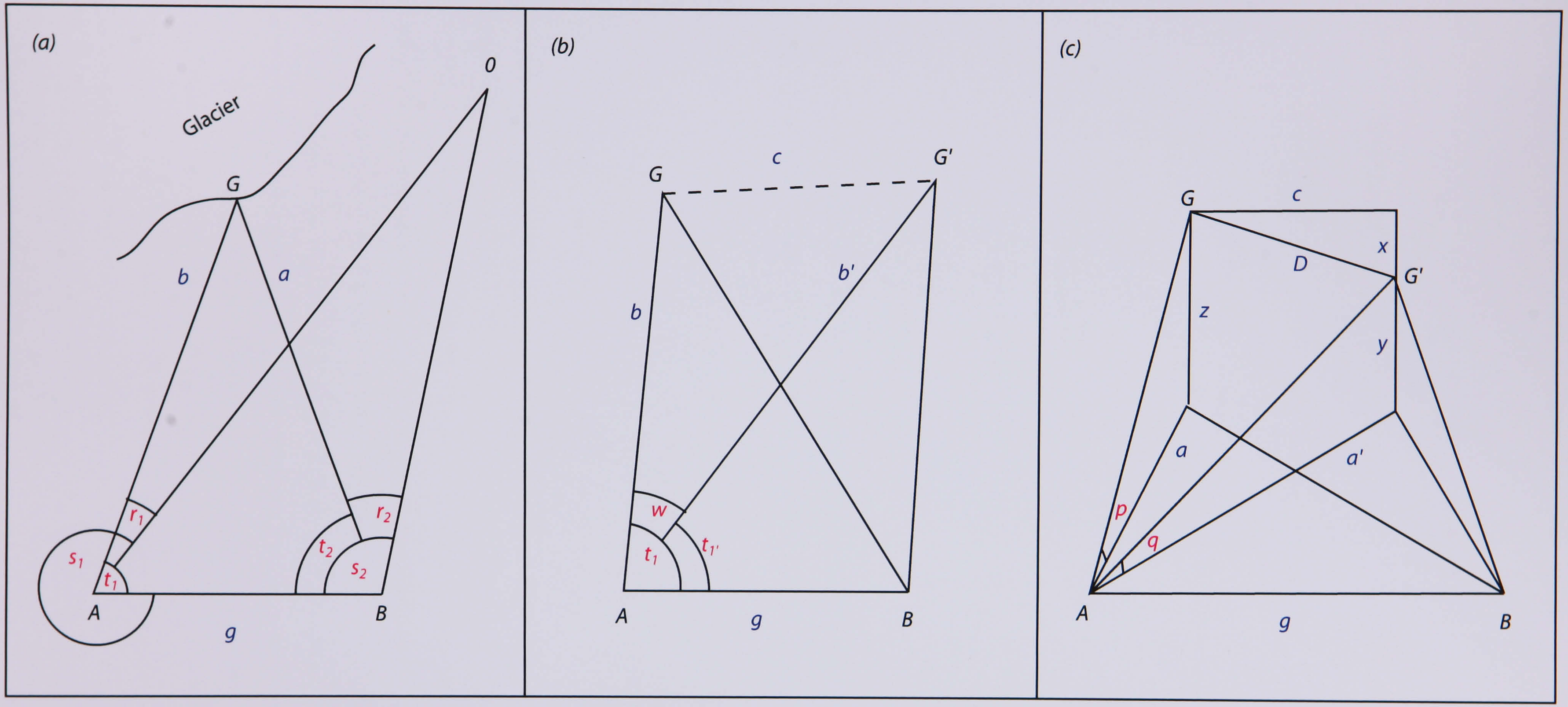

Figure 4.3 Sketches of the trigonometrical methods used to survey seracs and calculate ice velocities. (a) Survey of an ice serac from a 'zero' point. (b) Calculation of the horizontal displacement of the serac between surveys. (c) Calculation of the overall serac displacement, incorporating vertical displacement.

$$t_1 = 360 - s_1 + r_1 \quad \text{(Eq. 4.1)}$$

$$t_2 = s_2 - r_2 \quad \text{(Eq. 4.2)}$$

$$G = 180 - t_1 - t_2 \quad \text{(Eq. 4.3)}$$

$$b = \frac{g \sin t_2}{\sin G} \quad \text{(Eq. 4.4)}$$

The positions of the points can be plotted by finding x and y.

$$x = a \times \cos t_1 \quad \text{(Eq. 4.5)}$$

$$y = a \times \sin t_1 \quad \text{(Eq. 4.6)}$$

The horizontal displacement between the points is given by

$$c = \sqrt{\left[b^2 = b'^2 - \left(2 \times b \times b' \times \cos w\right)\right]} \quad \text{(Eq. 4.7)}$$

where

$$w = t_1 - t_1' \quad \text{(Eq. 4.8)}$$

(Figure 4.3b). The change in the measured vertical angle (p and q) for each serac is used to find z, to calculate the total serac displacement, by Pythagoras' theorem (Figure 4.3c).

$$x = a \times \tan p \quad \text{(Eq. 4.9)}$$

$$y = a' \times \tan q \quad \text{(Eq. 4.10)}$$

$$z = x - y \quad \text{(Eq. 4.11)}$$

$$D = \sqrt{\left(c^2 + z^2\right)} \quad \text{(Eq. 4.12)}$$

4.2.2.ii Ice velocity

Surveys using the triangulation methods (4.2.2.i) were used to monitor 19 seracs from November 8-17, 2001 and 35 seracs from October 17 to November 11, 2002, from survey location (1) (Figure 4.2). The ice surface velocity at each serac was found by calculating the displacement, S, over a known time period. Because the glacier is accessible only by boat from the north-east end of Lago Leones, and because the lake can be affected by strong winds, survey frequency was weather dependent and the typical interval between surveys was roughly 2-3 days, though with some longer gaps enforced by expedition logistics (Table 4.2). The seracs were not evenly distributed across the glacier but divided naturally into northern, central and southern groups as a result of the interaction between

glacier topography and lines of visibility from the survey baseline. Seracs were chosen primarily on or near the terminal ice cliff, with some points extending up-glacier to ~1km from the terminus. The number and distribution of surveyed seracs was somewhat different in the two years because they were selected opportunistically according to the requirement that they be unambiguously identifiable. In particular, the seracs selected in the central section of the glacier in 2002 were immediately behind the calving terminus, whereas those in 2001 were some tens of meters further back. The timing of the surveys was weather dependent, amounting to a total of 6 surveys in 2001 and 10 surveys in 2002 (Table 4.2).

2001	2002
08-Nov	17-Oct
10-Nov	18-Oct
12-Nov	20-Oct
13-Nov	24-Oct
15-Nov	26-Oct
17-Nov	04-Nov
	05-Nov
	08-Nov
	10-Nov
	11-Nov

Table 4.2 *Dates of ice velocity surveys at Glaciar León.*

It was not possible to account for rotation of the seracs in the survey, but this was assumed to have a negligible effect on ice velocity values, partly because ice velocities were high and partly because any significant rotation or shape-change of a serac rendered it unrecognisable, leading to its removal from the survey. Regular calving activity meant that several of the points were lost during the field season, and new points were added each time a survey was carried out. Instrumental error, derived from inconsistencies in the theodolite set-up on each survey, and visual limitations in repeatedly measuring the same part of the serac accurately, were deemed to be < 0.1 m, based on measurements of 'displacement' of the zero point, using the same method as for the moving seracs in the ice survey (4.2.2.i).

It was intended that some of the ice velocity seracs would be utilised to measure longitudinal stretching along the northern tributary but, as the final survey was not possible due to adverse weather conditions, these data are unattainable. Survey methods were also employed to carry out an additional ice velocity survey from a baseline on a small rock promontory, some 2 km from the glacier (survey location (2), Figure 4.2). This location gave the greatest choice of measurable seracs, and the entire terminus was visible. However, errors associated with the baseline calculations render these data unusable.

4.2.2.iii Terminus change

Comparisons of terminus position over time periods of years is possible using the vertical aerial photographs taken by the Instituto Geográfico Militar (IGM) of Chile in 1974, which cover all of the lower area of the glacier and the whole lake, as well satellite images and photos made available by Aniya (*pers. comm.*).

During the 2002 field campaign, the terminus fluctuations from October 24 to November 10 were also surveyed by triangulation (4.2.2.i) on five occasions to delineate the position of the central projecting cliff along the waterline. The change in position of the most forward-projecting visible point on the glacier, half way up the subaerial cliff, was also monitored. Frequent calving activity meant it was not possible to measure the position of the same points each time, but the method nonetheless allows the relative change in the cliff position to be measured, as well as documenting the change in terminus position between the two years' surveys.

4.2.2.iv Ice cliff geometry

Photogrammetry was used to record changes in the ice cliff geometry. It provided a visual record of the changes that occurred in terminus position and form, on a timescale of a few days, indicative of the nature of the calving events that took place. It is also possible to see small features on the photographs that would have been hard to identify unambiguously in the field for survey purposes, and tracking of these features is used in additional calculations of ice velocity and terminus change (4.3.1.ii, 4.3.1.iii). Pictures were taken from the rock knoll between November 7 - 16, 2001, and October 16-November 11, 2002, giving eight photographs in each field season. Photographs were

taken at a fixed focal length and field of view, and were co-registered in Adobe Illustrator using features in the background bedrock.

In conjunction with bathymetric data (4.3.2.i), measurement of the subaerial ice cliff height allows calculation of the 'height above buoyancy' of Glaciar León. Here, values of 55 m and 57 m were obtained on November 8, 2001, and November 5, 2002, for the most protruding central section. The scale on the photogrammetry sequence was calibrated using surveyed values of cliff height, above, which also permitted calculation of cliff heights on additional days. The values are given in Table 4.3.

Date	Cliff height (m)
08-Nov-01	55
12-Nov-01	69
16-Nov-01	78
16-Oct-02	56
20-Oct-02	59
26-Oct-02	56
05-Nov-02	57
06-Nov-02	61
08-Nov-02	61

Table 4.3 *Ice cliff heights at Glaciar León, calculated from survey and photogrammetric analysis, to the nearest meter.*

4.2.2.v Melt rates

Subaerial melting

To estimate subaerial melting at the terminus cliff, four ablation stakes were monitored over a period of 19 days in October, 2002. The stakes were placed on the southern glacier margin in slow-flowing dirty ice, the only safely accessible location (Figure 4.2). Plastic tubes with a diameter of 2.5 cm and a length of 60 cm were drilled 15 cm into the ice using an ice screw, at angles of 0, 30, 45 and 80 degrees to the vertical. On occasions when

access to the glacier was not possible and the stakes melted out, only minimum values could be recorded, and the stakes were redrilled.

To obtain more realistic values of melt rates of the clean ice of the subaerial calving cliff, the difference between advance rate and surface flow rate of distinctive 'prows' along the cliff was determined photogrammetrically, providing a measure of cliff melt rate. However, this method yielded unrealistic values, probably because of the short periods available for measurement between calving events, and the values were not used.

Waterline melt notch development

The perpendicular position of the survey baseline to the ice cliff allowed the use of the triangulation survey to follow the development and evolution of thermo-erosional waterline notches on the part of the ice cliff where the greatest calving activity took place. The horizontal depth of the notch was recorded, on four occasions in 2001 and six times in 2002, and provides a comparison of melt rates here with those of the subaerial portion of the ice cliff.

4.2.3 Limnological Observations

4.2.3.i Bathymetry

Both water temperature profiles and depth soundings were carried out from an Avon inflatable boat. A Lowrance LMS-350A echosounder with integral GPS was used in 2001 to take 475 depth soundings. The soundings were made every 100-200 m along intersecting transects across the lake, to provide a detailed sampling network. A greater density of soundings was acquired in the ice-proximal zone, for a more detailed picture of the bathymetric topography of the zone over which the glacier has retreated relatively recently. Safety considerations prohibited close approach to the ice front, but estimates of water depth at the ice front were obtained by extrapolating from 9 long-transects in the ice-proximal area which were continued to within ~150 m of the calving cliff. A greater density of soundings was also made around the area of the lake near the island (north side), where the lake-side geometry hinted at the presence of a ridge-like feature. Changes in lake stage were noted using fixed markers at either end of the lake.

4.2.3.ii Water Temperature

The temperature structure of the lake was studied in 2001 and 2002. A total of 235 vertical temperature profiles were obtained using an electronic temperature sensor with an accuracy of ± 0.1 °C and a maximum depth capability of 100 m, along a similar network of transects as those of the bathymetric measurements. Temperatures were measured every 5 m in the upper 20 m of the water column, and every 10 m thereafter, to a maximum depth of 100 m. Temperature transects in the ice-proximal area and a long-transect of the lake were repeated several times during both field seasons to examine the development of the thermal structure of the lake during the early part of the melt season.

To appreciate the significance of physical limnology for thermo-erosional melting at the waterline of the ice cliff, detailed measurements of the water temperatures in the immediate ice-proximal area are important. Safety considerations usually preclude such measurements being taken from an inflatable boat, but a radio-controlled boat offers the possibility of safely obtaining such data. Inductive temperature loggers are attached by a cord of known length under the boat, recording temperatures as the boat is navigated along the ice front. Unfortunately, loss of the boat in transit to Chile prevented these measurements from being made, but this field technique was utilised during a later field season, at Fjallsjökull, south-east Iceland (6.3.3.i).

4.2.3.iii Suspended sediment concentration

The suspended sediment concentration (SSC) may affect the thermal structure of lake, due to its effect on water density. Water samples were collected for analysis in 2002 using a custom-made sampler, comprising a cylinder whose two ends can be locked ajar (Figure 4.4a). The sampler is lowered to a known depth and, by tugging the string to shut the ends of the cylinder, the water is trapped, and can be decanted into a bottle once the sampler is raised back to the surface. Samples collected on October 22, 2002, were taken from two locations close to the ice front (Figure 4.4b), at the surface and at 10 m deep. It was hoped that samples could be collected at greater depths, but the drift of the boat made it impossible to keep the sampler rope vertical in the water. Samples collected on November 8, 2002, were only collected from the surface, due to problems with the closing mechanism of the sampler, but were taken from three locations, two believed to be in areas of meltwater input, and one which was not.

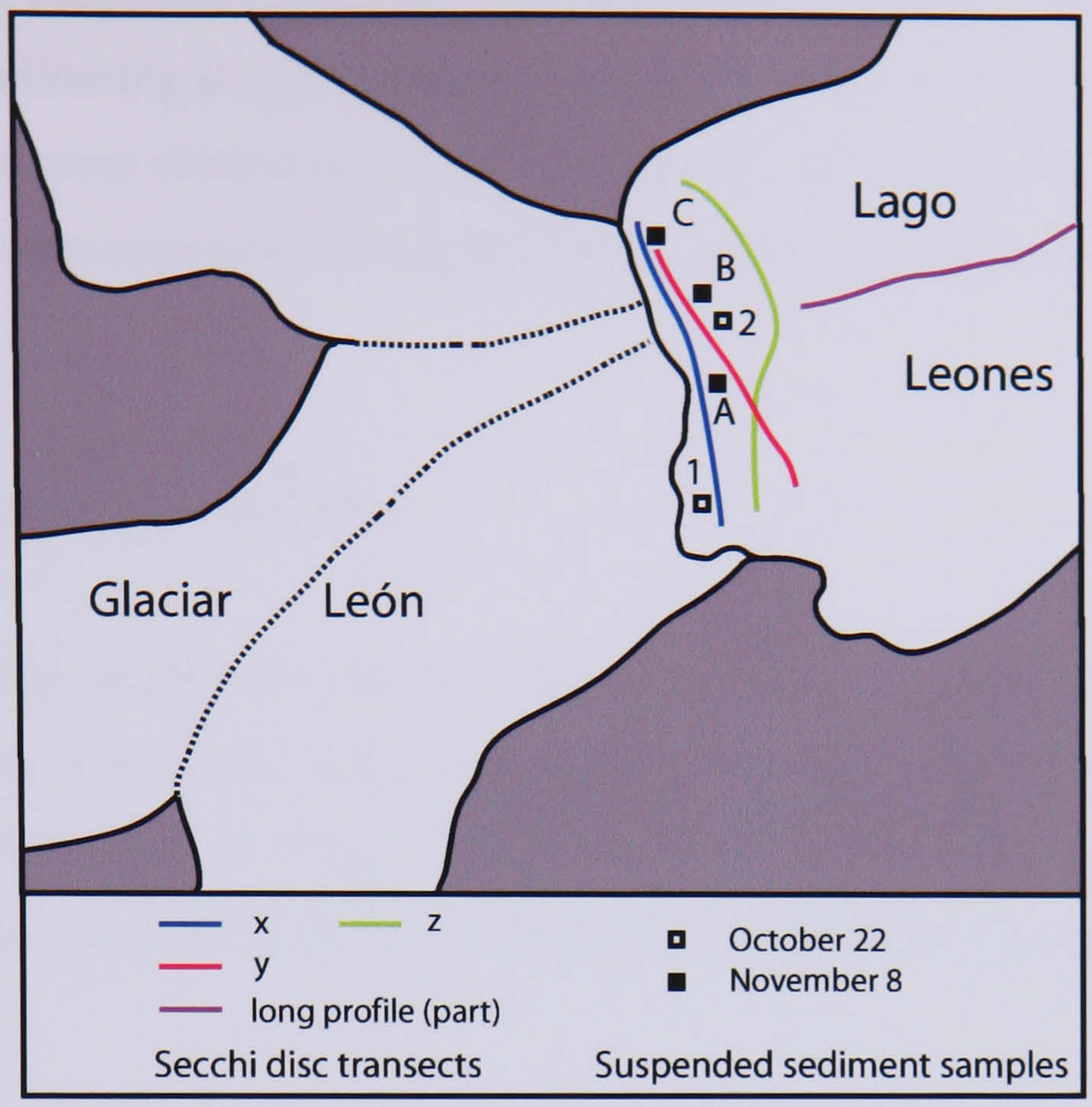

Figure 4.4 The locations of suspended sediment sampling in Lago Leones, 2002.

Figure 4.5 Typical ice cover in the ice-proximal zone of Lago Leones, protruding less than 1 m above the water surface. Note also the prominant waterline melt notch and the large, near-vertical crevasse in the central ice cliff (November, 2002).

The variability of suspended sediment concentrations was also assessed using Secchi disc measurements, following the protocol of Hutchinson (1975). Three cross-profiles totalling 44 measurements were carried out at distances of 50, 100 and 300 m in front of the glacier terminus, and 69 measurements along the length of the lake (Figure 4.4b).

4.2.4 Meteorological Observations

Measurements of precipitation, maximum and minimum temperatures and wind speed were taken using hand-held instruments, from October 9 to November 17, 2001, and October 15 to November 15, 2002. They were taken daily at the east end of the lake at basecamp, and on every occasion when the glacier was visited (Figure 4.2).

4.3 Field Results

4.3.1 Glaciological Observations

4.3.1.i Calving Characteristics

Observations of calving style were made throughout both field seasons, noting full and partial height (subaerial) events, ice disintegration, 'boulder' falls and subaqueous events. Calving occurs daily, mostly consisting of small-scale events which produce growlers (< 1 m above the water) (Figure 4.5). Occasional larger failures produce icebergs (> 5 m above the water) and bergy bits (1 – 5 m above the water) with estimated volumes of 20 000 - 50 000 m^3. Hereafter, all floating ice pieces are referred to as icebergs. Subaerial calving, especially along the central portion of the ice cliff, is cyclical, as illustrated in Figure 4.6. The result of the photogrammetry study in 2001 shows the evolution of ice cliff geometry during a nine-day period in November, 2001, for the projecting central section of the calving terminus. A prominent crevasse forms and grows, and calving progresses from thermal erosion of a melt notch at the waterline, to calving of lamellae, and then full-height slab calving, which occurred approximately every 4 days. In both years, the cliff height sometimes increases prior to a full-height calving event (Figure 4.6). In the example shown, cliff height increased by ~ 9 m, ~ 13 % of the original cliff height.

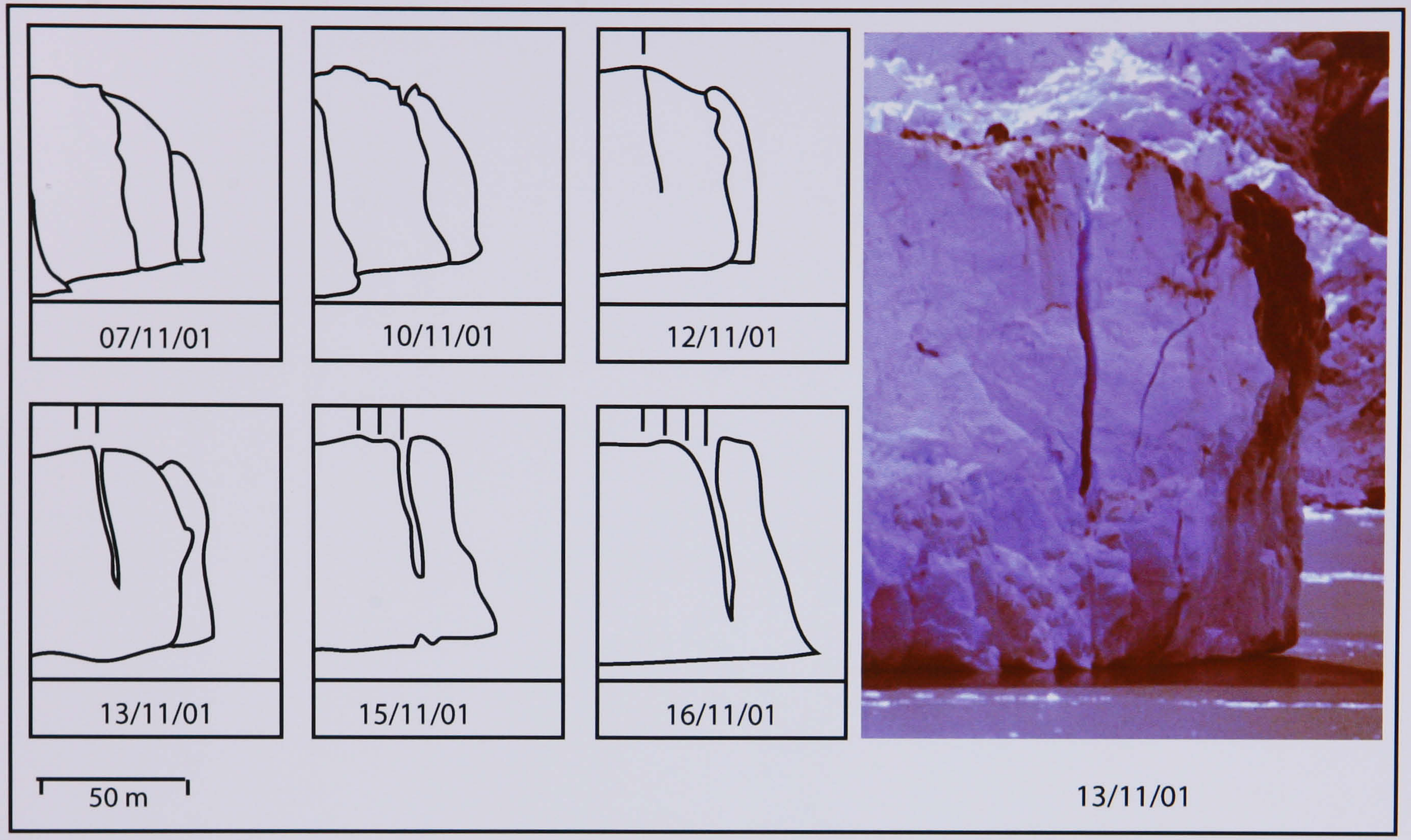

Figure 4.6 (a) Evolution of the central section of Glaciar León's calving cliff during the period 07/11/01 to 16/11/01 based on repeat photogrammetry using photographs taken from the south (true right) side of the terminus near the survey baseline (Figure 2.2). The sequence shows the development and translation of a large crevasse that preceded a full-height slab calving event; its successive positions are traced by the markers at the top of each panel. (b) The photograph of 13/11/01 from the above sequence.

Calving of subaqueous bergs was sometimes witnessed, following full-height subaerial calving events from the central ice cliff, which produced icebergs of similar dimensions to subaerially calved bergs. Subaqueous bergs were distinctive in their rich, blue colour, and often had black, debris-rich ice attached, indicating their basal origin. Waterline melting maintains a thermo-erosional notch which undercuts the base of the subaerial cliff by as much as 5 m (Figure 4.6). Such notches are present at all times except immediately after calving events. Notch growth appears to facilitate smaller calving events from the lower half of the subaerial cliff, events which return oversteepened sections of the ice cliff to a near-vertical condition.

Calving events were often heard during the night from the camp at the eastern end of the lake and, on some occasions the evidence for this was clear. For example, on November 4, 2002, three large bergs were present in the middle of the lake, with long axes of 50, 30 and 20 m, each. However, ambiguity arose as it was not always possible to distinguish between events heard at Glaciar León and those at Glaciar Fiero (Figure 3.2, p. 74). To monitor calving event timing in 2002, a pressure strain gauge was installed at the waterline on the rock knoll, south of the terminus (Figure 4.2), where the timing of the propagation of calving-induced waves was recorded for one month. However, it was not possible to retrieve the data from the logger. This field technique was utilised later at Fjallsjökull, southeast Iceland, in 2004 (6.3.3.ii). At Glaciar León, a qualitative record of calving event observations was kept instead.

Various styles of calving characterise different regions of the ice front. Small events consisting of disaggregated ice blocks calved mainly from the south side of the terminus, where the ice rests on bedrock with no contact with the lake. To the north of this section, the central portion of the ice cliff experiences the full calving cycle. Full-height calving events are less frequent at the most northerly cliff full-height. Instead of large ice blocks, full-height events comprised calving of oversteepening lamellae. The subaqueous events that were witnessed occurred from the central section of the ice cliff, implying the development of an ice foot here. On one occasion (November 5, 2002), a large berg (30 m long) calved from this section appeared to be grounded on a protrusion below, as it did not drift with the other icebergs which calved that day. However, it is possible that subaqueous ice projections also occur in the most northerly section because, on occasion, calved ice appeared to be resting at the base of the subaerial cliff, at the waterline.

Calving is closely linked with crevassing. The whole ice surface is highly crevassed, reflecting the steep gradient of the ice surface. The gradient was calculated here using the triangulation survey method (4.2.2.i) between selected seracs on five occasions in both 2001 and 2002, giving an average value of ~ 15° on the northern side, ~ 17° on the southern side, with slopes up to 85° on the steepest part of the northern tributary icefall. These values are larger than the 11.5° given by Aniya (1988), from aerial photo analysis. Ice flow into the terminus is not necessarily perpendicular to the ice front, evidenced by the orientation of crevasses. Crevasses are perpendicular to the ice front in the north, and calving appears to occur along existing crevasses. In contrast, the largest blocks produced in the central section appear to form along crevasses propagated immediately behind the ice cliff. The ice flux to this location is sourced from the southern tributary, which is the largest (Figure 4.1), and crevasses arrive oblique to the terminus. Full-height lamellae sometimes calve parallel to these crevasses, along existing crevasses, perpendicular to the large blocks described above (Figure 4.7). Calving of rubble along the southerly section above the rock base occurs as the buttressing support of the southern valley margin is lost, as the ice approaches the terminus from behind the rock knoll. As the ice is already pervasively fractured, it disintegrates over the ice cliff at this point.

Close-up inspection of the waterline melt notch was not possible due to safety restrictions. However, the wave train from one particularly large calving event had a low trough, such that the ice cliff immediately below the waterline became visible up to 1 m below the waterline, revealing scalloped features on the subaqueous ice face. The geometry of the ice face at that location is shown in Figure 4.8, and is similar to the geometry caused by melting of ice in laboratory tanks, in freshwater of 4 – 10 °C (Eijpen *et al.*, 2003). As well as the persistent presence of a melt notch at the waterline, 'caverns' were also witnessed, extending ~ 1-2 m in height above the waterline, sometimes indicative of subaqueous meltwater discharge (Syvitski, 1989). They were usually located in the most northerly section and the central part of the cliff (Figure 4.9). In the northern part of the ice cliff, where most calving took place as spalling of lamellae, cavern height increased to a maximum as flakes calved above the cavern, before decreasing as calving reached the 'back' of the cavern.

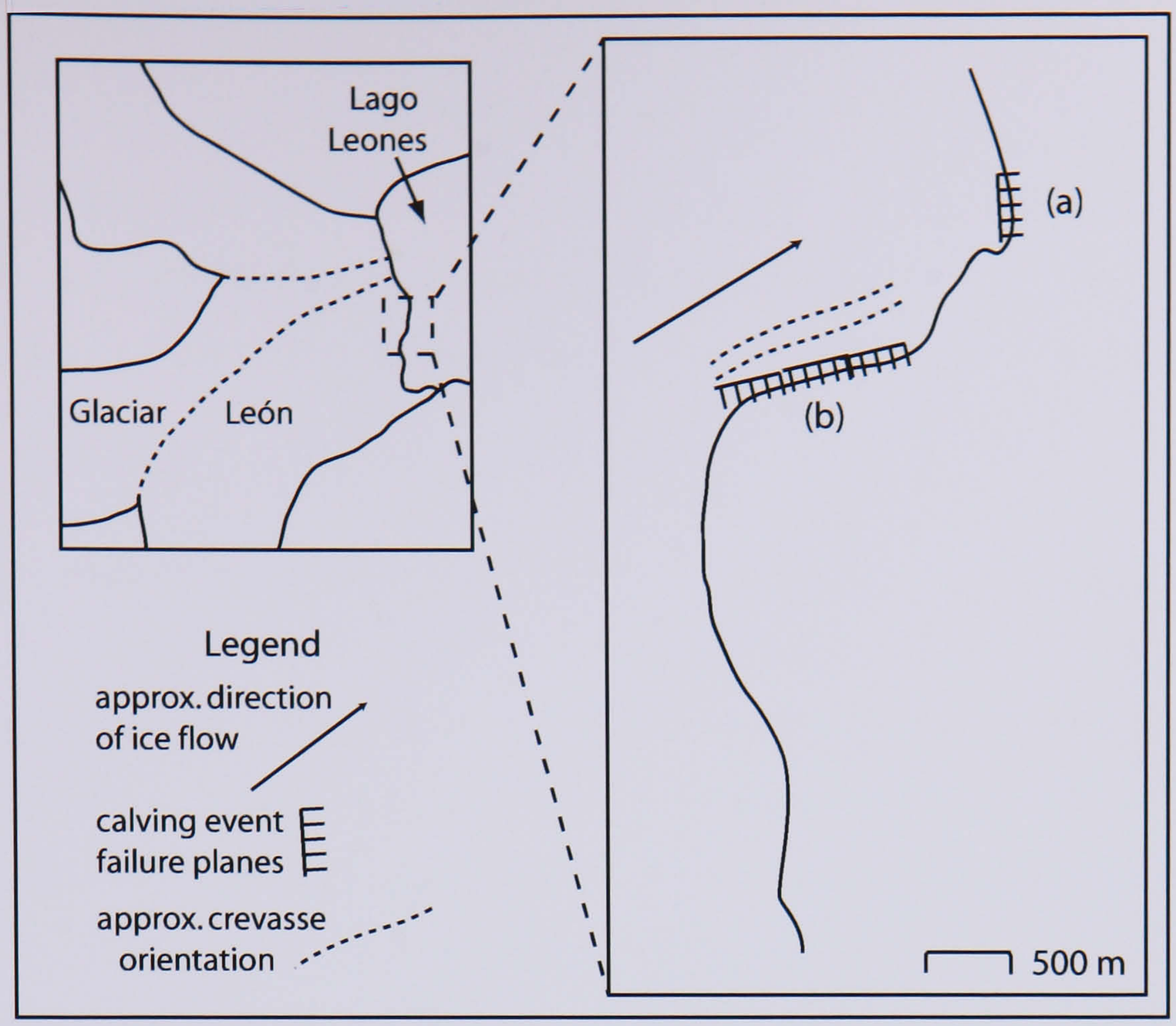

Figure 4.7 Orientation of crevasses and the propagation of calving fractures at Glaciar León. (a) Full-height events of large subaerial ice blocks occur perpendicular to the crevasses which are advected into the terminus, whilst (b) full-height lamellae calve parallel to these crevasses.

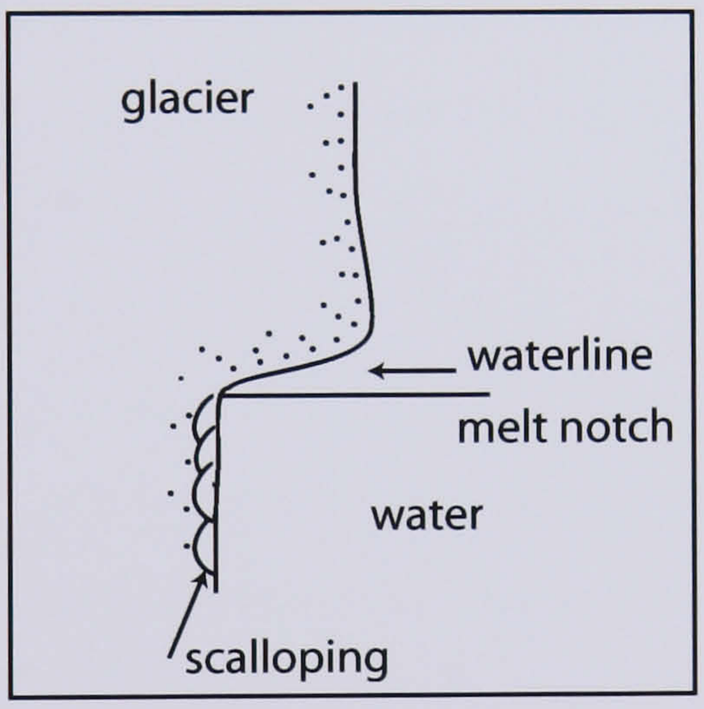

Figure 4.8 Schematic vertical cross-section of the geometry of the ice cliff at the waterline, November 2002, showing the presence of a thermo-erosional melt notch at the waterline and scalloping of the subaqueous ice face.

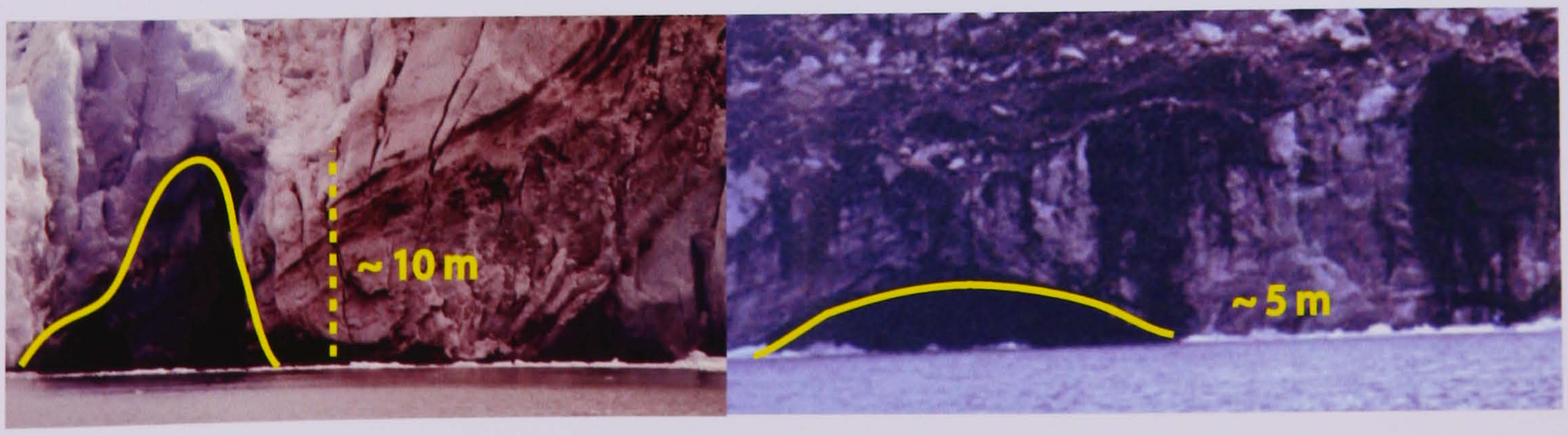

Figure 4.9 Caverns at the waterline., October / November, 2001 and 2002. (A) High, narrow caverns in the central section of the ice cliff, and (B) broad, low caverns to the north.

In the central section, a cavern was sometimes revealed, following several calving events at that point on the cliff that occurred during the previous 3-4 hours. Subaqueous events were sometimes observed to occur at such times. Caverns often re-developed in the same location.

As well as visual observations of calving activity, audible clues to the behaviour of the glacier were available. Before large calving events, loud cracking noises could be heard within the glacier. It is likely that this represents the opening of internal crevasses. On October 24, 2002, the sound was akin to rumbling of water, and was not always followed by a calving event, although ripples were observed to emanate from the southernmost corner of the ice face, which could not be attributed to wind action. Tiny streams also intermittently flowed over the bedrock underlying the ice in the southern section of the terminus, from November 4, 2002, providing evidence for a link between calving event timing and changes in glacier hydrology.

Floating ice covers very little of the lake surface beyond the immediate ice-proximal area, and all except the larger icebergs melt within 24 hours. Even large icebergs rarely reach the distal end of the lake, mostly melting within 3-4 km of the glacier. At the terminus, icebergs and brash ice are always present and sometimes form a continuous cover extending many tens of metres beyond the ice cliff (Figure 4.5). Although this floating ice is not static, and patches of open water within brash ice are sometimes maintained close to the ice front, there is no evidence of persistent, strong plumes of upwelling meltwater.

4.3.1.ii Ice surface velocity

Ice velocity was calculated for the maximum duration available for each serac (Appendix A). Ice surface velocities in each of the three zones across the glacier were distinctive, and are summarised in Table 4.4 and Figure 4.10.

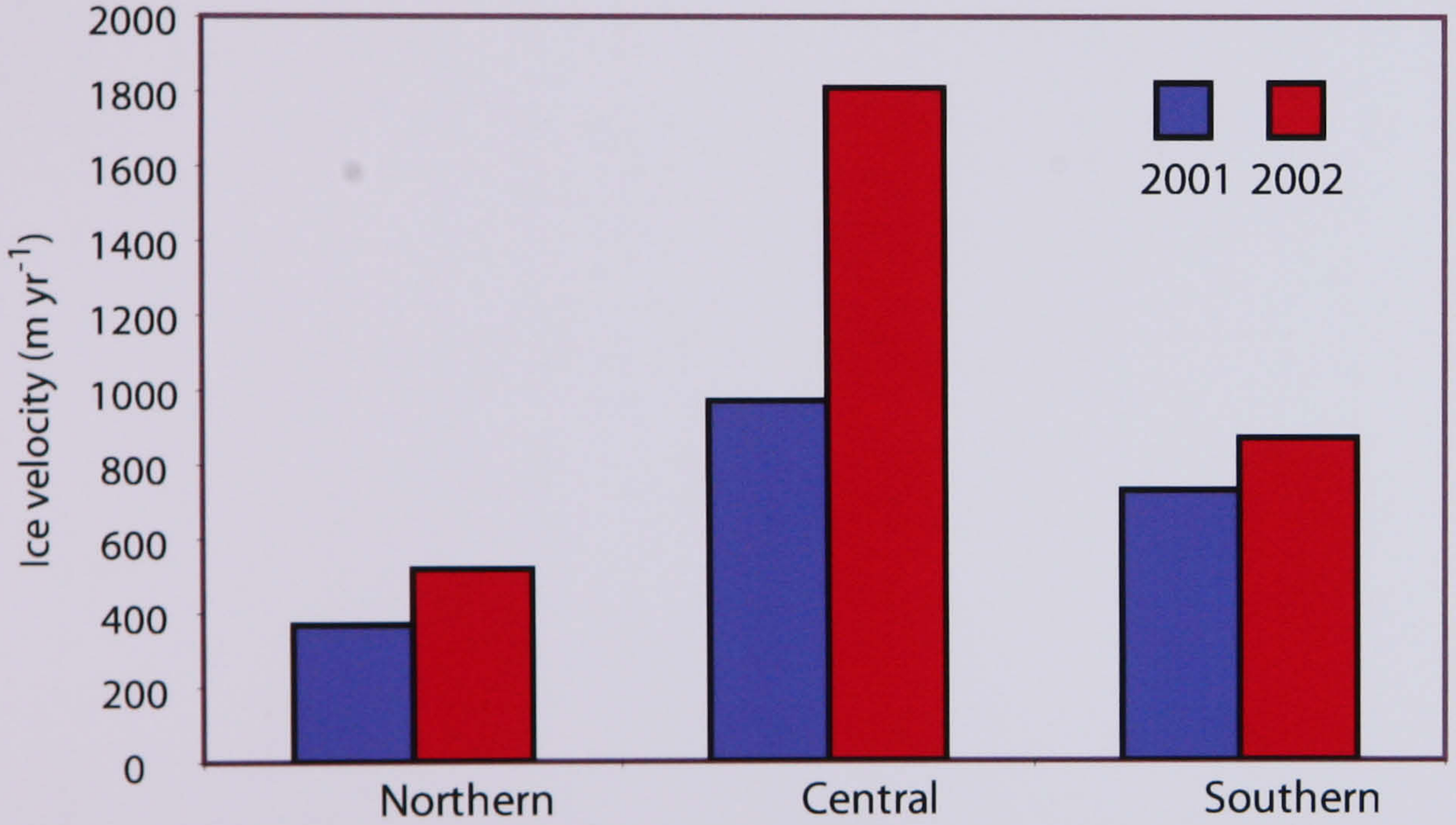

Figure 4.10 Ice surface velocities for each section of the terminus of Glaciar León in 2001 and 2002.

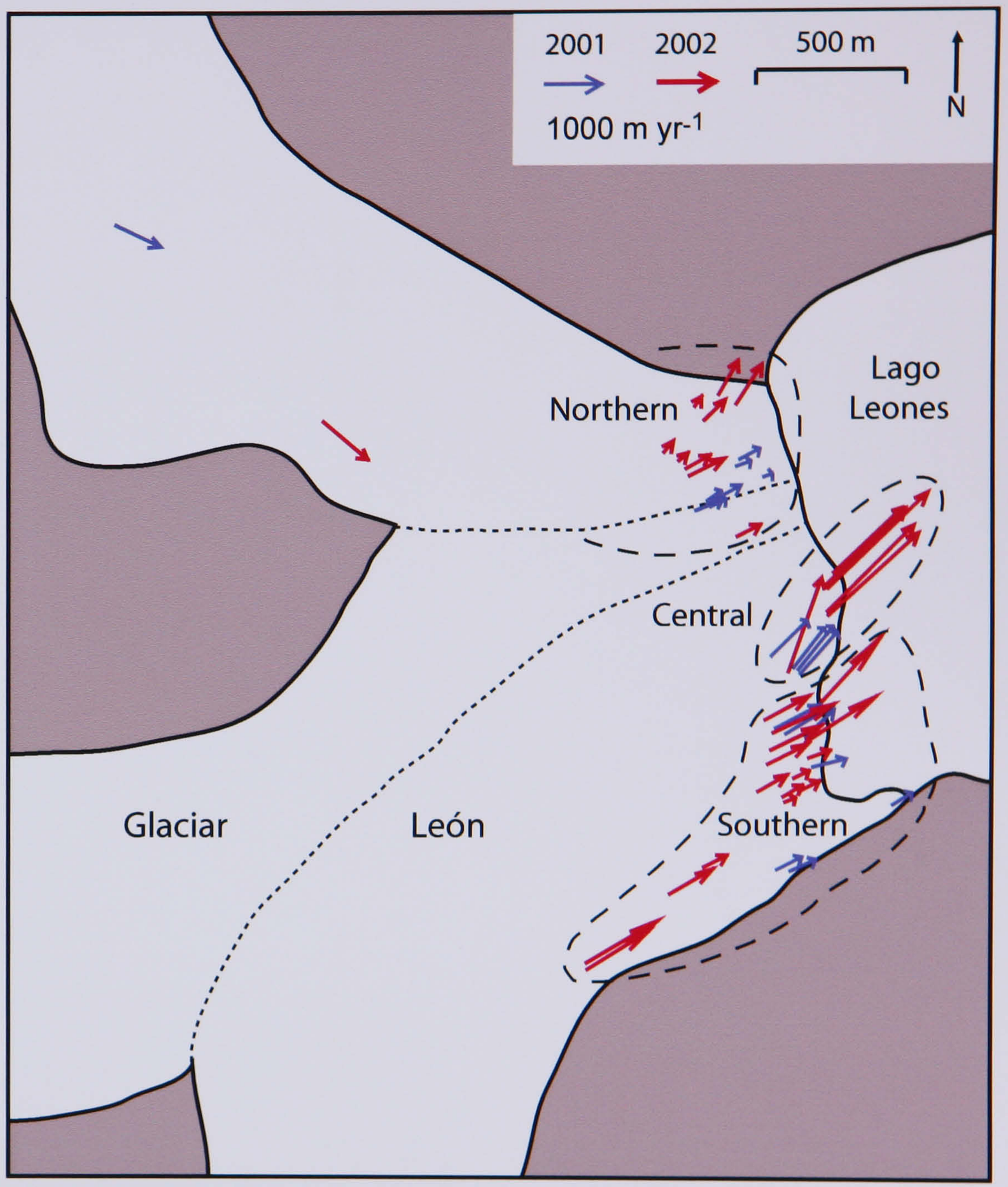

Figure 4.11 Ice velocity vectors for the terminus area of Glaciar León in November 2001 and 2002. Ice front position is for November 2002.

Glacier section	Ice velocity					
	2001		2002		Mean	
	(m d^{-1})	(m a^{-1})	(m d^{-1})	(m a^{-1})	(m d^{-1})	(m a^{-1})
Northern	1.0	370	1.4	520	1.2	450
Central	2.7	970	5.0	1810	3.8	1390
Southern	2.0	730	2.4	870	2.2	800
Width-averaged mean	1.9	690	2.9	1070	2.4	880

Table 4.4 *Surface ice velocities of Glaciar León measured over 36 days in the austral springs of 2001 and 2002. The values in m a^{-1} are unadjusted extrapolations of the values given in m d^{-1}.*

The individual serac velocities are plotted in Figure 4.11, which shows each ice velocity as a scaled vector, with the initial position of the serac located at the origin of each arrow. Calculated serac positions from survey data were transposed onto the base map, using the fixed markers of the survey baseline and the 'zero' point. The seracs are colour-coded to distinguish between the markers measured in each year. Ice flow is predominantly perpendicular to the terminus cliff except in the north, where flow towards the lateral margin is recorded. The fastest flow occurs closest to the central projecting section of the ice cliff, and fast flow is also notable in the steep icefall areas of the northern and southern tributaries. The distribution of the velocities is as expected, with slower velocities towards the lateral margins, where drag is higher. However, the range of individual serac values for each section is large (Table 4.5).

Glacier Section	Range (m a^{-1})	
	2001	2002
North	160-730 (570)	220-870 (650)
Central	910-1040 (130)	1590-2640 (1050)
Southern	350-1050 (700)	210-2040 (1830)

Table 4.5 *Maximum and minimum ice velocity values for each section of Glaciar León in each year, with this range given in brackets.*

The high velocities at Glaciar León are perhaps unsurprising, given the presence of large icefalls just up-glacier of the current location of the terminus, and that the lower glacier is steep and pervasively fractured. Ice velocities are in the middle of the range of those of Patagonian glaciers (Table 3.1). Those terminating in the sea on the west typically flow at speeds over ~1500 m a^{-1}, and are much greater than those located on the east side of the icefields, which flow at speeds in the region of a few hundred meters per year (Warren & Aniya, 1999). Lake-calving glaciers in New Zealand also flow much slower (Warren & Kirkbride, 2003). For comparison with published results for other calving glaciers, the width-averaged mean is also given, at 880 m a^{-1}.

The annual values extrapolated from the short-term surveys ignore seasonal variations. However, whilst surface ice velocities are known for only a few of Patagonia's lake-calving glaciers (Warren & Aniya, 1999), seasonal variations are thought to be negligible in Patagonia (~ 5 % summer-winter difference), due to high, year-round precipitation and relatively mild winters, permitting continuous basal sliding (Rott *et al.*, 1998; Skvarca *et al.*, 2003). Strain heating and sliding friction associated with high flow speeds will also contribute meltwater to the basal hydrological system, creating positive feedback for maintaining fast flow. However, given the different characteristics across the ice front e.g. exposed bedrock in the south, the separate source tributaries feeding each section, and the large range of velocities, the width-averaged value is of limited use for aiding our understanding of the processes responsible for these rates and the variations seen. Ice velocities also vary greatly between the two years, and with distance behind the terminus. Surface ice velocities are significantly and consistently faster in 2002 than in 2001. The most straightforward explanation of this is the greater frequency of rain days in 2002, combined with the higher minimum temperatures (4.3.2), both of which would increase meltwater volumes and enhance basal sliding. However, in the central section, where 2001 values are ~ 50 % of those in 2002, the position of the seracs in 2001, further back from the terminus, may account for these differences, as extensional flow characterises the terminus zone.

To examine ice velocities in greater temporal and spatial detail, ice velocities were calculated within three shorter periods in 2002. These provide velocity values with which to calculate calving rates for each zone, and over each time period (5.1), along with measurements of terminus changes (4.3.1.iii), and they are summarised in Table 4.6.

Zone	Ice velocity (m d^{-1}) (2002)		
	Period 1 (17-26 Oct)	**Period 2 (26 Oct-4 Nov)**	**Period 3 (4-11 Nov)**
Northern	1.5	2.0	1.6
Central	5.0	-	-
Southern	1.7	2.1	2.9

Table 4.6 *Ice velocities for each glacier section, calculated over three short periods in 2002.*

Ice velocities are generally higher in Period 2 than in Period 1. Some markers have slower ice velocities in Period 3 than in Period 2. However, not all the seracs were measurable in each period. In particular, it was impractical to select seracs in the central section close to the ice cliff, as calving was so rapid that markers rarely persisted from survey to survey. However, markers further back from the ice cliff were rarely available, as the terminus geometry often obscured the ice surface just back from the ice cliff.

In an alternative approach, photogrammetry was used to trace the path of features on the central ice cliff. Key features of the cliff geometry were identified between each pair of photos. The scale calculated from the ice cliff height calculations (4.2.2.iv) allowed the displacement between the 6–9 features on each pair to be measured, as shown in Figure 4.12. It was necessary to assume that displacement was purely perpendicular to the 2D plane of the photographs, and it was not possible to use all photos as corresponding features were not always available. The values obtained are shown in Table 4.7.

Values are only accurate to the nearest half-meter. Whilst more accurate measurement from the photo pairs is possible, delineation of the features and terminus outline is not precise enough to allow velocities of higher accuracy to be calculated. The complexity and rapidly changing nature of the terminus geometry required a balance between the camera focal length and the field of view available. Furthermore, the clarity of the photos is affected by the sun angle, particularly important for precise co-registering of the photos on the rock features, which were some 1.5 km away.

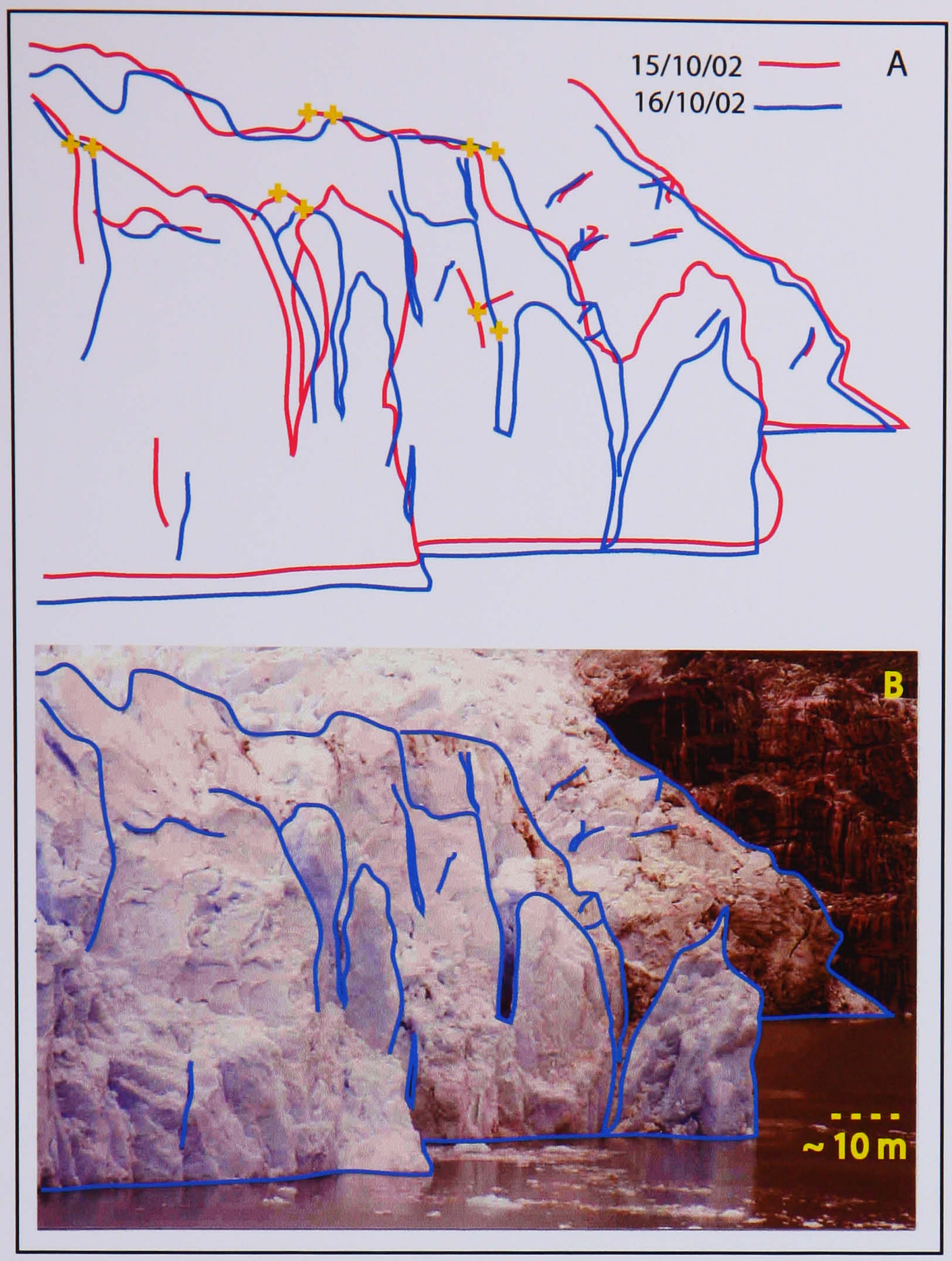

Figure 4.12 Calculating ice velocities using photogrammetric methods. (A) An example of a photo pair (15-16/10/02), and the selection of features used to calculate velocity (+). (B) The original photo (16/10/02) from which the above analysis was made . The scale relates to the ice cliff in the foreground.

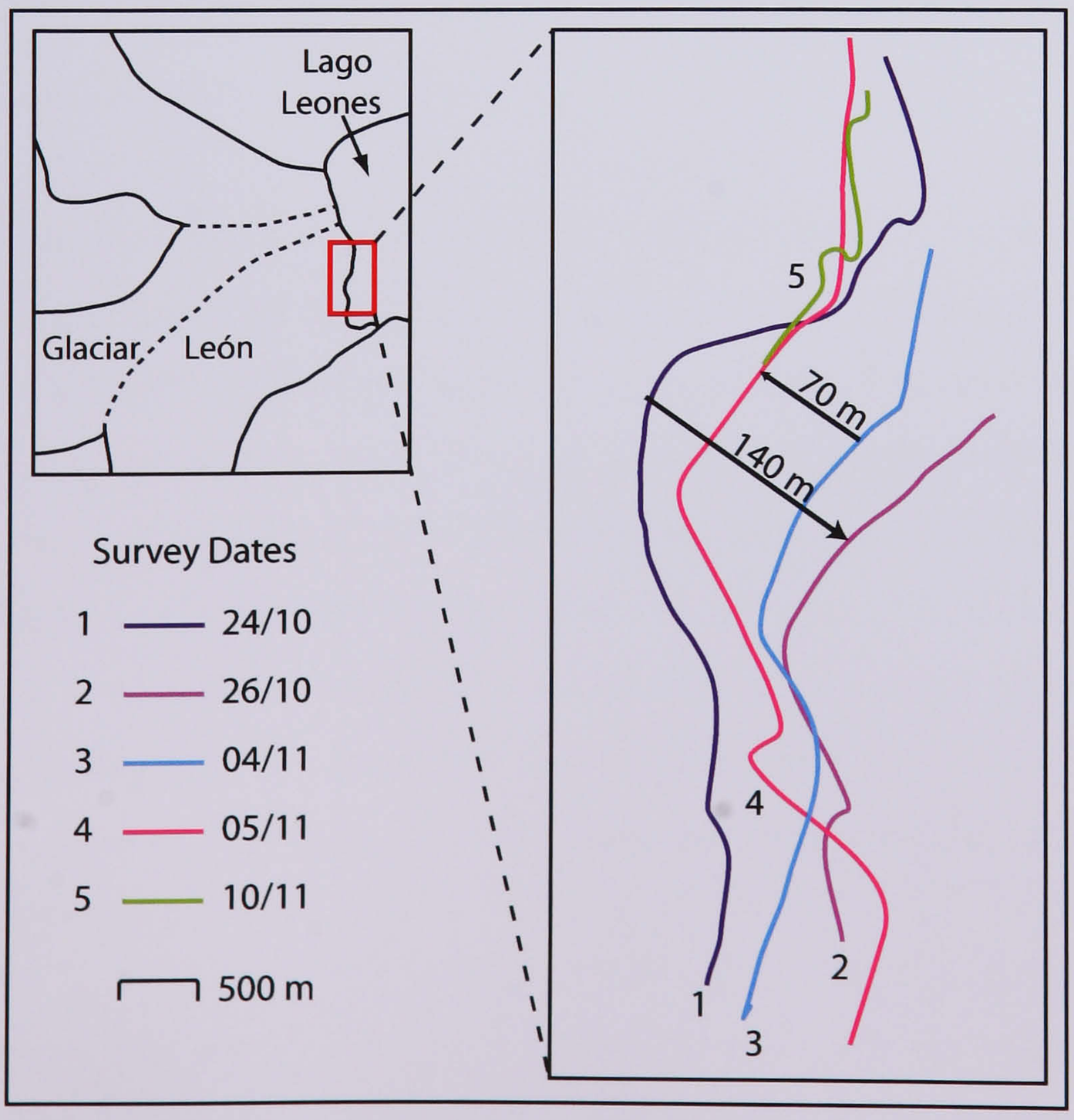

Figure 4.13 Terminus positions of Glaciar León between 24/10 and 10/11, 2002.

Date (2002)	Period	Average ice velocity (m d^{-1})
15-16 Oct	1	5.5
16-18 Oct	1	2.5
18-20 Oct	1	2.5
24-26 Oct	1	10.0
6-8 Nov	3	5.0

Table 4.7 *Ice velocities calculated from photogrammetric analysis, to the nearest 0.5 m, for the central section of Glaciar León during 2002.*

Ice velocities show a similar increase during the observation period to those calculated from the triangulation surveys (Table 4.6) for the northern and central sections, except for the large values seen from October 24 – 26. It was not possible to determine ice velocity during Period 2 (Table 4.6), as none of the initial features were recognisable at the end of the period. The average of the ice velocities calculated over this short time period using photogrammetrical methods is consistent with those calculated by survey. Although this average value may be extrapolated to give the same annual value as obtained in Table 4.4, large variations are observed. Processes affecting iceberg calving clearly vary on timescales of hours and days.

4.3.1.iii Terminus change

Annual terminus change was documented by calculating the displacement of the most forward projecting point of the central cliff top, between two sets of paired dates, as shown in Table 4.8. Although these are the only available measured values, they are very closely similar, and provide an indication of the order of magnitude of annual change. A visual comparison of photographs of the terminus between the two years also suggests that the northern and southern sections did not advance. Additionally, aerial photos taken at the end of November in 1998, 1999 and 2001 from a small plane also show that ice front variation is negligible in the south and north (Aniya, *pers. comm.*). This emphasizes the need to consider calving in each of the three zones separately, rather than using only width-averaged values.

Period	Terminus change (m)
08/11/2001-08/11/2002	-51
12/11/2001-11/11/2002	-52
Average	-52

Table 4.8 *Terminus change for the central section of the ice cliff between two sets of paired dates, between 2001 and 2002, positive in the direction of retreat, to the nearest meter.*

Over shorter timescales, during the field season in 2002, changes in terminus position were documented by surveying the position of the subaerial cliff along the waterline in the central and southern sections of the terminus. The plotted positions are shown in Figure 4.13, showing a clear advance between October 24-26, followed by a retreat between November 4-10, a sequence supported by photogrammetry. The fluctuations indicate displacements of up to ~ 140 m. However, these terminus oscillations are oriented obliquely to ice flow. These large oscillations represent calving activity that occurs along the crevasses advected to the terminus (4.3.1.i).

Quantitative measurements of short term terminus change were also calculated from triangulation surveys of the most forward projecting point on the ice cliff, in the central zone. The Cartesian grid on which ice velocities and displacements are plotted is such that the x-axis lies almost parallel with the direction of flow at this point on the terminus. The displacements of this point in the x-axis direction, over the measurement period, are given in Table 4.9. A rapid advance (3 m d^{-1}) occurred between October 24-26, in between two periods of rapid retreat (3 and 6 m d^{-1}, respectively). This advance coincides with that shown by the cliff positions changes described above, and with the rapid velocity measured using the photogrammetry. Although the net terminus change from October 26 to November 4 is retreat, it is possible that the sign of terminus change altered some time during this 10-day period, with terminus advance continuing for a few days before rapid retreat commenced.

Date (2002)	Displacement (m d^{-1})
17-20 Oct	1
20-24 Oct	3
24-26 Oct	-3
26 Oct-04 Nov	2
04-05 Nov	6
05-08 Nov	1
08-11 Nov	1

Table 4.9 *Terminus fluctuations of the central ice cliff, from survey analysis, positive in the direction of retreat.*

4.3.1.iv Melt rates

Subaerial melting

These can be estimated from the ablation stake data at the glacier margin (Table 4.10) and yield a mean rate of 0.04 m d^{-1}.

Date	Ablation rate (m d^{-1})
23-24 Oct	0.06
24-25 Oct	0.05
25-26 Oct	0.04
26-27 Oct	0.01
10-11 Nov	0.04

Table 4.10 *Ablation rates at Glaciar León, 2002, measured at the southern margin, (23/10-10-11), showing values obtained over 24-hour periods*

Whilst rates were consistent between the four stakes during each measurement period, the stakes melted out of the ice over periods longer than 24 hours, limiting the ablation record to the periods when access was possible every 24 hours. Melt rates on the debris-free, vertical cliff face are likely to be lower than this (perhaps by 50%, cf. Kirkbride and

Warren, 1997), so this figure provides an upper boundary. This average spring rate is lower than summer rates reported at New Zealand lake-calving glaciers (0.07 m d^{-1} (Kirkbride and Warren, 1997); 0.08 m d^{-1} (Purdie & Fitzharris, 1999); 0.06-0.1 m d^{-1} (Roehl, 2003); 0.05 m d^{-1} (Warren & Kirkbride, 2003)) and at the tidewater LeConte Glacier (0.1 md^{-1} (Motyka *et al.*, 2003)).

Waterline melting

The rate of waterline melting was assessed by surveying the size of waterline notches in October-November, 2002. On the central part of the ice cliff, where the greatest calving activity took place, notches with a horizontal depth of up to 6.3 m developed. The notch sizes are presented in Table 4.11, to the nearest 0.1 m.

Date (2001)	**Notch size (m)**	**Date (2002)**	**Notch size (m)**
08-Nov	0.0	24-Oct	5
10-Nov	4.7	26-Oct	0.8
12-Nov	3.1	04-Nov	4.6
13-Nov	6.3	05-Nov	1
15-Nov	4.2	08-Nov	5
17-Nov	0.6	11-Nov	3.3

Table 4.11 *Melt notch sizes at the waterline in the central ice cliff of Glaciar León, calculated from survey analysis, to the nearest 0.1 m.*

Some of the measured melt notches were used to calculate a linear melting rate, as summarised in Table 4.12, below. These values apply to the central section of the ice cliff.

Period	**Melt rate (m d^{-1})**
08-10/11 2001	2.3
12-13/11 2001	3.2
25-26/10 2002	0.8
08-11/11 2002	1.1
Average	1.9

Table 4.12 *Waterline melt rates at Glaciar León.*

Melt rates were greater in 2001 than 2002. This may be due to several factors. Greater input of meltwater is apparent in 2001 from lake level changes (4.3.2.i), and the extra meltwater discharge may lead to higher subaqueous melt rates (Weeks & Campbell, 1973). Alternatively, the higher velocities noted in 2002 may have caused the ice to disintegrate more extensively as it flows towards the terminus, causing calving events to occur more frequently, although it is not possible to know this without a continuous record of calving event timing and size (4.3.1.i). It is possible that calving of small flakes from the leading edge of the notch, undetected by survey or photogrammetry, have modified the melt notch under investigation, so that the apparent melt rate is lower than the true rate. Water temperature differences are not thought to be the cause, as surface temperatures are consistently warmer in 2002 throughout the field season (4.3.2.ii). Despite the uncertainty, waterline melt rates appear to be an order of magnitude greater than inferred rates of melting on the subaerial ice cliff. These waterline rates also provide an upper limit for subaqueous rates because maximum rates of aqueous melt are known to occur at the waterline (Eijpen *et al.*, 2003; Warren & Kirkbride, 1998).

4.3.2 Limnological Observations

4.3.2.i Bathymetry

The bathymetric data were formatted into a .csv file, for handling in ArcView. It proved difficult to GeoRegister the scanned map with the GPS coordinates using ArcInfo, so, in 2002, 456 positions of the lake perimeter were recorded on the GPS, providing ArcView with 0 m depths. This made it easier to create a 'point shape' file of the data, which could then be interpolated using the TIN (Triangulated Interpolation Network) method, with a known 0 m boundary. Contours were set at 50 m intervals. Transferring the TIN to Adobe Illustrator then permitted the conversion of these data to a contoured map, presented in Figure 4.14.

The data show that the lake comprises several basins, dissected by ridges believe to be moraines (Haresign *et al.*, submitted) at 3.5, 5.5 and 7 km from the glacier (Figure 4.15). They roughly correspond to slight bedrock narrowings in the valley sides. The ridges rise up to ~ 100 m from the lake floor. The basins become deeper towards the glacier (Figure 4.15), reaching a maximum depth of over 360 m in the deepest part of the lake.

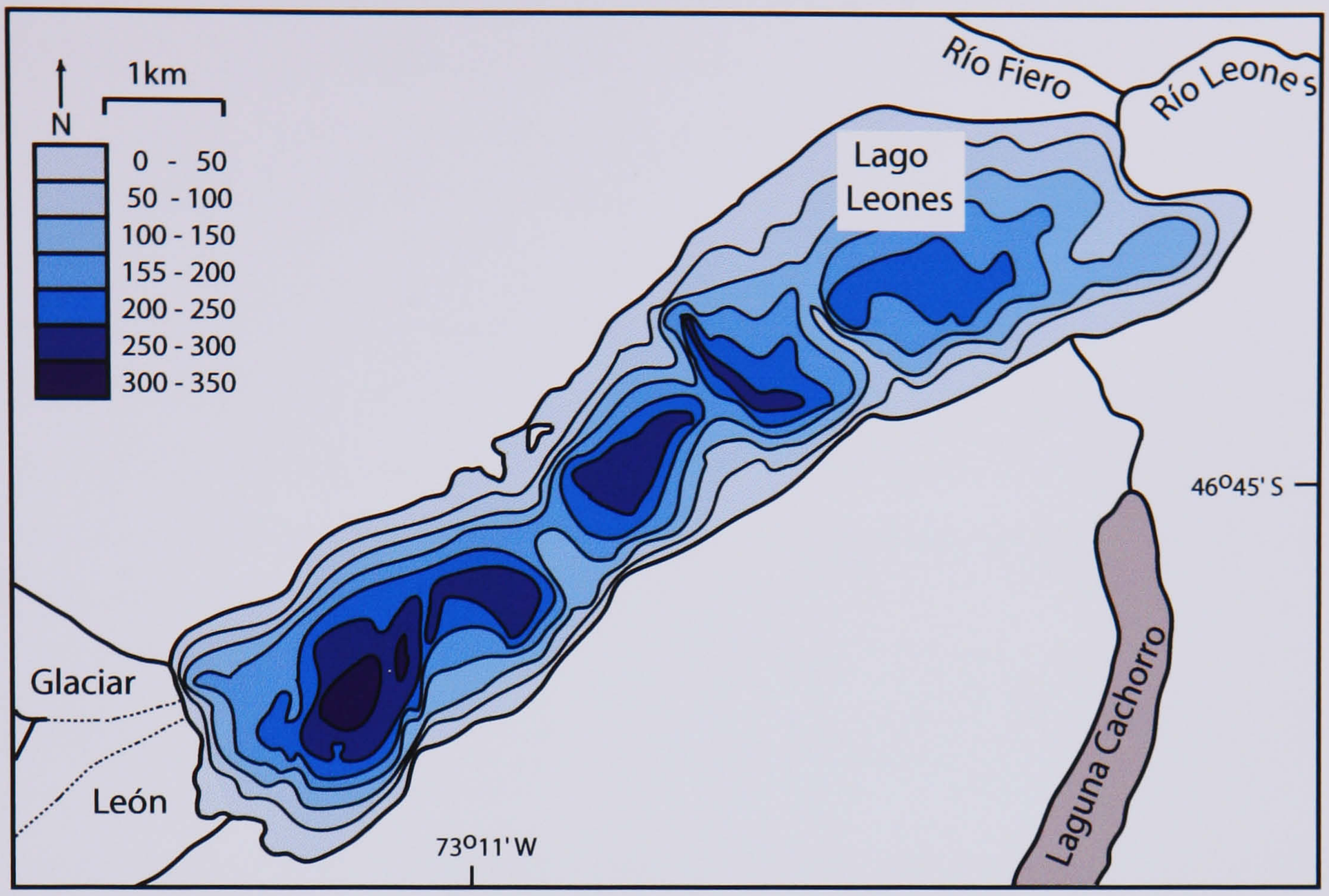

Figure 4.14 Bathymetric map of Lago Leones.

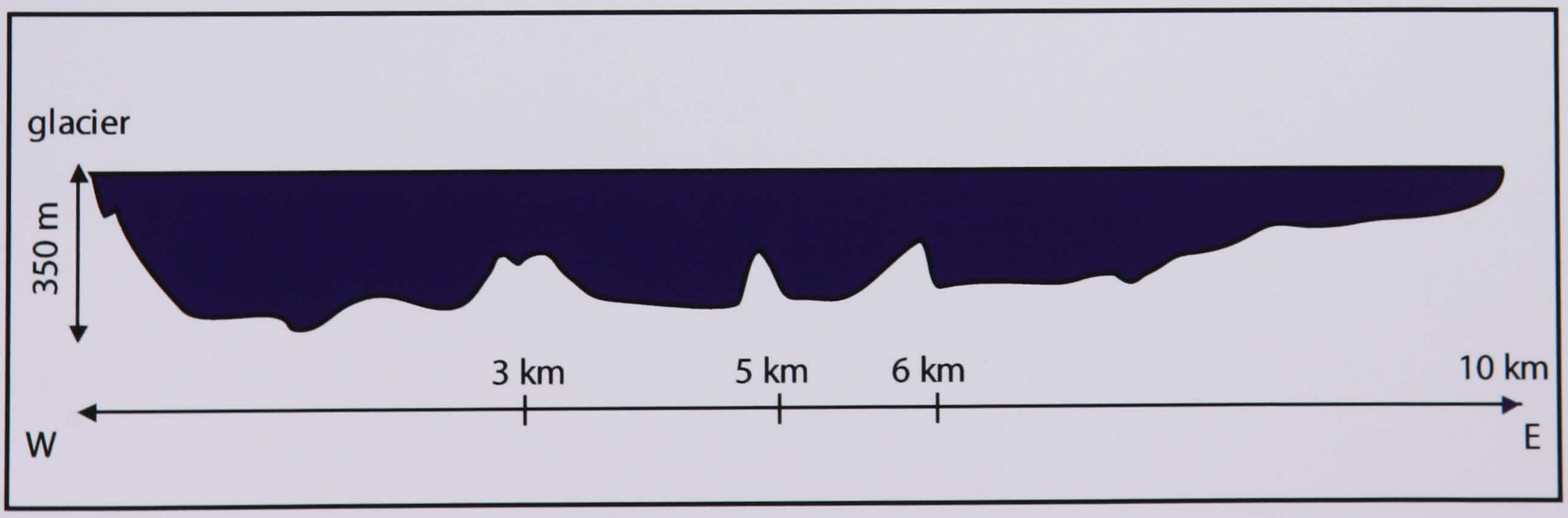

Figure 4.15 Bathymetric long profile of Lago Leones, illustrating the three ridges interpreted to be terminal moraines. Source: Haresign *et al.* (submitted).

However, the width-averaged ice-proximal depth is 65 m, shallow in comparison into maximum basin depths, and the lake floor must rapidly drop off into the basin over a relatively short distance. Cross-sections in the ice proximal area (Figure 4.16) show large variations in depth across the ice front, and it is possible that they relate to the three zones of ice velocity as well as the medial moraine.

During both 2001 and 2002 in the 'change-over period' (Table 4.1), the lake level rose at the end of October by 0.8 m and 0.3 m, respectively, indicating an input of meltwater of some 6 – 16 × 10^6 m^3, returning to its original level after about 5-10 days. In 2002, this coincides with the period of increased velocity and either follows or coincides with the localised terminus advance of the central section.

4.3.2.ii Water temperatures

Examples of temperature profiles seen in the ice-proximal area, mid-lake and the eastern end of Lago Leones are shown in Figure 4.17 (for the complete water temperature dataset, refer to Appendix B). Both stratified and isothermal conditions occur in the lake. Surface temperatures are typically 5-8 °C, cooling to about 4.5 °C at 100 m deep. Lake temperature conditions evolved through October and November from near-isothermal conditions with a warm surface (upper 5 m) layer in the ice-proximal area, to a thermal structure with more gradual cooling from the surface and weak thermocline development at 30-40 m deep, which develops westwards towards the glacier as the season advances (Figure 4.18). It is observed that the proximal-distal gradient was more pronounced in 2001 throughout the season than in 2002, where surface temperatures ranged from 5-8 °C throughout. There is no detectable diurnal warming.

Temperature range decreases with depth, and the greater range at the lake surface becomes more pronounced as the season progresses. In 2002, surface water temperature showed a larger seasonal range than 2001 and, at depth, warmer temperatures were experienced, although temperatures were warmer from 10-40 m in 2001. The water is generally warmer on the south than north side of the lake, as seen in the 2001 temperature profiles in Figure 4.19. Thermocline development on the south side of the lake is more clearly evident. The generally isothermal conditions seen on the north side may result from incoming meltwater to the lake being deflected to the left by Coriolis forcing.

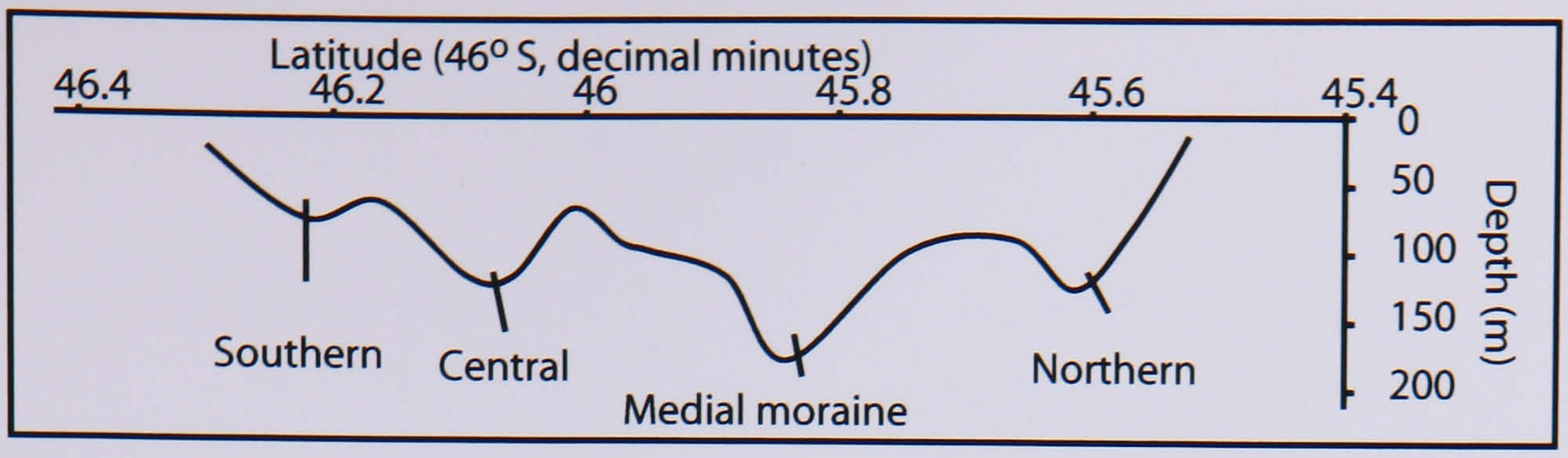

Figure 4.16 Ice-proximal bathymetric cross-section of Lago Leones, showing four deeper zones which coincide with the three zones characteristing the ice velocities, and a fourth zone which is aligned with the debris-rich medial moraine.

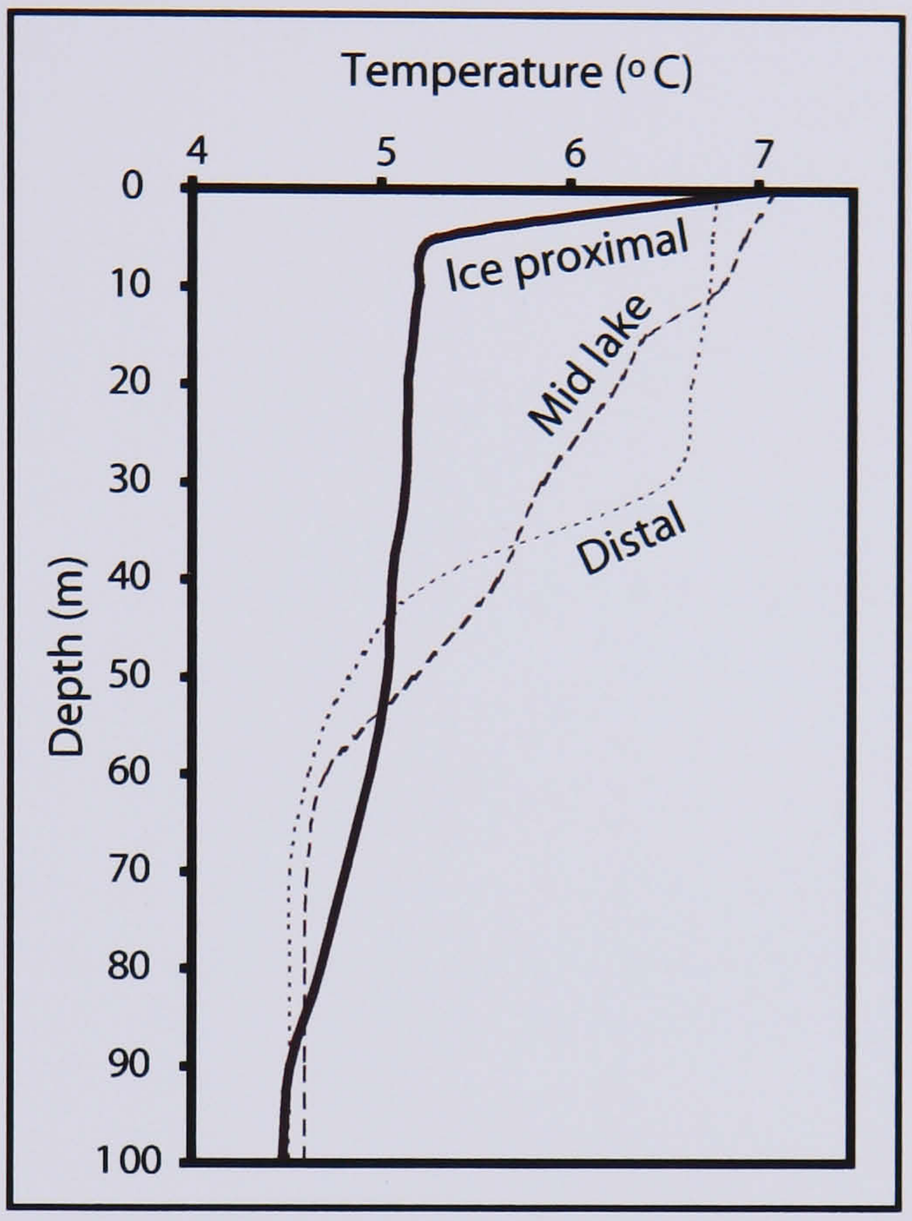

Figure 4.17 Examples of temperature profiles for Lago Leones, showing near-isothermal conditions in the ice-proximal waters and the development of a thermocline in the distal part of the lake.

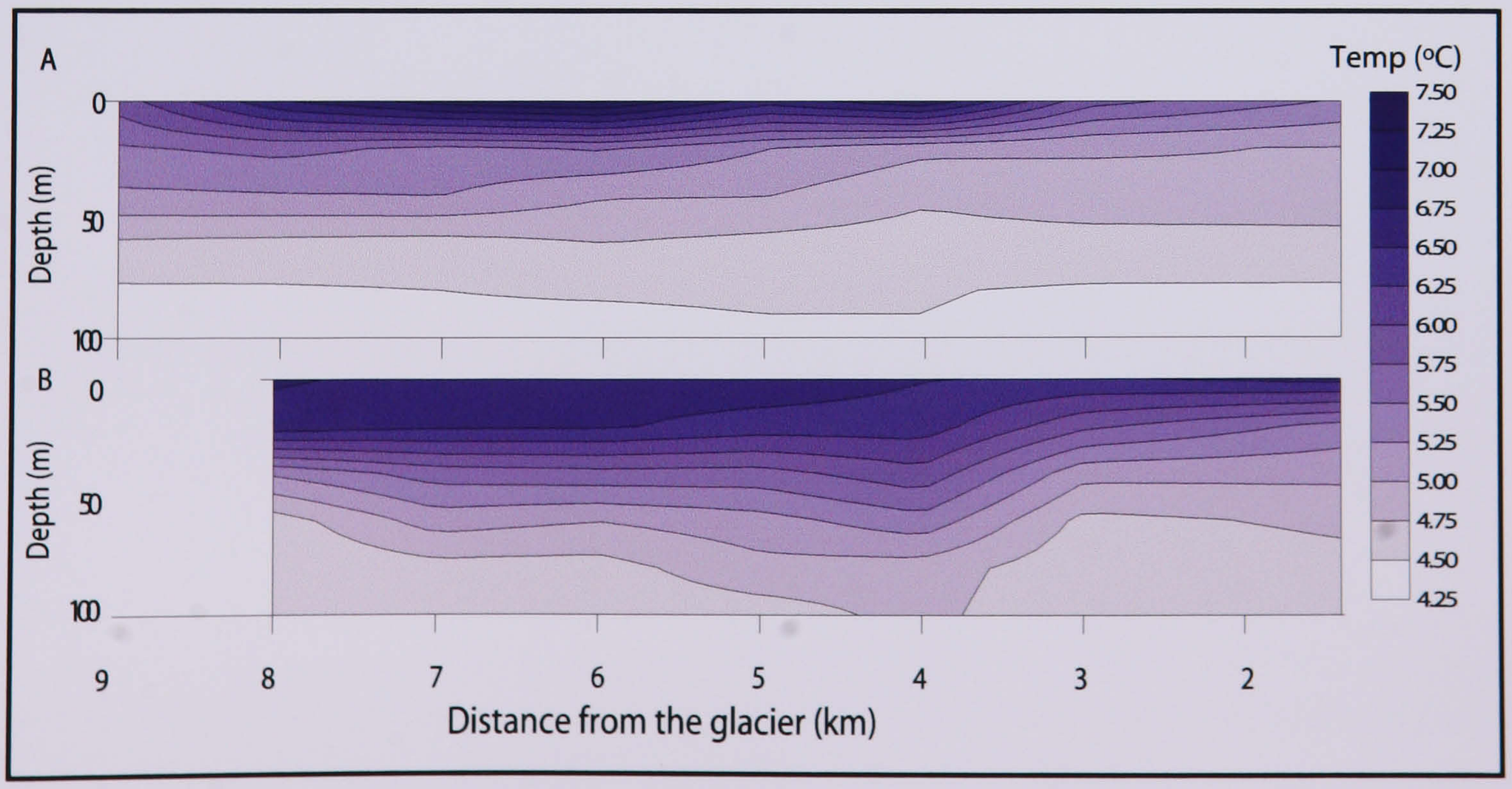

Figure 4.18 The evolution of water temperatures along the longitudinal cross-section of Lago Leones. Profile A (14/10/01) shows rapid cooling from a warm surface layer in the lake centre. Profile B (13/11/01) shows warmer water with more cooling at 30-40 m.

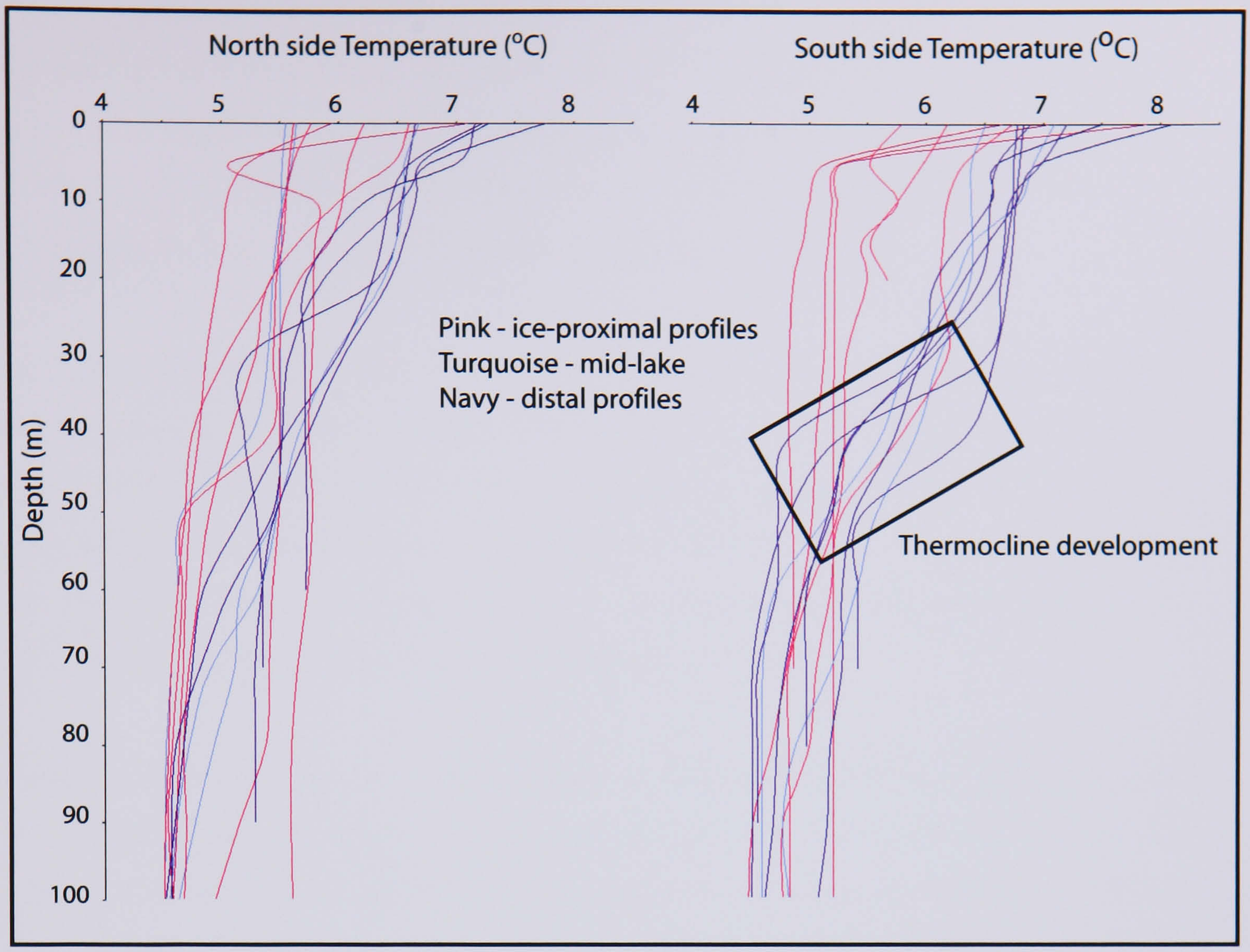

Figure 4.19 A comparison of temperature profiles from the north and south sides of Lago Leones in 2001. Generally isothermal conditions occur on the north side, whilst thermocline development is stronger in the south.

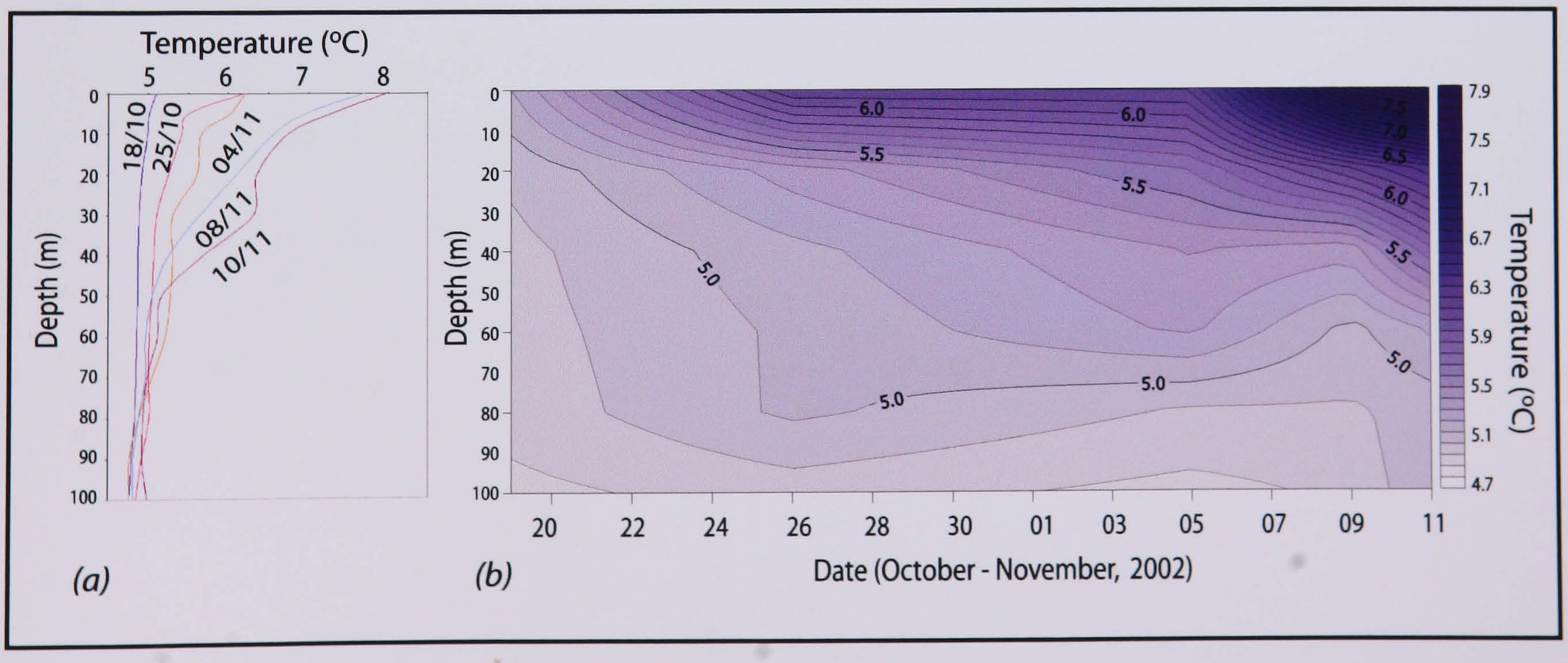

Figure 4.20 *(a)* Repeated temperature profiles taken from 46.7686°S 73.2115°W (see Figure 4.21, inset) between October 18 and November 10, 2002, showing progressively warmer temperatures. *(b)* Development of a thermocline at the location in *(a)* at ~ 30-50 m deep.

It is also possible that it result from lower insolation in the shadow of the mountain to the north of the lake. The thermocline development on the south side of the lake was also seen in 2002. Figure 4.20 illustrates this development in greater detail, with profiles taken from 46.7686°S 73.2115°W between October 18 and November 10, 2002.

Despite the general trend of cooling from the south to north side, there is little variation in temperature across the ice front (Figure 4.21a) although, in some cases, surface waters were slightly colder in the centre of the lake. On occasions, a second change in the cooling gradient in ice-proximal profiles occurs at 50-60 or 70-90 m (Figure 4.21b). Upwelling directly to the surface in front of the ice face is not expected at Glaciar León and these areas of cooling are perhaps indicative of an interflow of meltwater.

It was expected that an increased concentration of ice-proximal profiles in 2002 would reveal the locations of meltwater outflow from the glacier. Unfortunately, it was not possible to hold fixed GPS positions in the dinghy with sufficient accuracy to sample a dense enough network of temperature profiles to clarify this. It is only possible to identify tentatively a possible area of cooling at a depth of 50-60 m in the northern part of the lake in the ice-proximal zone.

4.3.2.iii Suspended sediment concentration

In the laboratory, the water samples were weighed along with Whatman filter papers of grade 542 (2.7μm), before the water was filtered and the sediment air-dried and weighed. Values range from 14-75 mg l^{-1}, as shown in Table 4.13. The average value was 37 mg l^{-1}.

Date	Location	Depth (m)	Concentration (mg l^{-1})
Oct-22	1	1	30
Oct-22	1	10	14
Oct-22	2	1	20
Oct-22	2	10	75
Nov-08	A	0.3	22
Nov-08	B	0.3	33
Nov-08	C	0.3	68

Table 4.13 *Values of suspended sediment concentration for Lago Leones in 2002.*

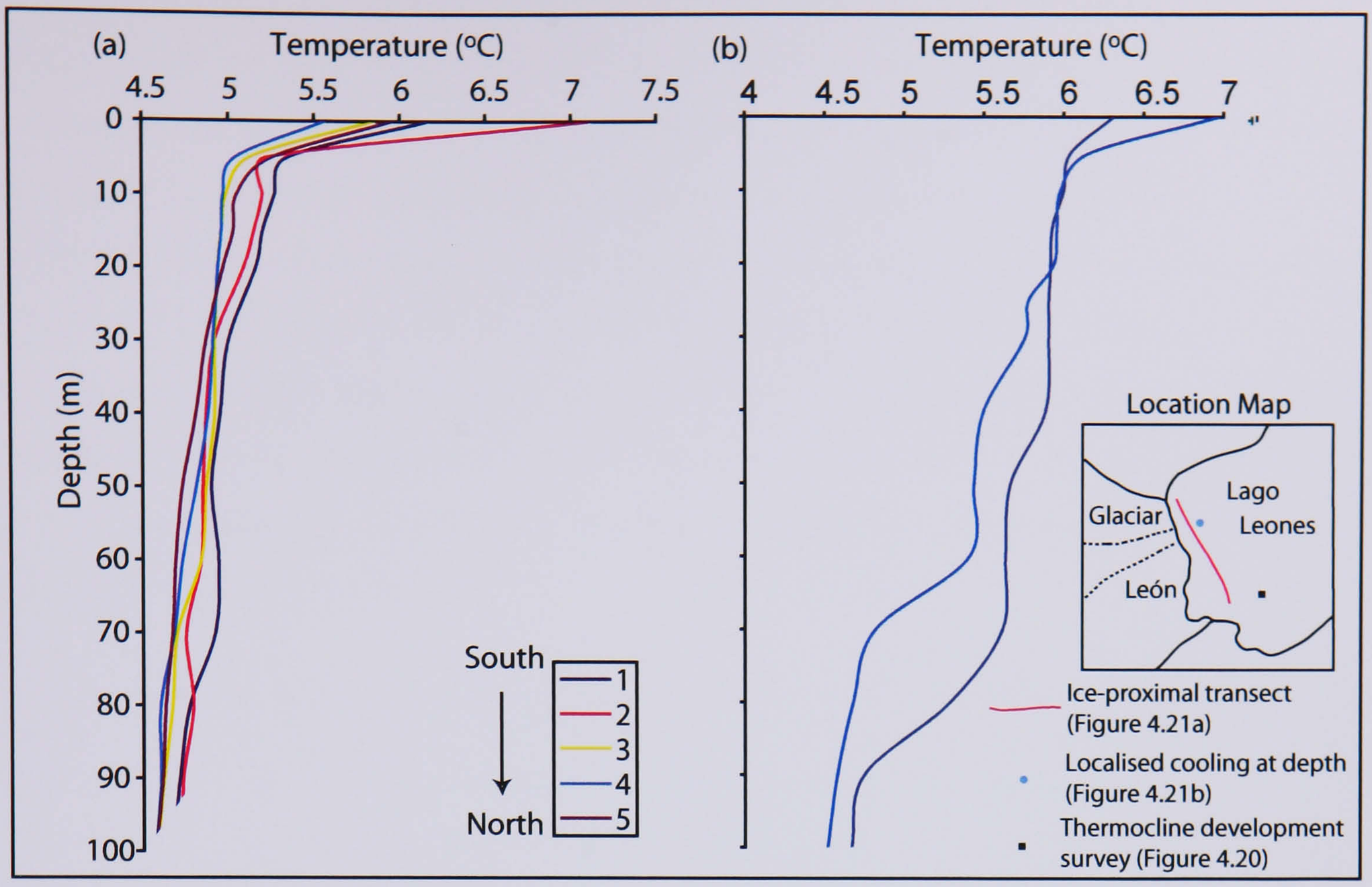

Figure 4.21 (a) Temperature profiles for an ice-proximal transect (inset) of Lago Leones, November 2002, showing cooling from south to north. (b) Localised cooling between 50 and 90 m deep.

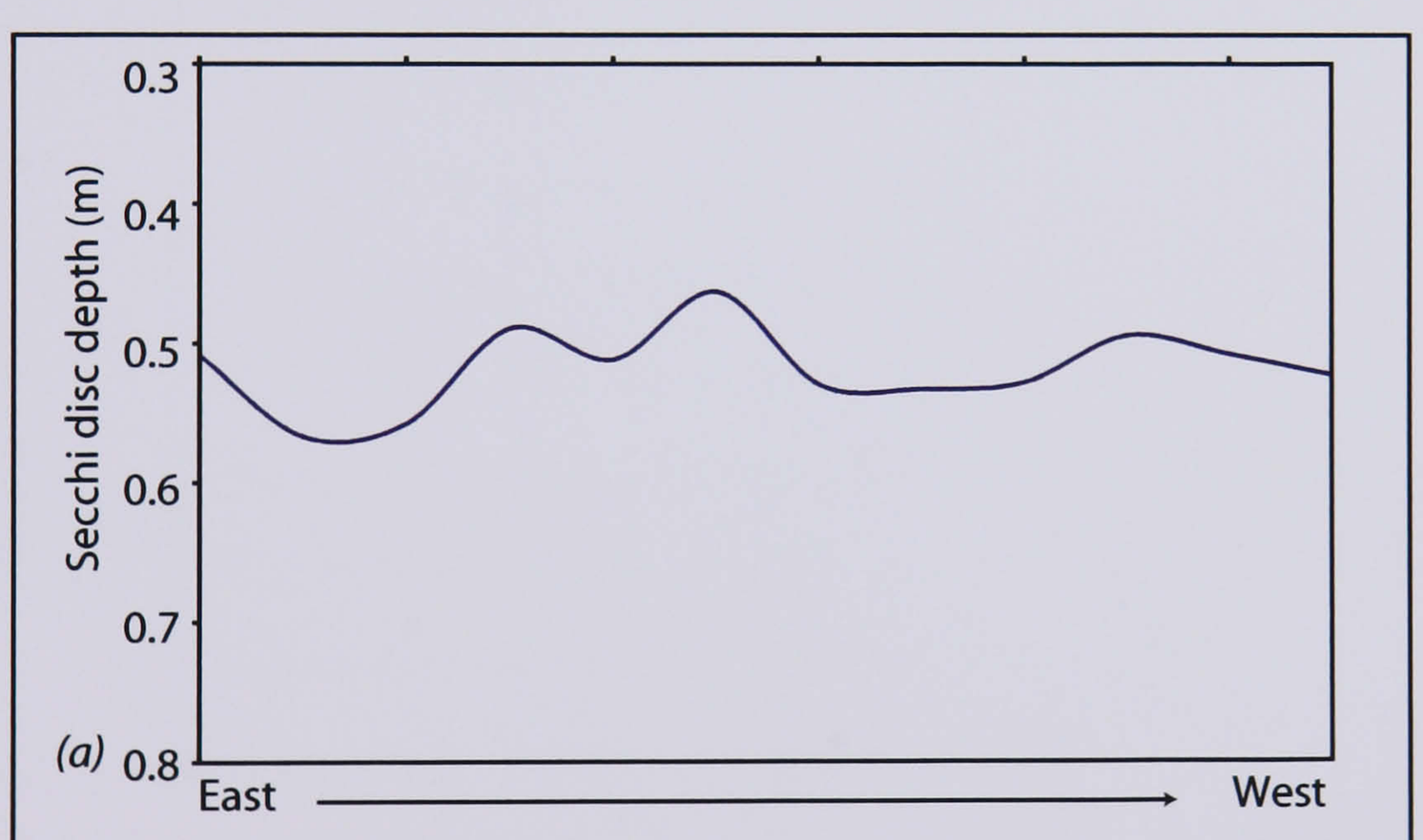

Figure 4.22 (a) Secchi disc measurements along the long profile of Lago Leones, October / November 2002. (b) Ice-proximal cross profiles of secchi disc measurements, as shown in Figure 4.4b.

The data show no obvious pattern of changes in SSC with depth, and no pattern across the front of the glacier. It was thought that samples A and B might lie in zones of concentrated meltwater input from the glacier. Sample A was taken directly in front of the central section of the ice cliff, where the presence of several caverns was suggestive of meltwater influx, (Figure 4.9). However, the values are not as high as expected (4.3.2.ii). It is also possible that the meltwater does not carry much sediment if there is little at the glacier bed. Given the steep nature of the terrain and the volcanic bedrock lithology (Clapperton, 1993), this may be true, in which case SSC may not be a reliable indicator of meltwater input at this site.

Lake	Ice contact	Concentration (mg/l)
Tasikutaaq Lake, Baffin Island		5.7
Hector Lake, Alberta		>8
Bow Lake, Alberta		15
Lower Waterfowl Lake, Alberta		17.2
Ape Lake, British Columbia		28.7
Garibaldi Lake British Columbia		30
Lillooet Lake, British Columbia		49
Lake Wakatipu, New Zealand		57
Stewart Lakes, Baffin Island	Y	109
Cascade Lake, Washington	Y	110
Hazard Lake, Yukon	Y	122
Unnamed, Purcell Mountains, B.C.		140
Sunwapta Lake, Alberta		380
Malaspina Lake, Alaska	Y	723

Table 4.14 *Maximum recorded concentration of suspended sediment particulate matter in the waters of glacial lakes (Menzies, 1995: modified from Gilbert & Desloges, 1987a).*

The SSC is low compared to that recorded at other ice-contact lakes (Table 4.14). Lake water density is not likely to be affected by sediment-rich meltwater influx i.e. sediment-stratified, although samples through the entire water column are not available for confirmation. Water at 0 °C is denser than that at 5-8 °C (2.2.2.i) so an overflow of

incoming meltwater is unlikely. However, meltwater inflow is known to be considerable on occasions (4.3.2.i), and must be dispersing into the lake as an interflow or underflow. This has been suggested by cooling in the water column at 50-70 m, but no further data are available.

The secchi disc measurements were taken after the lake level rise, in early November, and show consistent depths of ~ 0.52 m throughout the main body of the lake, indicative of thorough mixing (Figure 4.22a). In the immediate ice-proximal area, a mean Secchi disc depth of 0.50 m along the cross-profile closest to the glacier compared with a mean of 0.47 m from the cross-profile 300 m further down lake, indicating slightly clearer water close to the glacier (Figure 4.22b). In all three profiles, peaks in inferred suspended sediment concentration occurred in line with the central section of the ice cliff. Given the low values of SSC, the secchi disc values here are surprising, as they imply low transparency. Values of less than 1 m are usually only seen in the most sediment-choked proglacial lakes (Hutchinson, 1975). These large differences cannot be accounted for here. However, the SSC analysis is a less subjective, and more accurate, method, and these values are preferred as a reliable reflection of the state of sediment in Lago Leones.

4.3.3 Meteorological Observations

Maximum and minimum temperatures and rainfall figures are shown in Figure 4.23. Average values are shown in Table 4.15.

	Basecamp	**Glacier**
2001		
Temperature min (°C)	3.3	-
Temperature maximum (°C)	15.6	-
Rainfall (mm)	3	6.4
2002		
Temperature min (°C)	7.3	6.9
Temperature maximum (°C)	13.7	14.6
Rainfall (mm)	4.6	6.9

Table 4.15 *Weather data from Lago Leones in 2001(13/10 – 16/11) and 2002 (15/10 – 14/11), showing daily average values.*

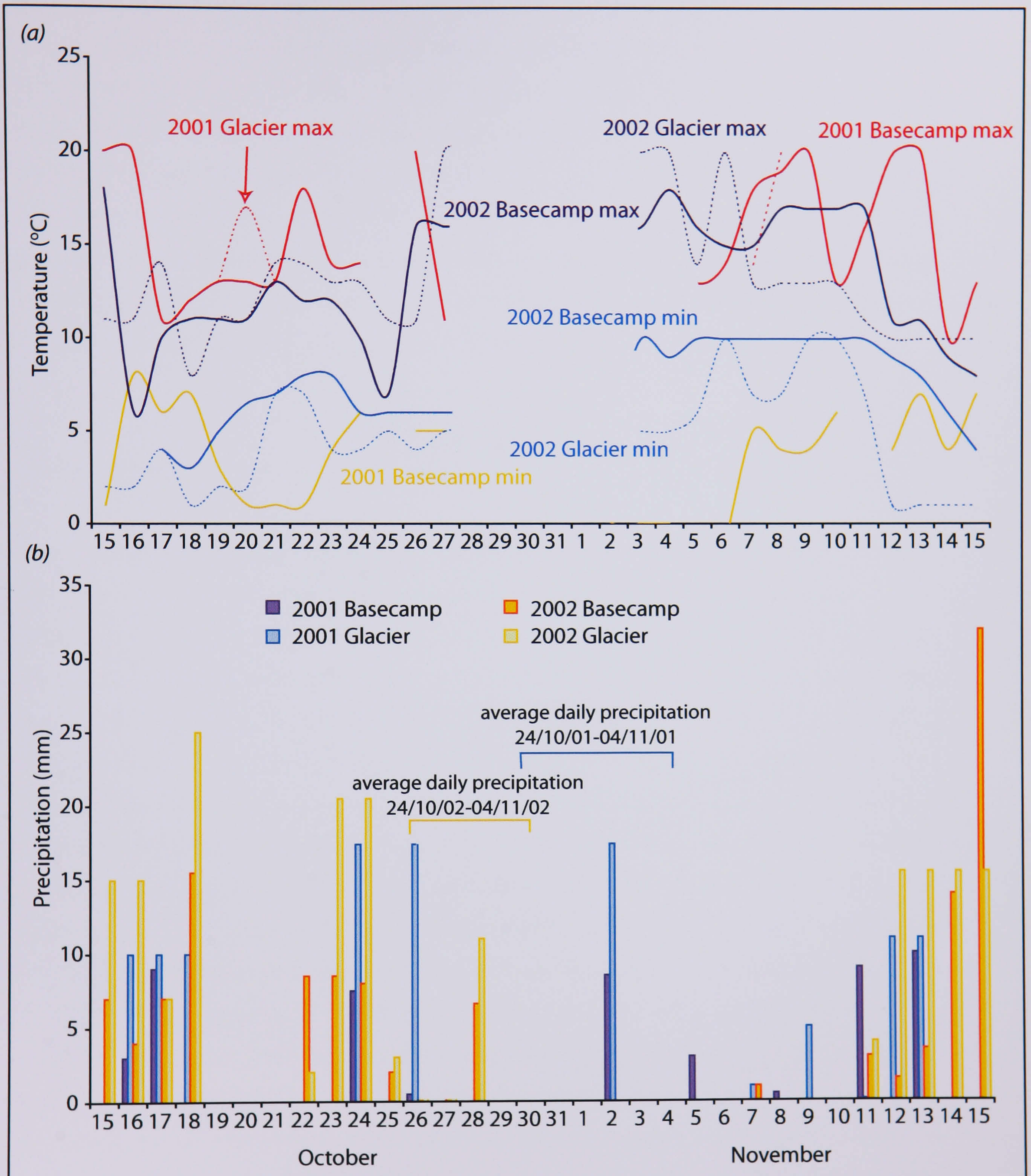

Figure 4.23 (a) Air temperatures for Glaciar León, at both basecamp and close to the glacier (Figure 4.2), for 2001 and 2002. (b) Precipitation values at Glaciar León, at both basecamp and close to the glacier, in 2001 and 2002. Where measurements were unavailable average daily figures are given for the highlighted periods.

Maximum temperatures occurred at ~ 1500 h. It was generally milder in 2002, with a smaller temperature range. Maximum temperatures at either end of the lake are comparable, whilst minimum temperatures are colder at the west end, by the glacier. Rain at the east end of the lake occurred on 43% of days in 2001 and 62% days in 2002. There is a substantial gradient in precipitation from the east to west end of the lake, of 0.3 mm km^{-1}. Precipitation quantities are often 30% greater by the glacier. The dominant winds were katabatic winds draining down the neighbouring Fiero valley (cf. Figure 4.2), typically in the afternoon. These predominated over katabatics from Glaciar León, typically leaving the ice-proximal area calm and free of waves. Winds of 16-22 km hr^{-1} were experienced most days, though gusts of up to 45 km hr^{-1} were recorded.

4.3.4 Summary

Glaciar León is an actively calving, lake-terminating glacier. Descending steeply from the NPI down an icefall, it terminates into water ~ 65 m deep with ice velocities in the austral spring up to an observed maximum of 10 m d^{-1}, although values of ~ 2-5 m d^{-1} are more typical, and a width-averaged annual rate of 880 m a^{-1}, which is high for lake-calving glaciers in Patagonia. Velocity varies spatially across the glacier front, with the highest values occurring in the central, most actively calving section, as well as temporally over diurnal timescales. Rates of terminus change are also variable, with short-term variations exceeding annually averaged diurnal rates. Terminus advance was observed during a period of increased ice velocity. Thermo-erosional waterline melt notches developed at rates up to ~ 3 m d^{-1}, several orders of magnitude greater than subaerial melt rates of ~ 0.04 m d^{-1}, and appears to facilitate calving by undercutting the subaerial portion of the ice cliff. Water temperatures at this site vary from ~ 4.5 °C at 100 m deep to a maximum of ~ 8 °C at the surface, with ice-proximal surface temperatures around 6-7 °C. Whilst the water is isothermal close to the glacier, a weak thermocline develops in the distal zone, extending towards the glacier as the season progresses. Despite low values of suspended sediment concentrations, large volumes of meltwater are implied by a lake level rise that occurred at the end of October 2001 and 2002. Precipitation occurred on ~ 50 % days, and was ~ 30% greater by the glacier. Daily average air temperatures ranged from 3.3-15.6 °C, and winds of 16-22 km hr^{-1} were experience most days.

CHAPTER 5

Glaciar León, Chilean Patagonia: Reduced Data and Discussion

5.1 CALVING RATES AT GLACIAR LEÓN

The calving rate (u_c in m a^{-1}) at Glaciar León can be obtained from the equation:

$$u_c = u_i - \frac{dL}{dt} - u_m \qquad \text{(Eq. 5.1)}$$

where u_i = ice velocity, dL/dt = rate of change in glacier length (between 2001 and 2002), positive in the direction of retreat, and u_m = melt rate at the calving face, all in m a^{-1} and width-averaged. In many calving studies, width-average values are used in this formula (Warren *et al.*, 1995a, 1995b; Warren, 1999; O'Neel *et al.*, 2001; Skvarca *et al.*, 2003). At this site, where the width-averaged terminus position is stable, (i.e. dL/dt is negligible), the ice velocity is balanced by the sum of calving and melting, i.e. $u_i = u_c + u_m$. For comparison with published 'calving rates' which disregard the melt term, the value of ($u_c + u_m$) at Glaciar León is therefore 880 m a^{-1}. However, the usefulness of determining calving in this way for understanding calving processes is limited (2.3.1), especially for glaciers where there is high spatial variability in ice velocity and changes in terminus position. Annual calving rates for each of the three sections are calculated from the 2002 ice velocity and terminus change data, shown in Table 5.1, by extrapolating from the short-term data. A large range of values is apparent.

Zone	Ice velocity (m a^{-1})	Terminus change (m a^{-1})	Calving rate (m a^{-1})
Northern	520	0	520
Central	1810	50	1770
Southern	870	0	870

Table 5.1 *Calving rates of each glacier section calculated from the 2002 annual ice velocities and values of terminus given in Tables 4.4 and Table 4.8.*

This large range is most likely to be attributable to differences in ice flux from each tributary to the terminus. However, extrapolating the data to provide calving rates for each section in this way is not without its limitations, as terminus change values for the northern and southern sections are not known precisely (4.3.1.iii). Furthermore, terminus retreat of ~ 40 m was measured at the central section even within a 36-day period in 2002 (Table 4.7), calling into question the value of using annually-averaged data to evaluate calving rates and their process-links (2.1.3, cf. Van der Veen, 2002a). Over a shorter timescale, daily calving rates were calculated for the periods between each ice velocity survey of the central cliff, in 2002 (Table 5.2).

Date	Ice velocity ($m\ d^{-1}$)	Terminus change ($m\ d^{-1}$)	Calving rate ($m\ d^{-1}$)
15-16 Oct	5.5	n/a	
16-18 Oct	2.5	1	1.5
18-20 Oct	2.5	1	1.5
20-24 Oct	n/a	3	
25-26 Oct	10	-3	13
04-05 Oct	n/a	6	
06-08 Oct	5	1	4
08-11 Oct	n/a	1	
Average	**5**	**1.5**	**3.5**

Table 5.2 *Calving rates for the central ice cliff in 2002, calculated from ice velocity and terminus change data (Table 4.7, Table 4.9).*

Values of calving rate are not available for all periods. However, diurnal calving rates appear to vary by an order of magnitude. If the largest calving rate of 13 m d^{-1} is extrapolated to give an annual value, the resulting massive value of 4745 m a^{-1} is over three times greater than the annual rate calculated for the central section in Table 5.1. Although it is improbable that such high calving rates are maintained for long periods at an otherwise stable terminus, it appears that, at that particular time, large calving rates occurred as the terminus advanced into deeper water at high ice velocities. The implication that calving is a response to changes in flow regime is discussed below, in section 5.4.2. The values of u_c given in Tables 5.1 and 5.2 are compatible with published

'calving rates' because most of these have ignored u_m, judging melt rates to be insignificant compared to rates of mean mass loss by the mechanical processes of calving. However, such values are in fact equal to $u_c + u_m$. In order to derive a value for u_c alone, it is necessary to partition mass loss into its mechanically and thermally driven components. This issue is discussed in section 5.3.

5.2 Thermal Structure of Lago Leones

The u_c / h_w relation has proved robust at sites around the world as a useful first-order predictor of calving speeds (2.1.1.i), but it is also apparent that the water temperature of proglacial water bodies may significantly influence calving rates and processes (Figure 2.7) (Kennett *et al.*, 1997; Warren, 1999; Warren & Kirkbride, 2003). Calving dynamics at some lake-calving glaciers are therefore intimately linked with the thermal regime of the lakes in which they terminate, yet very little attention has been given to the interaction between limnological and glaciological processes (Roehl, 2003).

Water temperatures recorded in Lago Leones are higher than in many ice-contact lakes, even though this work was carried out in spring whereas most data in other locations have been obtained in summer or autumn (Funk & Röthlisberger, 1989; Warren *et al.*, 1995a; Warren & Kirkbride, 1998; Warren, 1999; Warren *et al.*, 2001; Roehl, 2003). The greater warmth probably reflects the lake's relatively low latitude (46°S) and altitude (303 m), and also its large size (~ 20 km^2) which dilutes the influence of glacial meltwater input. Similar ice-proximal temperatures have been recorded in the much larger Lago Argentino (Warren, 1994), whilst maximum water temperatures of 0.48 °C are observed in Lago Nef (Warren *et al.*, 2001). At Tasman Lake, New Zealand, stratified and isothermal conditions have also been observed, despite cold water temperatures of 1–3 °C (Roehl, 2003). It is probable that these conditions prevail at times at other ice-contact lakes, but temperature measurements are too few to detect them. However, another factor affecting the thermal structure of Lago Leones is the absence of floating ice from most parts of the lake. As most of the icebergs produced are small (growler size), they melt quickly (cf. Smith & Ashley, 1996). This contrasts with many other ice-contact lakes in Patagonia where abundant icebergs prevent the development of stratification and deliver meltwater to all parts of the lake (Warren, 1999; Warren *et al.*, 2001).

Water in the ice-proximal area is isothermal below a depth of 5 m, presumably due to mixing driven by turbulent meltwater inputs. Evidence for substantial meltwater input is provided by the increases in lake level that occurred in both 2001 and 2002 (4.3.2.i). However, the existence of a warm layer in the upper 5 m, and the absence of obvious zones of upwelling suggest that this mixing is not vigorous, and that the meltwater does not form a buoyant overflow plume like that seen at the tidewater LeConte Glacier, Alaska (2.3.5.i) (Motyka *et al.*, 2003). Ice-proximal convective cells driven by meltwater inputs from the glacier are less powerful in freshwater than in tidewater because meltwater at 0 °C is 200 times more buoyant in saltwater than in freshwater, a contrast which is probably part of the explanation for faster calving rates in tidewater (Funk and Röthlisberger, 1989). Furthermore, the only evidence for inflow of meltwater was observed to occur at 50-60 or 70-90 m deep (4.3.2.ii). The temperature stratification of Lago Leones (Figure 5.1), which evolved during the late spring, with temperatures throughout the lake above 3.98°C (the density extremum for sediment-free water), and temperatures warming towards the surface, is indicative of a stable water column (2.2.3.ii).

The lake represents a large reservoir of heat which has the potential to melt glacier ice. The question, however, is whether this thermal potential can be realised through advection of warm waters to the calving front by, for example, convection, turbulent mixing and/or wind. Heat transfer to the ice face is implied by the distinct temperature gradient from the distal to proximal zones, and by the dominant wind direction. Heat may be advected along the whole length of the lake, by waves driven by the up-lake winds (2.3.5.iii) coming from Glaciar Fiero. Certainly, the depth of the thermocline at 30-45 m deep implies a deep level of wind-driven mixing and circulation.

The role of the physical limnology of the ice-contact water body on terminus dynamics varies, both temporally, over seasonal and shorter timescales, as well as spatially. Lake size is important; at larger lakes, such as Lago Leones and Lago Argentino, the presence of the glacier has little impact on distal water temperatures (Warren, 1994) and warmer conditions may be established, melting floating ice quickly and establishing a temperature gradient along which heat may be conducted towards the glacier and/or advected by thermally-driven circulation cells in the lake. There may also be a feedback between the lake conditions and calving activity from the glacier.

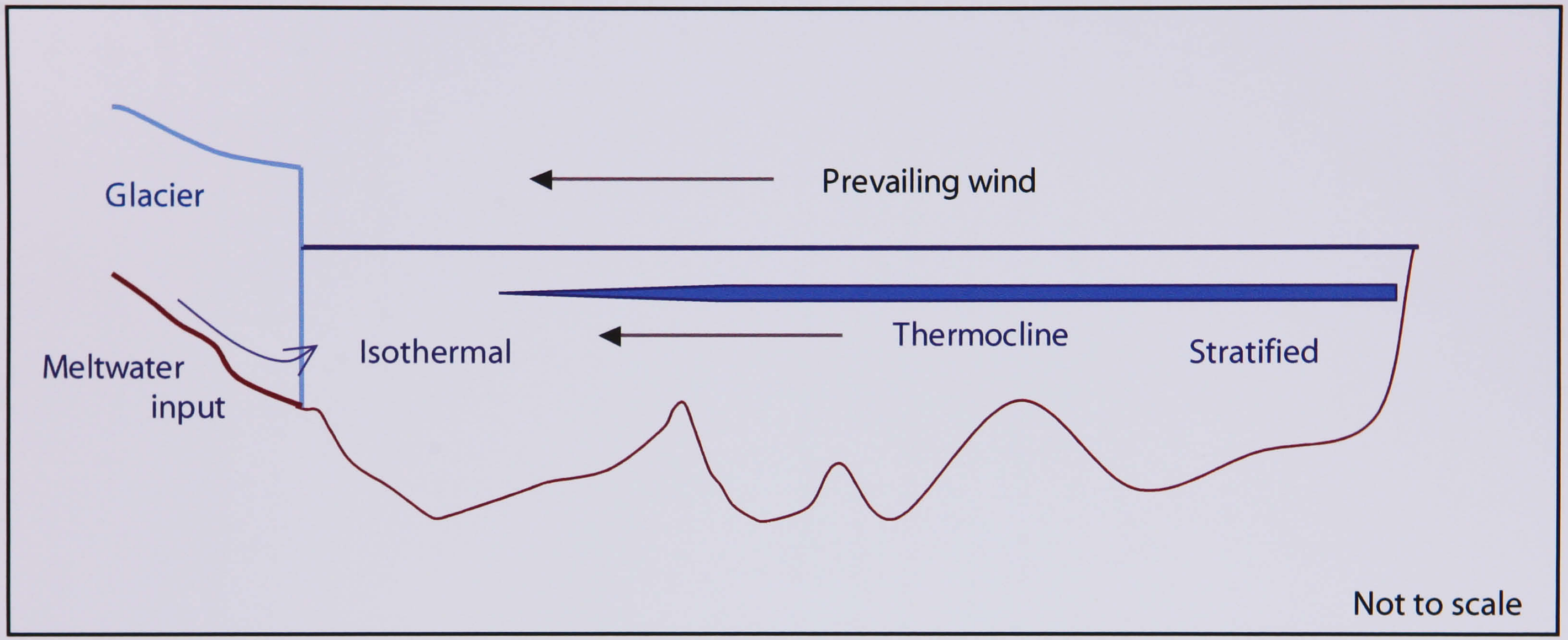

Figure 5.1 Schematic diagram of the thermal structure of Lago Leones. A thermocline develops in the distal zone, and extends towards the glacier from spring into early summer. Generally isothermal conditions are maintained by meltwater drainage, in the ice-proximal zone. The prevailing wind direction assists in advecting heat towards the glacier.

Therefore, by making a preliminary assessment of proglacial lake size and the influence of the presence of a glacier on its thermal behaviour, it is possible to anticipate other lake-glacier interactions which may be important for glacier dynamics.

If large quantities of ice enter the lake, then the melting potential of the ice-proximal water body is reduced, because the surface water is cooler and the bergs protect the calving front from wind-driven wave activity (Smith & Ashley, 1996), until all the ice has melted (2.3.4). Melt rates are therefore likely to vary on a day-to-day basis. However, without detailed observations of the boundary temperature that results from the interaction of advected heat with meltwater produced from melting of the subaqueous ice face and subglacial/englacial meltwater inflow, the precise influence of the thermal structure of the lake on subaqueous melt rates cannot be determined. Roehl (submitted) notes that the temperature at the back of the waterline melt notch correlates with the melt rate, and that the horizontal temperature gradient within the notch makes little difference although, presumably, the higher the lake temperature, the higher the temperature at the back of the notch. However, this confirms the need to know boundary conditions, and emphasizes the limitation of only knowing the thermal structure of the main body of the lake.

5.3 Glacio-limnological interactions: How important is melting?

5.3.1 Introduction

Melting has long been presumed unimportant at calving termini, both in absolute and process terms, but recent evidence has questioned this assumption, suggesting that it is inappropriate to incorporate melting within 'calving rates' (2.3.1), as highlighted in section 5.1. These two components of mass loss are strongly linked at lake-calving termini where waterline melting may be the rate-controlling process for subaerial calving (Kirkbride and Warren, 1997; Roehl, 2003; Warren and Kirkbride, 2003; Roehl, submitted). This close linkage makes it hard to separate them precisely. Nevertheless, a more complete understanding of processes operating at calving termini requires that mass loss should be partitioned into its thermal and mechanical components.

Whilst a knowledge of the thermal behaviour of the water body, as described in section 5.2, is useful in providing a first estimate of whether melt rates can be expected to be in the range of observed calving speeds (i.e. that there is the means to transfer energy to the ice face from far-field waters), a more direct way of calculating melt rates is required, in order to account for u_m accurately. An ice flux balance, discussed in Chapter 2.3.7, is discounted, due to the large uncertainties involved in calculating the ice flux (Warren *et al.*, 1995b; Motyka *et al.*, 2003a). For example, at Glaciar León, many of the large icebergs calved at night are greatly melted by morning. Another approach, recognising that melt rates will vary significantly above, below and at the waterline, is to consider melting in each zone of the terminus. In general terms, subaqueous melt rates are likely to be higher than subaerial melt rates, with the highest rates of all taking place at the waterline (El Tahan *et al.*, 1987). Each of these zones is now considered in turn, to evaluate their contribution to the calving rate ($u_c + u_m$).

5.3.2 Subaerial melting

Subaerial melt rates are reported in Chapter 4.3.1.iv. In terms of the width-averaged calving rate ($u_c + u_m$) of 880 m a^{-1}, a subaerial melt rate of 0.04 m d^{-1} implies that that u_m accounts for horizontal cliff retreat of 15 m a^{-1}, or just 1.7% of total ice loss ($u_c + u_m$) from the subaerial cliff. Even by using the short term calving rates calculated in 2002, subaerial melting may only account for up to 2.7%. Given that these rates provide an upper boundary (4.3.1.iv), subaerial melting is seen to make a negligible contribution to mass loss at the terminus.

5.3.3 Waterline melting

Using average values of calving rate ($u_c + u_m$ = 3.5 m d^{-1}; from Table 4.7, p. 116) and melt rate (1.0 m d^{-1}) for the central section of the ice cliff in 2002 (Table 4.12, p. 119), where notch development is most rapid, waterline melting-driven calving may account for up to ~ 29 % of mass loss at the terminus during spring. However, the range of melt rates is large, and it may be misleading to use average values. The only dates for which both calving rate and notch melt rate are available are October 25-26, 2002. Using the calving rate ($u_c + u_m$ = 13 m d^{-1}) and the melt rate (u_m = 0.8 m d^{-1}) for these dates, waterline melting-

driven calving during this 24-hour period accounts for only ~ 6% of the calving rate. Regardless of the combination of calving rate and melt rate used to calculate the contribution of melt to subaerial calving, waterline melting appears to account for less than half of mass loss at the terminus.

Although calving rates are not available in comparable detail for 2001, lower ice velocities imply lower calving rates for the central section. The higher melt notch rates seen in 2001 (average = 2.8 m d^{-1}) therefore imply that melting played a greater contribution to calving rates during spring of 2002. Lago Leones does not freeze over in winter, so waterline melting must continue throughout the year, and will probably increase through the summer into autumn, when maximum water temperatures are observed (Motyka *et al.*, 2003a).

In laboratory experiments, Eijpen *et al.* (2003) found that ice melt in freshwater at temperatures up to 8 °C resulted in a waterline melt rate of < 0.14 m d^{-1}. This is much lower than the rates given above, probably because the laboratory rates occurred only as a result of density-driven free convection, not the forced convection typical at calving glaciers. Although the percentage contribution to the calving rate is small, absolute melt rates at Glaciar León are greater than those seen at the slow-flowing Tasman Glacier, where waterline melting rate in cooler water, of 1-3 °C, controls calving rates (Roehl, submitted). This implies that the proportion of calving accounted for by waterline melt rates decreases with increasing ice velocity. It is suggested that calving rates exist along a continuum between slow rates in freshwater such as those in New Zealand, to the fastest rates at tidewater margins such as Columbia Glacier, Alaska (2.1.3) (Warren & Kirkbride, 2003). At Glaciar León, waterline melting cannot be the primary rate-controlling process for calving as it is at the slow-moving New Zealand glaciers (Warren & Kirkbride, 2003; Roehl, 2003, submitted). It nevertheless accounts for a significant fraction of subaerial calving and, by partially controlling the geometry of the calving cliff, modifies the stress distribution at the glacier terminus. Other factors are also important at Glaciar León; glacier flow regime was alluded to in section 5.1. This and other variables are discussed in section 5.4.

5.3.4 Subaqueous melt rates

Of the three zones at the terminus of a calving glacier, melt rates along the subaqueous portion of the ice cliff are the hardest to quantify. Melt rates of glacier ice in water have been studied in a variety of non-calving settings, but the rates and variability of subaqueous melt rates at calving termini are still highly uncertain (2.3.6). One approach is to derive temperature-dependent melt relations, either from laboratory studies or from observations of rates of iceberg deterioration in the open sea. Three of the best known such relations are those by Neshyba & Josberger (1980), Russell-Head (1980) and Weeks & Campbell (1973) (see equations 2.8, 2.9 and 2.11). Here, l (= 65 m), in equation 2.11 is ice thickness below water i.e. parallel to the expected dominant direction of buoyant upwelling. Additionally, values of v used here (= 0.1, 0.2 and 0.3 m s^{-1}) have previously been observed or estimated elsewhere (2.3.6), and provide estimates of current velocity in the range expected at Glaciar León (Hunter *et al.*, 1996a; Roehl, 2003). Melt rates, calculated using these velocities across the temperature range recorded in ice-proximal locations at Lago Leones, are presented in Table 5.3.

Equation	v (m s^{-1})	Melt rate (m d^{-1})			
		Temp (°C)			
		4	5	6	7
2.8	-	0.25	0.32	0.39	0.47
2.9	-	0.05	0.07	0.09	0.12
2.11	0.1	0.16	0.20	0.24	0.28
2.11	0.2	0.28	0.35	0.42	0.49
2.11	0.3	0.39	0.48	0.58	0.68

Table 5.3 *Ice melt rates from published equations (2.8, 2.9, 2.11) using ice-proximal water temperatures observed in Lago Leones in 2001 and 2002. All melt rates are in m d^{-1}.*

Equation 2.9 yields significantly lower values than the closely similar values from equations 2.8 and 2.11 (v = 0.2 m s^{-1}), and are somewhat lower than the rates indicated from the melt notches. Calving termini clearly represent very different contexts from either tabular icebergs melting in the open ocean or laboratory settings, and so there are obvious problems in attempting to apply relationships developed for the latter to calving

termini. This is illustrated by the disparity between the melt rates indicated here and calculated at the waterline melt notches (5.3.3, Table 5.3). To produce melt rates from the iceberg-derived equations comparable to those measured at the waterline, water temperatures of ~ 7 °C are required. This is an unrealistic condition for the ice-water interface zone, and it is also unlikely that current velocities are greater than 0.3 m s^{-1} (Hunter *et al.*, 1996a). At Glaciar León, given that there is no evidence for vigorous upwelling along the ice face (4.3.1.i), current velocity values are likely to be low. The notch melt rates therefore suggest that the iceberg equations under-predict melt rates. Furthermore, upwelling of meltwater outflow is not likely to be vertical, whereas at tidewater glaciers, near-vertical plumes are typical where meltwater emerging into a saline water body is highly buoyant (Motyka *et al.*, 2003a). Interflows at Glaciar León are inferred from the thermal structure of the lake (5.2), and the water is likely to flow out as a sub-horizontal layer. The effective length term is therefore likely to be less than 65 m, resulting in yet lower melt rates from iceberg equation calculations.

Melt rates at Glaciar León are an order of magnitude lower than those calculated for tidewater LeConte Glacier, Alaska (2.3.6) (Motyka *et al.*, 2003a). However, melt rates at other Alaskan tidewater glaciers appear to be similar to those at Glaciar León (Hunter *et al.*, 1996a). In the laboratory experiments of Eijpen *et al.* (2003), melt rates are highest directly below the waterline (Figure 2.11, p.58). In freshwater, with temperatures of 4–8 °C, rates range from 0.25–0.58 m d^{-1}. These rates are comparable to those predicted by equations 2.8, 2.9 and 2.11, unsurprising given the dependence only on temperature in both cases, with no consideration of other factors, such as forced convection (2.3.5). The observed subaqueous ice face geometry at Glaciar León (4.3.1.i), where melting left a vertical ice face undercutting the subaerial portion of the cliff by the depth of the melt notch, implies that melting below the waterline is not always significantly greater than that at the waterline, as indicated by the laboratory experiments. At Tasman Glacier, melting at the waterline is greater than that below, due to the greater rates occurring in the clean ice of the notch, compared to the insulating effect of debris on the subaqueous ice face (Roehl, submitted). At Glaciar León, where the ice face is debris-free, the occurrence of enhanced rates of waterline melting must relate to other factors, such as energy exchanges with the atmosphere and heat advected by wind-driven waves, which were not simulated in the laboratory experiments. These factors are considered in Chapter 8.1.

It seems, then, that since direct measurement is difficult and water current speeds are unknown at Glaciar León, available data do not enable rates of subaqueous melting to be calculated accurately. It is probable, though, that rates of mechanical loss (through subaqueous calving) exceed melt rates, as they do along the subaerial cliff. Even if waterline melting operates at as much as ~ 29 % of the rate of subaerial calving, subaqueous melting can only account for a small percentage of mass loss from the submerged portion of the face at this site. Moreover, melt rates decrease with increasing water pressure at depth (Huppert, 1980). Rapid calving of the subaerial cliff, leading to a projecting underwater 'ice foot', will expose submerged ice to increasing buoyant forces which will eventually trigger calving when buoyancy exceeds a critical stress for failure (cf. Hunter and Powell 1998). The observation that subaqueous icebergs are not consistently larger than subaerial ones is unusual, contrasting with the pattern typically observed at grounded calving termini, both in tidewater and freshwater (Warren *et al.*, 1995b; Warren and Kirkbride, 2003). It suggests that the basal part of the glacier is pervasively fractured, presumably through bottom crevassing driven by high flow speeds through the icefalls, so that the critical failure stress is similar throughout the ice thickness.

5.3.5 Summary

This discussion makes clear how difficult it is to quantify rates of melt at calving termini and to partition total mass loss ($u_c + u_m$) into its two primary components. At Glaciar León, this means that it is not possible to derive an accurate value for u_c alone. All that can be said with confidence is that calving accounts for a majority of mass loss, and waterline or subaqueous melting for a small but significant minority. From the few existing lake-calving studies, there is evidence that melting is of relatively greater significance (both as a process of mass loss and as a triggering mechanism for calving) when u_c is low and becomes progressively less significant as u_c increases. Thus at slow-flowing calving glaciers (such as those in New Zealand) waterline melting can be the rate-controlling process for calving, and cliff melting may account for significant percentages of the ice loss. For example, Purdie & Fitzharris (1999) suggest that melting accounts for 71 % of subaerial ice loss at the terminus of Tasman Glacier, and Roehl (submitted) suggests that the calving rate is directly controlled by the rate of thermal undercutting. By contrast, at sites with high flow speeds, pervasive crevassing and rapid calving,

including Patagonian glaciers like Glaciar León and Glaciar Ameghino (Warren 1999), the rate of waterline notch development is slow compared to u_c. In such contexts, melt-induced calving and cliff melting only account for a small portion of mass loss at the terminus.

5.4 Calving Dynamics at Glaciar León

5.4.1 Introduction

The cyclic pattern of subaerial calving recorded at Glaciar León, together with the associated repeating sequence of ice front geometries, closely reflects observations at lake-calving glaciers in New Zealand (Kirkbride & Warren 1997; Purdie & Fitzharris 1999). The cycle, however, is shorter, taking ~4 days at Glaciar León compared with ~15 days at the slower-flowing New Zealand glaciers, and is accompanied by faster change of terminus geometry. That waterline melting may drive calving at both freshwater and tidewater glaciers (2.3.1) (Vieli *et al.*, 2002; Motyka *et al.*, 2003a) suggests either that this style of subaerial calving is common to both freshwater glaciers and polar tidewater glaciers, and/or that it is a process which becomes progressively more important with decreasing calving speeds, as described in section 5.3.3. For example, waterline melting is insignificant for the Brown *et al.* (1982) dataset of 12 tidewater glaciers, in which the mean value of u_c is 1885 m a^{-1}, whereas at the 21 lake-calving glaciers in the Warren & Kirkbride (2003) dataset the mean value of u_c is 136 m a^{-1}, and melt-induced calving is common. At tidewater Hansbreen, where waterline melting is important for mass loss, u_c = 164 m a^{-1} (Vieli *et al.*, 2002).

It is clear from the analysis of the contribution of melting to the overall calving rate that waterline melting cannot be the only rate-controlling factor (5.3.3). If calving due to waterline melting accounts for around a quarter of mass loss in the central section, other processes must control the other three quarters. Furthermore, calving from the southern section cannot be controlled by waterline melting, as the cliff is not in contact with the water, but rests on bedrock instead (4.3.1.i). Here, the discussion considers the other factors influencing the calving rate, both at the central section of the terminus, and for the northern and southern sections. A model of terminus dynamics over the period October

24 - November 10, 2002, providing evidence for some of the rate-controlling factors, is presented below.

5.4.2 Model of terminus dynamics between October 24 – November 10, 2002

Changes in ice flow regime were suggested in section 5.1 to explain the short-term advance of the central section of the terminus seen at the end of October in 2002. In light of the observations described in Chapter 4.3.1.i, along with measurements of terminus change and ice velocity, which provide calving rates, the following scenario is proposed, illustrated in Figure 5.2. In mid-October, surface ablation and snow melt runoff increase, as air temperatures become warmer. These add increased volumes of water to the bed of the glacier, augmented by high daily rainfall at that time, of 15–25 mm d^{-1} (Figure 5.2a). Furthermore, the highly crevassed glacier surface both creates potential for high rates of surface melting and provides fast transport paths for surface water to reach the glacier bed. In combination, these conditions permit the subglacial hydrological system to alter. The exact nature of subglacial drainage is unknown, but it is probable that drainage occurs along efficient conduits all year round, in order to maintain fast ice velocities by basal sliding with little seasonal variation. However, this sudden increase in water to the system may not be accommodated solely by the conduits and, by lubricating the entire bed, causes the effective pressure to decrease, and accelerated ice flow close to the terminus (Table 4.7, p. 116), which results in a small terminus advance (Table 4.9, p. 118) (Figure 5.2b). The hydrological system subsequently adjusts to the increasing volume of water, perhaps by accelerated expansion of conduits by melting, and the large volume of water is flushed out, reflected in the increased lake level (Figure 5.2c).

Whilst no direct measurements are available for the basal conditions e.g. from borehole data, and this scenario is speculative, such switches in basal hydrology are known to occur (Willis, 1995). Seasonal variations in ice velocity and calving rate have been attributed to basal conditions at tidewater Columbia and LeConte glaciers, in Alaska (2.1.1.ii) (Kamb *et al.*, 1994; Meier *et al.*, 1994; Krimmel, 1997; Pfeffer *et al.*, 2000; Motyka *et al.*, 2003a). The timing of glacier acceleration, resultant terminus advance and the large increase in lake water volume at Glaciar León is unlikely to be coincidental, and is modelled in Figure 5.3, which graphs the changes in the relevant variables over this period.

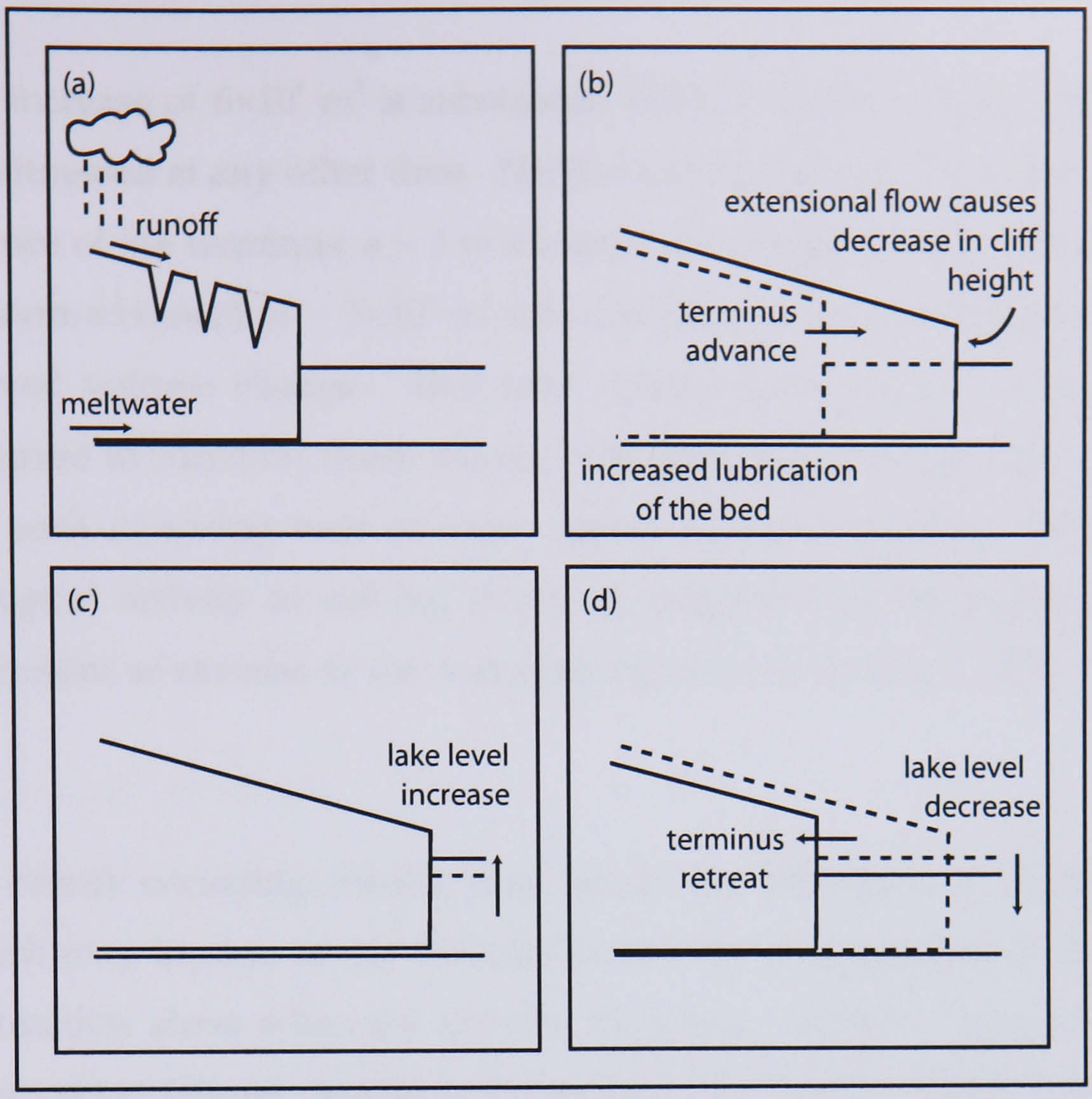

Figure 5.2 Short-term terminus dynamics at Glaciar León. (a)Spring melt increases water to the glacier bed. (b) Increased sliding causes a terminus advance. (c) Lake level increases as basal water is expelled. (d) Reduced ice velocities result in terminus retreat by calving.

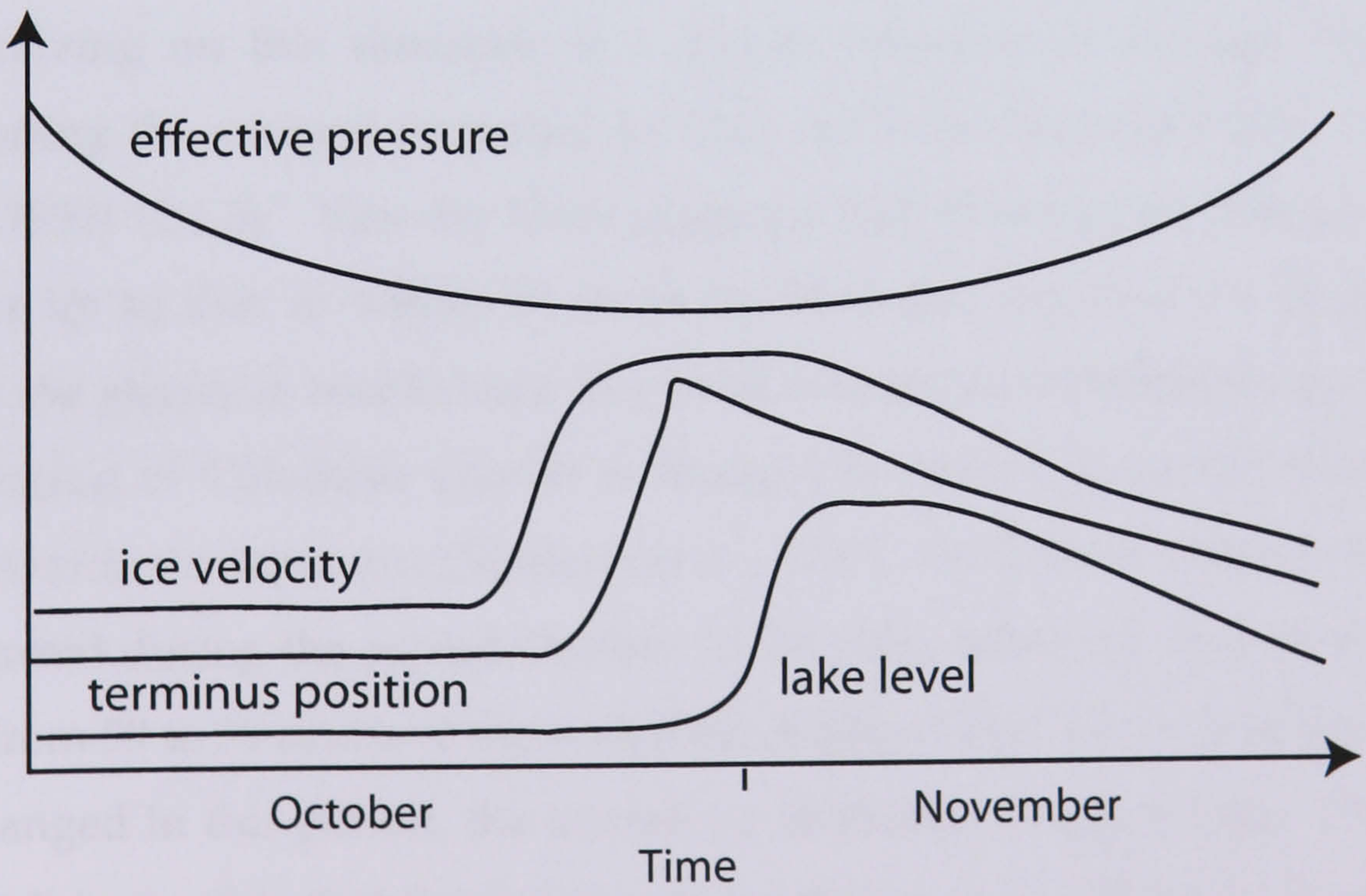

Figure 5.3 Schematic diagram of the timing of terminus dynamics at Glaciar León in the spring of 2002, illustrating the timing of changes in key variables, as described in section 5.4.2.

A lake volume increase of 6×10^6 m^3 is substantial (4.3.2.i), and no comparable lake level changes were witnessed at any other time. Neither can the volume increase be accounted for by the advance of the terminus: a ~ 3 m advance corresponds to an estimated volume (assuming uniform advance) of ~ 3×10^5 m^3 into the lake, an order of magnitude smaller than the observed volume change. That lake volume increases of a similar order of magnitude occurred at identical times during both 2001 and 2002 implies a seasonally-derived cause, such as spring melt of snow higher in the catchment. Other evidence linking hydrological activity to calving events is suggested by meltwater conduits at Glaciar León, present as caverns at the waterline (4.3.1.i) (cf. Syvitski, 1989; Theakstone, 1989).

Large calving events occurring during this period are preceded by audible internal fracturing, which may be due to the inability of the ice to accommodate the increased strain by deformation alone when ice velocity increases. Internal crevassing was also inferred at Mittivakkat Glacier, southeast Greenland, by Hasholt (2002) from a sudden drop in the lake water temperature immediately prior to a calving event. It is interpreted as a sudden outflux of subglacial meltwater resulting from the internal crevassing, triggering calving (Hasholt, 2002), although few observations exist to support this. The terminus advance at Glaciar León is followed by reduced ice velocities and retreat by calving, whilst lake level returns to its original position (Figure 5.2d, Table 5.2). This suggests that calving on this timescale is a glacier response to changes in terminus position, supporting the concept proposed by Van der Veen (Van der Veen, 1996, 1997; Venteris *et al.*, 1997) (2.1.2). Van der Veen suggests that thinning or changes in water depth cause the ice to thin to within 50 m of the thickness required for flotation, and calving permits the glacier to recede back to a point where this ice thickness is once again exceeded. Thinning of Columbia Glacier is thought be due to increased stretching by basal sliding towards the terminus (Venteris *et al.*, 1997). At Glaciar León, a decrease in cliff height occurred during the period October 25-26, 2002, when the terminus advanced was recorded, from 59 to 50 m above the waterline (Figure 5.2b). Given that the lake level remained unchanged in this period, the overall ice thickness changed from ~ 52 to 43 m above flotation. It is possible that the decrease in ice thickness to within the 50 m criterion proposed by Van der Veen (2.1.3) is just sufficient to trigger a calving response to buoyancy forces. Vieli *et al.* (2001) propose a modified flotation criterion, where the amount exceeding the flotation thickness is replaced by a small fraction q of the flotation

thickness at the terminus. The terminus moves to the position where ice thickness corresponds to $h_c^{'}$:

$$h_c^{'} = \frac{\rho_w}{\rho_i}(1+q)d = \frac{\rho_w}{\rho_i}d + h_o^{'} \qquad \text{(Eq. 5.2)}$$

Because it is likely that the 50 m criterion applies specifically to Columbia Glacier, this fraction criterion is more readily applicable to other calving glaciers, such as Glaciar León, and the changes in subaerial cliff height described above may be significant for buoyancy forces to become more dominant.

Interestingly, cliff height does not always decrease with terminus advance. As Figure 4.6 (p. 106) shows, the ice appears to thicken as it advances, in the build up to a large, full-height slab calving event. This particular sequence was observed several days after the lake level had returned to its original level, and ice flow had decreased. It is possible that this results from temporary ice thickening as the ice flux into the terminus adjusts to the slower ice and lower basal water pressures.

5.4.3 Evaluation of rate-controlling processes

The model above offers suggestions to account for the remaining three quarters of calving from the central section that cannot result from undercutting at the waterline by melting, namely extensional flow towards the terminus (i.e. increasing longitudinal strain rates) and buoyancy of ice in the terminal water body. Whilst detailed terminus ice velocities and calving rates are not available from the northern and southern sections, this information can be used to evaluate the balance of rate-controlling factors operating at these locations.

The ice flux to the southern section of the ice cliff is sourced from the same tributary as that flowing to the central section. However, ice flow and calving rates are 40 % smaller here. Calving in the southern section cannot be driven by waterline melting or buoyancy forces, as it is not in contact with the lake. Ice velocities are not as rapid as in the terminus centre, and this will relate to thinning towards the ice cliff, as well as increased frictional drag from the valley side and the rock knoll, to which it flows more closely that the central section. Extending flow is therefore likely in the last few hundred meters, once the

ice is no longer buttressed by the rock knoll at this point, and the ice is pervasively fractured on reaching the ice cliff. The force balance at the terminus ice cliff is described by the balance of ice overburden pressure and water pressure acting in the opposite direction (Figure 2.3, p. 26). At the southern part of the terminus, where there is no water body, and the force balance relates solely to the overburden pressure, maximum values will occur at the base of the cliff. Any imbalance in this force, arising from the arrival of ice flowing into the cliff, will lead to the movement of the centre of gravity of the ice face as the cliff tends towards oversteepening (cf. Iken, 1977). The ice immediately at the cliff, in this case highly disintegrated, will adjust to the force imbalance by calving of small lamellae and ice 'boulders' (4.3.1.i). A similar force balance probably operates at the cliff in the central section, causing small lamellae in the lower half of the subaerial ice cliff to break off.

In the northern section, waterline melt rates are expected to be similar to those in the central section, given the fairly uniform surface water temperatures across the ice front (4.3.2.ii). Calving losses due to undercutting at the waterline would, therefore, constitute a greater proportion of the overall calving rate, estimated to be up to ~80 %, assuming a melt rate of ~365 m a^{-1} (1.0 m d^{-1}), and a calving rate of 450 m a^{-1}. The significance of this contribution to the calving rate probably relates to the enhanced undercutting the melting causes, as the widest caverns are found here, and spalling of lamellae expanding the cavern leads to an increasing overhang of the subaerial cliff. The cliff force balance is therefore moderated by waterline melt rates.

It is unlikely that the ice cliff force balance constitutes the main control on calving losses at Glaciar León. It can only account for calving of a thin lamella from the ice cliff, and this mechanism does not account for the majority of ice loss, given the observations of calving of subaerial seracs and full-height calving events. This must be the case for most fast-flowing calving termini, where the rapid ice flux to the terminus dictates that calving resulting from thinning, either by longitudinal stretching or buoyant forces predominates. The force balance is, instead, of greater importance for calving at ice faces where there is little mass flux to the terminus, e.g. the supraglacial lakes of the debris-covered glaciers in the Himalaya, which expand primarily by melting of the base of the pond and calving of lamellae at the sides (Yamada, 1998; Chikita *et al.*, 1998, 2000a, 2000b; Sakai *et al.*, 2000a, 2000b; Reynolds, 2000; Benn *et al.*, 2000; Hands, 2004). At Patagonian glaciers, however,

the majority of calving is most likely to relate to the factors that permit greater mass loss i.e. undercutting of the cliff by waterline melting, longitudinal stretching and buoyancy.

5.4.4 Summary

Calving dynamics at Glaciar León are complex, involving several processes which control the style, timing, size and rate of calving. Four key forces are apparent: waterline melting, longitudinal stretching, buoyancy and the force balance at the cliff margin. These vary in their influence on calving, both across the ice face, and over time. This is partly dictated by factors affecting the ice flux through the terminus, e.g. the steep slopes, pervasive fracturing of the ice, and the effect of the topographic pinning point on terminus position. In turn, these factors are important for evaluating the nature of the hydrology of the glacier, a key parameter affecting ice flow. Calving appears to form an output of the processes of ice flow, basal hydrology and terminus fluctuations, supporting the concept of Van der Veen (1996, 1997, 2002a) that calving is the 'slave' to other glacier dynamics, rather than the driving force, or 'master', as described by Meier and others (2.1.3) (Meier & Post, 1987; Meier, 1994, 1997; Meier *et al.*, 1994).

5.5 Climatic response of Glaciar León

5.5.1 Introduction

Glaciar León is unusual amongst Patagonian outlet glaciers. During Neoglacial tim,e most NPI glaciers have terminated on land and so their response to climate forcing has not been modulated by calving dynamics; most of the present ice-contact lakes are just a few decades old. Lago Leones, by contrast, has existed for at least 3000 years (Haresign *et al.*, submitted) meaning that Glaciar León has been a calving glacier throughout that time, subject to the peculiar sensitivity to topographic controls which is one of the hallmarks of calving glaciers. This sensitivity is apparent in León's post-LIA fluctuation history (Haresign *et al.*, submitted), as outlined below.

5.5.2 Neoglacial fluctuations

An OSL date of 3.0 ka for the terminal moraine at the end of Lago Leones indicates that the glacier retreated from this moraine sometime before that date and therefore that a lake (of variable size) has existed in the valley for at least 3000 years (Haresign *et al.*, submitted). The glacio-climatic and glaciological significance of this date is that it represents a minimum age, firstly, for the significant Neoglacial advance which constructed the major moraine itself, and, secondly, a maximum age for the transition from non-calving to calving following retreat off this moraine. No dates are available for the two large moraines between the lake-end moraine and the LIA maximum revealed by the bathymetric survey (Figure 5.4, Figure 4.15, p. 121), but they must represent stillstands or readvances during Neoglacial time. It is tempting to equate the Lago Leones moraines with Clapperton and Sugden's (1988) scheme of four Neoglacial advances (at *c.* 3.6 ka, *c.* 2.3 ka, *c.* 1.4 ka and the LIA) (3.4.3). The lake-end moraine would then represent the first period of advance and the two subaqueous moraines would date from 2.3 and 1.4 ka respectively, but this neat solution remains speculative at present.

5.5.3 The LIA maximum

The maximum position reached by Glaciar León during the LIA is marked by a small till-covered bedrock peninsula extending from the northern shore of Lago Leones some 3.5 km from the ice front. Glacier retreat from this location has been dated by dendrochronology to 1867, providing a minimum date for the maximum LIA advance in this valley (Figure 5.4) (Haresign *et al.*, submitted). The timing of the LIA maximum at this site is closely similar to that for other NPI outlet glaciers. Retreat from a LIA maximum position began around 1860-1870 at Glaciar Nef (Winchester *et al.*, 2001), and an LIA maximum at Glaciar Soler was reached some time between 1600-1900 (Glasser *et al.*, 2002). Retreat from LIA maxima at Gualas, Reicher, San Rafael and San Quintin glaciers on the west side of the ice cap all began in the 1870s (Harrison & Winchester, 1998; Winchester & Harrison, 1996) while, on the east side, retreat of the Colonia, Arenales and Arco, glaciers began in the late 1870s to early 1880s (Harrison & Winchester, 2000).

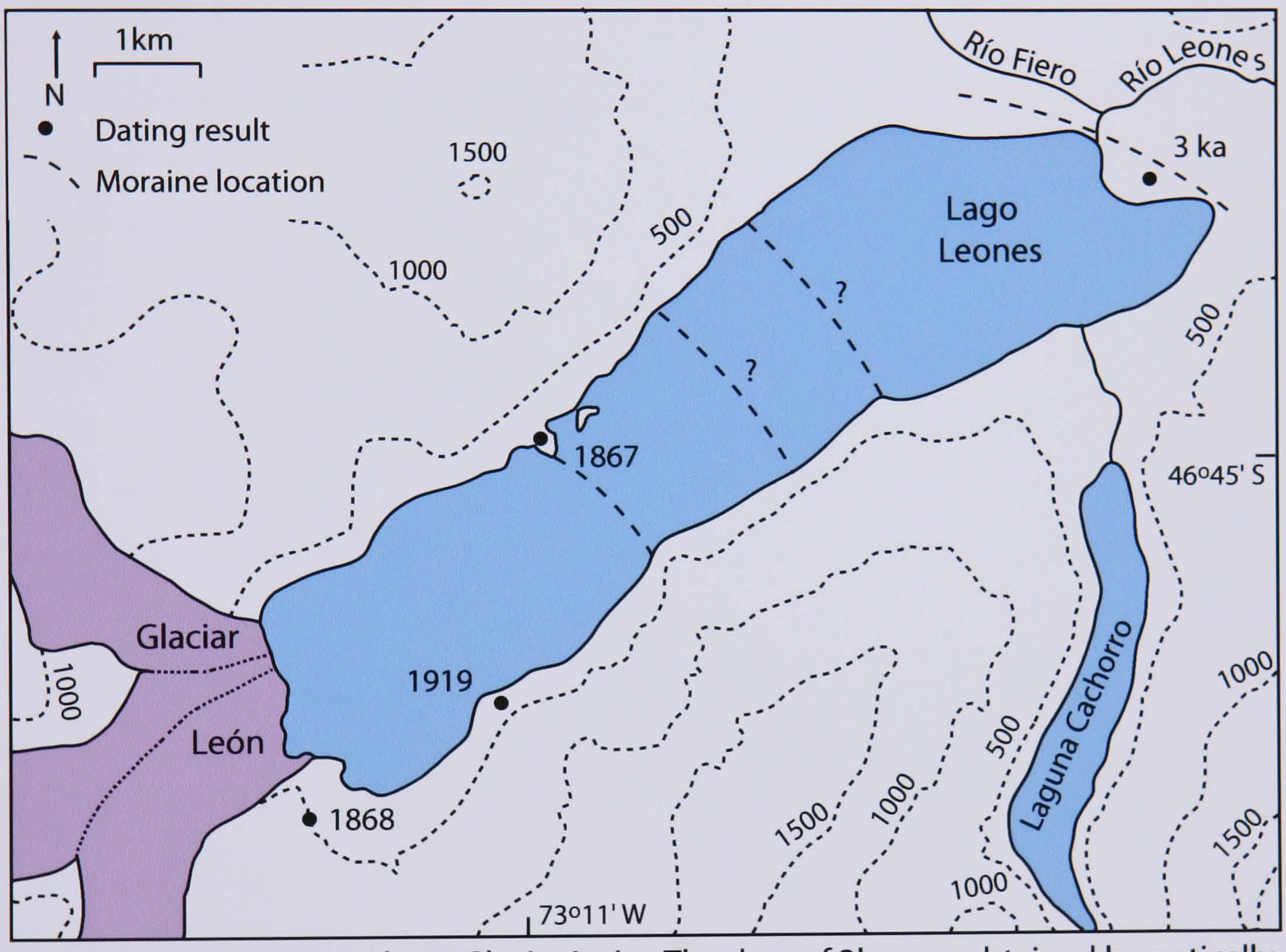

Figure 5.4 Dating results at Glaciar León. The date of 3ka was obtained by optically stimulated lumiscence, and the others from dendrochronology and lichenometry. Dates of the two other moraine ridges are uncertain.
Adapted from Haresign *et al.* (submitted).

The data from Lago Leones thus strengthen the argument made by Harrison & Winchester (2000) for largely synchronous behaviour of glaciers on both sides of the icefield at the end of the LIA (3.4.3). In conjunction with LIA dates for 17th and 18th centuries at east-side SPI glaciers Upsala, Tyndall and Ameghino (Aniya, 1995; Aniya, 1996), these data from Glaciar León support the idea of synchronous icefield response to climatic forcing (3.4.3).

5.5.4 Historic fluctuations

Thinning and retreat of Glaciar León, in the second half of the 19th and early 20th Centuries, is suggested by dates on the southern lake shore within the LIA limit (Figure 5.4, Haresign *et al.*, submitted). A reconnaissance map of the NPI based on 1945 aerial photographs (Lliboutry, 1956), shows the terminus only ~ 300 m in advance of its position in 1991 (Aniya, 2001). Between 1994 and 1999, there was a small readvance of ~ 190 m, before retreating (in common with the other eastern side NPI glaciers) from 1999-2000, by ~ 100 m (Aniya, 2001) (3.3.3). In the late 20th Century, synchrony across the NPI was less apparent due to the increasing influence of calving dynamics and topographic controls as glaciers retreated into overdeepened troughs and experienced rapid calving retreats (Warren and Aniya, 1999; Harrison *et al.*, 2001) (3.5.2). The post-LIA behaviour of Glaciar León illustrates the sensitivity of calving glaciers to the topographic geometry of their valleys. Both the LIA and present locations of the terminus are topographic pinning points, providing the glacier terminus with a greater measure of stability relative to the deeper, wider parts of the lake. Retreat through the 360 m-deep intervening basin appears to have been rapid and largely uninterrupted. Conversely, the present location is so stable that the terminus position has changed little since 1945, a 58-year period during which most NPI glaciers have seen significant changes (Aniya, 2001) (3.3.3). However, several of the western calving outlets of the NPI (San Quintin, San Rafael, Gualas, Reicher) recently exhibited slowed retreat or slight advance following high precipitation in the 1970s and 1980s (Warren, 1993; Winchester & Harrison, 1996; Harrison & Winchester, 1998), which may have caused the 1990s readvance of Glaciar León. Again, this would imply synchrony across both sides of the icefield, similar to that inferred from LIA dating the investigations, above.

5.5.5 The role of calving for long-term glacier fluctuations

Two main points arise regarding the interaction of calving with the retreat behaviour of Glaciar León. Firstly, the glacier's post-LIA behaviour and contemporary calving characteristics echo those of other freshwater calving glaciers (Warren and Aniya, 1999; Warren and Kirkbride, 2003). This is apparent in its sensitivity to topographic geometry (especially the cross-sectional area of the calving terminus). During Neoglacial time, the glacier could therefore have been expected to exhibit a 'jerky' response to climate change as it jumped between topographically defined points of stability in the lake basin (cf. Vieli *et al.*, 2002) (2.1.1.i). Although the dating resolution is insufficient to identify anomalies caused by calving dynamics over Neoglacial timescales, given the considerable depth of individual basins within the lake ($\leq$ 360 m), it is likely that Neoglacial fluctuations consisted of a pattern of 'punctuated equilibria', in which topo-climatically defined stillstands were interspersed with relatively short periods of rapid retreat. The geomorphological evidence supports such a scenario. The most stable location of all is at the north-eastern end of the lake where the glacier could maintain a non-calving terminus. Here, the substantial dimensions of the lake-bounding terminal moraine attest to an extended stillstand (or stillstands). Once the terminus retreated into deep water, rapid calving retreat would have ensued through each of the lake's four basins, punctuated by topo-climatic stillstands at relatively shallower and/or narrower locations.

The second relevant aspect concerns calving mechanisms. At present, thermal undercutting at the waterline is an integral part of the calving process, driven by ice-proximal surface water temperatures of 5-8°C. In the early Neoglacial, as the glacier retreated from the lake-end moraine and Lago Leones began to form, meltwater would have been the dominant water source and water temperatures would have been close to zero, minimising aqueous melt rates. At later times, however, with increasing lake size and inputs from valley-side streams, including the substantial Cachorro catchment (Figure 5.4), water temperatures would probably have been high enough to drive the thermal undercutting process and accelerate calving. It is also likely that, during retreat through the deepest parts of the lake, the terminus approached or reached flotation, a point at which different and highly efficient calving mechanisms become dominant (2.1.2) (Warren *et al.*, 2001; Motyka *et al.*, 2003b).

CHAPTER 6

Fjallsjökull, South-East Iceland: Field Observations

6.1 ICELANDIC GLACIERS

6.1.1 Introduction

There are several ice caps in Iceland, and the largest of these, Vatnajökull, is located on the southeast side of the island. It comprises 70% of all glacierized land in Iceland, and covers an area of 8100 km^2 (in 1991 by Landsat image (Sigurdsson, 1998)). It feeds 38 named and several unnamed glaciers (Evans & Twigg, 2002) (Figure 6.1). Compared to the rest, those on the south-eastern margin are smaller, steeper and non-surging, fed by the independent Öræfajökull which merges with Vatnajökull on its north side (Sigurðsson, 1998). Most Icelandic glaciers are presently in recession (6.1.3), in response to climatic warming (6.1.2), and for some this is the result of post-surge downwasting. For others, this downwasting is concurrent with retreat through a proglacial lake. About twenty glacier-margin lakes were recorded in the 1970s (Björnsson, 1976). Most are found along the more active southern to eastern edge of Vatnajökull from Skeiðarájökull to Eyjabakkajökull. Whilst particular interest has been focused on lateral lakes, having the greatest potential for jökulhlaups (Björnsson, 1976), there are several sizeable proglacial lakes including those at Breiðamerkurjökull, Heinabergsjökull, Tungnaájökull, Langjökull and Fjallsjökull. Glaciers currently known to be calving include Heinabergsjökull (Thorarinsson, 1939; Bennett *et al.*, 2000) and Hoffellsjökull on the east side, and Breiðamerkurjökull and Fjallsjökull on the south-eastern margin. Jökulsárlón at Breiðamerkurjökull formed in the 1930s, and the other lakes have formed in the last 30-40 years, suggesting that continued retreat of Vatnajökull's outlet glaciers will result in the formation of glaciolacustrine termini at other locations. Therefore, calving is imminently to become even more important for ice cap mass balance.

Systematic monitoring of glacier fluctuations has been carried out since 1930, and published in the journal *Jökull*, and many of these studies are carried out by local inhabitants who make regular reports (Sigurðsson, 1998). At present, 19 named outlet glaciers from Vatnajökull are monitored using ground measurements.

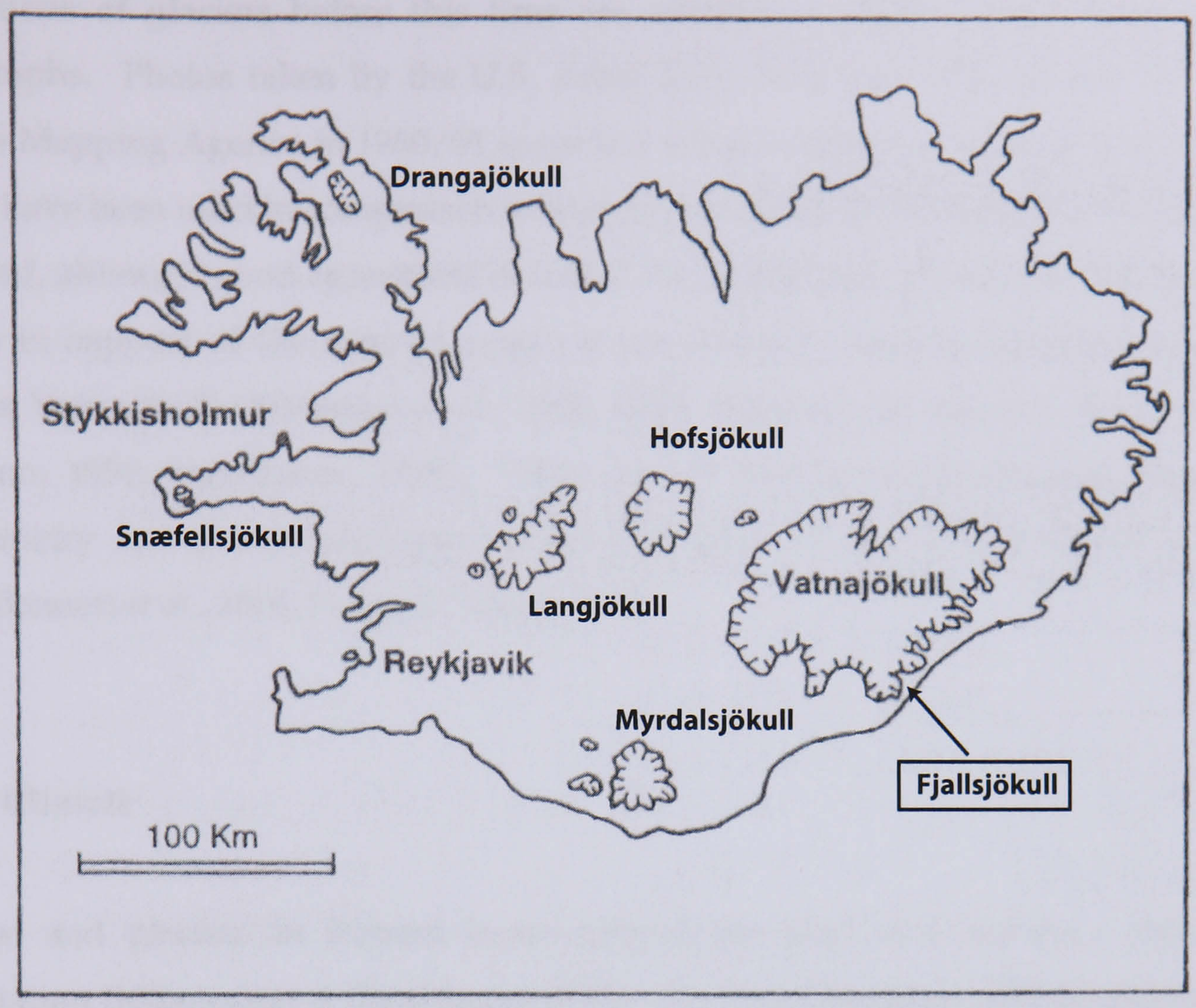

Figure 6.1 Map of Iceland showing the primary icecaps, including Vatnajökull. Source: Kirkbride (2002).

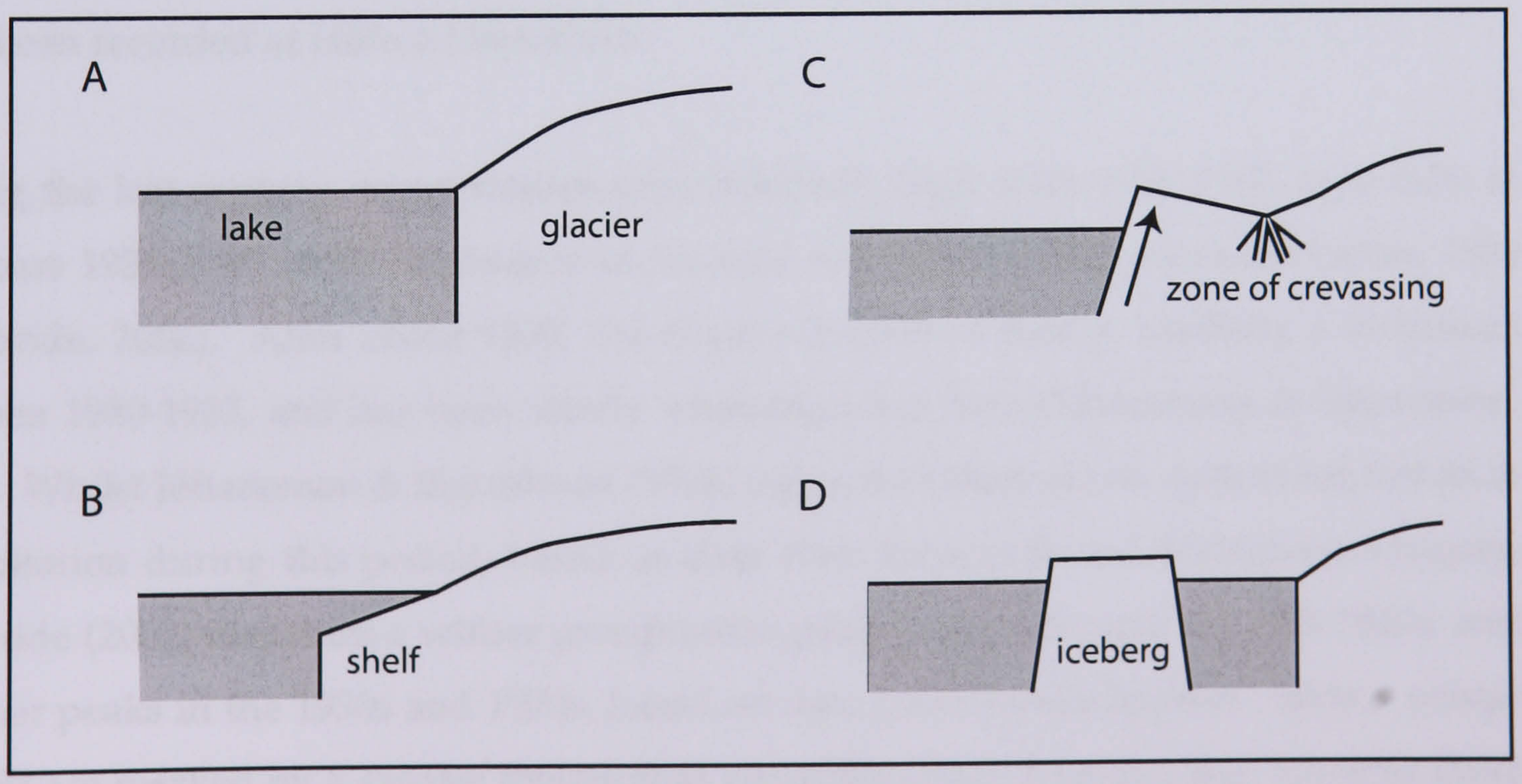

Figure 6.2 The suggested mechanism for the calving of icebergs from a submerged ice front, adapted from Howarth & Price (1969).

Fluctuations of glaciers before this time are sometimes inferred from maps or aerial photographs. Photos taken by the U.S. Army Map Service in 1945/46 and by the U.S. Defence Mapping Agency in 1960/61 cover the whole of Iceland. More recently, Landsat images have been used in comparison to the ground-based measurements (Williams *et al.*, 1997) and, although good agreement is found, the importance of 'local knowledge' of the glaciers in support of the remote images is emphasized. Several mass balance studies exist for Vatnajökull (Björnsson *et al.*, 1992, 1998; Björnsson & Pálsson, 1998; Pálsson & Björnsson, 1999; Sigurðsson, 1998). Other glacier history studies include those using lichenometry and geomorphological techniques (Rose *et al.*, 1997; Evans *et al.*, 1999a, 1999b; Bennett *et al.*, 2000; Evans & Twigg, 2002).

6.1.2 Climate

Ice caps and glaciers in Iceland cover 10% of the land and receive ~ 20% of the precipitation (Jóhanesson & Sigurðsson, 1998). The Stykkisholmur climate record, on the east coast, is the longest instrumental record in Iceland. Although precipitation shows high spatial variability (Kirkbride, 2002), temperature records show good correlation across the island (Einarsson, 1991; Jóhanesson & Sigurðsson, 1998). The annual summer temperature on the south coast is 11 °C, and the area receives 80 % of its precipitation between September and May. From 1971 to 2001, winter temperatures down to – 7 °C have been recorded at Höfn a Hornafirdi.

During the last century, temperatures were relatively high from 1931-1960, especially in the years 1931-1940, with an absence of the cold winters that had prevailed before 1920 (Kirkbride, 2002). After about 1960, the climate cooled markedly, reaching a minimum between 1980-1985, and has been slowly warming since then (Jóhanesson & Sigurðsson, 1998). Whilst Jóhanesson & Sigurðsson (1998) argue that there are no systematic trends in precipitation during this period, based on data from Reykjavík and Kirkjubæjarklauster, Kirkbride (2002) identifies a winter precipitation peak from 1920 until the mid-1940s, and summer peaks in the 1930s and 1970s, based on data from Stykkisholmur. Wetter winter periods are marked by a greater interannual variability than drier periods, whereas there is high interannual variability for summer precipitation.

6.1.3 Glacier Variations

There is a clear correlation between glacier variation and climate in Iceland. The response time of most glaciers is 2-5 years (Sigurðsson, in press). Most of the non-surging glaciers retreated strongly during the early half of the period 1930-1995, with stabilization or a readvance around 1970. These fluctuations have been interpreted to relate to variations in temperature rather than precipitation (Jóhanesson & Sigurðsson, 1998). They argue that climatic warming on the order of 0.3 °C per decade has temporarily increased glacier runoff from some Icelandic ice caps and glaciers by more than 50% and may lead to a decrease in volume by approximately 40% of some glaciers over the next century.

Kirkbride (2002) examines the response of Iceland glaciers to climate in more detail, accounting for the role of shifts in the location and intensity of the Icelandic Low, in terms of the North Atlantic Oscillation (NAO). Larger glaciers in the 19th and 20th Centuries were favoured by low-NAO index, cool dry winters. Decades of cool, cloudy low-index summers, following decades of wet winters, have caused late-20th Century glacier advances, and is probably more important than either occurring alone. The wet winters from 1920-1945 provided increased mass flux whose downstream transfer would have progressively reduced terminus retreat rates, aided by reduced ablation in the cool summers of the 1970s. However, not all mass balance changes are climatically induced. Volcanic activity results in tephra on the glacier surface, which may inhibit or promote surface ablation, depending on the tephra thickness. The fallout resulting from the eruption of Hekla in 1947 triggered contrasting advances and retreats on different parts of Eyjafjallajökull over a 7-year period (Kirkbride & Dugmore, 2003).

Most of the large, lobate outlet glaciers are surge-type with surge periods of less than 10 years up to ~ 80 years. In studies relating glacier fluctuations to climate changes, only the non-surging glaciers are used, due to the non-climatic controls on decadal-scale changes. However, little consideration has been given to the non-climatic control of calving dynamics on terminus positions. Those glaciers presently calving into proglacial lakes have all retreated since 1930 (Table 6.1), although Hoffellsjökull and Fjallsjökull have maintained a fairly stable terminus position since around 1990 (Sigurðsson, 1998), and Heinabergsjökull has recently advanced in response to an increase in the size of its proglacial lake (Evans *et al.*, 1999a). At first glance, therefore, these glaciers have also

responded to climatic forcing, and not become decoupled from climate by calving dynamics.

Glaciar	Time period	Overall retreat (m)
Breiðamerkurjökull	1950-95	1363
Fjallsjökull		
calving section	1933-95	705
north	1951-95	133
south	1950-93	455
Heinabergsjökull	1935-90	1330
Hoffellsjökull	1930-69	415

Table 6.1 *Terminus position fluctuations of calving glaciers on the Vatnajökull icecap (Sigurðsson, 1998).*

6.1.4 Calving in Iceland

Proglacial lakes are recognized in the sedimentological record in studies of glacier fluctuation histories and jökulhlaup events (Thorarinsson, 1939; Williams *et al.*, 1997; Geirsdóttir *et al.*, 2000; Bennett *et al*, 2000; Björnsson, 2002). However, they have rarely been examined with respect to calving dynamics, either in terms of their influence on current glacier dynamics, or how they may have modified the climatic response of a glacier. The only studies attempting to examine the significance and role of the proglacial lakes of Vatnajökull on glacier dynamics are those carried out adjacent to Breiðamerkurjökull (Derbyshire, 1974; Harris, 1976 and Howarth & Price, 1969; Björnsson *et al.*, 2001; Landl *et al.*, 2003). Bathymetric surveys have been carried out on some of the lakes (Howarth & Price, 1969; Derbyshire, 1974; Boulton *et al.*, 1982), which have formed due to the removal of thick, unlithified sediments during the Little Ice Age advance (rather than overdeepening of a rock basin) and the retreat of Breiðamerkurjökull during the warm conditions of the 20th century (Björnsson, 1996). Breiðamerkurjökull has retreated 4 km since its maximum position in 1890, and areas covered by 200 m-thick ice are now ice-free (Björnsson *et al.*, 2001).

Harris (1976) studied the seasonal development of a thermocline and the intrusion of saline water into Jökulsárlón. Warm seawater feeds the lagoon at high tide. During the winter the water was entirely isothermal and, in spring, a saline wedge intruded along the lake bed. Glacial meltwater flushed the saline waters out during the summer, but a thin bottom layer remained. During the summer months, the surface waters approach the temperature of maximum density (~ 4 °C), but more often the surface layer does not exceed 2 °C. Below a depth of 5 – 10 m, where a weak thermocline prevents mixing of warmed surface waters to lower depths, the temperature is usually below 1 °C. Landl *et al.* (2003) have quantified the energy fluxes of Jökulsárlón to consider melting of ice in the lake. Seawater provides ~ 60 % of the required energy on a yearly basis, radiation 43 %, and the study identified turbulent fluxes as the greatest source of uncertainty in the energy balance. However, the implications of this balance for linear melt rates on either the icebergs or the ice face are not discussed in any detail. Further work is required to use this information to estimate the contribution of subaqueous melting to the overall calving rate, and the implications for future lake expansion and glacier retreat.

A floating portion of the terminus of Breiðamerkurjökull, observed in the Northern Stemmárlón, along with observations of icebergs, crevasses, and rates of subaerial versus subaqueous melting, was used to suggest a calving mechanism, whereby subaerial melting causes ice thinning, resulting in buoyancy-driven uplift. This cause an apparent increase in size of the submerged ice 'shelf', as the subaqueous portion is revealed, before buoyancy forces cause the detachment of an iceberg (Figure 6.2) (Howarth & Price, 1969). However, the first attempt to quantify calving fluxes at an Icelandic glacier was conducted at Breiðamerkurjökull (Björnsson *et al.*, 2001). Field observations, taken in 1997-99 indicate an average ice flow velocity of 258 m yr^{-1}, and suggest a calving rate, from a combination of measure and calculated values of calving flux and calving front area, of 582 m yr^{-1}. Using data for ice flow and calving rates, they predict a similar pattern of retreat for the next ~ 70 years as for recent years, of 200 m yr^{-1}, as the glacier recedes inland where the bed slopes from 200 m to 300 m below sea level. If the present negative mass balance continues, retreat from the lake is expected in ~ 200 years.

6.2 FJALLSJÖKULL: PHYSICAL SETTING

6.2.1 Location

Fjallsjökull (64°01′ N 16°23′ W) is located immediately south of Breiðamerkurjökull, on the south-east side of Vatnajökull (Figure 6.3). It is 15 km long, with an ice surface area of 48 km^2 (Sigurðsson, 1998). It descends from the east slopes of Öræfajökull, with a maximum altitude of 2040 m, over a series of ice falls to form a highly-crevassed piedmont lobe debouching into Fjallsárlón, on the western edge of Breiðamerkursandur, at 40 m A.S.L (Figure 6.4).

6.2.2 Previous studies at Fjallsjökull

Recession has been documented in this area by maps since 1903, and by aerial photos since 1945. Breiðamerkurjökull has frequently been mapped in detail, and the east half of Fjallsjökull usually appears of the edge of such maps, the most recent being that by Evans & Twigg (2002). Despite the attention Breiðamerkurjökull and Jökulsárlón (amongst its other lakes) have received, in terms of glaciological and limnological observations (Howarth & Price, 1969; Björnsson, 1996; Björnsson *et al.*, 2001), Fjallsjökull has received very little attention. Indeed, there are no published studies examining the current glaciological characteristics of the glacier, in terms of its ice dynamics. Geomorphological and sedimentological studies of Fjallsjökull during its recession allude to the historic fluctuations as well as the subglacial processes that take place (Evans & Twigg, 2002). The farm at Fjall (Figure 6.3) was abandoned at the end of the 17th Century as the glacier advanced to reach its maximum position around 1850. It then retreated only to readvance again to approximately the same limit in 1894, followed by twentieth century retreat. The recession of Fjallsjökull slowed considerably in 1952 and numerous small readvances characterized a period of ice marginal stability between 1952 and 1990. Part of the glacier is presently undergoing a phase of modest readvance as documented by the stacking of push moraines on part of the foreland (Evans & Twigg, 2002). The rest of the terminus is relatively stable at present, except for the section of the ice cliff that calves into Fjallsárlón, which is retreating slowly (Evans, D., *pers comm.*), although this is negligible compared to the rapid retreat rates of > 200 m a^{-1} at Breiðamerkurjökull (Björnsson, *et al.*, 2001).

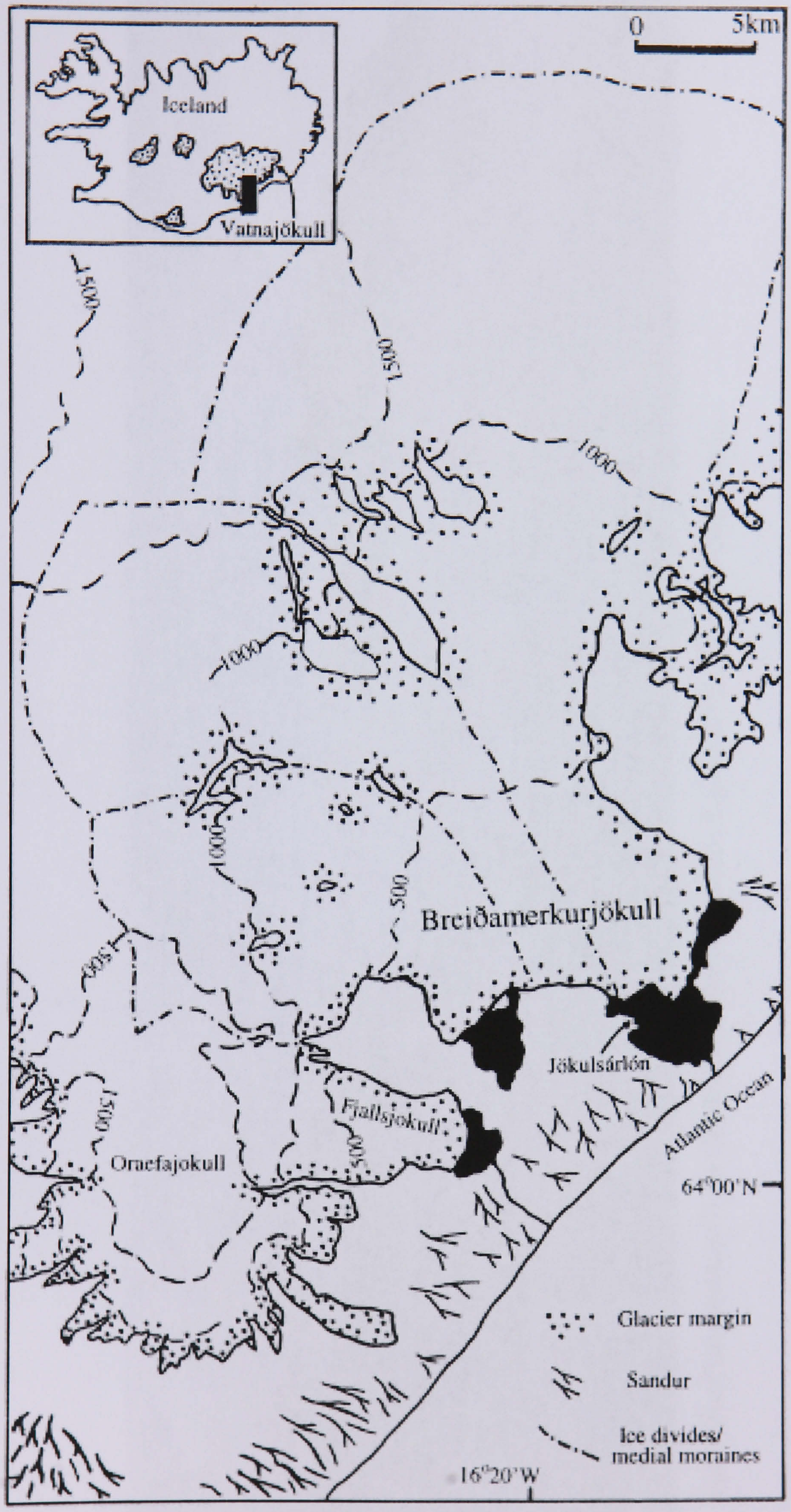

Figure 6.3 Location maps of Fjallsjökull and Breiðamerkurjökull, Iceland. The larger scale map shows the drainage areas of the glaciers with contours in metres. Source: Evans & Twigg (2002).

Figure 6.4 Fjallsjökull descending from Öræfajökull into Fjallsárlón, August 2003. Source: Andy Casely.

6.2.3 Current glacier characteristics

At present, the calving front is ~ 2 km wide and the glacier terminates into water ~ 75 m deep, immediately in front of the ice cliff (Eijpen, unpublished data). The present lake of Fjallsárlón has existed since around 1945, when Fjallsjökull was still confluent with Breiðamerkurjökull. By 1960, major drainage from Breiðamerkurjökull into Breiðárlón flowed into Fjallsárlón at the north eastern end, along the river Breiðå, when the glacier had separated from Breiðamerkurjökull (Figure 6.5). At present, Fjallsárlón is < 2 km^2 in area, and ~ 30-50 m deep in the centre of the lake. On the south margin, it is drained by the river Fjallså, travelling some 4.5 km to the sea.

6.3 FIELD DATA

6.3.1 Introduction

The outcomes of the field studies at Glaciar León show that surveying the thermal structure of the lake, whilst providing an indication of the potential heat transfer to the ice face, is insufficient for supplying accurate boundary water temperatures with which to calculate melt rates. Measurements of melt notch growth rates give an estimation of waterline melt rates. However, the notches on the central section are amongst the largest on the ice cliff at Glaciar León and, because melt rates may vary along the cliff, errors arise in the application of these rates to other sections. Alternative methods of acquiring water temperatures of the boundary layer are required. Furthermore, terminus dynamics at Glaciar León are variable over short timescales, particularly in response to short-term lake-level fluctuations. At Fjallsjökull, the paucity of data for lake-calving dynamics, as well as the opportunity to pursue the issues outlined above, initiated a field season in 2003. In order to tackle these concerns, two novel field techniques were tested. They had been intended for use at Glaciar León in 2002, but failed due to problems with the equipment. One is the continuous monitoring of water level using a pressure sensor, to infer calving event timing and size. The other is the use of a radio-controlled boat to deploy water temperature loggers at the ice-water interface (4.3.2.ii). Fjallsjökull was chosen because it is actively calving, but has a lake of a manageable size for gathering such data, and is easily accessible from the main road.

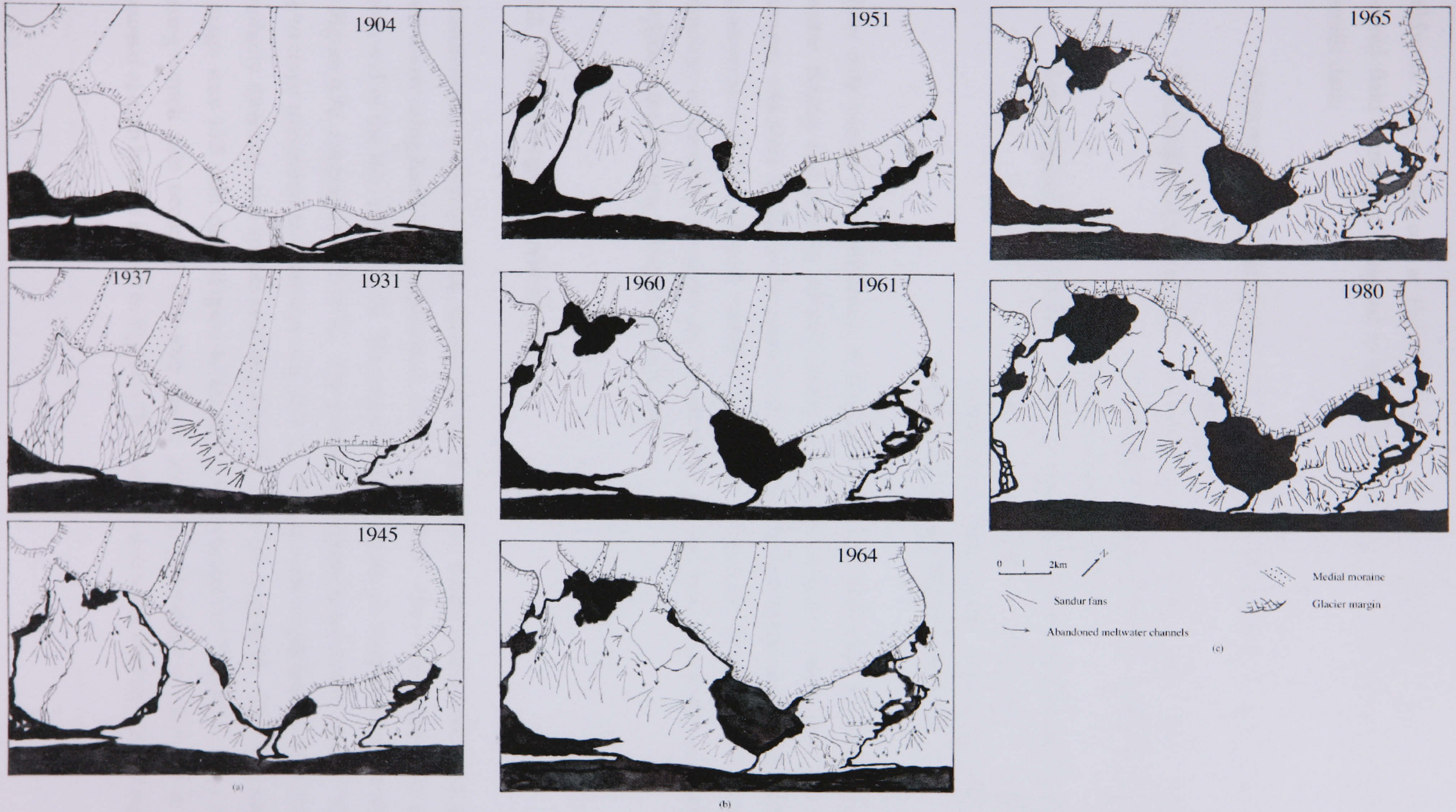

Figure 6.5 Maps of Breiðamerkurjökull and Fjallsjökull showing the evolution of the drainage system. The diversion of the meltwater drainage from west Breiðamerkurjökull after 1960, in the corridor between Breiðárlón and Fjallsárlón, led to the long term progradation and incision of glacifluvial sediments around moraine and till-covered topographic high points . Source: Evans & Twigg (2002).

Fieldwork was carried out at Fjallsjökull from August 5–17, 2003. This was a short, focused field campaign, designed to test novel techniques and to obtain the following specific data:

Meteorological observations:	Air temperature, precipitation, wind speed and direction
Glaciological observations:	Calving event timing and size, ablation measurements, waterline melt notch development and ice front geometry
Limnological observations:	Water temperatures (both mid-lake and at the ice-water interface), suspended sediment concentration, lake stage and river discharge estimations of both Breiðå and Fjallså

These data permit an examination of calving over short timescales, by comparing the precise timing and size of calving events with meteorological inputs and lake level changes, and aims to clarify the range of rate-controlling factors operating at Fjallsjökull. Measurement of limnological variables permits an evaluation of the role of physical limnology on terminus dynamics and, in particular, the importance of water-ice boundary conditions for affecting subaqueous melt rates.

6.3.2 Meteorological Observations

Measurements of precipitation, maximum and minimum temperatures and wind speed were taken using hand-held instruments, from August 5-17. They were taken daily at the south end of the lake (Figure 6.6). Maximum and minimum air temperatures are shown in Figure 6.7a, ranging from 5-19 °C. The average minimum temperature was 6.5 °C and the average maximum temperature was 13.4 °C. Winds were negligible, or light, with a southerly direction, and speeds reaching 8 km hr^{-1} only on August 15. The daily rainfall average was 13.5 mm day^{-1} (Figure 6.7a), and rain occurred on 77% days. The hours during which rain occurred was also noted, and the percentage of days when rain occurred at each hour is shown in Figure 6.7b. It shows that more rain occurred at night.

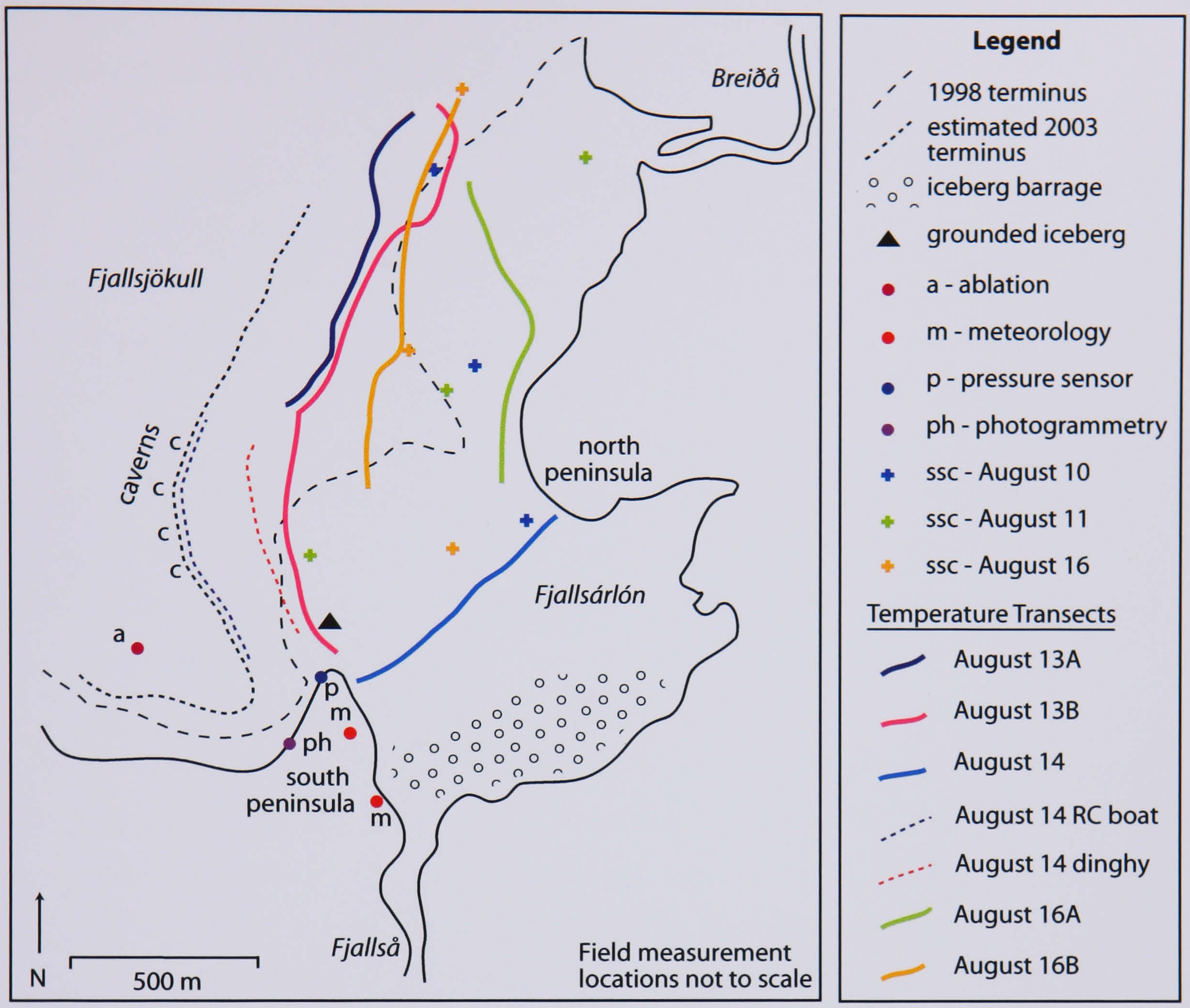

Figure 6.6 Field map of Fjallsárlón and the terminus of Fjallsjökull, showing the location of the field measurements. Based on the 1:30 000 scale map produced by Evans & Twigg (2000).

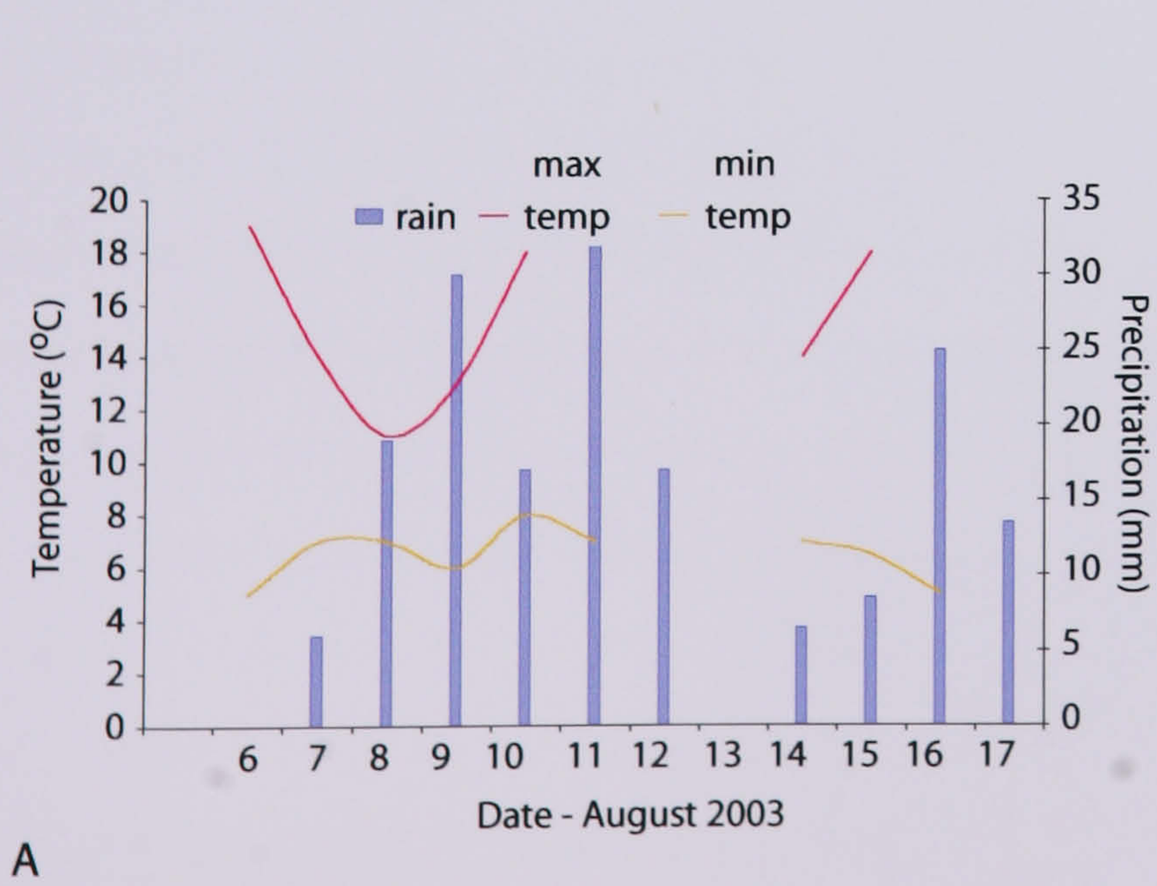

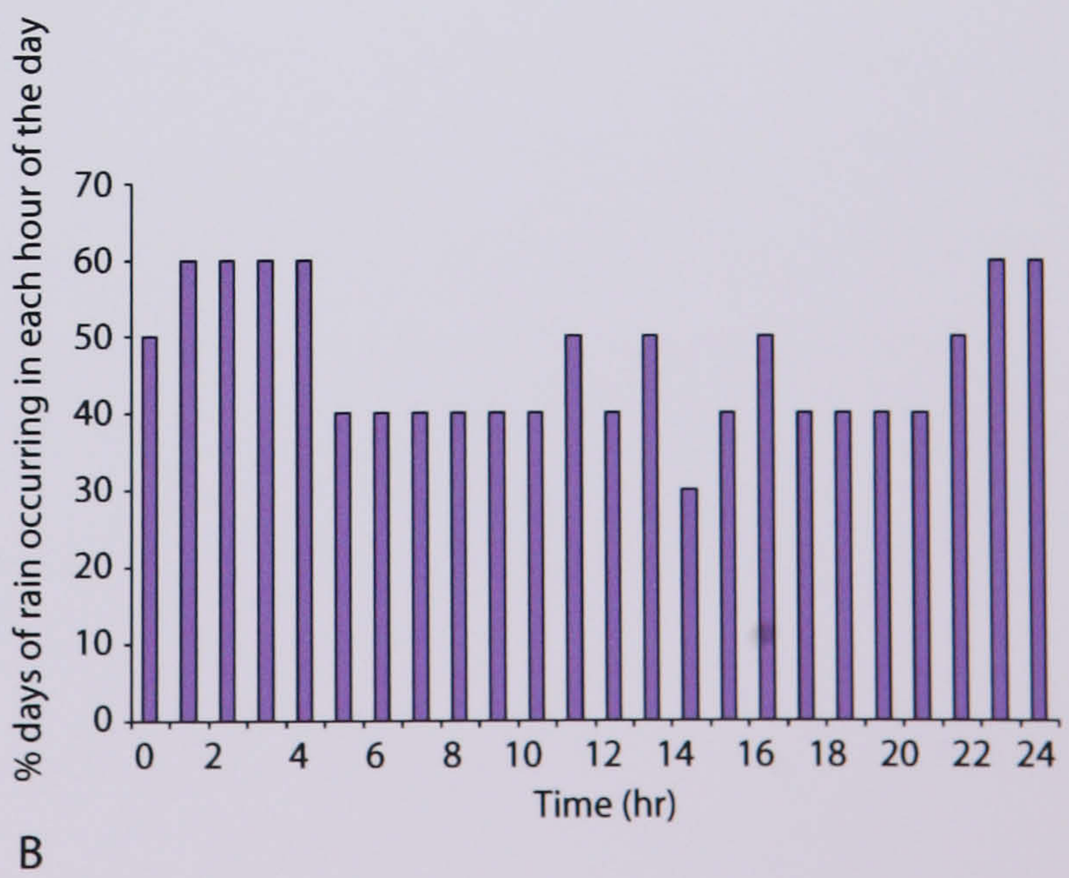

Figure 6.7 (A) Air temperature and rainfall at Fjallsjökull. (B) The percentage of days where precipitation occurs during each hour over the measurement period.

6.3.3 Glaciological Observations

6.3.3.i Glacier and Calving Characteristics

The surface of the glacier is highly crevassed, as it descends the steep slopes of the ice fall. There is very little debris on the ice surface, except at the typically non-calving lateral margins, where the ice flow is negligible and downwasting is taking place (Evans, D., *pers comm.*). Some 200-300 m up-glacier of the ice cliff in the centre of the terminus, in the zone shown on Figure 6.8, the slope direction begins to change, and slopes upwards to the glacier terminus at an angle of 5-10° (Figure 6.9). In the zone where the glacier surface is at its lowest, crevasse traces close up, and new crevasses typically re-open along the crevasse traces as they are advected towards the ice cliff in the area of the reverse surface gradient, as shown in Figure 6.9. The largest crevasses were observed to open up at least as far as the water level.

Calving takes place along all parts of the ice face, which varies in height, with some parts barely protruding above the water level, and other areas estimated at ~ 15-20 m above the water (Figure 6.8). Calving occurs daily, mostly consisting of small-scale events but with occasional larger failures which produce icebergs of estimated volumes of 5 000 – 30 000 m^3. The largest icebergs were grounded close to the glacier in the middle of the lake for several days before disintegrating, and one was present at the southern end of the lake (Figure 6.6) for the entire measurement period (Figure 6.8). Another large berg constituted a fragment of the terminus which simply detached from the main glacier, grounding immediately in front of the ice cliff, and maintaining the original surface geometry. Calving at a given section of the ice cliff was observed to be cyclical for the most part, progressing from thermal erosion of a melt notch at the waterline, to calving of lamellae, and then full-height calving events. The periodicity of these calving cycles is unclear, but was longer than the measurement period of 11 days along parts of the cliff, as repeated cycles on each portion of the ice cliff were not observed. Other parts, however, exhibited more regular calving activity, and this tended to occur along sections of the cliff where the subaerial portion was highest. Evidence for subaqueous events was also seen on August 10 and 13, at the southern end of the lake, where large icebergs with grooved channels, 0.15-0.2 m in diameter (Figure 6.10), and debris-rich sections were observed.

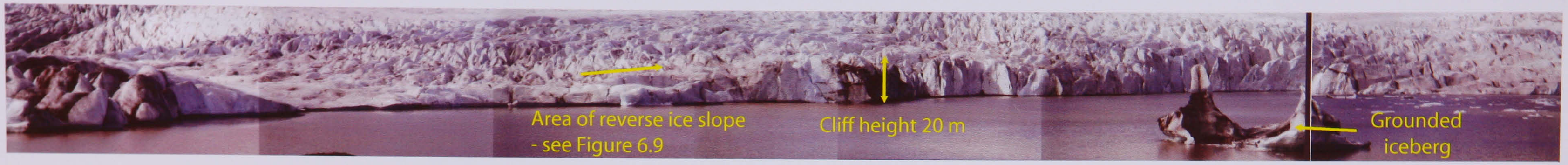

Figure 6.8 Panoramic view of the southern part of Fjallsjökull terminus, August 2003, showing the variation in subaerial ice cliff height, the reverse ice surface slope in the last few hundred meters of the terminus, and the large grounded iceberg that was present through the field season.

Figure 6.9 View of Fjallsjökull terminus, showing the gently rising ice surface to the cliff, and the propagation of crevasses along old crevasse traces immediately behind the ice cliff.

Figure 6.10 Iceberg in Fjallsárlón exhibiting a scalloped surface, indicative of subaqueous melting.

A thermo-erosional melt notch was present along all sections of the ice cliff, except at times when a large calving event removed the overhanging ice cliff (Figure 6.11). The notches often exhibited up to six subsidiary layers, spanning an estimated vertical distance of ~ 0.5-1 m (Figure 6.12), suggesting changes in water level position relative to the ice face, reflecting either lowering of the water level, or a rising ice cliff. This varied along the ice face, and portions of the ice cliff with no, or only one, notch layer could lay adjacent to a section with six. On a few occasions, a 'cavern' at the waterline was seen, which enlarged as progressive calving occurred, extending up to ~ 1 m in height (Figure 6.13).

Floating ice covers the lake surface primarily in the south and, whilst the smaller bergs melt within 24 hours, many bergs last several days, and congregate in a 'barrage' near the river exit of Fjallså, where they overturn as they melt until they are clear of the lake bed, to move down the river (Figure 6.14; Figure 6.6). Bergs often move quickly away from the ice cliff. In the fastest instance, bergs took less than 5 minutes to move from the terminus across to the northern peninsula. Despite the dynamic nature of iceberg drift in the lake, there is no evidence of persistent, strong plumes of upwelling meltwater.

A photogrammetric study of the ice face was carried out to examine the development of waterline melt notches and the changes in ice front geometry that took place. However, access to a suitable site was limited to the southerly end of the glacier, where calving activity was infrequent. Seven photos were taken from August 6–18 from the lake shore (Figure 6.6), but the low light conditions and the dark mountain background meant that co-registering the images onto fixed markers with sufficient accuracy for quantitative analysis was not possible. An effort to chart the evolution of a distinctive portion of the cliff with a large notch by taking repeat photos from a boat was also unsuccessful because the water currents meant that it was not possible hold an exact position using a GPS.

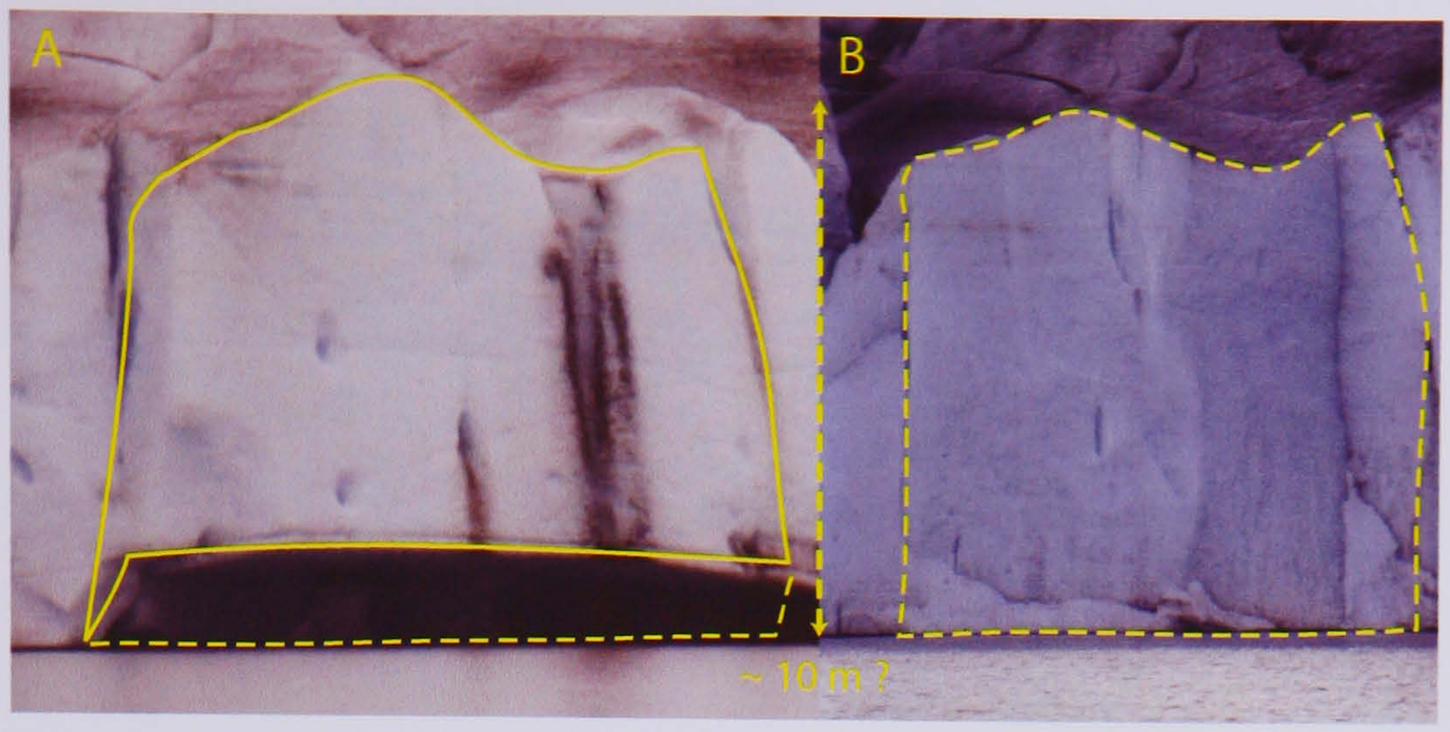

Figure 6.11 Photos before and after a calving event which caused the overhanging portion of the cliff to be removed, leaving a cliff with no waterline notch.

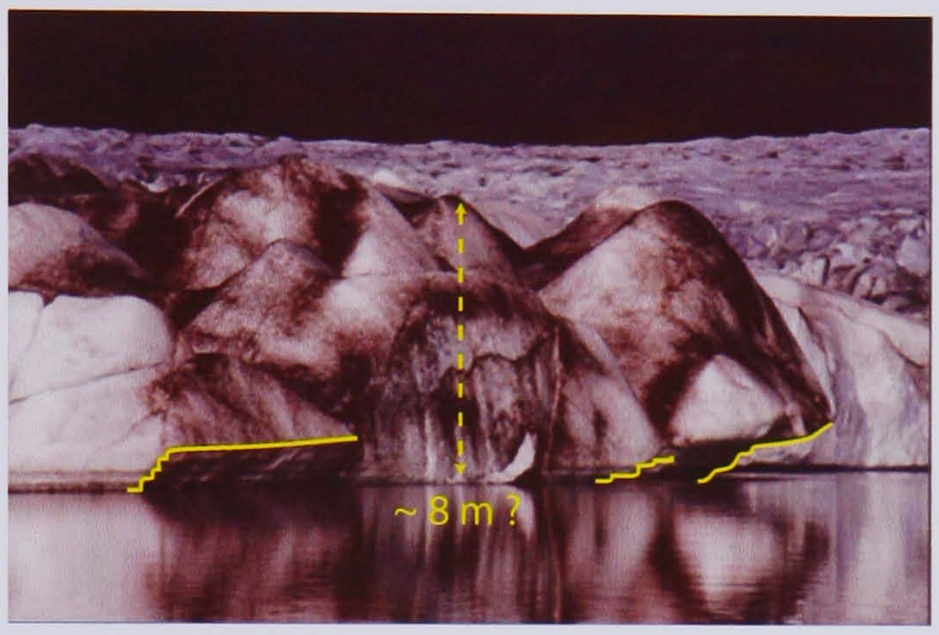

Figure 6.12 The southerly end of the ice cliff, illustrating some examples of the multi-layered waterline melt notches.

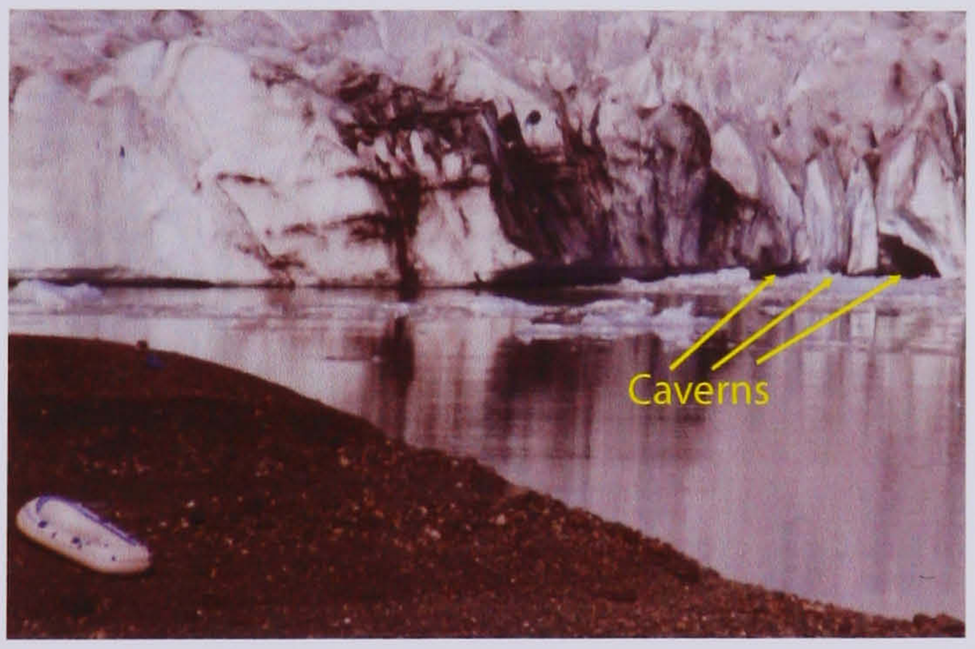

Figure 6.13 Caverns at the water line, at the southern end of Fjallsjökull terminus.

Figure 6.14 The barrage of icebergs that persisted at the downstream end of the lake.

6.3.3.ii Monitoring Calving Event Timing and Size

Rationale

Continuous monitoring of the timing and size of calving events is difficult, especially at night time. One possibility for monitoring ice front change is the use of automated repeat photogrammetry, from a fixed position near the terminus. This has been done at several sites (Krimmel & Vaughn, 1987; Walters & Dunlap, 1987; Kirkbride & Warren, 1997) and provides useful information, but it can only record terminus change at fixed intervals, and is not a continuous size/frequency record of calving activity. An indirect technique for obtaining such a dataset has been developed by Japanese workers, at Glaciar Moreno, Patagonia (Kobayashi *et al.*, 2001; Iizuka *et al.*, 2004), and at Mittivakkat Glacier, southeast Greenland (Hasholt, 2002). Abrupt changes in water level i.e. wave activity, identified from a record of pressure changes, can be used as a proxy for the size and timing of calving events. However, the criteria on which the interpretation of a calving event was based is not clear in the complex record at Glaciar Moreno and, at Icefall Lake, Mittivakkat Glacier, the record was very short. At Icefall Lake, the criteria that were derived for predicting the timing of calving events, using the pressure sensor, require further work before the method can be used on a wide scale to monitor calving activity, and contribute to an improved understanding of glacier and lake processes. At Fjallsjökull, a continuous proxy record of calving magnitude and frequency was obtained over a 10-day period, from August 7-16, 2003.

Calving waves

There are few descriptions of calving waves in glaciological literature, mainly because they pose little threat if they occur in remote locations. The effect of calving waves washing onto a dam at the Unteraargletscher, Switzerland, were investigated using a hydraulic model (Funk & Müller, unpublished). On a larger scale, long calving waves in Greenland may have wave lengths of tens of kilometres, wave heights up to ten meters, and a wave period of 1 – 10 minutes (Reeh, 1985). The wave period can be attributed to the oscillatory motion of the iceberg on the water surface, and typically have long wave lengths. The period of oscillation is sensitive to the water depth beneath the iceberg, and the iceberg size, where the wave length of the initial wave is of the same order of magnitude as the diameter of the iceberg (Weigel, 1955 *cf.* Syvitski, 1989; Reeh, 1985). The

wave amplitude depends on the net potential energy of the calving iceberg, where the trough that follows the first crest is one to three times larger in amplitude than that of the first crest. At Fjallsjökull, where berg sizes and water depths are small, compare to the fjords of Greenland (Reeh, 1985), wave amplitude is expected to be less than ~ 1 m, and wave periods are only a few minutes.

Field Methodology

A standard strain gauge pressure sensor, with an output of 100 mV at a full-scale range of 1 bar, was connected to a Campbell Scientific CR510 data logger facility. The sampling interval was one second, and the data were summarised to give a maximum, minimum and average value every minute. The sensor was located on a small peninsula at the south-west end of the lake, adjacent to the fixed marker used for lake stage (Figure 6.6). It was placed near the lake shore in water depth of 0.2 m, and fixed securely in place by several boulders. The location was ideal in that the peninsula protruded into the lake such that most calving waves were likely to be recorded. Moreover, waves generated by the overturn of icebergs were rare. Icebergs tended to overturn when they had been present for several days, and these icebergs were situated in the iceberg barrage (Figure 6.6), where their deterioration over this period resulted in geometries which became unstable due to their new mass distribution, and resolved by overturning. To confirm the correct identification of calving events from the pressure record, a record of the timing of both observed and audible events was also kept. The latter was useful when the glacier was not visible in poor weather and at night.

Interpreting The Pressure Record

The pressure readings (in volts) were calibrated to give relative change in lake stage (in cm), using the average of the eleven measurements taken from fixed stage markers (6.3.4.iv). The converted raw data (Appendix C) are presented in Figure 6.15. It shows the changes in lake stage that occurred relative to the initial reading, with maximum, minimum and average values plotted at one-minute intervals for the 10-day period.

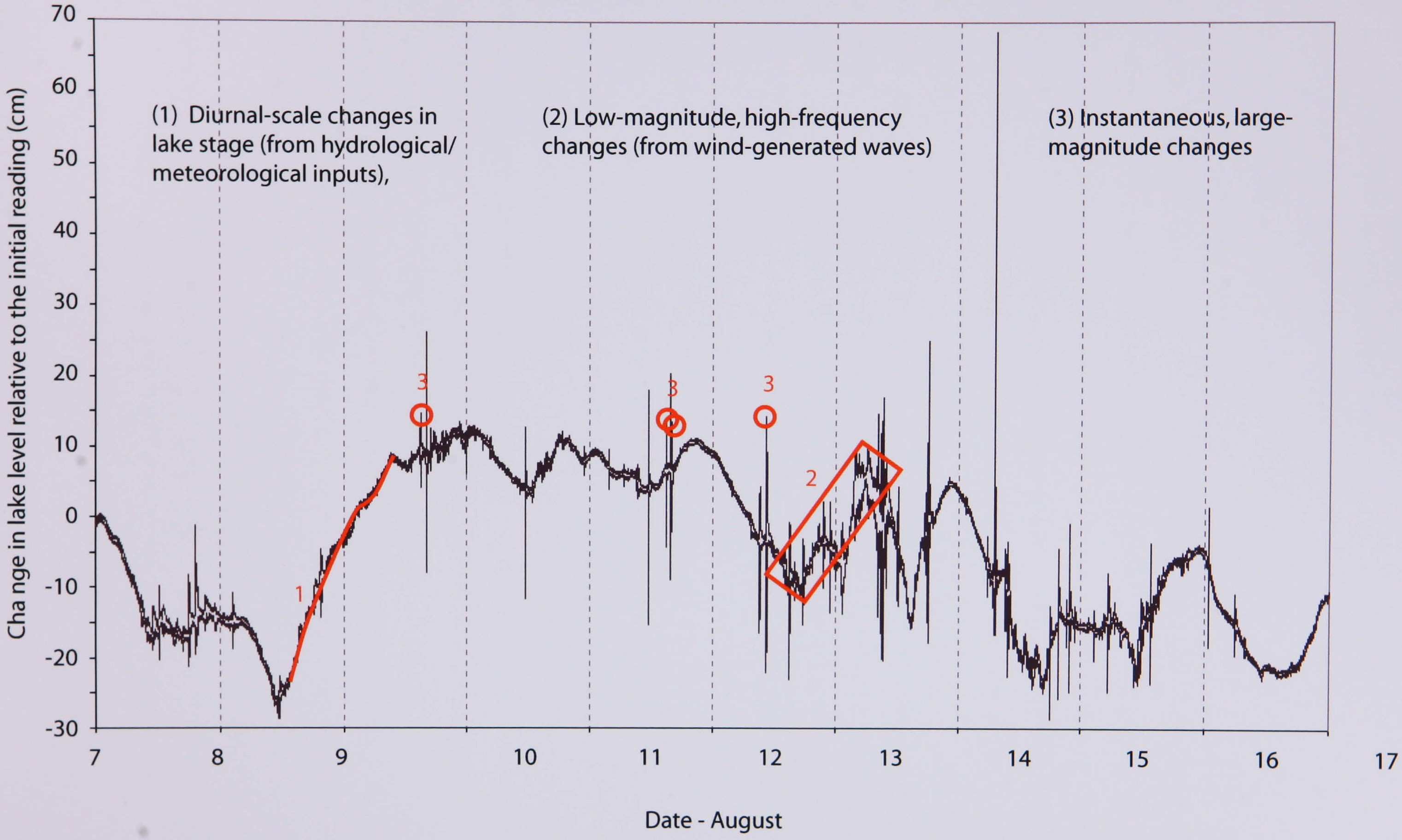

Figure 6.15 The recorded changes in relative lake level at Fjallsjökull, including maximum and minimum values measured every minute.

It displays:

1 Diurnal-scale changes in lake stage

2 Instantaneous, large-magnitude changes

3 Low-magnitude, high-frequency changes

Lake level changed from day to day (6.3.4.iv), in response to changes in input of precipitation, glacier drainage and discharge from Breiðå. The low magnitude changes are interpreted to reflect small wind-generated waves. The lake surface conditions were generally calm, reflecting the general absence of measurable winds in the meteorological data (6.3.2), and the wave amplitude (i.e. maximum minus minimum water level)was often as low as ≤ 0.005 m. The exceptions to this were the windy conditions recorded on August 13 and 15, when wave amplitudes were greater, with values of 0.04-0.10 m.

The large-magnitude changes are interpreted as the arrival of wave trains generated by calving events. Despite the calm conditions, there is some ambiguity in the origin of some of the peaks. These may relate to iceberg overturn events nearby in the lake, so it is necessary to define a calving criterion to determine which events in the record represent calving. At Fjallsjökull, two criteria were applied: the water level peak was reached within 2 minutes, and the change in water level was ≥ 0.04 m. The water level change was defined as the maximum difference between the maximum and minimum water level during the event. This allows comparison of event sizes with those observed at other calving glaciers (Hasholt, 2002; Iizuka *et al.*, 2004). On occasions when calving events were witnessed, those occurring from the southern portion of Fjallsjökull produced a calving wave that took ~ 1 minute to reach the pressure sensor. The application of these two criteria appears to identify calving events successfully. However, whilst most event peaks occurred within two minutes, there were some that have been interpreted as calving events, even though the time taken to reach the maximum peak was slightly longer. They were included if their amplitude dictated that it could only be a calving event or, in some cases, precursor events occurred during the rising limb (Figure 6.16a). There were also events which were not included, despite their sudden onset, as the time taken for the wave amplitude to dampen substantially was long, and more likely to reflect the sudden onset of wind blowing across the lake surface (Figure 6.16b).

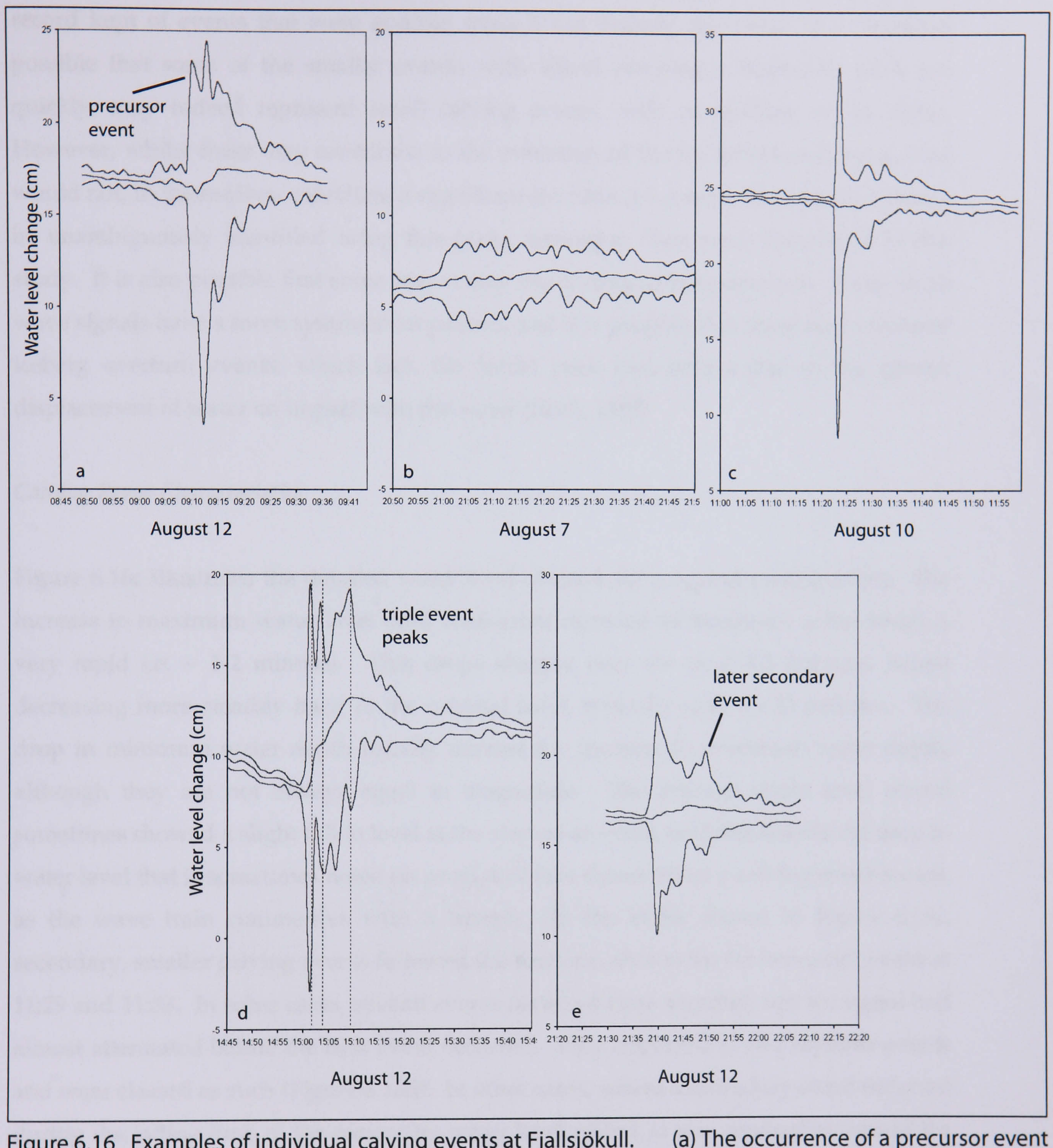

Figure 6.16 Examples of individual calving events at Fjallsjökull. (a) The occurrence of a precursor event before the maximum peak. (b) The signal produced by wind-driven waves on the lake surface. (c) A typical calving event, showing the rapid rise in maximum water level, and slower falling limb. Smaller, secondary events are seen, as well as the slight drop in average water level at the beginning of the event. (d) Several events in close succession constitute a single event. (e) A secondary event occurring during the falling limb of the main event.

However, it is important to note that only the very largest peaks can be correlated with a record kept of events that were audible, even if not directly observed. It is therefore possible that some of the smaller events, with waves reaching a maximum peak less quickly, may indeed represent small calving events, such as spalling of ice flakes. However, whilst these may contribute to the evolution of the ice terminus stresses, they would not, in themselves, constitute a significant ice mass loss event. Because they cannot be unambiguously identified using this proxy technique, they were discounted in this study. It is also possible that some waves may result from iceberg overturn. Some small wave signals have a more symmetrical pattern, and it is possible that these may represent iceberg overturn events, which lack the initial peak that occurs due to the greater displacement of water on impact with the water (Reeh, 1985).

Calving Event Characteristics

Figure 6.16c illustrates the detailed water level changes for a typical calving event. The increase in maximum water level (and concurrent decrease in minimum water level) is very rapid i.e. ~ 1-2 minutes. This drops sharply over the next 4-5 minutes, before decreasing more steadily back to the original level, typically over 15-30 minutes. The drop in minimum water depth usually mirrors the increase in maximum water depth, although they are not always equal in magnitude. The average water level record sometimes showed a slight fall in level at the start of an event, and this reflects the drop in water level that is sometimes noted on proglacial lake shores when a calving event occurs, as the wave train commences with a trough. In the event shown in Figure 6.16c, secondary, smaller calving events followed the first one, shown by the two small peaks at 11:29 and 11:33. In some cases, several events occurred close together, but the signal had almost attenuated before the next event occurred. They appeared as two separate events and were classed as such (Figure 6.16d). In other cases, where a secondary event occurred during the falling limb of the maximum water level record, it was counted as part of the same event (Figure 6.16e).

Calving Event Size

The water level change generated by most events ranges from 0.04 – 0.15 m (Figure 6.17), with the exception of a particularly large event on August 14, of 0.85 m, which washed icebergs far up the lake shore.

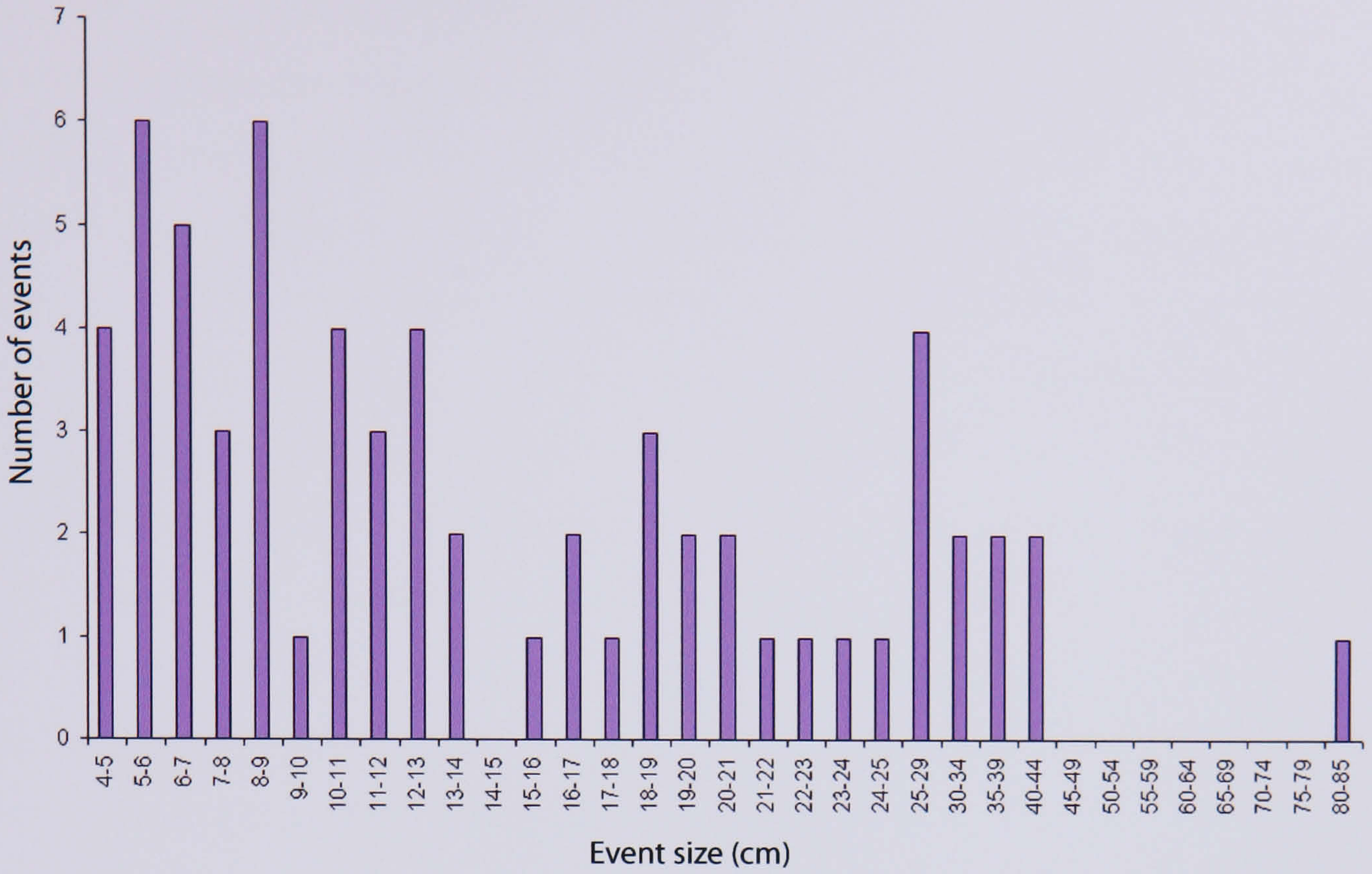

Figure 6.17 The number of calving events at Fjallsjökull occurring at each size interval (in centimeters, water level change).

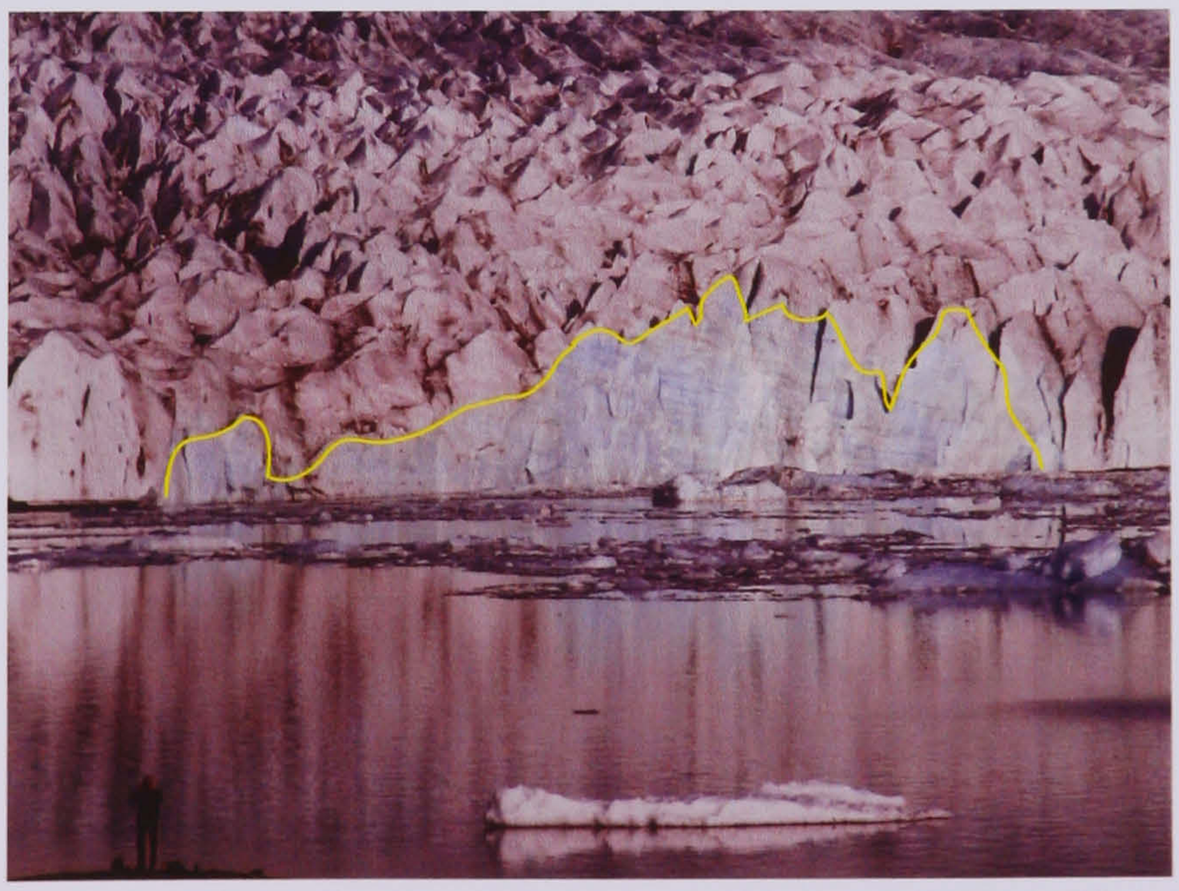

Figure 6.18 The scar resulting from calving event at Fjallsjökull at 0700h on August 14, 2002. Full-height subaerial calving occurred above the waterline in ice with crevasses occurring obliquely to the cliff.

The 'scar' on the calving terminus, outlining the extent of this calving event can be seen in Figure 6.18. The average peak size is 0.16 m. Most calving events are <0.20 m (peak size) and occur frequently (within 2 hours of the previous event). At Icefall Lake, the peak size for the two calving occurrences was ~ 0.10 - 0.15 m. The results at both Fjallsjökull and Icefall Lake contrast with the observations reported by Iizuka *et al.* (2004). Whilst calving events at Glaciar Moreno, Patagonia, created similar water-level change geometries, many of the events appear to be larger, ~ 0.2 – 0.4 m (Iizuka *et al.*, 2004). Whilst larger icebergs often calve at Glaciar Moreno, they reported only the 'largest' calving events, and there is no indication what the criteria were for determining the occurrence of a calving event from the pressure record. At other lake-calving glaciers, such as Maud Glacier, New Zealand, where there is a stable terminus position, combined with a low slope gradient and ice velocities, calving events are large and infrequent (Warren & Kirkbride, 1997). The similar pattern of calving of small icebergs at Fjallsjökull and Glaciar León (4.3.1.i), which also descends a steep icefall only a few hundred meters back from the ice cliff, suggests that crevasse density, dictated by the steep underlying topography, plays an important role in determining the size of icebergs produced.

Timing of Calving Events

Inspection of the data indicates that 64 inferred calving events occurred during the 10-day period. Calving events occur, on average, every 3 hours. Although the intervals between events were, at longest, 18 hours, many events occurred within less than an hour of the previous event (Figure 6.19). Analysis of the timing of the calving events on different time scales allows investigation of the factors that influence the occurrence and timing of calving events. The number of calving events was examined on an hour-by-hour and day-by-day basis. Figure 6.20 shows the number of calving events that occurred each day. A clear increase in the daily number of events occurred prior to August 14, the day that the largest event took place, at 0704h.

Rainfall totals per day (6.3.1, Figure 6.7) show little correlation to the number and size of events occurring on the same day, although more than half of all calving events occurred during periods of no rain. However, if a 3-day time-lag period is used, diurnal rainfall amounts correlated better with the number of events, with an R^2 value of 0.54 and peak rainfall, on August 11, matching the day of largest calving events, August 14.

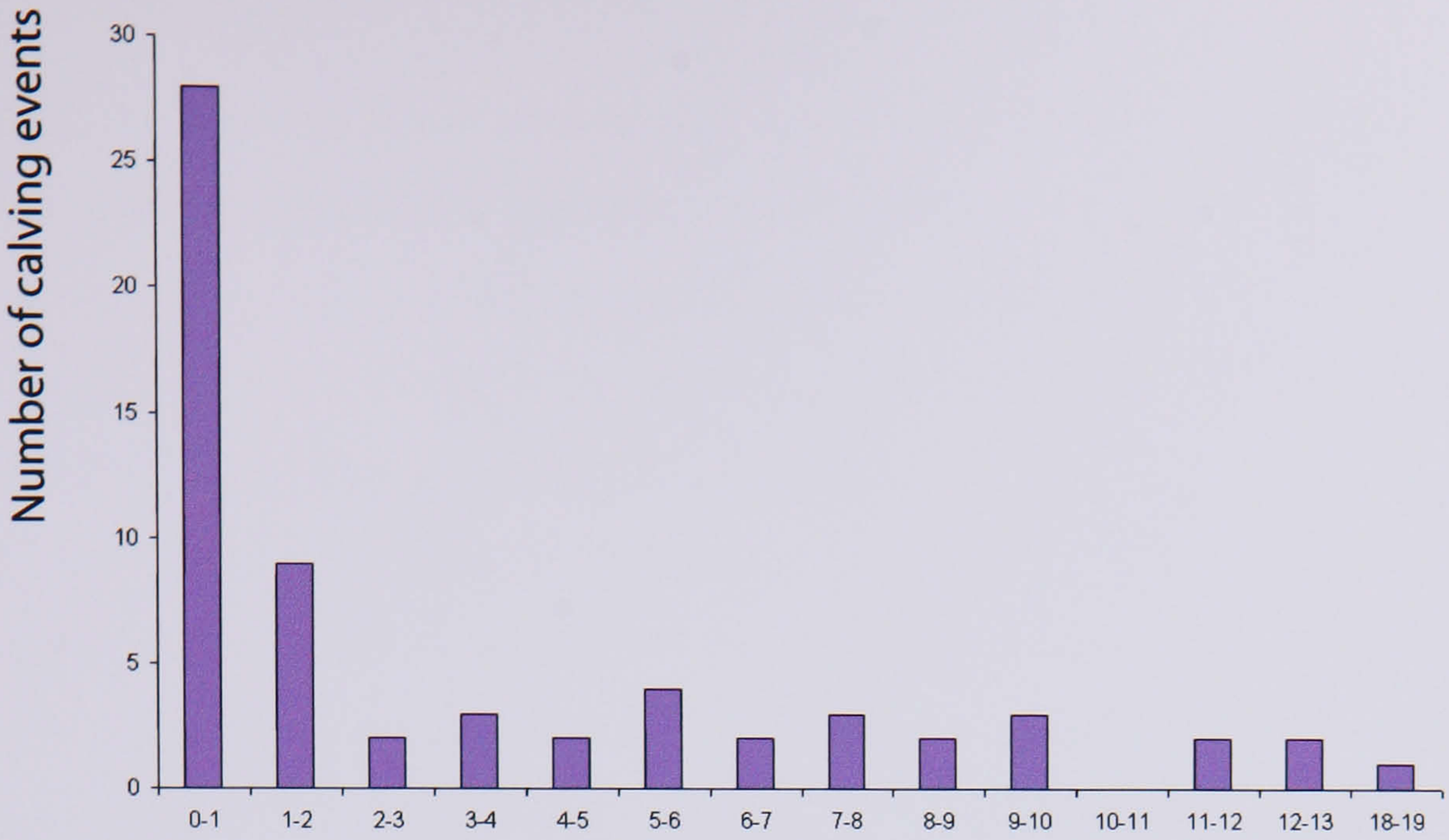

Figure 6.19 The frequency of the interval between calving events at Fjallsjökull, August 2003.

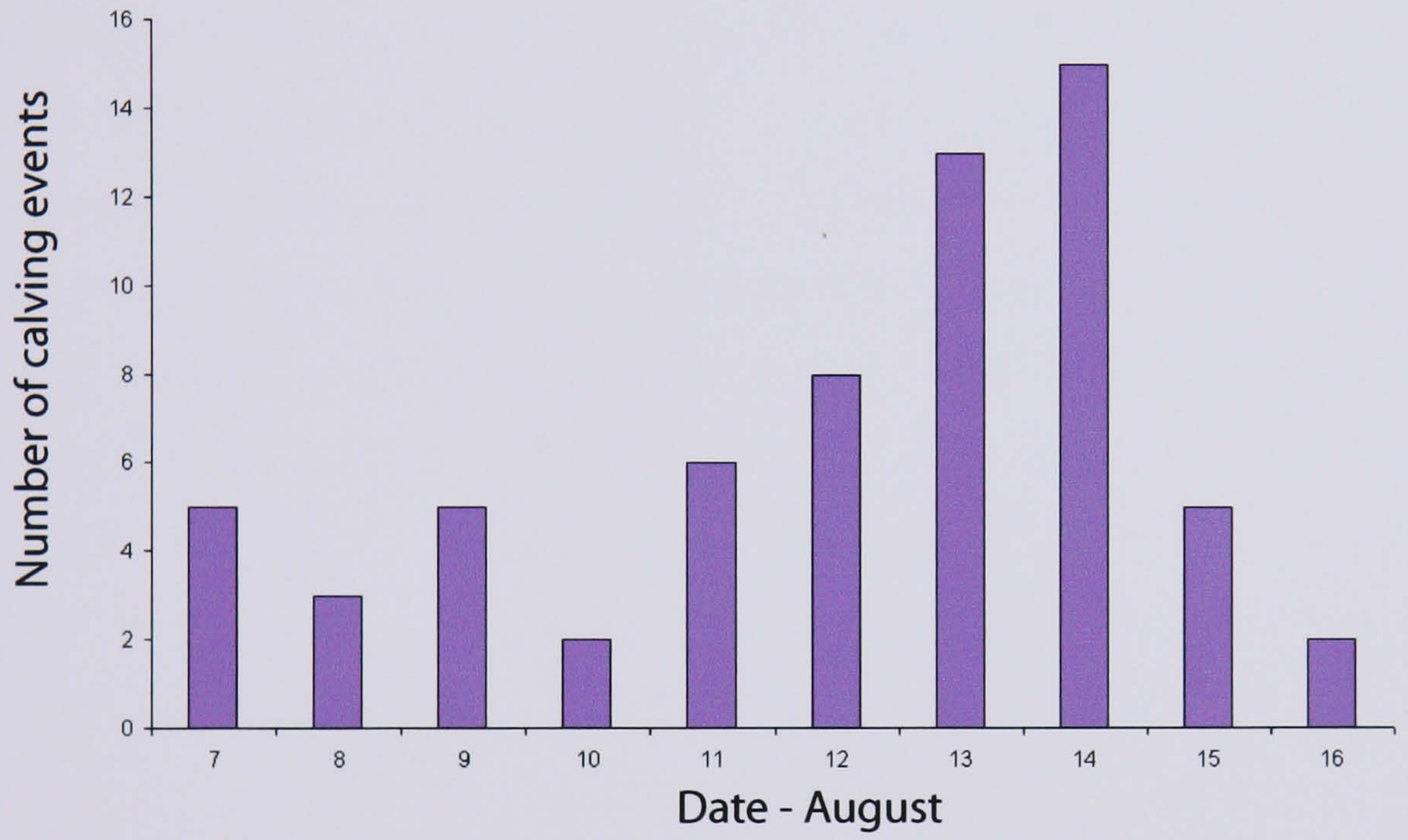

Figure 6.20 The number of calving events occurring each day at Fjallsjökull, August 2003.

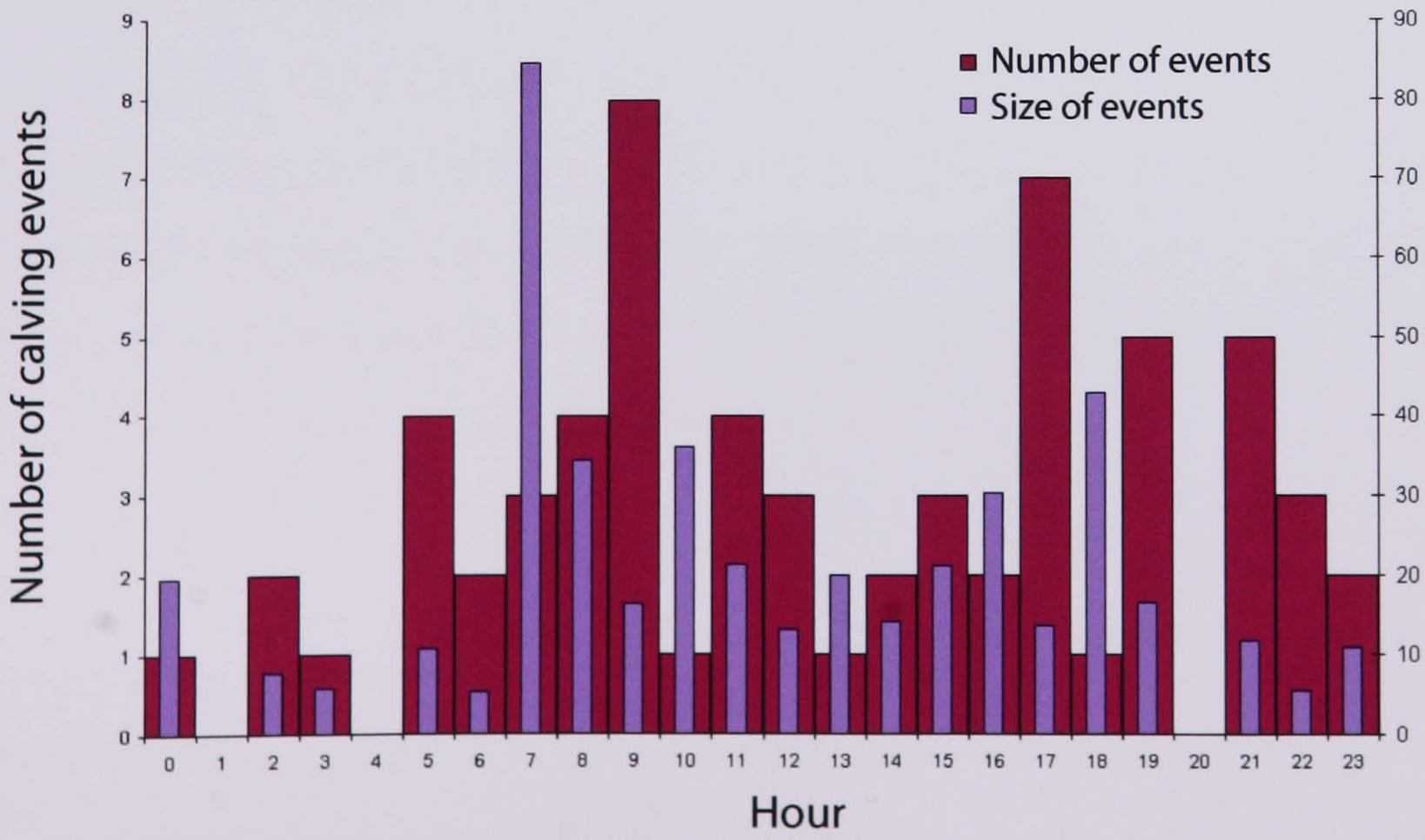

Figure 6.21 The number and size of calving events occurring during each hour over the measurement period at Fjallsjökull, August 2003.

However, the R^2 value is not necessarily indicative of a causal link, as the time series is too short to observe sufficient patterns of either rainfall or calving event occurrences. Furthermore, it is unlikely that any precipitation falling into the glacier would take more than one day to travel through the ice to the glacier bed, as the highly crevassed nature of the ice surface provides a fast route for precipitation to the glacier bed (cf. O'Neel *et al.*, 2001). Over a one-day lag, it is possible that precipitation could cause an increased number of calving events: increased ice velocities, due to decreasing basal drag, might trigger an unstable period, to which the glacier adjusts by calving rapidly. Furthermore, if calving events occur over cycles of more than ten days, the dataset here is not long enough to investigate thoroughly whether there is an autocorrelation with precipitation.

Figure 6.21 shows the number of calving events occurring each hour during the measurement period. In general, more events occur during the daylight hours, with 86 % of events occurring during between 0500 to 2200h. Additionally, the average event size is typically higher between these hours. However, the correlation coefficients for these comparisons are low, and a longer series would be necessary in order to examine them more thoroughly. Iizuka *et al.* (2004) also note a peak during the day, with most events occurring between 1100 and 1800h. They comment that when there were more events i.e. during the day and over the period December 6-9, 1999, the maximum amplitude recorded was also large. At Fjallsjökull, however, the correlation between event frequency and size was low, where $R^2 = 0.40$.

Over the period of 10 days, it appears that there are two peak times for the occurrence of events - 0900h and 1700h, with 8 and 7 events occurring at these times, respectively. Iizuka *et al.* (2004) report that the largest number of calving events at Glaciar Moreno occurred at 1600h and 1700h (6 and 7, respectively, of a total of 68 events over the 12-day period in December). Similarly, at Icefall Lake, both calving events in the recorded observations occurred late in the day, at 1700h and 2200h (Hasholt, 2002). At Fjallsjökull, the occurrence of two key time periods for calving events is much stronger than that at Moreno, although both records span only 10 and 12 days. If this apparent trend is real, it is tempting to speculate about the causes for this temporal pattern.

Using radiation data and air temperature variations, Iizuka *et al.* (2004) suggest that there is a relationship between the hourly number of events in a day and the hourly air temperature rise, which ranged from 2.8 to 19.6 °C. However, the daily temperature range

at Fjallsjökull is much lower (6.5 - 13.4 °C), and net radiation received is likely to be lower due to the persistent cloud cover. Detailed records are not available here. However, Meier & Post (1987) note that maximum daily ice velocity at Columbia Glacier occurred 7-8 hours after maximum insolation/air temperature, evidence that glaciers can respond over shorter timescales. Hasholt (2002) logged water temperature concurrently with water level, and commented that maximum water temperatures were reached at 1500h each day. With reported water temperatures of ~ 9 °C at Icefall Lake, it is likely that subaqueous melting rates are high (Eijpen *et al.*, 2003), and it is possible that these diurnal trends of warming provide a trigger for calving late in the day, by exacerbating subaqueous melt rates, undercutting the subaerial ice cliff to a critical threshold. The time taken for this warming to affect the ice cliff may also help explain the relatively high frequency of calving events until 2200h, as also evidenced at Icefall Lake. Rainfall at Fjallsjökull peaked between 2100-0500h (Figure 6.7b). It is possible that the peak in number of calving events at 0900h corresponds to a response to this high rainfall and that the peak in events at 1700h relates to ice oversteepening following subaqueous melt due to several hours of insolation warming the lake water.

Over timescales of less than one hour, Hasholt (2002) noticed that water temperature dropped by > 0.5 °C over ~ 15 minutes, reaching a minimum ~ 15 minutes before the calving event took place. However, the logger was situated some distance from the ice front, and this phenomenon was observed on so few occasions that it is just as likely that cooler water drifted past the logger at that time. Comparably detailed water temperature data are not available here. Water temperatures in Fjallsárlón, and their implications for calving at Fjallsjökull, are discussed in section 6.3.4.i. Hasholt also noted a rise in water level, of 0.01 – 0.02 m, up to an hour before the calving event. The combination of these events was interpreted as the release of cold water at the glacier front, due to opening of crevasses, and he suggests that these features can be used to predict glacier calving. The effects of water level changes, over timescales of a few hours at Fjallsjökull, on the timing of calving events are reported in section 6.3.4.iv.

Finally, the time between events was also studied to see if there was a pattern relating the timing of calving events of various sizes. Of particular interest was whether the observed cycles of calving, described in section 6.3.3.i, could be detected. However, there is no pattern in the record. This is partly because one part of the ice cliff will be at a different stage in the calving cycle compared to another section, and it is not possible to extract the

signal of cyclicity without knowing from which part of the ice cliff a particular high-stage calving event occurred. However, cycles are unlikely to be registered on the pressure record until it is possible to distinguish between iceberg overturn events and flake calving.

6.3.3.iii Ablation

To estimate subaerial melting at the terminus cliff, two ablation stakes were placed on the glacier, close to the terminus in clean ice (Figure 6.6). Wooden stakes with a diameter of 2 cm and a length of 50 cm were drilled 15 cm into the ice using an ice screw. One stake was placed on a horizontal surface, and the other a vertical surface, with an aspect comparable with much of the ice cliff i.e. east-south-east, both in an initial ice depth of 15 cm. Ablation was monitored over an eleven-day period, from August 6. Access to the glacier was restricted by weather conditions, and redrilling was undertaken, as necessary, when the stakes melted out. The ablation record is therefore limited to periods when access was possible every 24 hours, as shown in Table 6.2.

Date	**Ablation Rate (m d^{-1})**	
	Horizontal Ice	**Vertical Ice**
06-07/08	0.07	0.03
15-16/08	0.07	0.12

Table 6.2 *Ablation rates at Fjallsjökull, August 2003, showing values obtained over 24-hour periods.*

On the horizontal ice surface, ice melt rates in both periods were 0.07 m day^{-1}, whilst values on the vertical ice face were 0.03 and 0.12 m day^{-1}, giving a mean of 0.08 m day^{-1}. These values are likely to be similar to those at the ice cliff, and less than those occurring under debris at the lateral margins (6.3.3.i). They are comparable to other clean ice rates at lake-calving glaciers, including those measured in this study, at Glaciar León (4.3.1.iv). Rates at Maud Glacier, New Zealand, are ~ 0.05 m d^{-1} (Kirkbride & Warren, 1997) and 0.06 – 0.10 m d^{-1} at Tasman Glacier, New Zealand, (Roehl, 2003).

6.3.4 Limnological Observations

6.3.4.i Water temperatures

Rationale

Melting can be important at both tidewater and lake-calving glaciers, as discussed in Chapters 2.1.5 and 2.3 (Vieli *et al.*, 2002; Motyka *et al.*, 2003a; Warren & Kirkbride, 2003). Various field approaches have been undertaken to examine melt rates (2.3.3), but there is still no satisfactory method with which rates of melting may be accurately calculated. This is due to the dangerous nature of obtaining direct measurements (Hands, 2004). Water temperature has been identified as one of the key factors influencing melt rate (Weeks & Campbell, 1973; Neshyba & Josberger, 1980; Russell-Head, 1980; Eijpen *et al.*, 2003), along with salinity and current speed (Josberger & Neshyba, 1980; Keys & Williams, 1984; El-Tahan *et al.*, 1987; Syvitski, 1989). However, it is not satisfactory to use far-field values of water temperature to calculate rates of melt at the ice face. Upwelling of cold, buoyant water occurs along the ice face, from either sub- or en-glacial meltwater outflow, or that produced from direct melting of the ice face itself. Thus, the ice-water boundary zone is likely to exhibit a complex thermal regime, whose temperatures are likely to differ from those in the surrounding water body, particularly if large volumes of meltwater are present. It is often impossible to gain access to the ice face closer than ~ 100 - 200 m (Walters *et al.*, 1988; Warren *et al.*, 1995a; Warren, 1999), and the relevant water temperature measurements may be missed. In this study, the issue of safety was overcome by using a small, radio-controlled (RC) boat which enabled water temperatures to be measured in the immediate ice-proximal zone.

Method

Water temperatures in the lake were surveyed on August 13, 14, and 16. An array of Gemini inductive aquatic temperature loggers (Appendix D) were operated from both an inflatable dinghy in mid-lake areas (Figure 6.22a) and the RC boat in the ice-proximal area, immediately adjacent to the ice cliff (Figure 6.22b). The logger array was attached to the boat on a string at marked intervals, with a float attached in case the array became separated from the boat.

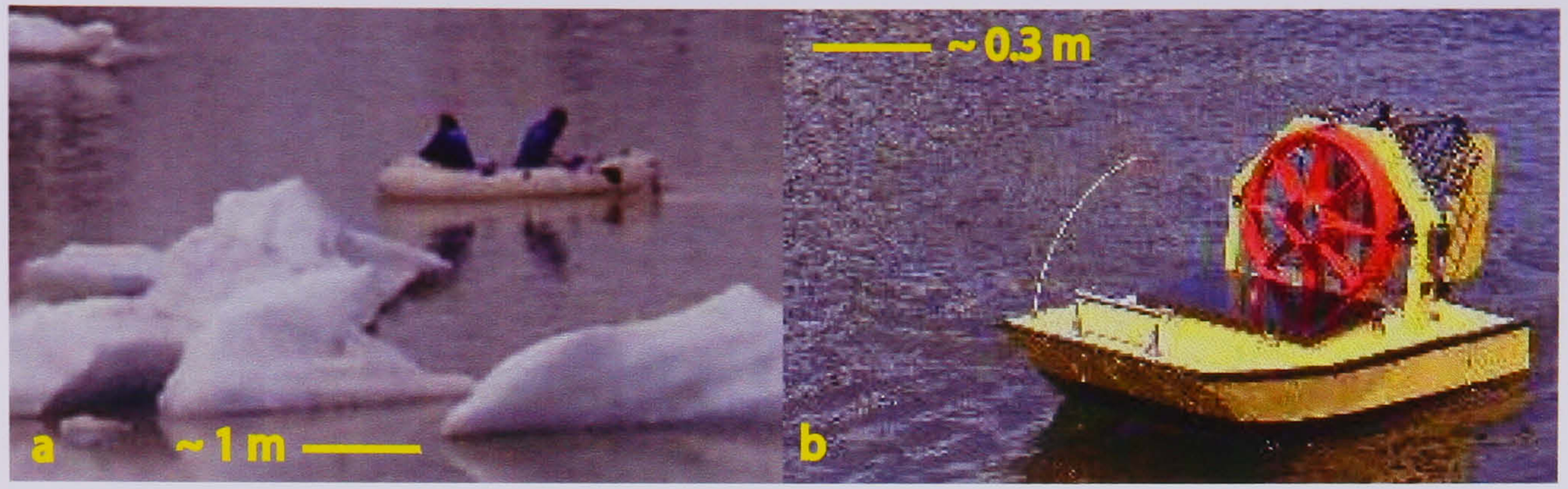

Figure 6.22 The boats from which water temperature measurements were collected at Fjallsjökull, August 2003. (a) The inflatable dinghy, and (b) the radio -controlled boat. Scales apply to the boats dimensions.

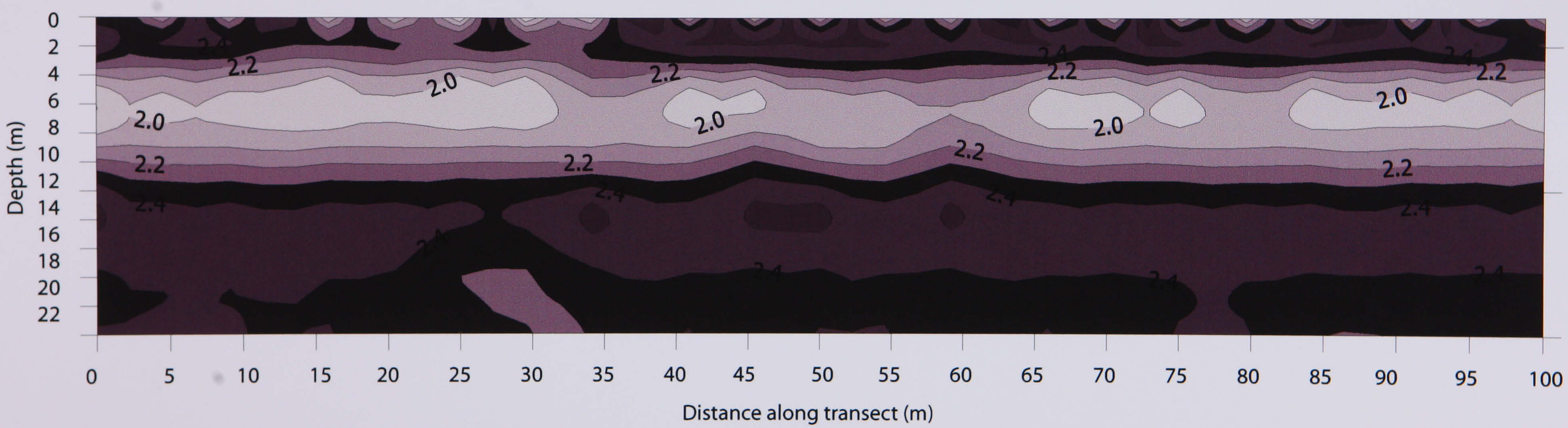

Figure 6.23 2-D profile of lake temperatures in Fjallsárlón, August 16 (B), 2003, showing the cool layer at ~ 4 m deep.

The RC boat, designed and built for the purpose, is driven by a 2 horse-power petrol engine, through an air propeller. The radio unit has a signal range of 400 m, permitting operation at a safe distance from the calving cliff in the inflatable boat.

The seven loggers had a logging interval of 1 minute. When using the RC boat along the ice front, on August 14, five loggers were used, at lengths of 0, 2.5, 5, 10 and 15 m, whilst the other two were employed on the dinghy, mid-lake, at 0 and 5 m. This gave a simultaneous comparison of water temperatures between the ice front and mid-lake. Previous attempts to utilise all the loggers with the RC boat, down to 25 m, proved unsuccessful, as the loggers created excessive drag, inhibiting the manoeuvrability of the boat, or became lodged against ice protrusions or the lake bed at depth. Problems arose in balancing the need to weight the logger array to keep its orientation vertical and the need to retain forward momentum and steerage. Regardless of the weights applied, the loggers did not remain vertical when used from the dinghy. On the RC boat, too much weight caused the array to act like an anchor, immobilising the boat, whilst too little weight caused the array to trail out at the surface. On August 13, 14, and 16, the loggers were also used on the dinghy alone, attached at lengths of at 0, 2.5, 5, 10, 15, 20 and 25 meters. For all measurements, the array depths were corrected for an estimated trailing angle of 60° to the vertical, and the corrected depths to the nearest meter are used (due to limitations in accuracy), hereafter, as shown in Table 6.3.

Length of string (m)	**Actual depth (nearest m)**
0	0
2.5	2
5	4
10	9
15	13
20	17
25	22

Table 6.3 *Converted depths of the temperature logger array in the water column, to account for the angle at which the array trailed in the water.*

An in-built GPS unit was not available on the RC boat, and the locations of temperature measurements are approximate (Figure 6.6). On the dinghy, however, a hand-held GPS was used to record the position at minute intervals, so that the positions could be recorded. When the loggers were used on the dinghy alone, transects were made of the ice-proximal area, some ~200-300 m from the ice cliff. Transects were made both south-north and north-south, at different distances from the ice cliff (Figure 6.6). The northerly limit of measurement was constrained by the inflow of Breiðå, as it was not possible to overcome the strong current and take measurements further north. On occasions, when measuring water temperatures from the dinghy, large amounts of brash ice were present, usually in a restricted zone and their location was recorded for comparison with measured water temperatures.

Results

The seven loggers recorded data continuously from 1200h on August 13 until their memories were full, on August 18. The precise times at which temperature transects were made were noted, and these were extracted from the overall record, allowing 10 minutes at the start of each measurement period, during which the loggers adjusted to the temperature difference between air and water, as indicated in the Gemini manual. As a result, some transects have been shortened to allow for erroneous data where the adjustment time had not been fully accounted for in the field. The data were subsequently analysed in Microsoft Excel and Golden Software Surfer.

In August 2003 the lake was characterised by temperatures of 1.5 – 2.5 °C, comparable with those seen at neighbouring Jökulsárlón (Harris, 1976). A layer of warmer water was persistent across all measured areas of the lake at a depth of ~ 2 m. Cooling, sometimes to the minimum values observed, occurs at depths of ~ 4 - 9 m, before warming down to ~ 13 m, followed by slight cooling to the bottom of the profile at ~ 22 m (Figure 6.23). The cool surface layer may reflect the frequent iceberg cover on the lake, which provides a source of 0 °C meltwater to the water surface. The cool layer between 4 – 9 m may reflect meltwater entering the lake as an interflow (2.2.4). Interestingly, the transect of August 14 exhibits some of the warmest temperatures seen in the lake, at a depth of 22 m, with values up to 2.7 °C on the north side. The transect is located between the two peninsulas (Figure 6.6), and is the transect made at the greatest distance from the glacier. Reasons for this are not clear.

Water temperatures in the mid-lake area were recorded on August 13, 14 and 16, at ~ 2000h, 2000h and 1500h, respectively. The temperature transects, and their averages, are plotted in Figure 6.24 and Figure 6.25. A temperature gradient indicates cooling towards the south (August 13 and 14). This probably relates to an influx of melt water coming from the south end of the glacier, evidenced by the cavern that subsequently developed on August 15 (Figure 6.13). Additionally, the large grounded iceberg that was present throughout the measurement period caused a decrease in water temperatures in the immediate vicinity, coinciding with this transect. However, localised cooling in both the north and south occurs on August 16, which may relate to an increase in meltwater coming from Breiðå, following the warm sunny weather of the previous few days, although the low lake level on August 16 conflicts with this suggestion. These profiles indicate an overall warming trend towards from the glacier (Figure 6.6 and Figure 6.25), and occurs even between the two transects on August 13. However, weather conditions varied between transects on the different days and may explain this trend: whilst August 13 was sunny and windy, August 14 was sunny with rain in the evening, and persistent rain fell during August 16. The notably cooler water on August 14 may reflect the increased input of meltwater and icebergs in conjunction with the high amount of calving activity occurring that day. This trend is, therefore, not reliable.

Using the radio-controlled boat close to the glacier generated the coolest temperature measurements, as low as 1.49 °C. Although more variable than the mid-lake temperatures, the profiles exhibited similar vertical profiles geometry (Figure 6.26). The comparison between measurements at 4 m deep at the ice-water boundary and those taken simultaneously in the mid-lake area shows the consistent difference in temperature, with cooling towards the north, similar to measurements on the mid-lake profiles (Figure 6.27). This strengthens the argument for suggesting the location of meltwater influx in this area. The data confirm the hypothesis that water temperatures at the ice-water boundary are cooler than those mid-lake, and that it is not appropriate to use mid-lake temperatures as proxies for the boundary conditions when calculating rates of ice melt. The implications of this temperature difference on melt rates are discussed in Chapter 7.2.

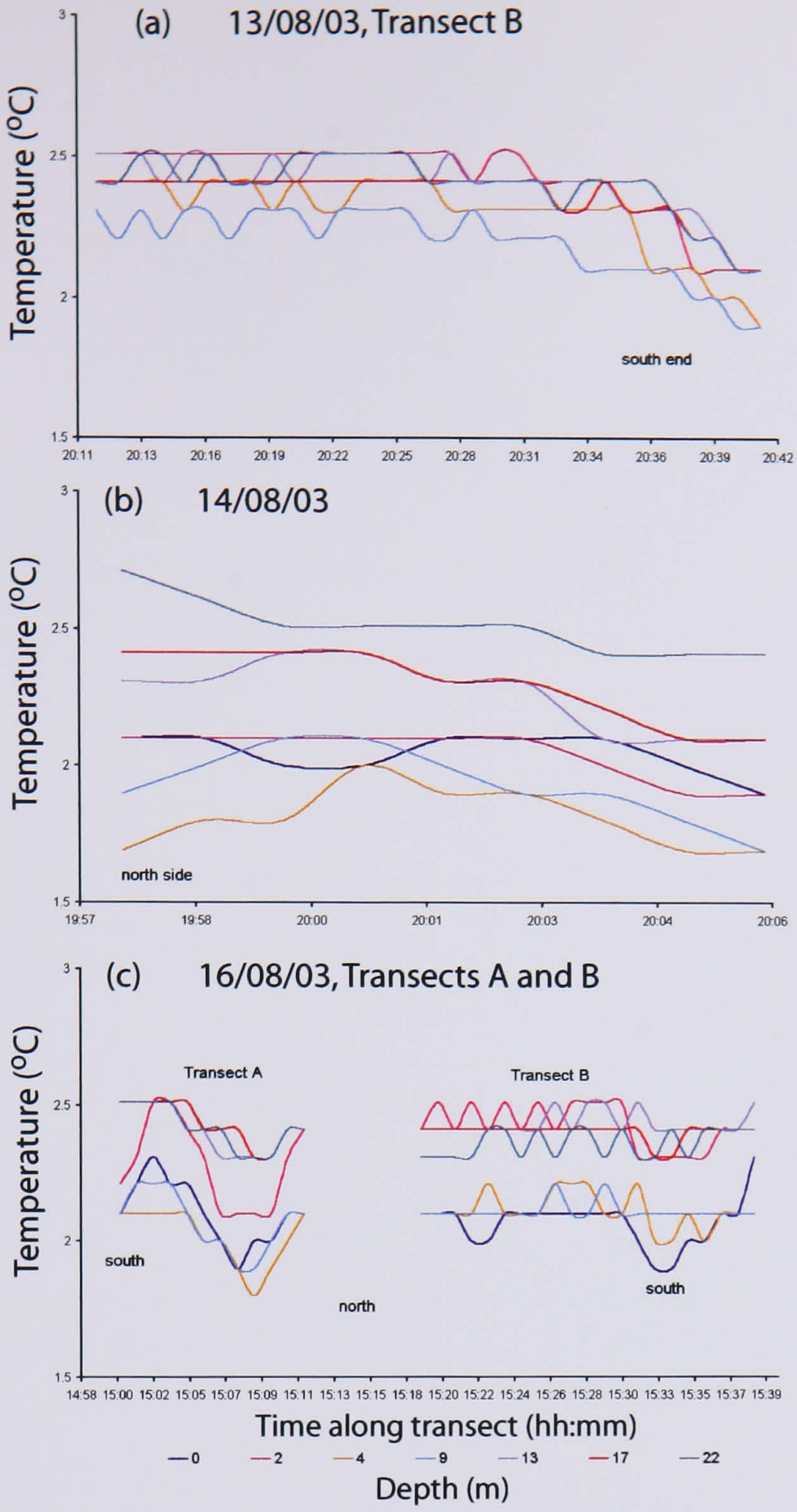

Figure 6.24 Water temperatures along each transect in Fjallsárlón, August 2003. For locations of transects, see Figure 6.6 (p. 160).

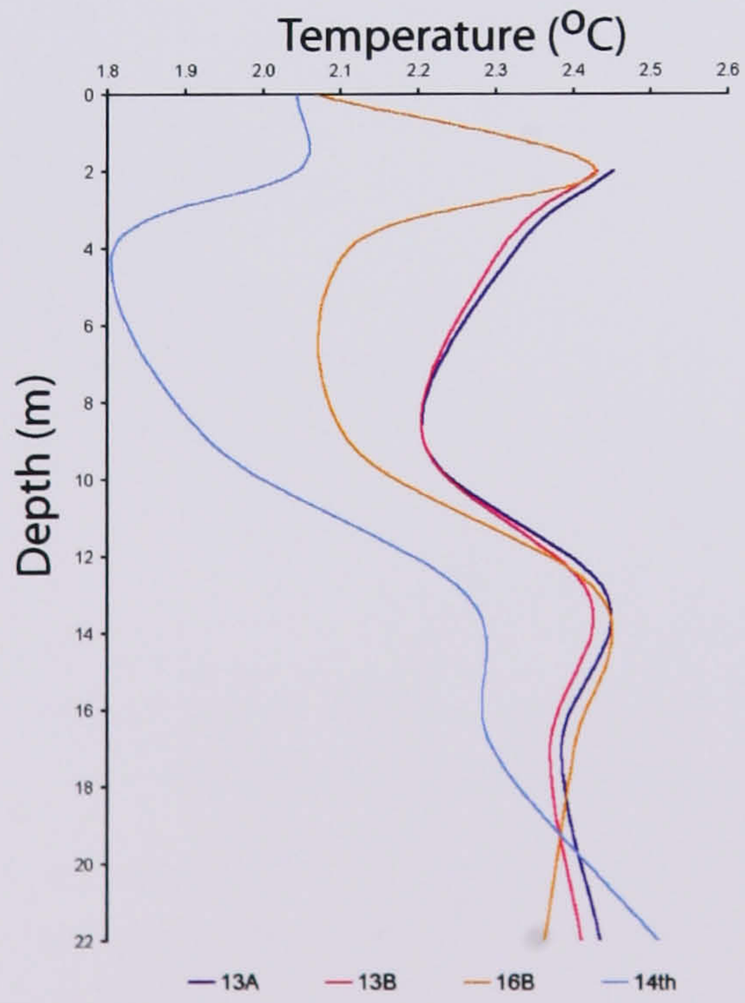

Figure 6.25 Depth-averaged temperatures for August 13, 14 and 16, 2003, in Fjallsárlón (cf. Figure 6.6, p. 160), showing a warm layer at 2 m, minimum temperatures at ~ 4 m deep, and a general cooling trend away from the glacier.

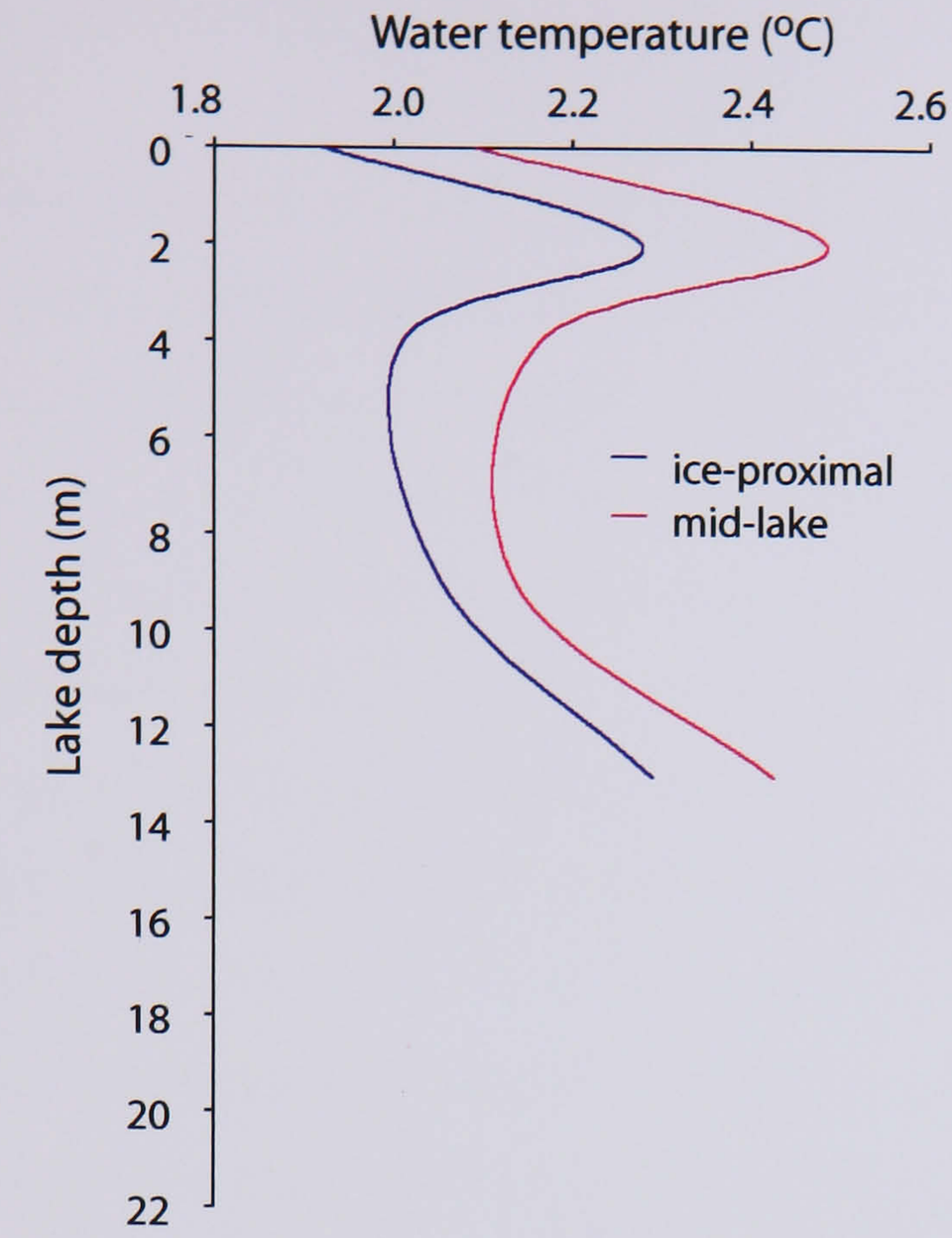

Figure 6.26 A comparison of depth-averaged temperatures measured near the calving terminus of Fjallsjökull using the radio-controlled boat with temperatures measured mid-lake on August 14, 2003, showing warming away from the glacier. For location, see Figure 6.6 (p.160).

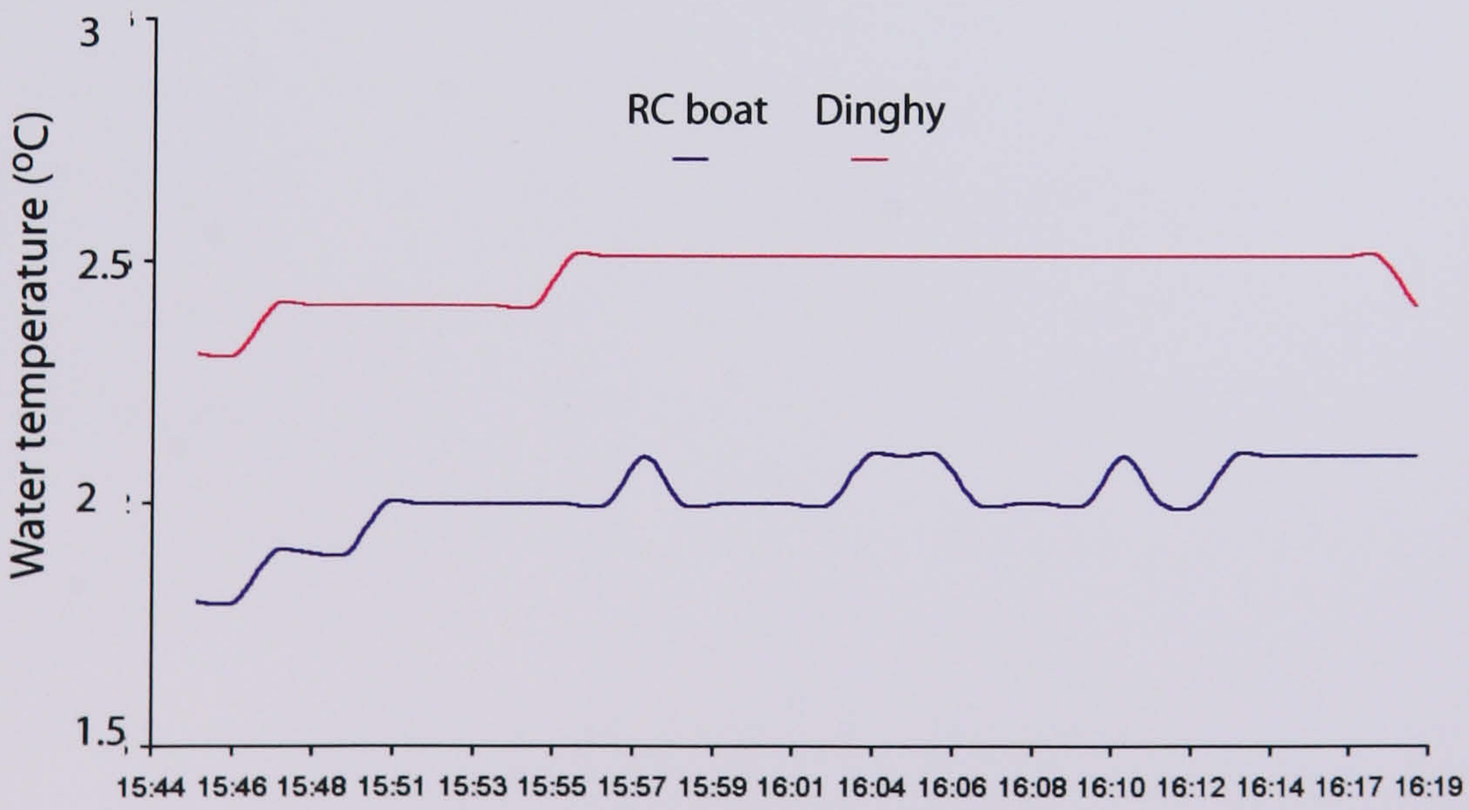

Figure 6.27 Comparison of water temperatures at 4m depth on August 14, 2003, near the ice using the radio-controlled boat and mid-lake with the dinghy. For location, see Figure 6.6.

6.3.4.ii Suspended sediment concentration and salinity

Surface water samples were collected to determine the suspended sediment concentration (SSC) and salinity of Fjallsárlón, which may affect the thermal structure of lake, due to its effect on water density. Due to the proximity of Fjallsárlón to the sea, salinity measurements, taken using a Pinpoint salinity monitor, yielded values of ~ 0.8 ‰, verifiying the lack of influence of marine waters to the lake. Samples were taken along both a long-transect of the lake (August 10), and twice in front of the ice cliff (August 11 and 14), totalling 10 samples (Figure 6.6). Similar laboratory procedures were carried out on those samples collected from Lago Leones (4.3.2.iii). However, due to the small water sample size, and the fine-grained nature of the ash-dominated sediments found in Iceland, a cellulose-nitrate filter paper, with a pore size of 0.8 μm was used. Values ranged from 41–546 mg l^{-1}, as shown in Table 6.4, and the average value was 235 mg l^{-1}.

Date	Sample	Location	Concentration (mg l^{-1})
10-Aug	1	28W 0431789 UTM 7100366	324
10-Aug	2	28W 0431070 UTM 7100126	174
10-Aug	3	28W 0431344 UTM 7099920	272
10-Aug	4	28W 0431703 UTM 7099767	77
11-Aug	A	28W 0432042 UTM 7099545	41
11-Aug	C	28W 0432001 UTM 7100612	207
14-Aug	α	28W 0432428 UTM 7099921	325
14-Aug	β	28W 0432330 UTM 7099712	546
14-Aug	γ	28W 0432257 UTM 7099503	152

Table 6.4 *Values of suspended sediment concentration at Fjallsárlón, August 2003.*

There is variation within the samples taken on the same day, as well as the variation between days, and the water is not well mixed. Sample C and sample α were both taken in the northern part of the lake, where high concentrations of SSC can be expected to relate to the turbulent influx of water from Breiðå. However, surface SSC values are highly sensitive to the transient nature of the presence of icebergs in the lake, and the high

level of variability in volume and lake surface coverage on any given day. The particularly low value of 41 mg l^{-1} was measured adjacent to a large iceberg.

The SSC is high compared to those recorded at other ice-contact lakes (Table 4.13, p. 124). The large range is not uncommon for ice-contact lakes, where rapid fluxes of incoming and outgoing water may occur. Concentrations in Ape Lake, British Columbia, for example, ranged from 28.7 to 1248 mg l^{-1}, before and after draining (Gilbert & Desloges, 1987). Large quantities of suspended sediment cannot be carried in overflows, due to the increased water density, and interflow and underflows are more common, sometimes alternating between the two (Gustavson, 1975).

6.3.4.iii River discharge

Accurate data for the discharge of both the incoming Breiðå and outflowing Fjallså (Figure 6.6) are not available. However, estimates were made for the discharge of these fast-flowing rivers, using estimates of river depth, width and surface velocity near to their junctions with Fjallsárlón. Ten icebergs were timed along a measured distance of the river, and averaged to provide a surface velocity. A comparison of icebergs grounded on the riverbed with those that were floating permitted an estimation of water depth. Discharge is estimated at ~ 90 m^3 s^{-1} for Breiðå, and ~ 125 m^3 s^{-1}, with higher discharge occurring in Fjallså, where higher surface velocities were seen and the river was deeper. Although these figures provide a rough guide only, it is not unreasonable to expect higher discharge on the outflowing river, where discharge from the incoming Breiðå will be augmented by meltwater from Fjallsjökull.

6.3.4.iv Lake stage

Direct observations of lake stage were made against a fixed marker on the southwest shore of the lake, and were used to calibrate the continuous record of the pressure sensor (6.3.3.ii). The values of average water level were smoothed by calculating hourly averages, and is shown by the stage record in Figure 6.15 (p. 167). Lake stage ranged over 0.23 m, and varied by at least 0.05 m each day. With the exception of August 9, there was a cyclic lowering of lake level, with the lowest lake stage each day occurring during the daylight hours of 1000-1700h. Water inputs to lake from the glacier come from surface ablation and precipitation. If diurnal variability in ablation and hydrology affected the

water level of the lake, one might expect higher surface melting during hours of insolation to result in more water entering the lake during the day, raising the lake stage, so clearly the lake level is not controlled by ablation inputs. The other primary input of water to the lake is from precipitation. Given the tendency, during the measurement period, for more rainfall from 2100 – 0500h, this provides a more likely explanation of the higher water level during night time. Not only will rain enter via the glacier's hydrological system, but water routed in from Breiðamerkurjökull, via the river Breiðå, will contribute substantially to this variation. This would also explain the lack of lake lowering that took place on August 9. Rain fell continuously during this 24-hour period, totalling 37 mm. By comparing the lake level changes to tidal data from Hornafjörður (64.1500° N, 15.1200° W), the timing of the changes is such that tidal influences can be eliminated as a stage control.

The lowering of lake stage during the day coincides with the timing of many of the calving events. It is possible that the peak in number of events occurring at 0900h relates to a threshold, where lowering of lake stage, due primarily to meteorological controls, causes a release in tensile stresses at the ice cliff, and the reduced buttressing of the ice cliff triggers calving activity. In fact, 60 % of the calving events occurred during periods of generally falling stage. Furthermore, within 40 minutes of the calving event time, there is a small fall in lake stage of ~ 0.05 m, for 90 % of calving events (Figure 6.16). Whilst the lake level change is small, it is easily perceptible, and it appears that the event size increases with the magnitude of this change. Most events experience a pre-event lake level drop of ~ 0.01 cm, whilst the largest events occur after a fall of ~ 0.05 m. It is also interesting that, following 60 % of calving events, lake level is higher by a few centimetres. This may reflect the increased mass in the lake. However, the additional volume in the lake indicated by the lake level rise cannot be solely attributable to calved ice volumes and if bergs are causing higher lake levels, it is expected that this should occur after all calving events. On the contrary, it is more pronounced for the larger calving events, and it is possible that only the largest bergs make a noticeable difference in lake level due to the displacement. This is discussed further in Chapter 7.5.2.

6.3.5. Summary

Fjallsjökull is an actively calving, lake-terminating glacier, which descends steeply from Öræfajökull down an icefall, into Fjallsárlón. Calved icebergs take a variety of forms, ranging from small flakes to large, 'tabular' icebergs, several tens of meters long, which preserves the original glacier surface morphology. The ice cliff exhibits a multi-layered notch, with up to six subsidiary notches, spanning a vertical height of ~ 0.5–1 m.

Continuous monitoring of the timing and size of calving events is difficult, especially at night time. At Fjallsjökull, abrupt changes in water level, indicative of wave activity, were identified from a record of pressure changes, and used as a proxy for the size and timing of the 64 calving events which occurred over a 10-day period in August 2003. The pressure changes also provided a record of general lake stage changes, which were rapid, over hourly and daily scales, and with a maximum amplitude of 0.23 m. The record shows that lake-level fluctuations are intrinsically linked to calving behaviour, in terms of calving event timing and size over diurnal and hourly timescales. 90% of calving events occur after a rapid fall in stage (within 1 hour of the calving event), of ~ 0.05 m, and 60% of calving events occurred during periods, of generally falling stage. Furthermore, calving events are larger and more frequent when lake stage is lower during the daytime. Comparison of the heights of multi-layered melt notches, with the maximum amplitude of lake-level fluctuations reveals that the melt notch height range exceeds that of lake-level changes.

High concentrations of suspended sediment in the lake indicate that large volumes of meltwater enter the lake, both from Fjallsjökull as well as from Breiðamerkurjökull via Breiðárlón. This meltwater maintains cool temperatures in the lake, which range from ~ 1.5-3 °C, with temperatures immediately adjacent to the ice cliff typically ~ 1 °C cooler than those mid-lake. The vertical profile appeared to be isothermal, disturbed by apparent cooling at ~ 2 m deep, which more likely results from exacerbated surface cooling from floating ice. Further cooling, from 4-9 m deep, may represent meltwater entering the lake as an interflow. Precipitation occurred on ~ 77 % days, averaging 13.5 mm day^{-1}, with most occurring during night-time. Daily average air temperatures ranged from 5-19 °C, and winds were negligible most days.

CHAPTER 7

Fjallsjökull, South-East Iceland: Reduced Data and Discussion

7.1 THERMAL STRUCTURE OF FJALLSÁRLÓN

Little attention has been paid to the influence of the physical limnology of ice-contact lakes on calving behaviour, despite the clear correlation between lake temperature and calving speed (Warren & Kirkbride, 2003). The late summer water temperatures at Fjallsárlón are comparable to many other ice-contact lakes. Summer water temperatures in the upper 20 m of the water column at the Tasman Glacier, New Zealand, are 1.9 – 2.3 °C (Roehl, 2003), and ~ 1.7 °C in the upper water column at the Hooker Glacier (Warren & Kirkbride, 2003). Although warmer than the ~ 0 °C temperatures at high-latitude Heiavatnet, Norway (Kennett *et al.*, 1997), and 0.48 °C water in iceberg-choked Lago Nef (NPI) (Warren *et al.*, 2001), temperatures are slightly cooler than the lake temperatures seen at Glaciar Ameghino, which is also heavily littered with floating ice (Warren, 1999). The temperature range of 0-3 °C seen at these lakes probably reflects their similar, moderate sizes, compared to warmer temperatures in larger lakes, such as Lago Argentino and Lago Leones (5.2) (Warren, 1994; Rott *et al.*, 1998).

The observed stratification occurs across much of the lake, and is interpreted as the result of cooling of an otherwise isothermal water column (1) at the surface, by melting of floating icebergs, and (2) at 4-9 m deep, from incoming meltwater as an interflow, as illustrated in Figure 7.1. This is the opposite of what is expected in late summer (2.2.3.ii). The sensitivity of the thermal structure of the lake to iceberg melting is also indicated by the localised cooling in the southern part of the lake, due to the presence of a large grounded iceberg (> 15 m high) throughout the field season. Additionally, cooler temperatures at the ice-water interface than those mid-lake reflect both meltwater produced directly from melting of the subaqueous ice face and incoming en- or subglacial meltwater.

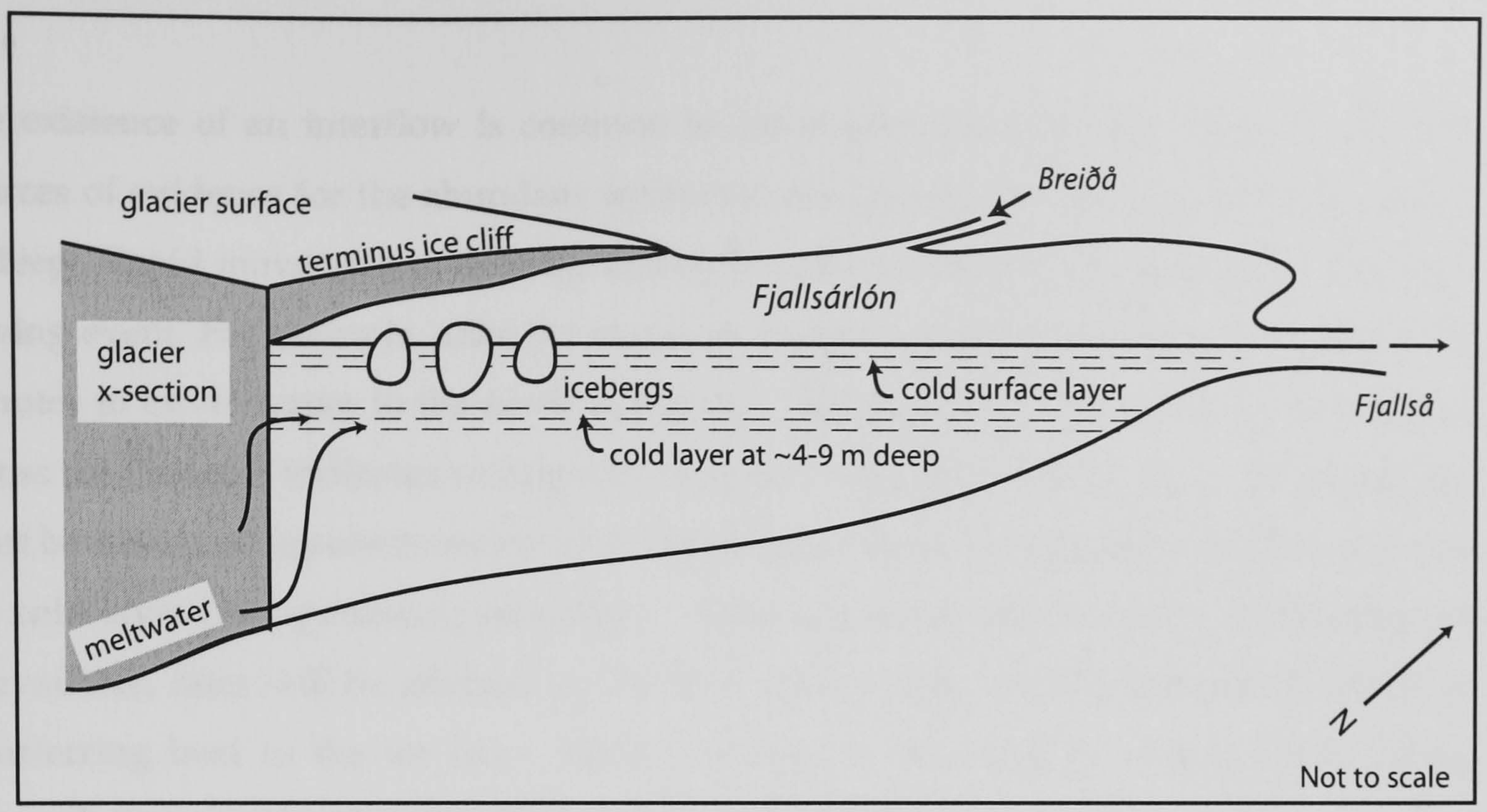

Figure 7.1 Thermal structure of Fjallsárlón, August 2003, as a 3D cross section, showing the input of meltwater from Fjallsjökull, as well as the incoming and outflowing rivers. The lake cross-section shows the cool layers in the water column, which result from iceberg cooling at the surface and cooling by meltwater ~ 4-9 m deep.

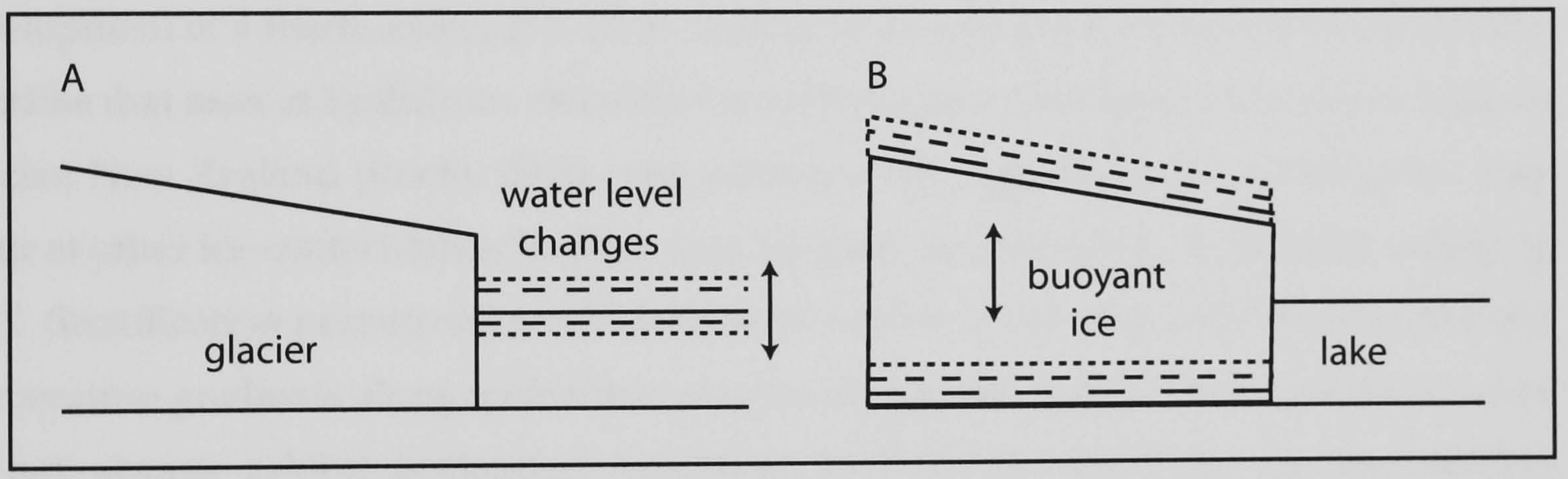

Figure 7.2 Possible explanations for the multilayered waterline melt notches observed at Fjallsjökull, August 2003. They may result from (A) changes in lake level, or (B) uplift of the glacier terminus due to buoyancy forces.

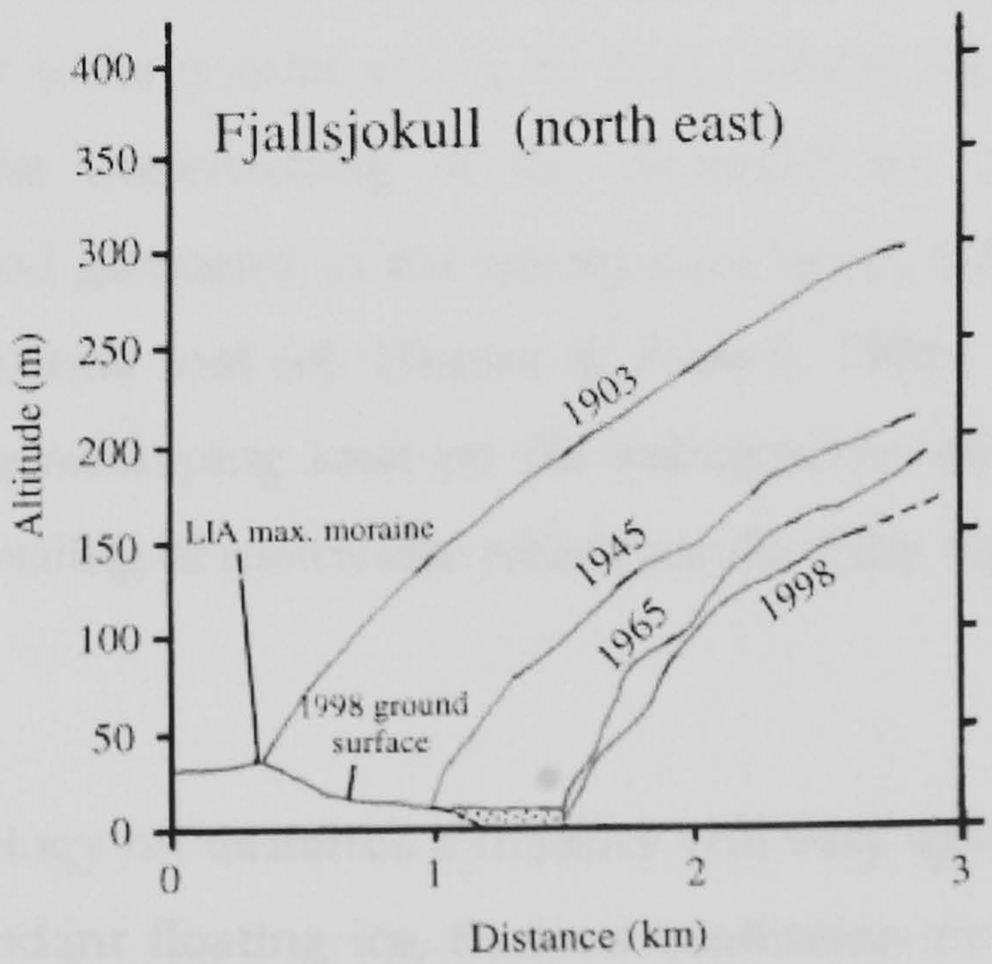

Figure 7.3 Profiles of the surface of Fjallsjökull.
Source: Evans & Twigg (2002).

The existence of an interflow is common in ice-contact lakes (2.2.4). There are several sources of evidence for the abundant meltwater interpreted to cause the cool layer at 4-9 m deep. Rapid movement of icebergs across the lake was sometimes observed to follow a calving event. For example, after the event on August 14, 0704h, icebergs took only 1 – 2 minutes to travel across to the north peninsula. The cool layer, 4–9 m deep, is persistent across the lake and indicates widespread input of meltwater into the lake. The input rate must be rapid, as turbulent mixing of slow-moving currents is otherwise likely to prevent the cold layer from persisting so widely. Although meltwater current velocity data are unavailable, rates will be affected by the flow of incoming river Breiðå, which assists in transferring heat to the ice face. Heat may also be advected by wind-driven waves, although they may be attenuated by the floating ice present.

The thermal structure differs from that at neighbouring Jökulsárlón, which is influenced by a saline intrusion (6.1.4) (Harris, 1976). Although both are stratified, the weak development of a thermocline, at 5–10 m deep, above isothermal conditions at Jökulsárlón is unlike that seen at Fjallsárlón. Stratified conditions have also been observed at Tasman Glacier, New Zealand (Roehl, 2003), strengthening the suggestion that stratification may occur at other ice-contact lakes, but has thus far gone undetected by insufficient sampling (5.2). Stratification permits the concentration of warmer water at specific depths, creating temperature gradients along which heat may be transferred (2.2.4). That ice-contact lakes do not always exhibit isothermal conditions is therefore important for the melting potential of the subaqueous portion of the ice face.

The development of waterline notches at Fjallsjökull provides evidence for melting at the ice face. Melting is likely to be greater at ~ 2 m deep, where higher temperatures are recorded, exacerbating the undercutting of the subaerial ice cliff, and is perhaps responsible for the observed geometry of the subaqueous bergs, which may have calved from a protruding subaqueous foot (cf. Hunter & Powell, 1998). Further evidence of subaqueous melting is the scalloping seen on the subaqueous icebergs (Figure 6.10, p. 162), indicative of the upwelling of meltwater which results from direct melting of the ice face (2.3.5.ii).

The role of physical limnology on terminus dynamics will vary spatially and temporally. In a small lake, with abundant floating ice, thermal conditions are likely to be constant across the whole lake (cf. Warren, 1999; Warren *et al.*, 2001). In addition, the sensitivity of

water temperature to grounded icebergs at Fjallsárlón is evident: there is a tendency for icebergs to accumulate in the distal part of the lake, probably against a sill at the river mouth (2.1.2) (cf. Duck & McManus, 1985), over which icebergs can flow only once their draft is reduced after deterioration by melting or breaking (2.3.4) (Savage *et al.*, 2000). These icebergs will prevent any clearly defined ice-proximal–distal temperature gradient from being established, despite the evidence for cooling against the ice face (Figure 6.26, p. 182). Iceberg cover on the lake varies from day to day, altering the temperature gradient towards the ice face, with consequences for the subaqueous melt rates of the ice cliff.

The thermal regime of the lake will also influence calving over seasonal timescales. Jökulsárlón is known to be completely frozen over from January to April (Landl *et al.*, 2003), and it is likely that Fjallsárlón experiences similar conditions. Calving at Fjallsjökull is therefore seasonal, with little calving taking place in winter. Any calving that occurs probably relates to the launch of subaerial seracs due to oversteepening of the ice cliff against the lake ice.

In summary, the physical limnology of Fjallsárlón is complex, with high variability in spatial and temporal patterns of thermal structure. Water and heat are advected by several processes, and floating ice from calving activity provides a feedback through its influence on thermal structure and subsequent melt rates. However, the consistently lower temperatures in the ice-water boundary zone, obtained by the radio-controlled boat (Figure 6.6, p. 160), confirm the need to obtain accurate boundary conditions in order to calculate the effect of water temperature on ice face melt rates precisely.

7.2 Glacio-limnological interactions: How important is melting?

Observations of well-developed melt notches, subaqueous bergs and scalloping (6.3.1.i) indicate that melting at and below the waterline of the ice cliff may be important. Limnological processes are, therefore, important for ice dynamics at the terminus of Fjallsjökull. Existing empirical equations derived for iceberg melting all depend on water temperature (equations 2.8, 2.9 and 2.11; p. 54 and 59). Analysis of the thermal condition of the lake indicates that water temperatures vary by ~ 1 °C between mid-lake locations

and those immediately adjacent to the ice face. Using these equations for melting as a first estimate, the effect of this 1 °C difference in temperature is investigated. Melt rates for water temperatures at 1.5 and 2.5 °C are compared in Table 7.1. Using the same approach as that taken in Chapter 5.3.4, values of v (equation 2.11) range from 0.1 to 0.5 m s^{-1}, where the highest value of ~ 0.5 m s^{-1} is observed in conjunction with bubbling of upwelling water at the surface (Hunter *et al.*, 1996a; Roehl, 2003; Motyka *et al.*, 2003a), and may be equivalent to values resulting from the incoming river Breiðå. The length term in equation 2.11, l, is approximated to the ice thickness below water i.e. parallel to the expected dominant direction of buoyant upwelling, at 70 m (Eijpen, unpublished data).

Equation	v (m s^{-1})	Melt rates (m d^{-1})		Difference (m d^{-1})
		1.5	2.5	
2.8		0.11	0.16	0.05
2.9		0.01	0.03	0.02
2.11	0.1	0.06	0.09	0.03
2.11	0.2	0.10	0.16	0.06
2.11	0.3	0.14	0.23	0.09
2.11	0.4	0.17	0.28	0.11
2.11	0.5	0.20	0.34	0.14

Table 7.1 *Ice melt rates from equations (2.8, 2.9 and 2.11) using mid-lake (2.5°C) and ice-proximal (1.5°C) water temperatures from Fjallsárlón.*

Regardless of the parameters included in the relationship, and the differing values obtained by the different equations, a difference of 1 °C results in very different melt rates. Melt rates obtained for a temperature of 2.5 °C show an increase of 50-200 % from rates at 1.5 °C, indicating the sensitivity of melting to differences in water temperature. Furthermore, melt rates increase by between ~ 20-80 % with every 0.1 m s^{-1} increase in current velocity. The large discrepancy in melt rate emphasises the need to obtain accurate boundary water temperatures and current velocities, in order to calculate melting of the ice face. It is inadequate to assume that mid-lake conditions are a suitable analogue for boundary conditions when considering the role of subaqueous melting at calving termini. Observations of a temperature gradient even within a waterline melt notch at Tasman Glacier, New Zealand (Roehl, submitted) further emphasize the need to pursue accurate boundary conditions.

To assess the significance of this melting requires a comparison between the subaqueous melt rate and the calculated calving rate, which is unavailable from Fjallsjökull. The large errors of using incorrect water temperatures will result in the over- or underestimation of the contribution of melting to the overall calving rate. The presence of ice cover on the lake during winter (cf. Landl *et al.*, 2003) means that these values of melting and calving represent summer rates, and cannot be extrapolated to give an annual figure, because ice terminus stress and melt rates will differ under the influence of an ice cover and must be addressed independently.

The problems of applying melt equations derived for icebergs in the ocean have already been discussed (2.3.6, 5.3.4). The values of current velocity used here have been calculated or observed elsewhere, although it is suggested that values of 0.5 m s^{-1} are the maximum likely to be observed at a grounded calving ice face (Hunter *et al.*, 1996a; Motyka *et al.*, 2003a). At Fjallsjökull, however, the incoming flow of Breiðå may substantially increase this value. High values of subaqueous melting may explain the observation of a substantially overhanging subaerial ice cliff. It is unlikely that the calculated subaerial melt rates of 0.03–0.12 m d^{-1} are misleading, as they are comparable to those recorded nearby at Breiðamerkurjökull (Howarth & Price, 1969). Instead, it appears that the iceberg melt rates severely underpredict subaqueous melting, as suggested previously in Chapter 5.3.4. This is possible, given the dissimilarity in environmental setting of icebergs in open ocean, compared to a grounded ice terminus. Either explanation of the overhanging cliff (higher current velocities or underprediction of melt rates from the existing equations) may be valid.

The laboratory experiments of Eijpen *et al.* (2003) support the expectation that melt rates are at a maximum just below the waterline. However, they suggest that melting does not occur just below the waterline at temperatures of less than 4 °C in any salinity. Although the scaling from laboratory ice blocks to the glacier margin is uncertain, evidence from subaqueous bergs (6.3.3.i) suggests that melting at and below the waterline at Fjallsjökull are comparable, displaying a similar geometry to that seen at Glaciar León on one occasion (4.3.1.i). Despite boundary water temperatures of only ~ 1.5 °C, melting was clearly evident, and the laboratory results reflect the simplification of more complex natural conditions, where melt rates at < 2 °C are less than 0.1 m d^{-1}.

Whilst melting is sensitive to water temperature, other factors such as current speed are important in determining the melt rate. It has also been observed that melt notch growth is sensitive to lake level changes (Roehl, submitted). Fluctuations of over 0.15 m occur within 24 hours at Tasman Glacier, New Zealand, i.e. within the range of those observed at Fjallsjökull, and are thought to reduce notch formation significantly. Furthermore, the horizontal temperature gradient within the notch does not correlate with melt rate as well as water temperature at the back of the notch (Roehl, submitted), although this may arise from a differential in melt rates on the clean ice within the notch and the subaqueous face, which is assumed to be debris-covered. The gradient restricts water circulation towards the notch, slowing notch formation (Roehl, submitted), although it is questionable whether the steep subaqueous ice face could support the thickness of debris cover required to insulate it from melting. At Fjallsjökull, where the ice cliff is debris-free, this may not be the case, although measurements conducted using a similar method to Roehl would be required to test this. Whilst the radio-controlled boat has proved valuable in ascertaining more realistic boundary water temperatures, the method may still not provide sufficiently precise boundary conditions for calculating waterline and subaqueous melting, and another approach is required to quantify melting accurately, before its contribution to calving rates can be fully understood. This is considered in Chapter 8.4.2.

7.3 Calving dynamics at Fjallsjökull

7.3.1 Introduction

Calving at Fjallsjökull appears to follow the pattern of cyclic calving seen at other lake-calving glaciers, with a cycle length that is shorter than some New Zealand glaciers, but longer than that seen at Glaciar León (4.3.1.i) (Kirkbride & Warren 1997; Purdie & Fitzharris 1999). Calving occurs by spalling of lamellae from the subaerial ice cliff; launch of subaerial seracs; full-height calving events; subaqueous events (Figure 1.1, p. 4); and the detachment of large 'tabular' slabs from the glacier (6.3.3.i). Subaqueous events at Fjallsjökull produce bergs larger than those by subaerial launch, in common with observations from other slow-flowing glaciers, although unlike the bergs seen at Glaciar León (4.3.1.i). On occasions, the detachment of large portions of the terminus occurs,

which are large enough to maintain their surface morphology and prevent overturning, thus emulating the tabular geometry of the much larger bergs which are typically the product of flat ice shelves. These 'tabular' bergs ground only tens of meters from the ice cliff for some days before disintegrating into smaller fragments that float away. Four factors believed to control the majority of calving at Glaciar León were suggested in Chapter 5.4, and are: waterline and subaqueous melting, longitudinal stretching, buoyancy forces and the force balance at the terminal cliff. The influence of these factors on calving at Fjallsjökull is now considered.

7.3.2 Evaluation of rate-controlling processes

The cyclic nature of calving sequences appear to be driven partly by the rate of waterline melt notch development. Observed calving above such notches acts to 're-zero' the notch, although this is not always the case, and other factors must also control calving. Lake level changes, with their own cyclicity, also influence the timing and size of calving events (6.3.4.iv); as well as modifying the rate of thermo-erosional melt notch development (Roehl, submitted), lake level changes may affect the buoyancy of the terminus in the water body (increasing with lake level rise), ice cliff force balance (due to changes in the buttressing of the cliff by the water body) and longitudinal stretching towards the terminus (due to the influence of water depth on basal water pressures). The relative importance of these factors is explored, below.

Melt notches in the ice cliff were described in Chapter 6.3.3.i., and provide evidence for the role of buoyancy forces at Fjallsjökull. Whilst it is possible to argue that frequent changes in lake level are responsible for their multi-layered nature (Figure 7.2a), there is uncertainty in this interpretation, as notches were not identical along the whole ice cliff. Instead, buoyancy forces may be responsible (i.e. the ice moves vertically, relative to the water level; Figure 7.2b). This would account for the presence of notches along some parts of the ice cliff and not others, i.e. no notch reflects the 're-zero-ing' of the notch following a large, full-height calving event. The variable presence of notches around the lake may also be explained by lake level changes acting along the ice face, which is at different stages of the calving cycle (6.3.3.i). Nevertheless, the height range of the notches (0.5 m) exceeds the amplitude of lake level changes (0.23 m), and can only have occurred

by the displacement of the ice face relative to the water level, providing unequivocal evidence in favour of a buoyancy argument for explaining the multi-layered notches.

Further evidence for the role of buoyancy on terminus dynamics comes from examining the height of the terminus above flotation. Given that the water depth at Fjallsjökull terminus is ~ 75 m, and the average subaerial ice cliff height is ~ 10 m (6.2.3) (Eijpen, unpublished data), then the glacier is only ~ 1-2 m above flotation. Regardless of the definition of the height above flotation (5.4.2) (Van der Veen, 1996; Vieli *et al.*, 2001), it is likely that the ratios of ice thickness and water depth seen here result in conditions suitable for at least transient flotation of the terminus (2.1.2) (cf. Warren *et al.*, 2001).

The notches and the terminus height above flotation, described above, provide evidence that buoyancy forces are important for Fjallsjökull. However, it is unclear over what timescales buoyancy becomes important. The influence of diurnal lake level changes on buoyancy can be assessed by calculating the resulting adjustment to the height above flotation (equation 2.5, p. 22). In a water depth of 75 m, flotation occurs when h_i = 83 m. Using a value of 15 m for the height of the ice cliff above the waterline, the glacier is therefore 6.7 m above flotation. When water depth increases/decreases by 0.23 m, the height above flotation is reduced/increased to 6.4/6.9 m. Given the poor accuracy of the known subaerial freeboard and the bathymetry, these alterations to the buoyancy of the glacier are negligible and are unlikely to be responsible for instantaneously inducing a large mass loss by calving. Furthermore, calving events occurred more often when lake level was lower during the day, with 90 % of events occurring after a rapid fall in lake level, of ~ 0.05 m (6.3.4.iv). For increased buoyancy forces to trigger calving events over short timescales, the lake level would be expected to rise, decreasing the height above flotation. Therefore, buoyancy forces cannot be the immediate cause for calving events in response to lake level changes, and an explanation must lie elsewhere.

The calving of 'tabular' icebergs, grounded close to the ice cliff, appears to relate to forcing mechanisms other than waterline melting, because such melting did not undercut the entire subaerial cliff which subsequently calved. Furthermore, these events occur infrequently, suggesting that ice stresses have built up over time before reaching a failure threshold. This implies that the buoyancy of the terminal cliff increases over time, perhaps due to ongoing surface downwasting, such that the terminus slowly moves upward, away from the glacier bed. This would explain the progressive development of

the multi-layered melt notches. However, specific data to confirm buoyancy as the cause of calving in this manner is not available, and this situation remains speculative at present.

In support of the role of buoyancy for calving over timescales greater than hours and days, buoyancy forces are expected to become increasingly important for future calving at Fjallsjökull over monthly and annual timescales. Bathymetric data show that the lake is deepest close to the ice front (6.2.3), and that the glacier is receding into deeper water (Eijpen, unpublished data). Thus, the reverse ice surface slope (6.3.3.i) may reflect the combined effect of bottom topography and an upwardly lifting buoyant terminus. As the glacier retreats into progressively deeper water, buoyancy forces will become increasingly important as the subaerial freeboard forms a progressively smaller fraction of the overall ice thickness, and the height above flotation correspondingly decreases. Furthermore, downwasting of the terminus was noted between August 2002 and August 2003 (6.3.3.i) and it is feasible that this is causing thinning of the glacier, which becomes more buoyant as a result. Rapid retreat is therefore expected once the height above flotation is small enough to make the terminus unstable. Whilst retreat will probably not be as dramatic as that seen at neighbouring Breiðamerkurjökull (Björnsson *et al.*, 2001), this scenario is indicative of the potential for calving glaciers to decouple from climatic forcing. With continued glacier recession in Iceland, calving termini may become more widespread, particularly on the southeast side on Vatnajökull, where unlithified sediments which were removed during the LIA provide lake basins in which glaciers can terminate (Björnsson, 1996). It is important that the implications of such retreat by calving on the overall mass balance and stability of the Vatnajökull ice cap are not overlooked.

Lake level changes also affect the force balance at the ice cliff, in terms of a buttressing effect (Figure 2.3, p. 26), and appears to affect the spalling of thin lamellae from the subaerial ice face (5.4.3) and, like buoyancy forces, alters with lake level changes. When lake level decreases, the buttressing of the ice cliff is reduced, and maximum ice pressure at the waterline increases. The potential for a calving event due to the cliff force balance is therefore promoted by lower lake level. On both diurnal and pre-event timescales (Figure 6.16, p. 174, 6.3.4.iv and Appendix C), calving events at Fjallsjökull are concentrated during periods of lowered lake level, suggesting that the removal of the water body buttress may result in calving. However, like with buoyancy forces, the magnitude of the lake level changes recorded at Fjallsjökull result in little difference in this buttressing.

Furthermore, calving at Fjallsjökull does not occur solely as thin lamellae, thought to be the product of cliff force imbalances (7.3.1). Therefore, the mass loss volume resulting from an ice cliff force imbalance is not substantial, and changes in lake level will not independently affect the contribution of mass lost in this way to the overall calving flux.

The other major control of lake level changes on calving behaviour is the influence they have on basal water pressures. Despite the practical difficulties in obtaining direct measurements for the subglacial water pressure, an estimate can be made. At the glacier terminus, meltwater is expelled from the glacier. Water pressures must therefore be at least equal to the water pressure at the lake bed, p_w, which provides a first approximation for basal water pressure close to the terminus:

$$p_w = \rho_w g h_w \qquad \text{(Eq 7.1)}$$

It is well known that fast rates of glacier flow take place primarily by basal sliding (Kamb *et al.*, 1994; Meier *et al.*, 1994; Van der Veen, 1996), which depends on the gravitational driving stress and the effective pressure, facilitated by subglacial water which lubricates the glacier bed (2.1.1.ii). Given that the subaerial freeboard of the terminus is relatively small, and the basal water pressure will therefore be similar to the overburden pressure (equation 2.3), the effective pressure will already be low. Additionally, the high crevasse density further up-glacier offers an easy route for surface-melt runoff and precipitation to reach the bed over diurnal timescales, and subglacial water pressure is probably higher than this basal threshold.

An increase to the basal water pressure will permit an increase in basal sliding, resulting in longitudinal stretching (2.1.1.ii). However, a small change in basal water pressure has an amplified effect on sliding velocities, due to the power relationship between sliding velocity, v_b, and effective pressure, p_e:

$$v_b = k\tau_b^m p_e^{-r} \qquad \text{(Bindschadler, 1983)} \qquad \text{(Eq 7.2)}$$

Therefore, in comparison to the apparently limited influence of lake level changes in triggering calving through changes to the buoyancy of the terminus or the ice cliff force balance, lake level changes may be significant for ice velocities. An increased lake level may induce longitudinal stretching of the terminus zone as ice velocities increase in response to lower effective pressures. Such stretching usually results in glacier thinning and, for glaciers already close to flotation, often results in a calving response (2.1.3, Van der Veen, 1996, 1997).

Evidence of extensional flow conditions at the terminus comes from observations of crevasse patterns. Intense crevassing towards the terminus of calving glaciers is indicative of extensional flow and increasing longitudinal stretching towards the ice cliff. At Fjallsjökull, crevasses advected down the icefall close up as it levels out at the bottom. When the ice surface begins to exhibit a reverse gradient close to the terminus (6.3.3.i), crevasses are re-propagated along the crevasse traces, i.e. at these points of weakness, and may propagate below the waterline (cf. Theakstone, 1986; Motyka *et al.*, 2003b). This implies that longitudinal stretching, over the reverse slope towards the terminus, may be taking place. However, compressional flow would normally be expected on a reverse slope, and would contradict this suggestion. Further data are needed to clarify this matter.

7.3.3 Model of terminus dynamics at Fjallsjökull

Calving as described by Van der Veen (1997, 1997), where glacier thinning due to longitudinal stretching induces a calving response, implies the significance of buoyancy. For glaciers close to flotation, such stretching and thinning causes the glacier to calve back to a thickness where buoyancy forces no longer stress the ice to failure point. This makes it difficult to separate the varying influences of longitudinal stretching and buoyancy from each other, and emphasizes the need to examine the interaction of the controls on calving. For example, glacier thinning due to surface downwasting will affect both stretching and buoyancy. This is known to be occurring at Fjallsjökull (6.3.3.i) and both reduces the effective pressure at the bed, allowing faster rates of basal sliding as well as altering the buoyancy of the glacier in the water body. To separate the resulting effect of such thinning in terms of calving behaviour is very difficult without detailed measurements of ice velocity and longitudinal strain rate, basal water pressure and ice thickness. However, it is possible to envisage the interaction of calving rate-controlling forces at Fjallsjökull in the context of the observed lake level changes, as described below.

Crevasses immediately behind the ice cliff develop due to undercutting at the waterline. Following an increase of water to the glacier bed, due to a precipitation event, ice accelerates towards the terminus in response to increased basal sliding. These crevasses expand as extensional flow occurs, effectively lowering the glacier surface, and become

deep enough that, when the water level returns to a lower level during the day, the removal of the buttressing support is sufficient to trigger a calving event. Furthermore, the decrease in basal sliding with the drop in water level may cause a transient increase in oversteepening. Calving, due to the combined effect of the removal of buttressing with increased oversteepening in the upper ice column, would allow the terminus position to retreat to its location prior to the reduction in lake level, returning the ice cliff height to one of greater stability, in terms of its buoyancy.

The model given above suggests that basal water pressures increase directly due to external inputs e.g. precipitation, and that a lake level increase results from this added water coming through the system i.e. lake reflects existing basal conditions. Alternatively, it is possible that changes to the discharge of Breiðárlón, the river coming into Fjallsárlón has a greater effect on a lake level rise than subglacial meltwater from Fjallsjökull, and that basal pressures respond to the changes in water depth (equation 7.1). Without the appropriate data, it is not possible to qualify the cause and effect of these changes in basal water pressure and lake level change in more detail.

However, this scenario illustrates the manner in which the cliff force balance may contribute to mass loss by calving. Of the factors described above, the ice cliff force balance is the only one which links to the observed timing of calving at Fjallsjökull i.e. calving events occur when lake level falls, whereas both buoyancy forces and longitudinal stretching would induce calving when lake level rises, which is not observed. Although if operating independently from other rate-controlling factors, mass loss due to the cliff force balance is negligible (7.3.2), its significance becomes enhanced when working in conjunction with the other factors of buoyancy, longitudinal stretching rate, and undercutting of the subaerial cliff by waterline melting, as suggested in this model.

The effect of short term water level changes on terminus dynamics has also been described for LeConte Glacier, Alaska (O'Neel *et al.*, 2001), which provides a useful comparison to the observations at Fjallsjökull. Minimum speeds occurring on semi-diurnal timescales, at high tide (2.1.1.ii) suggest that the restraining force of the water column overrides the high rates of sliding that would be expected when basal water pressures are elevated. Because most of the drag at the terminus comes from the valley sides, basal sliding is little altered by the increased water at the bed. Furthermore, the

terminus is so close to flotation that increased basal water pressure is thought to cause uplift of the terminus without increased sliding.

In contrast to LeConte Glacier, most of the drag at the terminus of Fjallsjökull comes from the glacier base, and higher rates of sliding may override the increased restraining force that results from increased basal water pressures at higher lake stage. It is not possible to confirm whether or not uplift of Fjallsjökull terminus occurs when the lake level is high. However, it is possible to speculate that maximum velocities occur at maximum water level, the opposite situation to that seen at LeConte Glacier. In this case, the terminus may experience a slight advance, which would cause increased stretching of the terminus. If this extension cannot be accommodated by the tensile strength of the ice, fracturing must occur (Figure 2.7, p. 43), and this could explain the observed pattern of crevassing below the icefall. Prolonged terminus acceleration would lead to unstable glacier thinning, and retreat by calving would be necessary to regain equilibrium of buoyancy.

7.3.4 Summary

Like Glaciar León, calving from the terminus of Fjallsjökull is a complex process, involving the interaction of several rate-controlling factors, outlined in Chapter 5.4. These four key factors appear to operate over a variety of timescales. Most immediate to a given calving event appears to be a drop in lake level, which removes some of the restraining force at the terminus within an hour of a calving event. Over a diurnal time period, basal water pressures are thought to respond to additional inputs of precipitation and discharge from Breiðå, causing extensional flow and thinning, which will necessitate retreat by calving, in order to regain sufficient height above flotation. Buoyancy forces are thought to be important over longer periods. Downwasting by surface melting causes glacier thinning and uplift, which is illustrated by the presence of multi-layered notches. As the glacier recedes into increasingly deep water, the height above flotation approaches zero, leading to accelerated retreat until the basal topography changes slope direction. All these conditions conform to a theory of calving as a response to other terminus dynamics, i.e. ice thickness, effective basal pressure and ice velocity (2.1.3).

It is particularly interesting that the terminus exhibits a sensitivity to internal (glacier dynamics) and external forcing (meteorological and hydrological) factors on timescales of

a day or less. Previous calving studies have suggested that rapid glacier response to diurnal variations is limited to tidewater settings, where cyclic tidal fluctuations have been attributed to diurnal trends in calving activity (Warren *et al.*, 1995b; O'Neel *et al.*, 2001). At lake-terminating Glacier Moreno, the number of calving events was correlated with increased global radiation during the day (6.3.3.ii, Iizuka *et al.*, 2004), although this was not explained in terms of a process link. This study at Fjallsjökull has demonstrated a link between calving and meteorological as well as hydrological variables over diurnal timescales, most probably through their influence on effective pressure and sliding velocity. Where rapid transport of such water inputs to the bed occurs, lake level changes are then also important in altering the restraining force at the ice cliff.

7.4 Climatic response of Fjallsjökull

Fjallsjökull is one of only a few Icelandic outlet glaciers which terminates in an ice-contact lakes (6.1.1). Most Icelandic glaciers have terminated on land during historic time, and so their response to climate forcing has not been modulated by calving dynamics. Although it is known that the current Fjallsárlón has only existed since ~ 1945 (6.2.3, Figure 7.3, p. 187), it is not clear from the literature whether a lake has ever been present in the past. The existence of a previous lake here is important for understanding the climatic sensitivity of Fjallsjökull, when comparing its terminus fluctuations to those of other outlet glaciers in the region. The present Jökulsárlón has existed since the 1930s, and it has been suggested that previous lakes may have existed, as it is thought to have formed from the removal of sediment during the LIA, rather than overdeepening of bedrock (Björnsson, 1996). It is suggested that this could be true for the whole of the coastal plain south of Vatnajökull (Björnsson, 1996). Fjallsjökull is therefore likely to have undergone similar methods of excavation to produce a depression to hold a lake (Rose *et al.*, 1997).

The retreat of Fjallsjökull in the late 19th and early 20th Centuries is punctuated by several readvances, detailed in Chapter 6.2.2. Other Icelandic glaciers stabilised or advanced around 1970, in response to the extra mass available from increased precipitation between 1920 and 1945, perhaps in combination with cooler summer temperatures during the 1970s (Kirkbride, 2002). This suggests that Fjallsjökull responds more to changes in precipitation than to changes in temperature, the small fluctuations from 1952-1990 being a result of calving activity moderating terminus position. Furthermore, the calving

history of Fjallsjökull will have been affected by the fluctuations of Breiðamerkurjökull, via outflow of meltwater from Breiðálón.

However, Fjallsjökull lacks the confinement by topographic geometry seen at many calving glaciers, and is therefore like to be reasonably sensitive to climatic controls. If retreat did not occur by punctuated equilibria, as through a valley with topographic pinning points, then the readvances must have related to other controls on terminus position. In comparison to the rapid retreat by calving at Breiðamerkurjökull from 1950-1960 (Björnsson *et al.*, 2001), the post-LIA behaviour of Fjallsjökull echoes the overall trend of recession of other Icelandic glaciers. Given their proximity to each other, their different behaviours illustrate the ability of calving glaciers to become partially decoupled from climatic forcing. At Breiðamerkurjökull, ice extends ~ 300 m below sea level (Björnsson, 1996). Calving is much more rapid in deeper water, and ice flux to the terminus is likely to be greater than at Fjallsjökull. This ice margin is therefore more unstable and is decoupled from climatic signals to a greater extent.

7.5 Field Technique Evaluation

7.5.1 Introduction

This section provides an assessment of the two main field techniques that have been employed in gathering empirical data at Fjallsjökull: the pressure sensor and radio-controlled boat. As preliminary studies into their suitability for gathering data from calving glacier margins, several possibilities for their further use in providing information about the nature of calving behaviour at lake-terminating glaciers, and the process links that they may reveal, have come to light during the course of this research.

7.5.2 Monitoring calving event timing and size using a pressure strain gauge

7.5.2.i Interpreting calving events from the pressure record

The technique used here to monitor calving event timing and size has successfully recorded calving activity. The sampling interval of 1 second, with values averaged every

minute, appears to provide a satisfactory level of detail. All rapid changes in water level, notably the maximum and minimum water levels, illustrate in fine detail the particular nature of an event e.g. two ice blocks calving in close succession. At Icefall Lake, a sampling interval of 1 minute was selected, and found to be adequate for providing sufficient detail about the changes in lake stage that took place (Hasholt, 2002). Sampling at this frequency was adequately powered using a 12 V 'gel cell' battery over the time period. To operate the logger over longer periods, some way of knowing the battery level without disconnecting it from the logger would be necessary, in order to maintain a constant supply of power. Hasholt (2002) also recommends that monitoring of lake stage over prolonged periods could be powered by having several loggers on a time-delay.

Many further observations of calving are required to calibrate accurately the pressure record into a clear picture of wave activity in the lake. Noting the timing of even the smallest flakes, along with the observations of iceberg overturn events should clarify what amount of calved ice produces a given signal. Furthermore, the wave height is affected by the lake-basin scale, in particular the lake depth and horizontal distance. The accuracy of using a pressure sensor in this way would be improved by installing several around the lake, to account for the influence of lake basin geometry on the timing and magnitude of the signals. By comparing the timing and water level change magnitude between loggers, it should be possible to determine the location from which an iceberg is produced. This would allow the observed cyclicity of events (6.3.1.i, 7.3) to be extracted from the overall record, and any zones of concentrated calving activity to be identified.

Whilst it is most likely that the definition of a large magnitude event will vary in scale between lakes, this attention to detail in terms of calibrating the record should then permit comparisons of calving behaviour from site to site. This is valuable in terms of identifying process links, by analysing the dominant size of iceberg produced and what the frequency of calving events tells us about the rate-controlling forces. Without this consistent approach, only preliminary comparisons of calving behaviour can be made between Fjallsjökull, Glaciar Perito Moreno and Mittivakkat Glacier, the three glaciers where calving has been monitored using a pressure sensor. By making the assumption that small calving events were negligible at Glaciar Moreno (from the description that Iizuka *et al.* (2004) focused on 'large' events), it appears that calving style here is dominated by subaerial calving of seracs along crevasses advected into the terminus. This contrasts

with the dominance of small spalling events combined with occasional calving of large bergs, formed along crevasse traces advected into the terminus, at Fjallsjökull.

The record of calving events is particularly clear at Fjallsjökull due to the very light winds (6.3.2, 6.3.3.ii). Negligible winds were also experienced at Icefall Lake in August 2002, resulting in a 'noise' level of 0.01 m (Hasholt, 2002). Steady, moderate breezes can be accommodated in the record without disguising the signal, as it is usually possible to pick out a peak and corresponding trough, to signal a calving event. However, it is possible that the interpretation of the record may become problematic if winds are strong and gusty. Although a sudden gust would probably produce a wave with a shorter wavelength than that of a calving-induced shock wave, the possibility of missing some calving event occurrences for this reason cannot be overlooked.

The other main source of ambiguity in the record is the possible confusion of a calving event with water level change resulting from iceberg overturn events. Again, it is possible that some small calving events have been missed in the analysis. For example, there may have been some small, precursory events taking place as a buildup to the large event on August 14, 0704h.

7.5.2.ii Glacio-limnological interactions

The size of calving events, inferred from the pressure record, may be calibrated to give an ice volume, by combining these data with detailed theodolite surveys of subaerial ice volume, during the buildup to a calving event. By providing a first-order quantification of the subaerial ice flux, the proportion of ice flux through the terminus attributable to small or large calving events can be determined. This would be useful in making process links. For example, if most ice loss relates to very small events such as the spalling of ice flakes, it implies that perhaps the ice cliff force balance (7.3.3.) is the most important factor. The force balance depend primarily on the rate of undercutting of the ice cliff by waterline melting and differential ice flow, tending towards oversteepening. Alternatively, if bergs are primarily produced by fracturing along crevasses advected into the terminus, then processes occurring behind the terminus are important, such as the stress regime associated with the presence of crevasses. Here, the controlling factors include stretching associated with extensional flow towards the terminus, glacier hydrology and the role of water in crevasse opening (7.3.4). Other events of a similar size,

but calved along crevasses formed immediately behind the ice front, would reflect a combination of undercutting at the waterline with destabilisation of the terminus zone by buoyancy forces (7.3.1, 7.3.4). At a larger scale still, 'tabular' bergs reflect the dominance of buoyancy forces, as seen at Glaciar Nef, Patagonia (7.3.2) (Warren *et al.*, 2001). Detailed studies would be required to calibrate the signal in the pressure record associated with the varying styles of calving.

On future occasions, installing an automated weather station would be useful for determining whether or not there is a relationship between either the timing or size of calving events and rainfall amount. It is possible that basal water pressures require a minimum rain intensity, to meet a threshold level where the change in effective basal pressure is significant enough to cause an observable difference in ice velocity, and subsequent calving speed. Given that calving event timing is sensitive to inputs to the lake, manifested as lake level changes, and that, in part, these relate to glacier meltwater volumes, installation of a temperature logger below the water surface of the lake would also be valuable, similar to that used by Hasholt (2002). The interpretation that meltwater enters the lake as an interflow indicates that loggers at a range of depths is required, as measuring only surface temperatures may be insufficient for detecting increased input of meltwater immediately prior to a calving event.

7.5.3 The use of a radio-controlled boat to measure boundary water temperatures

7.5.3.i Problems

- Despite the bright colours of the boat, and the positioning of the red propeller cover on the front, it was sometimes very difficult to identify the direction in which the boat was moving. With only two pairs of hands to operate both the dinghy and radio-controlled boat simultaneously, extra measures such as the use of binoculars were restricted. The steering became problematic mainly because the boat circled if the logger array caught on an ice projection underwater, and it was difficult to maintain a smooth line of travel in only one direction.
- It was sometimes hard to be certain that the boat remained close enough to the ice front at all times. According to Roehl (submitted), the water temperature at the back of the melt notch correlates most closely with melt rate, and implies that a radio-

controlled boat does not yield data sufficient close to the ice face. However, at glaciers where such access is impossible, a radio-controlled boat provides a means to obtain more representative data for calculating melting than those occurring in mid-lake areas.

7.5.3.ii Improvements and recommendations

- It is impossible to keep the logger array vertical under the boat, when the boat is moving. Further testing is required to find an accurate method of calculating the angle at which the array trails, for a given boat speed, water viscosity and logger weight distribution.
- Given the uncertainties about the exact depths of each logger, one way to avoid extrapolating the data between ambiguous logger depths is to have a greater concentration of loggers on the array.
- Improved control of the handling of boat is required. A bigger rudder to supplement the air rudders on this model is recommended.
- Although the range of the boat is adequate to overcome the safety issue being addressed here, a better method for improving the visual link to the boat is necessary.
- An automated GPS facility would permit a precise means of recording the travel path of the boat. This would both provide a simple means of documenting the position of the terminus if survey methods are unavailable, and provide a means of monitoring locations of meltwater entering the lake, outlined in more detail below.

7.5.3.iii Potential use

With an automated GPS facility attached, detailed spatial analysis of the water column will allow the detection of zones of incoming subglacial or englacial meltwater. These may then be related precisely to variations in surface ice velocity, from ice cliff surveys, development of thermo-erosional melt notches at different sections of the cliff, and observed occurrences of calving events. This will greatly improve our ability to evaluate process links between the controls on calving, linking the glaciological system and lake environment to evaluate the importance of glacio-limnological interactions, by analysing how ice flow regime and glacier hydrology interact with the physical limnology of the ice-contact lake, and their control on the timing and size of calving events.

CHAPTER 8

Synthesis and Conclusions

8.1 GLACIO-LIMNOLOGICAL INTERACTIONS AT FRESHWATER-CALVING GLACIERS

This work emphasises that the calving dynamics of lake-calving glaciers cannot be understood without detailed knowledge of the physical limnology of their ice-contact lakes. It highlights the fact that ice-contact lakes have a more complex thermal structure than has previously been thought, with rapidly changing stratification that varies spatially and temporally in its extent and duration. This stratification is important for considering heat transfer to the ice face, required for subaqueous and waterline melting. In large lakes, such as Lago Leones, warming in the distal area is largely unaffected by the presence of the glacier terminus, and a temperature gradient between the ice-proximal and distal areas may be established, important in advecting heat to the ice face. However, knowledge of the thermal structure of the lake alone is insufficient for understanding fully the role of the physical limnology of the ice-contact lake for calving dynamics. It is necessary to identify the precise conditions at the ice-water interface. Even in small lakes, where the temperature gradient between the distal and ice-proximal zones may be weaker, water temperatures close to the ice face may be at least 1 °C cooler than those further away. This has implications for the melt rate of the subaqueous portion of the ice face, which depends, amongst other factors, on water temperature.

Calculating melt rates of the waterline melt notch and the subaqueous ice face is difficult. As a result, melt rates at calving termini have often been calculated using temperature relationships developed from iceberg studies (Dowdeswell & Murray, 1990; Powell, 1981; Powell & Molnia 1989; Syvitski, 1989; Hunter *et al.*, 1996a, 1996b; Vieli *et al.*, 2001, 2002). As these equations are limited in their applicability to melt rates at grounded calving margins, it is doubtful whether such estimates of melt rates at calving glaciers are accurate, and there is still no satisfactory means of calculating waterline and subaqueous melting at grounded calving glaciers.

With the increasing recognition of the potential of subaqueous melting to make a significant contribution to calving and mass loss at the terminus, other approaches to

calculating melting have been attempted. These primarily involve calculating heat and water budgets for the ice-proximal zone (2.3.7) (Funk & Röthlisberger, 1989; Sakai *et al.*, 2000a; Motyka *et al.*, 2003a; Landl *et al.*, 2003). By calculating the inputs and outputs, the residual value is the heat available for melting. However, none of the existing studies successfully account for all components of heat transfer within an ice-contact lake. Whilst the energy exchange calculations at Unteraargletscher, Switerland, assumed uniform weather conditions, no surface heat losses and no heat advection within the lake (Funk & Röthlisberger, 1989), calculations of the energy available for melting at Jökulsárlón over each season applied only to the floating ice of the lake, and not the grounded ice cliff, and are therefore limited in their applicability to calving margins. Meanwhile, energy exchanges with the atmosphere are neglected entirely in the heat and water balance calculated for LeConte Glacier, Alaska (Motyka *et al.*, 2003a). The calculated linear melting rate, of 12 m d^{-1}, which contributed some 57 % of the total mass loss at the terminus, represents the largest absolute (and proportional) melt rate calculated for a tidewater calving glacier, where melting is generally considered a negligible mass loss in comparison to calving fluxes. Whilst the study is useful in highlighting the potential of subaqueous melting to form a significant component of the ablation system, it is essential to account for the lake-atmosphere interaction in order to confirm this significance.

Despite their short-comings, these studies provide a basis for future investigations into waterline and subaqueous melting. Lake-calving glaciers are better suited to such studies than tidewater settings, as the bounded nature of ice-contact lakes permits the components of heat exchange to be accounted for more easily. Additionally, their typically smaller size often makes direct access to the calving front possible. In this case, one way to determine melting is by direct measurement of thermo-erosional melt notch development. At Glaciar León, this is achieved using survey methods to calculate notch growth rate (4.3.1.iv) (Haresign & Warren, in press). An alternative method is employed at the slow-flowing Tasman Glacier, New Zealand, using floating pipes to measure melt notch depths (Roehl, submitted).

Direct measurement of subaqueous melt rates has not been conducted at calving glaciers, and, as it is not easy to envisage a method by which this may be successfully achieved, an alternative is required. As subaqueous melting is sometimes at a maximum just below the waterline (Eijpen *et al.*, 2003), waterline melt rates calculated directly also provide a minimum estimate for subaqueous rates. The results from Glaciar León imply that the

iceberg-derived relationships under-predict actual melt rates. This might be expected as a result of the forced circulation at calving termini from pressurized meltwater entering the water body. It appears, therefore, that the optimal approach to assessing subaqueous melting combines the use of a heat budget with direct measurements of the waterline melt notch, which provide a means to confirm the reliability of the heat budget. Only by validating such theoretical approaches with empirical evidence can we hope to further our understanding of this complex and inaccessible process.

8.2 CALVING INTO FRESHWATER

One well established statistical correlation for calving glaciers is the linear relationship between calving speed (u_c) and water depth (h_w) (2.1.1.i). For the relatively small number of calving glaciers worldwide for which u_c and h_w are available (Table 2.1 and Table 2.2), this correlation is robust, although not fully understood. However, the slope coefficient of this linear relationship varies significantly for different populations of calving glaciers: temperate, polar, freshwater, tidewater, and combinations of these. In particular, u_c at temperate tidewater glaciers is typically an order of magnitude faster in any given water depth than at temperate lake-calving glaciers. For a width-averaged water depth of 65 m, as at the terminus of Glaciar León, the tidewater relationship of Brown *et al.* (1982) predicts u_c = 1762 m a^{-1} while the freshwater relationship of Warren and Kirkbride (2003) predicts u_c = 167 m a^{-1}. The observed calving rate of 880 m a^{-1} at Glaciar León is therefore something of an anomaly, plotting in an intermediate position, and demonstrates that fast rates of calving are not limited to ice margins in water several hundreds of meters deep. However, given that all three tributaries have large icefalls just upstream of the current location of the terminus and that the lower glacier is steep and pervasively crevassed, the high flow speeds and high calving rate are perhaps unsurprising. Alternatively, this high value of u_c could prove not to be anomalous if further work reveals that the u_c / h_w correlation for freshwater is non-linear, as tentatively suggested by Warren *et al.* (1995a), but adequate data still do not exist to test this.

The u_c / h_w relationship has previously provided a useful first step in the pursuit of an understanding of calving rates and processes. However, it is insufficient to investigate the correlation between calving rate and water depth without also considering the

mechanisms by which calving occurs. It is therefore necessary to gather suitable empirical data to demonstrate the controls on calving, which also explain the link between calving rate and water depth. It is suggested that the water depth at the terminus affects the force balance at the ice cliff, due to the buttressing effect of the water body. It affects the tendency of the terminus towards flotation, and also the degree of extensional flow towards the terminus as a result of the influences of water depth on the basal water pressure and, hence, the sliding rate. The contribution of these factors to terminus dynamics at Glaciar León and Fjallsjökull is evident from this research.

As well as the factors which are reflected in the water depth correlation, other controls may operate at calving margins. Of particular interest has been the order of magnitude difference in calving rates between tidewater and freshwater calving glaciers. Research at slow-flowing lake-terminating glaciers in New Zealand implies that the rate of thermo-erosional melt notch development is the rate-controlling factor for calving rates at these sites (Kirkbride & Warren, 1997; Roehl, submitted), whereas, at faster-flowing glaciers, other controls such as buoyancy and longitudinal stretching are more important. Calving due to waterline melting is also apparent at Glaciar León and Fjallsjökull. However, it is not the dominant factor determining calving rates at either glacier, constituting approximately only a quarter of the overall calving rate at Glaciar León. For example, as the terminus advances into deeper water, buoyancy forces on the glacier increase as the effective pressure is reduced. Accelerating flow into the terminus results from increased longitudinal stretching, which then controls calving as crevasse density increases, and the ice disintegrates. Crevassing results from the glacier ice being unable to accommodate all the longitudinal strain by pure shear, resulting in void spaces, i.e. crevasses. The component of pure shear, however, causes the ice to thin allowing the buoyancy forces, which initiated the increasing in longitudinal stretching, to apply torque to the glacier, causing calving as flotation is achieved. Calving from these glaciers exhibits characteristics akin to both freshwater and tidewater glaciers. This scenario of stretching and buoyancy is more spectacularly illustrated by the retreat of Columbia Glacier, Alaska (Meier, 1994; Van der Veen, 1996, 2002a). However, the similarities in behaviour imply that perhaps there is not a systematic difference in calving mechanisms between tidewater and freshwater settings, as has previously been thought.

Not only is there no simple link between rate-controlling processes and calving, but these factors themselves inter-relate. For example, forces of buoyancy and longitudinal

stretching are often coincident, as described above. Thinning may lead to increased buoyancy which, by decreasing the effective pressure, results in glacier stretching and fracture. Similarly, increased longitudinal stretching due to decreasing effective pressure (from an increased input of water to the bed), will lead to thinning, resulting in increased buoyancy. However, care must be taken not to assume that buoyancy and longitudinal stretching always operate together. For example, at Glaciar Nef, Patagonia, the absence of open transverse crevasses from the lowermost part of the glacier indicates that the terminus is not undergoing longitudinal stretching, and that buoyancy operates independently, driven by high rates of surface melting (Warren *et al.*, 2001). In comparison, water-filled crevasses up to 40 m back from the ice cliff indicate longitudinal stretching at Mendenhall Glacier, Alaska, where calving occurs by buoyancy as the glacier recedes through a progressively deeper lake (Motyka *et al.*, 2003b). At Glaciar León, buoyancy appears to become transiently activated in response to a seasonal advance of the terminus, whilst at Fjallsjökull, buoyancy operates over longer timescales, as the glacier retreats into progressively deeper water, in a similar manner to Mendenhall Glacier (Motyka *et al.*, 2003b). It is interesting that waterline melt notches at Glaciar León and Fjallsjökull appear to evolve at similar rates and to similar sizes as the New Zealand glaciers. Whilst visual observation of the ice front geometry might imply that waterline melting is the dominant control, the closer the glacier terminus is to flotation, the greater role buoyancy plays in controlling calving relative to waterline melting. This would also explain how the melt notches seen at Glaciar Nef (Warren *et al.*, 2001) do not drive calving, as they might if the terminus was not as close to the threshold of flotation. Like the deep water-terminating Glaciar Upsala, Argentina (Skvarca *et al.*, 2002, 2003), calving at near-floating termini Glaciar Nef and Mendenhall Glacier is driven by buoyant forces of such high magnitude and is so dominant a process that it renders melting insignificant.

Short-term variations in calving rates cannot be accounted for in the water depth relationship, where water depth is prescribed in absolute terms. Ironically, it is emerging that it is relative water depth fluctuations which may modify terminus dynamics over short timescales. If the water depth at the terminus constrains basal water pressures, it is logical that changes in water depth will alter the basal conditions. At fast, temperate calving glaciers, ice flow is highly sensitive to the effective basal pressure, and the pervasively fractured nature of calving termini means that they can respond rapidly to cyclic fluctuations of water to the bed, causing terminus acceleration. This has been demonstrated at tidewater LeConte Glacier, Alaska (O'Neel *et al.*, 2001). However, the

existence of diurnal cycles in calving at freshwater glaciers has not previously been investigated. The research at Fjallsjökull in this thesis has revealed a correlation in the timing and size of calving events with diurnal fluctuations in lake level change, which result from both meteorological inputs and the glacial hydrological system. It is possible that this correlation relates to ice flow acceleration due to increases to the basal water pressure, although no data exist to test this. Over even shorter timescales of less than an hour, it is possible that changes to the cliff force balance, linked to a small drop in lake level, destabilises the terminus, triggering a calving event. Again, further work is required to test this correlation and establish whether a causative link exists.

Previous short-term observations at Maud Glacier identified a link between hydrological changes, resulting from a rainfall event, and glacier motion (Kirkbride & Warren, 1997). However, it was thought that these parameters neither affect nor are affected by calving activity. This contrasts with the observations at Glaciar León and Fjallsjökull. Whilst there appears to be a diurnal cycle in calving relating to lake level changes at Fjallsjökull, the terminus dynamics of Glaciar León at the end of October indicate that changes in terminus position resulting from a change in the basal hydrology and sliding regime were followed by a calving response, in order for the glacier front to regain an equilibrium position. In other words, up-glacier processes do interact with calving activity. Another explanation for the observations at Maud Glacier exists. It is possible that the generally low velocities means that although increased flow occurs, tensile stresses do not exceed the tensile strength of the ice, which can accommodate the resulting strain. The exception occurs at the terminus, where the force imbalance in conjunction with small water depths leads to the formation of crevasses only directly behind the terminus, along which full-height calving events occur.

The question of whether or not calving relates to up-glacier dynamics is central to the calving debate (2.1.3), which seeks to describe calving as either the 'master' or 'slave' of other glacier dynamics such as ice flow and terminus fluctuations. Field observations from both Fjallsjökull and Glaciar León suggest that calving occurs in response to changes in terminus dynamics, and is therefore the 'slave' to changes in water depth, basal sliding and water pressures, which alter the ice cliff force balance, ice velocity and the buoyancy of the terminus in the water body. The concept of calving glaciers operating along a continuum (2.1.3) is useful for accommodating the contributions of the various rate-controlling factors, where the full range of calving mechanisms combine in different ways

to produce the observed diversity of calving behaviours without the requirement that these forces operate mutually exclusively. However, it would therefore be more useful to consider this continuum in terms of a range of calving mechanisms relating to ice velocity, rather than as a scale defined by calving rate (Warren & Kirkbride, 2003), if it is indeed the case that changes in ice dynamics lead to a calving response. This may be represented by the conceptual model shown in Figure 8.1, which illustrates a continuum of glacier speed as a function of the dominant calving mechanism, and gives the positions of Glaciar León and Fjallsjökull, based on the findings in this study. Such a model provides a foundation with which to approach future studies of calving dynamics.

8.3 Climatic response of freshwater-calving glaciers

Glaciers and ice sheets provide a record of the general patterns of climatic change, and their expansion and retreat allows us to document long-term trends of cooling and warming. However, with decreasing timescales, the growth and decay of ice masses is increasingly modified by the influence of other factors, such as the local topography and catchment meteorology, and the internal dynamics of the ice mass. As a result, such glacier margins do not exhibit a direct linear response to climate. In particular, calving glacier termini become decoupled from climatic forcing over decadal and centurial timescales. The glacier instability that iceberg calving introduces means that calving glaciers may be insensitive to climate change. Whilst climate may initiate an advance or retreat phase, calving dynamics may subsequently dominate, such that the fluctuation of the terminus may bear little relation to the climatic trend. At the global scale, calving is a key mechanism for the Earth-climate system, as it provides a link between the cryosphere and the hydrosphere and, in turn, with the atmosphere.

It is possible to consider the climatic sensitivity of a calving glacier in terms of its position on the calving glaciers continuum (8.2). In this case, slow-flowing lake-terminating glaciers such as those in New Zealand constitute those calving termini which are most sensitive to climate, responding to high levels of precipitation (Fitzharris *et al.*, 1997; Warren & Kirkbride, 2003). At the insensitive end of the spectrum are fast, tidewater margins, and this continuum may be extended to include land-terminating glaciers, which are the most sensitive to climatic changes.

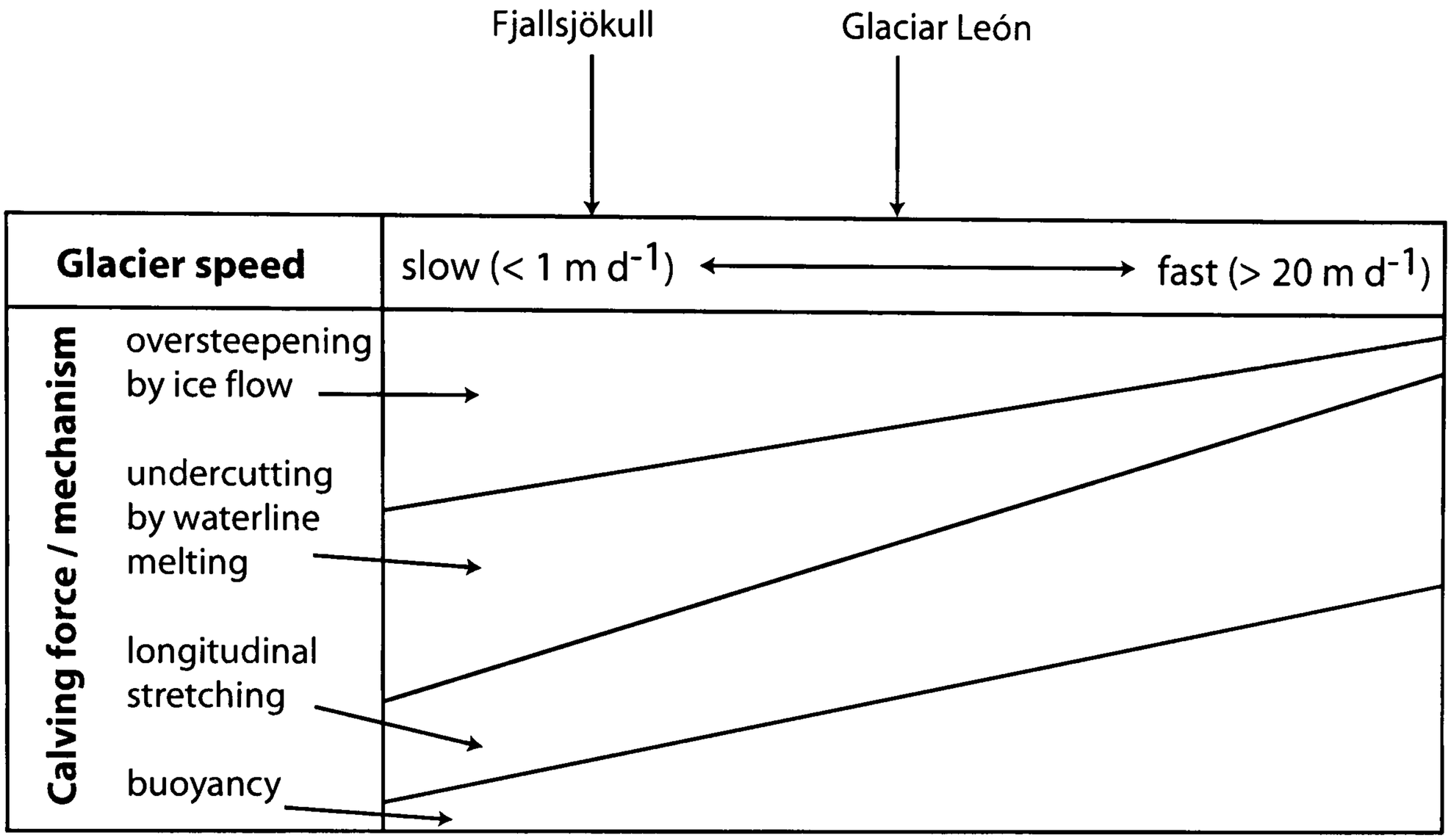

Figure 8.1 Conceptual model to illustrate a calving continuum, which relates the calving mechanism to ice velocity. This qualitatively illustrates the change in relative importance of each mechanism at different ice speeds. Oversteepening by ice flow dominates at the slowest glaciers, becoming negligible at the fast speeds. Undercutting by melting may operate at all speeds, but ceases to control calving when another mechanism dominates. Longitudinal stretching is negligible where oversteepening by ice flow is the rate-controlling factor, and buoyancy operates at all speeds, becoming increasingly important at faster speeds where, as flotation is approached, it may account for calving of large 'tabular' portions of the terminus. Beyond this extreme lie floating ice shelves, which are highly susceptible to buoyant forces. At the other end of the scale, land-terminating ice cliffs will be controlled by ice cliff oversteepening and, at the furthest extreme lie non-calving land-terminating glacier termini.

The suggested positions of Glaciar León and Fjallsjökull on this continuum are also shown. Glaciar León plots in an intermediate position, being fast for lake-calving glaciers, and reflects the dominance of longitudinal stretching and buoyancy forces on calving compared to the influence of waterline melting. At Fjallsjökull, whilst buoyancy forces are important for calving over longer timescales, most calving depends on the interaction of undercutting at the waterline with the force balance at the ice cliff, where frequent changes in water level influence the timing of calving events as the force balance adjusts. Other lake-calving glaciers such as those in New Zealand would plot to the left, whilst rapidly disintegrating tidewater glaciers, such as Columbia Glacier, would plot to the far right.

Mass balance and terminus changes at calving glaciers do not become entirely isolated from climatic forcing once calving has been initiated, demonstrated by the pattern of retreat at some lake-calving termini. For example, following thinning, glaciers in the Southern Alps of New Zealand experienced lake formation during the 20th century (Chinn, 1996; Kirkbride, 1993; Kirkbride & Warren, 1997), and their retreat rates increased from a mean of 12 m a^{-1} to 50 m a^{-1}, demonstrating that climatic sensitivity was reduced, but that calving dynamics still responded to mass balance changes. Similarly, lacustrine Mendenhall Glacier, Alaska, formed a lake in the 1930s, and whilst retreat rates have increased since calving was initiated, it is thought that most of the glacier shrinkage is primarily due to warming and that calving losses are secondary (Motyka *et al.*, 2003b). In Iceland, Breiðamerkurjökull has retreated rapidly through the deep basin during the last century whilst, in contrast, the retreat of neighbouring Fjallsjökull has been punctuated by decelerations in the retreat rate at times, similar to still-stands or readvances experienced by other, land-terminating Icelandic glaciers. This is thought to relate to periods of increased precipitation in conjunction with later cooling of summer temperatures (Kirkbride, 2002), and suggests that Fjallsjökull is sensitive to regional climatic forcing.

Like the above glaciers in Alaska and Iceland, many lake-calving glaciers began calving in the mid twentieth century in Patagonia. The Patagonian Icefields are a key record of climate for the southern hemisphere, where land mass is scarce. The increasing numbers of calving outlets is thus influencing the clarity of the climatic record that the icefields provide. In particular, Glaciar León differs from many outlets, having commenced calving some 3000 years ago. Any significant retreat of Glaciar León will lead to the cessation of calving and the margin will lose contact with Lago Leones. An advance of the terminus will occur into deep water, causing the calving rate to increase, limiting the amount of terminus advance (2.1.1.i). In combination, these scenarios imply that, at its current terminus position, Glaciar León is climatically insensitive, responding instead to the topographic control of the pinning point at which the terminus is held. This is substantiated by the recent history of the terminus position, which has altered little in the last 50 years. Furthermore, field data in this thesis indicate that short-term terminus fluctuations, which occur as the glacier responds to internal glacier dynamics by calving, exceed annual figures. Thus, the terminus position can be considered to exhibit relatively large-scale 'noise' around an otherwise static terminus.

The terminus position of Glaciar León contrasts starkly with neighbouring Glaciar Soler (Figure 3.2), whose lake has only formed in the last 10 years (Glasser *et al.*, 2002), and neighbouring Glaciar Fiero, whose debris-covered slope is low in surface gradient, and has far to retreat before it will lose contact with its ice-contact lake. Its slower retreat probably relates to the debris cover, which will cause greater rates of down wasting in relation to retreat rates, as at Tasman Glacier, New Zealand. Although ice velocities for this glacier are not known, they are likely to be slower due to the shallower surface gradient, inhibiting the rate of crevasse formation and the frequency of calving events. As Glaciar Fiero is also debris covered, it may be likened to the New Zealand calving outlets, and demonstrates the influence that calving dynamics can have on glacier response to regional climatic forcing. In the near future, fluctuations of Glaciar León and Fjallsjökull are likely to be quite different. Whilst Glaciar León is likely to cease calving, and fluctuate little, Fjallsjökull may experience an accelerated retreat, as it recedes into deeper water. Despite this contrast, the rate of retreat of the relatively stable Fjallsjökull terminus is still not expected to be as dramatic as seen at many tidewater glaciers.

8.4 Recommendations for future research

8.4.1 Introduction

As stated by Van der Veen in 1997, there is still a pressing need to add to the calving glacier database. This is particularly the case for freshwater-terminating margins, where few data exist. In order to gain a full understanding of the mechanisms involved in the process of calving, and the rate-controlling factors, it is necessary to make comprehensive measurements of a wide range of glaciological, limnological and meteorological variables, and measurements are required over a range of timescales, from interannual, to seasonal, to diurnal and hourly.

Of course, many factors inhibit the feasibility and practicality of conducting such detailed investigations over these time scales, but it is possible to consider what forces are at work and reflected in glacier behaviour. The outcomes of this thesis support the concept of rate-controlling factors operating along a continuum (Warren & Kirkbride, 2003). These factors are numerous and, as well as affecting various modes of calving, they interact with

each other, such that it is often difficult to disentangle their separate signals. Only by investigating these factors at a high level of spatial and temporal resolution, at a large number of glaciers, can we hope to understand and predict calving behaviour over longer timescales, and distinguish between the calving signal and that of climatic forcing.

8.4.2 Glacio-limnological interactions: evaluating melting

Research at Glaciar León and Fjallsjökull has shown that waterline and subaqueous melting, whilst not the dominant control on calving dynamics at these sites, facilitates subaerial calving by undercutting the ice cliff above the waterline. Although the use of a radio-controlled boat yielded important information about ice-water interface temperatures, it was not possible to measure melt notch growth directly, as was the case at Glaciar León, because of the restricted access to a view of the glacier margin parallel to the terminus. In such cases, a modelling approach is required, such as those outlined above. Here, a conceptual outline of a possible approach to understanding the energy fluxes involved in the transfer of heat to the ice face is presented for lake-calving glaciers, such as Glaciar León and Fjallsjökull.

In its basic form, melting (or freezing) of ice in contact with water depends on the temperature gradients in both media, and their thermal conductivities, k_i and k_w, respectively. Where the ice is isothermal at 0 °C, the melt rate, M, is given by:

$$M = \rho_i L k_w \left(\delta T_w / \delta x\right) \qquad \text{(Paterson, 1994)} \qquad \text{(Eq. 8.1)}$$

where ρ_I is the ice density, L is the latent heat of fusion, and $(\delta T_w/\delta x)$ is the temperature gradient in the water normal to the ice face. Where the ice is < 0 °C, freezing will occur due to conduction of heat into the ice. Despite its apparent simplicity, in the real-world situation at a glacier terminus this model is difficult to apply because the temperature gradient term constantly evolves in response to energy exchanges, production of meltwater, density-driven convection, and water advection resulting from wind-driven, tidal, and other currents. It is proposed here that it is possible to address this problem using two complementary models. In the first model, the heat flux equation (equation 8.1) could be coupled to a model of density-driven convection, in which water sinks or rises in response to heat exchange with the ice, and far-field water is drawn in to preserve

continuity. Far-field water temperature evolution would be forced by energy fluxes at the upper (atmospheric) and lower boundaries, and internal conductive and convective exchanges. Additional terms would be added sequentially to incorporate the effects of suspended sediment, inputs of meltwater from up-glacier, and externally-driven currents, e.g. inflow of Breiðå at Fjallsárlón. By implementing the model in 2-D finite-difference form, it could be used to calculate melting rates along vertical transects through submerged ice faces under varying boundary conditions.

The second model would develop the bulk heat budget approach used in earlier ice-melt calculations calculating melting by summing all other energy exchange and storage terms for the water body (equations 2.12 and 2.18-2.21, p. 62 and 66) (Sakai *et al.*, 2000a; Motyka *et al.*, 2003a), with the additional inclusion of the heat components from atmospheric exchange and the lake bed:

$$M = \left(Q_{atm} + Q_{bed} + Q_{in} - Q_{out} - \delta S / \delta t\right)\rho_i L^{-1} \qquad \text{(Eq. 8.2)}$$

where the terms in the first set of brackets are energy exchanges with the atmosphere, sea- or lake bed, incoming water, outflowing water, and change in heat storage, respectively. Model output is in the form of total loss per unit width for the whole submerged ice face. This approach does not consider physical processes at the melting face, but has the advantage that subaqueous melt can be estimated from relatively low-resolution field data, and is hence more appropriate for complex real-world situations. In order to overcome the problems experienced by previous researchers with regard to the oversimplification of the components in the heat budget, model testing using field data will allow comparison with empirical data on melt rates, calving rates, and water-body characteristics. The first model would be employed in detailed studies of waterline notch evolution at easily accessible ice faces at a suitable lake-calving terminus, whilst model two would be used to compute bulk subaqueous melt rates, using meteorological data as input. The models may then be refined and optimised at a range of spatial and temporal scales. The kinds of field data required include:

(1) Water body characteristics — A surface and 3D network of water temperatures and its temporal evolution. Although this was accomplished for the upper 100 m of Lago Leones in this thesis, suggestions for more comprehensive surveys include the use of time-lapse thermal imaging of the lake surface from elevated vantage points

which would permit the determination of advective heat fluxes, i.e. currents, to be calculated. Circulation patterns may be determined by radio-tracking neutrally-buoyant drifting buoys, which are less susceptible to destruction by icebergs than static, moored current sensors. A high frequency network of vertical temperature profiles and suspended sediment concentration will allow the evolving thermal structure and water density to be determined, with measurements close to the ice terminus gathered using a radio-controlled boat, as at Fjallsjökull (6.3.4.i, 7.5.3).

(2) Energy exchanges with the atmosphere The full water surface energy balance may be determined using meteorological data (shortwave and longwave radiation, air temperature, pressure, humidity and wind speed data, combined with albedo measurements) obtained from automatic weather stations installed close to the lake site.

(3) Water and ice outputs and inputs Heat losses from water exiting the lakes may be determined using stage recorders and thermistors located at efflux points. Pressure sensors installed below the lake surfaces could be used to record short-term (wave-induced) and longer term (water volume-controlled) changes in water depth, as at Fjallsjökull (6.3.3.ii, 7.5.2).

(4) Calving and waterline melt rates Repeat theodolite surveys of subaerial ice faces, like that carried out at Glaciar León (4.3.1, 5.3.3), would provide independent data on calving losses and waterline notch development. Subaerial melt losses can be found from ablation stake data.

In combination, this modelling approach, validated with such comprehensive energy balance data, would yield more detailed information on ice-contact lakes and glacio-limnological interactions than has hitherto been possible, contributing to the understanding of the role of subaqueous melting for calving mass losses.

8.4.3 Calving mechanisms

One area of particular concern is an understanding of the basal regime: the effective pressure including basal water pressure, and the response of the sliding rate, longitudinal stretching, buoyancy and ice cliff force balance that result from alterations to this regime. It is likely that the responses of these parameters involve thresholds, where one becomes dominant over another at certain levels of basal water pressure. For example, any ice mass terminating in water is subject to forces of buoyancy, but buoyancy only affects calving significantly once it reaches a threshold level, at which it overrides other forces, such as calving by undercutting at the waterline.

Inevitably, the fast-flowing nature of calving glaciers compared to land-terminating glaciers means that crevasse density often inhibits access to the glacier to make direct measurements of the basal conditions. However, at some lake-calving glaciers where ice flow is slower, such as Fjallsjökull, such measurements may be possible. Additionally, where calving may occur less frequently at lacustrine margins, the ice cliff is more accessible for gathering data such as waterline melt notch growth rates and ice-water boundary temperatures. This research has highlighted novel ways in which detailed records of calving events and monitoring processes at the ice face may be conducted (7.5), and provides a basis for investigations at other freshwater-calving glaciers.

A question that has arisen from the field studies at Glaciar León and Fjallsjökull is whether calving occurs along pre-existing crevasses or those advected into the terminus from up-glacier. This is important for addressing the issue of whether up-glacier processes affect calving or whether calving dynamics are limited to the ice terminus itself. It is not a straightforward question, as a sinuous glacier may advect crevasses into the terminus which are no longer transverse to the main direction of ice flow. Calving may then occur along these crevasses, i.e. obliquely to the ice front, or propagate parallel to the terminus, obliquely to the existing crevasses. Studies at lake-calving glaciers may, again, provide a simpler environment in which to investigate calving from a perspective of crevassing where crevasse density is often lower than for tidewater glaciers.

8.5 Conclusions

The main conclusions of this thesis are as follows:

- The studies of Glaciar León and Fjallsjökull have added to the expanding database of lacustrine calving glaciers. Ice surface velocities at Glaciar León are ~ 880 m a^{-1} and, with little terminus change taking place, calving rates are ~ 800-900 m a^{-1}. Calving occurs into water with a width-averaged water depth of ~ 65 m.

- Existing data suggest that the relative significance of melting decreases with increasing calving speeds. At slow-flowing lake-calving glaciers, waterline melting may be the rate-controlling process for calving, but with increasing calving rates the proportion of mass loss that is caused by melt-induced calving declines. Other factors controlling the majority of calving at these sites include buoyancy, glacier sliding and basal pressures, and the force balance at the terminal cliff. These forces operate contemporaneously, and vary in their relative importance for calving, both spatially and temporally.

- Water temperatures at the terminus are ~ 4.5–8 °C at Glaciar León, and ~ 1.5 °C at Fjallsjökull. Calving by undercutting of the subaerial ice cliff due to waterline melting accounts for a minority of mass loss from the terminus of Glaciar León. Neither is it likely to account for all mass loss at Fjallsjökull. Therefore, thermo-erosional melt notches are not always the primary control on calving at freshwater calving glaciers. Nevertheless, by undercutting the subaerial part of the calving cliff, melting at the waterline plays a significant role in facilitating subaerial calving.

- The physical limnology of ice-contact lakes is important for determining the potential for heat transfer to calving termini. Their thermal structure exhibits a high degree of spatio-temporal variability and a large lake may establish of a temperature gradient between the distal and ice-proximal ends, important for advecting heat to the ice face.

- Subaqueous melting may be important, but with present knowledge it is not possible to estimate its magnitude, variability or relative significance. Existing temperature-dependent melt relations, which largely relate to marine environments and ignore forced convection, are inadequate tools for

calculating subaqueous melt rates, especially at freshwater sites. To improve our understanding of calving, both in lakes and in tidewater, it will be necessary to investigate the immediate ice-proximal aqueous environment in greater detail, paying particular attention to water temperatures, upwelling rates and their spatio-temporal variability. Improved methods of obtaining accurate subaqueous and waterline melt rates are required. This study has made advances in overcoming some of the challenges of gathering data with which to make these calculations, by surveying waterline melt notch growth rates, and using a radio-controlled boat to gain improved access to water temperatures at the ice-water interface. However, further work is required before these techniques will yield accurate data for both the waterline and subaqueous portions of the ice face.

- Lake-level fluctuations may be both seasonal (Glaciar León) and diurnal (Fjallsjökull), and are integral to calving behaviour. Prior to this study, diurnal variations have only been considered of significance for tidewater glaciers, from tidal variations. This study has demonstrated the role of lake-level changes for seasonal terminus dynamics of Glaciar León, from the timing of terminus advance, changes in ice velocity and lake level changes. Additionally, lake-level fluctuations at diurnal and hourly scales influence the timing and size of calving events at Fjallsjökull, as seen from a record of pressure changes.

- The complex range of factors identified in this thesis, which control calving behaviour, lend support to a view of calving glaciers as being located along a continuum, between slow-flowing freshwater and fast-flowing tidewater glaciers at each extreme. This continuum is best defined in terms of a range of calving mechanisms, rather than a linear calving rate, if calving is considered to occur in response to other glacier dynamics.

- The climatic response of calving glaciers is sensitive to their position on the calving continuum. At present, interannual terminus change at Glaciar León can be expected to be insensitive to climatic forcing, relating instead to topographic controls. In Iceland, Fjallsjökull appears to have largely conformed with climatic changes, although it is expected that more rapid retreat may occur in the near future as the glacier recedes into deeper water.

REFERENCES

Abdalati, W. and Krabill, W.B. 1999. Calculation of ice velocities in the Jakobshavn Isbrae area using airborne laser altimetry. *Remote Sensing of Environment* 67, 194-204.

Alley, R.B. 1991. Sedimentary processes may cause fluctuations of tidewater glaciers. *Annals of Glaciology* 15, 119-124.

Alley, R.B. and MacAyeal, D.R. 1994. Ice-rafted debris associated with binge/purge oscillations of the Laurentide Ice Sheet. *Palaeoceanography* 9, 503-511.

Amos, J. 2004. Patagonian ice in rapid retreat [online]. Available at: http://news.bbc.co.uk/1/hi/sci/tech/3662975.stm (27/04/04).

Anandakrishnan, S. and Alley, R.B. 1997. Tidal forcing if basal seismicity of ice stream B, West Antarctica, observed far inland. *Journal of Geophysical Research* 102, 15183-15196.

Anderton, P.W. and Chinn, T.J. 1978. Ivory Glacier, New Zealand, I.H.D. representative basin study. *Journal of Glaciology* 20, 67-84.

Aniya, M. 1988. Glacier inventory for the Northern Patagonian Icefield, Chile, and variations 1944/45 to 1985/86. *Arctic and Alpine Research* 20, 179-187.

Aniya, M. 1992. Glacier variation in the Northern Patagonian Icefield, Chile, between 1985/86 and 1990/91. *Bulletin of Glacier Research* 10, 83-90.

Aniya, M. 1995. Holocene glacial chronology in Patagonia: Tyndall and Upsala glaciers. *Arctic and Alpine Research* 27, 311-322.

Aniya, M. 1996. Holocene variations of Ameghino Glaciar, southern Patagonia. *The Holocene* 6, 247-252.

Aniya, M. 1999. Recent glacier variations in of the Hielo Patagónicos, South America and their contribution to sea level change. *Arctic, Antarctic and Alpine Research* 31, 144-152.

Aniya, M. 2001. Glacier variation of Hielo Patagónico Norte, Chilean Patagonia, since 1944/45, with special reference to variations between 1995/1996 and 1999/2000. *Bulletin of Glaciological Research* 18, 55-63.

Aniya, M. and Enomoto, H. 1986. Glacier variations and their causes in the Northern Patagonian Icefield, Chile, since 1944. *Arctic and Alpine Research* 18, 307-316.

Aniya, M. and Sato, H. 1996. Recent glacier variations in the Patagonia Icefield. *Seppyo* 58, 43-52.

Aniya, M. and Wakoa, Y. 1997. Glacier variations on Hielo Patagonico Norte, Chile, between 1944/45 and 1995/96. *Bulletin of Glacier Research* 15, 11-18.

Aniya, M., Sato, H., Naruse, R., Skvarca, P. and Casassa, G. 1996. Remote sensing application to inventorying glaciers in a large remote area – Southern Patagonian Icefield, South America. *Photogramm. Eng. Remote Sensing* 62, 1361-1369.

Aniya, M., Sato, H., Naruse, R., Skvarca, P. and Casassa, G. 1997. Recent glacier variations in the Southern Patagonian Icefield, South America. *Arctic & Alpine Research* 29, 1-12.

Aniya, M., Naruse, R., Casassa, G. and Rivera, A. 1999. Variations of Patagonian glaciers, South America, utilizing RADARSAT images. *Proceedings of the International Symposium on RADARSAT Application Development and Research* Opportunity (ADRO), Montreal, Canada, October 13-15, 1998. CD-ROM.

Aniya, M., Park, S., Dhakal, A.S. and Naruse, R. 2000. Variations of some Patagonian glaciers, South America, using RADASAT and Landsat images. Science Reports, Institute of Geoscience, University of Tsukuba, Section A 21, 23-38.

Arakawa, M. and Maeno, N. 1997. Mechanical strength of polycrystalline ice under uniaxial compression. *Cold Regions Science and Technology* 26, 215-229.

Aristarain, A.J. and Delmas, R.J. 1993. Firn-core study from the southern Patagonia ice-cap, South America. *Journal of Glaciology* 39, 249-254.

Ashley, G.M. 1995. Glaciolacustrine Environments. In: Menzies, J. (ed.) 1995. *Modern Glacial Environments - Processes, Dynamics and Sediments.* Butterworth-Heinemann, Oxford. 417-444.

Ashley, G.M., Smith, N.D. and Shaw, J. 1985. *Glacial Sedimentary Environments*. SEPM Short Course, 16.

Ashley, G. and Smith, N.D. 2000. Marine sedimentation at a calving glacier margin. *Geological Society of America Bulletin* 112, 657-667.

Ashley, G.M. and Warren, W.P. 1997. The ice-contact environment. *Quaternary Science Reviews* 16, 629-634.

Barber, D.C. Dyke, A., Hillaire-Marcel, C., Jennings, A.E., Andrews, J.T., Kerwin, M.W., Bilodeau, G.,McNeely, R., Southon, J., Morehead, M.D. and Gagnon, J.M. 1999. Forcing of the cold event of 8,200 years ago by catastrophic drainage of Laurentide lakes. *Nature* 400, 344-348.

Benn, D.I. and Evans, D.J.A. 1998. *Glaciers and Glaciation*. Arnold, London. pp 734.

Benn, D.I., Wiseman, S. and Warren, C.R. 2000. Rapid growth of a supraglacial lake, Ngozumpa Glacier, Khumbu Himal, Nepal. *Debris-Covered Glacier (Proceedings of a workshop held at Seattle, Washington, USA, September 2000)*. IAHS Publ. 264, 177-186.

Bendall, M.S. and Gebhart, B. 1976. Heat transfer and ice melting in ambient water near its density extremum. *International Journal of Heat Mass Transfer* 19, 1081-1087.

Bennett, K.D., Haberle, S.G. & Lumley, S.H. 2000. The last Glacial-Holocene Transition in Southern Chile. *Science* 290, 285-286.

Bennett, M.R., Huddart, D. and McCormick, T. 2000. The glaciolacustrine landform-sediment assemblage at Heinabergsjökull., Iceland. *Geografiska Annaler* 82, 1-16.

Bigg, G.R., Wadley, M.R., Stevens, D.P. and Johnson, J.A. 1997. Modelling the dynamics and thermodynamics of icebergs. *Cold Regions Science and Technology* 26, 113-135.

Bindschadler, R.A. 1983. The importance of pressurized subglacial water in separation and sliding at the glacier bed. *Journal of Glaciology* 29, 3-19.

Bindschadler, R.A. and Rasmussen, L.A. 1983. Finite-differences model predictions of the drastic retreat of Colombia Glacier, Alaska. *United States Geological Survey Professional Paper* 1258-D.

Björnsson, H. 1976. Marginal and supraglacial lakes in Iceland. *Jökull* 26, 40-50.

Björnsson, H. 1996. Scales and rates of glacial sediment removal: a 20 km long, 300 m deep trench created beneath Breiðamerkurjökull during the Little Ice Age. *Annals of Glaciology* 22, 141-146.

Björnsson, H. 2002. Subglacial lakes and jökulhlaups in Iceland. *Global and Planetary Change* 35, 255-271.

Björnsson, H. and Pálsson, F. 1998. Icemass: Mass balance and meteorological observations on Vatnajökull 1998. *European Union Field Report* RH-14-98, 14pp.

Björnsson, H., Pálsson, F. and Guðmundsson, M.T. 1992. Breiðamerkurjökull, results of radio echo soundings 1991. *Science Inst. Univ. of Iceland* RH-92-12, 19pp.

Björnsson, H., Pálsson, F. and Guðmundsson, M.T. 1998. Mass balance and meteorological observations on Vatnajökull 1997. *Science Inst. Univ. of Iceland* RH-03-98, 20pp.

Björnsson, H., Pálsson, F. and Guðmundsson, M.T. 2001. Jökulsárlón at Breiðamerkursandur, Vatnajökull, Iceland: 20th century changes and future outlook. *Jökull*, 50, 1-18.

Bond, G. and Lotti, R. 1995. Iceberg discharges into the North Atlantic on millennial timescales during the last glaciation. *Science* 267, 1005-1010.

Bond, G., Heinrich, H., Broecker, W., Labeyrie, L., McManus, J., Andrews, J., Huon, S., Jantschik, R., Clasen, S., Simet, C., Tedesco, K., Klas, M., Bonani, G. and Ivy, S. 1992. Evidence for massive discharges of icebergs into the North Atlantic Ocean during the last glacial period. *Nature* 365, 143-147.

Boulton, G.S., Harris, P.W.V. and Jarvis, J. 1982. Stratigraphy and structure of a coastal sediment wedge of glacial origin inferred from sparker measurements in glacial lake Jökulsárlón in southeastern Iceland. *Jökull* 32, 37-47.

Broecker, W. 1994. Massive iceberg discharges as triggers for global climate change. *Nature* 372, 421-424.

Brown, C.S., Meier, M.F. and Post, A. 1982. Calving speed of Alaska tidewater glaciers with applications to the Columbia Glacier, Alaska. *U.S. Geological Survey Professional Paper* 1258-C. 13 p.

Budd, W.F., Jacka, T.H. and Morgan, V.I. 1980. Antarctic iceberg melt rates derived from size distributions and movement rates. *Annals of Glaciology* 1, 103-112.

Burgos, J.J., Ponce, H.H. and Molion, L.C. 1991. Climate change predictions for South America. *Climate Change* 18, 223-239.

Campbell, W.J. 1973. Structure and inferred circulation of South Cascade Lake, Washington, U.S.A. *International Association of Scientific Hydrology publication 95*, 259-262.

Canadian Ice Service. Available at: http://www.cis.ec.gc.ca/pictures/picturew.html (22/06/04).

Carrasco, J.F., Casassa, G. and Rivera, A. 2002. Meteorological and climatological aspects of the Southern Patagonian Icefield. In: Casassa, G., Sepúlveda, F.V. and Sinclair, R.M. (eds.) *The Patagonian Icefields: a unique natural laboratory for environmental and climate change studies. Series of the Centro de Estudios Científicos*. Kluwer Academic. 29-42.

Casassa, G. 1987. Ice thickness deduced from gravity anomalies on Soler Glacier, Nef Glacier and the Northern Patagonia Icefield. *Bulletin of Glacier Research* 4, 43-58.

Casassa, G. 1995. Glacier inventory in Chile: current statistics and recent glacier variations. *Annals of Glaciology* 21, 317-322.

Casassa, G. and Marangunić, C. 1987. Exploration history of the Northern Patagonia Icefield. *Bulletin of Glacier Research* 4, 163-175.

Casassa, G., Brecher,H., Rivera, A and Aniya, M. 1997. A century-long recession record of Glaciar O'Higgins, Chilean Patagonia. *Annals of Glaciology* 24, 106-110.

Casassa, G., Rivera, A., Aniya, M. and Naruse, R. 2002. Current knowledge of the Southern Patagonian Icefield. In: Casassa, G., Sepúlveda, F.V. and Sinclair, R.M. (eds.) *The Patagonian Icefields: a unique natural laboratory for environmental and climate change studies. Series of the Centro de Estudios Científicos*. Kluwer Academic. 67-84.

Chikita, K., Jha, J. and Yamada, T. 1998. The basin expansion mechanism of a supraglacial lake in the Nepal Himalaya. *Jor. Fac. Sci., Hookaido Univ., Ser VII (Geophysics)* 11, 501-521.

Chikita, K., Jha, J. and Yamada, T. 1999. Hydrodynamics of a supraglacial lake and its effect on the basin expansion: Tsho Rolpa, Rolwaling Valley, Nepal Himalaya. *Arctic, Antarctic and Alpine Research* 31, 58-70.

Chikita, K., Jha, J. and Yamada, T. 2000a. Sedimentary effects on the expansion of a Himlayan supraglacial lake. *Global and Planetary Change* 28, 23-34.

Chikita, K., Joshi, S.P., Jha, J. and Hasegawa, H. 2000b. Hydrological and thermal regimes in a supraglacial lake: Imja, Khumbu, Nepal Himalaya. *Hydrological Sciences Journal* 45, 507-521.

Chinn, T.J. 1995. Glacier fluctuations in the Southern Alps of New Zealand determined from snowline elevations. *Arctic and Alpine Research* 27, 187-198.

Chinni, G.A. and Warren, C.R. submitted. The 2004 outburst flood at Glaciar Perito Moreno, Argentina. *Journal of Glaciology*

Churski, Z. 1973. Hydrographic features on the proglacial area of Skeiðarárjökull. *Geographia Polonica* 26, 209-254.

Clapperton, C.M. 1983. The glaciation of the Andes. *Quaternary Science Reviews* 2, 83-155.

Clapperton, C.M. 1990. Quaternary glaciations in the southern hemisphere: an overview. *Quaternary Science Reviews* 9, 299-304.

Clapperton, C.M. 1993. Quaternary Geology and Geomorphology of South America. Elsevier Science. pp. 779.

Clapperton, C.M. 1998. Late Quaternary Glacier Fluctuations in the Andes: Testing the Synchrony of Global Change. *Quaternary Proceedings* 6, 65-73.

Clapperton, C.M. and Sugden, D.E. 1988. Holocene glacier fluctuations in South America and Antarctica. *Quaternary Science Reviews* 7, 185-198.

Clapperton, C.M., Sugden, D.E. and Pelto, M. 1989. Relationship of land terminating and fjord glaciers to Holocene climatic change, South Georgia, Antarctica. In: Oerlemans, J. (ed.) *Glacier Fluctuations and Climatic Change*. Kluwer, Dordrecht, 57-75.

Clapperton, C.M., Sugden, D.E., McCulloch, R.D. and Kaufmann, D.S. 1995. The last glaciation in centrall Magellan Strait, southernmost Chile. *Quaternary Research* 44, 133-148.

Clark, P.U., Marshall S.J., Clarke, G.K.C., Hostetler, S.W., Licciardi, J.M. and Teller, J.T. 2001. Freshwater forcing of abrupt climate change during the last glaciation. *Science* 293, 283-287.

Clarke, G.K.C. 1990. Fast Glacier Flow: Ice streams, surging, and tidewater glaciers. *Journal of Geophysical Research* 92 (B9), 8835-8841.

Clarke, G.K.C., Marshall, S.J., Hillaire-Marcel, C., Bilodeau, G. and Veiga-Pires, C. 1999. A glaciological perspective on Heinrich Events. In: Clark, P.U., Webb, R.S. and Keigwin, L.D. (eds). *Mechanisms of Global Climate Change at Millennial Timescales*. American Geophysical Union, Washington D.C. pp. 243-262.

Clarke, G.K.C., Leverington, D.W., Teller, J.T. and Dyke, A.S. 2004. Paleohydraulics of the last outburst flood from glacial Lake Agasiz and the 8200 BP cold event. *Quaternary Science Reviews* 23, 389-407.

Crocker, G.B. 1993. Size distributions of bergy bits and growlers calved form deteriorating icebergs. *Cold Regions Science and Technology* 22, 113-119.

Denton, G.H., Heusser, C.J. Lowell, T.V., Moreno, P.I., Anderson, B.G., Heusser, L.E., Schlüchter, C. and Marchant, C.R. 1999. Interhemispheric linkage of palaeoclimate during the last glaciation. *Geografiska Annaler* 81, 107-153.

Depetris, P.J. and Pasquini, A.I. 2000. The hydrological signal of the Perito Moreno Glacier damming of Lake Argentino (southern Andean Patagonia): the connection to climate anomalies. *Global and Planetary Change* 26, 367-374.

Derbyshire, E. 1974. The bathymetry of Jökulsárlón, southeast Iceland. *Geographical Journal* 140, 269-274.

Doake, C.S.M. and Vaughan, D.G. 1991. Rapid disintegration of the Wordie Ice Shelf in response to atmospheric warming. *Nature* 350, 328-330.

Dowdeswell, J.A. 1987. Processes of glacimarine sedimentation. *Progress in Physical Geography* 11, 52-90.

Dowdeswell, J.A. and Dowdeswell, E.K. 1989. Debris in icebergs and rates of glacimarine sedimentation, observations from Spitsbergen and a simple model. *Journal of Glaciology* 97, 221-231.

Dowdeswell, J.A. and Murray, T. 1990. Modelling rates of sedimentation from icebergs. In: Dowdeswell, J.A. and Scourse, J.D. (eds.) *Glacimarine Environments: processes and sediments*. London: Geological Society of London Special Publication 53, 121-37.

Drewry, D. 1986. *Glacial Geologic Processes*. Edward Arnold, London pp. 167-237.

Drewry, D.J., Jordan, S.R. and Jankowski, E. 1982. Measured properties of the Antarctic ice sheet, surface configuration, ice thickness, volume and bedrock characteristics. *Annals of Glaciology* 3, 83-91.

Duck, R.W. & McManus, J. 1985. Short-term bathymetric changes in an ice-contact proglacial lake. *Norsk Geografiska Tidschrift* 349, 39-45.

Eijpen, K.J., Warren, C.R. and Benn, D.I. 2003. Subaqueous melt rates at calving termini. *Annals of Glaciology* 36, 179-183.

Einarsson, M. 1991. Temperature conditions in Iceland, 1901-1990. *Jökull* 41, 1-20.

El-Tahan, M., Ventakesh, S. and El-Tahan, H. 1987. Validation and quantitative assessment of the deterioration mechanisms of arctic icebergs. *Journal of Offshore Mech. Arct. Eng.* 109, 102-108.

Elverhoi, A., Lonne, O. and Sealand, R. 1983. Glaciomarine sedimentation in a modern fjord environment, Spitsbergen. *Polar Research* 1, 127-149.

Enomoto, H. and Abe, 1983. Reconnaissance studies of meteorology and glaciology in Steffen and Jorge Montt Glaciers, Patagonia. In: Naruse, R. (ed.) *Glaciological studies in Patagonia Northern Icefield, 1983-1984.* Data Center for Glacier Research, Japanese Society of Snow and Ice, pp. 7-14.

Enomoto, H. and Nakajima, C. 1985. Recent climate fluctuations in Patagonia. In: Nakajima, C. (ed.) *Glaciological Studies in Patagonia Northern Icefield, 1983-1984.* Data Center for Glacier Research, Japanese Society of Snow and Ice, 7-14.

Escobar, F., Vidal, F., Garin, C. and Naruse, R. 1992. Water balance in the Patagonian Icefield. In: Naruse, R. and Aniya, M. (eds.) *Glaciological Researches in Patagonia 1990.* Japanese Society of Snow and Ice, 109-119.

Evans, D.A. and Twigg, D.R. 2000. Breiðamerkurjökull, 1998. 1:30 000 scale map. University of Glasgow and Loughborough University.

Evans, D.J.A. and Twigg, D.R. 2002. The active temperate glacial landsystem: a model based on Breiðamerkujökull and Fjallsjökull, Iceland. *Quaternary Science Reviews* 21, 2143-2177.

Evans, D.J.A., Archer, S. and Wilson, D.J.H. 1999a. A comparison of the lichenometric and Schmidt hammer dating techniques based on data from the proglacial area of some Iceland glaciers. *Quaternary Science Reviews* 18, 13-41.

Evans, D.J.A., Lemmen, D.S. and Rea, B.R. 1999b. Glacial landsystems of the southwest Laurentide Ice Sheet: modern Iceland analogues. *Journal of Quaternary Science* 14, 673-691.

Fastook, J.L. and Schmidt, W.F. 1982. Finite element analysis of calving ice fronts. *Annals of Glaciology* 3, 103-106.

Field, W.O. 1937. Observations on Alaskan coastal glaciers in 1935. *Geographical Review* 37, 369-99.

Fischer, M.P. and Powell, R.D. A simple model for the influence of push-morainal banks on the calving and stability of glacial tidewater termini. *Journal of Glaciology* 44, 31-41.

Fitzharris, B.B., Chinn, T.J. and Lamont, G.N. 1997. Glacier balance fluctuations and atmospheric circulation patterns over the Southern Alps, New Zealand. *International Journal of Climatology* 17, 745-763.

Fujiyoshi, Y., Kondo, H., Inoue, J. and Yamada, Y. 1987a. Characteristics of precipitation and vertical structure of air temperature in the northern Patagonia. *Bulletin of Glacier Research* 4, 15-23.

Fujiyoshi, Y., Nakajima, C., Inoue, J. and Nagao, I. 1987b. Cooling of water and the overlying air by melting ice at Lagoon San Rafael in the northern Patagonia. *Bulletin of Glacier Research* 4, 97-102.

Fukami, H. and Naruse, R. 1987. Ablation of ice and heat balance on Soler Glacier, Patagonia. *Bulletin of Glacier Research* 4, 37-42.

Funk, M. and Müller, D. Waves induced by calving of Unteraargletscher. ETH, Switzerland, unpublished report.

Funk, M. and Röthlisberger, H. 1989. Forecasting the effects of a planned reservoir which will partially flood the tongue of Unteraargletscher in Switzerland. *Annals of Glaciology* 13, 76-81.

Gade, J.W. 1979. Melting of ice in sea water: a primitive model with application to the Antarctic Ice shelf and icebergs. *Journal of Physical Oceanography* 9, 189-198.

Gade, J.W. 1993. When ice melts in sea water: a review. *Atmosphere-Ocean* 31, 139-165.

Gagnon, R.E. and Gammon, P.H. 1995. Characterisation and flexural strength of iceberg and glacier ice. *Journal of Glaciology* 41, 103-111.

Geirsdóttir, A., Hardardóttir, J. and Sveinbjörnsdóttir, A.E. 2000. Glacial extent and catastrophic meltwater events during the deglaciation of Southern Iceland. *Quaternary Science Reviews* 19, 1749-1761.

Gilbert, R. 1971. Observations on ice-dammed Summit Lake, British Colombia, Canada. *Journal of Glaciology* 10, 351-356.

Gilbert, R. and Desloges, J.R. 1987. A delta built by ice rafting in outflow from a glacial lake. *Geografiska Annaler* 69A, 375-378.

Gilbert, R. and Shaw, J. 1981. Sedimentation in proglacial Sunwapta Lake, Alberta. *Canadian Journal of Earth Sciences* 18, 81-93.

Ginot, P., Schwikowski, M., Gäggler, H.W., Schotterer, U., Kull, C., Funk, M., Rivera, A., Stampfli, F. and Stichler, W. 2002. First results of a palaeoatmospheric chemistry and climate study of Cerro Tapado Glacier, Chile. In: Casassa, G., Sepúlveda, F.V. and Sinclair, R.M. (eds.) *The Patagonian Icefields: a unique natural laboratory for environmental and climate change studies. Series of the Centro de Estudios Científicos.* Kluwer Academic. 157-168.

Glasser, N.F., Hambrey, M.J. and Aniya, M. 2002. An advance of Soler glacier, North Patagonian Icefield at *c.* AD 1222-1342. *The Holocene* 12, 113-120.

Glasser, N.F., Harrison, S., Winchester, V. and Aniya, M. In press. Late Pleistocene and Holocene palaeoclimate and glacier fluctuations in Patagonia. *Global and Planetary Change.*

Godoi, M.A., Shiraiwa, T., Kohshima, S. and Kubota, K. 2002. Firn-core drilling operation at Tyndall Glacier, Southern Patagonian Icefield. In: Casassa, G., Sepúlveda, F.V. and Sinclair, R.M. (eds.) The Patagonian Icefields: a unique natural laboratory for environmental and climate change studies. Series of the Centro de Estudios Científicos. Kluwer Academic. 149-156.

Gornitz, V. 1995. Sea level rise: a review of recent, past and near-future trends. *Earth Surface Processes and Landforms* 20, 7-20.

Greisman, P. 1979. On upwelling driven by the melt of ice shelves and tidewater glaciers. *Deep Sea Research Part A. Oceanographic Research Papers* 26, 1051-1065.

Gustavson, T.C. 1975. Bathymetry and sediment distribution in proglacial Malaspina Lake, Alaska. *Journal of Sedimentary Petrology* 45, 450-461.

Hajdas, I., Bonani, G., Moreno, P.L. and Ariztegui, D. 2003. Precise radiocarbon dating of Late-Glacial cooling in mid-latitude South America. *Quaternary Research* 59, 70-78.

Hands, K.A. 2004. Downwasting and supraglacial lake evolution on the debris-covered Ngozumpa Glacier, Khumbu Himal, Nepal. Unpublished Ph.D. thesis, University of St. Andrews.

Hanson, B. and Hooke, LeB. R. 2000. Glacier calving: a numerical model of forces in the calving speed/water-depth relation. *Journal of Glaciology* 153, 188-196.

Haresign, E. and Warren, C.R. In press. Melt rates at calving termini: a study at Glaciar León, Chilean Patagonia. *Geological Society Special Publications*.

Haresign, E., Winchester, V., Warren, C.R. and Harrison, S. Submitted. Neoglacial history of Glaciar León, Chilean Patagonia: The significance of calving dynamics. *Global and Planetary Change*.

Harris, P.W.V. 1976. The seasonal temperature-salinity structure of a glacial lake: Jökulsárlón, south-east Iceland. *Geografiska annaler* 58A, 329-336.

Harrison, S. 1992. A large calving event of Ventisquero San Rafael, southern Chile. *Journal of Glaciology* 38, 208-209.

Harrison, S. and Davenport, J. 1998. Small-scale iceberg grounding structures and associated biological diversity on boulder beaches at Laguna San Rafael, Chilean Patagonia. *Glacial Geology and Geomorphology* rp02/1998.

Harrison, S. and Winchester, V. 1998. Historical fluctuations of the Gualas and Reicher Glaciers, North Patagonian Icefield, Chile. *The Holocene* 8, 481-485.

Harrison, S. and Winchester, V. 2000. Nineteenth and twentieth century glacier fluctuations and climatic implications in the Arco and Colonia valleys, Hielo Patagónico Norte. *Arctic Antarctic and Alpine Research* 32, 55-63.

Harrison, S., Warren, C.R., Winchester, V. and Aniya, M. 2001. Onset of rapid calving and retreat of Glaciar San Quintin, Hielo Patagnico Norte, Southern Chile. *Polar Geography* 25, 54-61.

Harrison, S., Glasser, N. and Aniya, M. 2004. Morphostratigraphy of moraines in the Lago Tranquilo area, Chilean Patagonia. *Bulletin of Glaciological Research* 21, 45-48.

Hasholt, B. 2002. Measuring calving in Icefall Lake, SE Greenland, using a "Diver" pressure transducer with a built-in datalogger. *Geografisk Tidsskrift* 101, 106-109.

Heinrich, H. 1988. Origin and consequences of cyclic ice rafting in the northeast Atlantic Ocean during the past 130 000 years. *Quaternary Research* 29, 142-152.

Hennigan, T. 2004. Glacier marches on to Nature's explosive finale. *The Times* 26/2/04.

Heusser, C.J. 1993. Late-glacial of southern South America. *Quaternary Science Reviews* 12, 345-350.

Heusser, C.J. and Rabassa, J. 1987. Cold climate episode of Younger Dryas age in Tierra el Fuego. *Nature*. 328, 609-611.

Hicks, D.M., McSaveney, M.J. and Chinn, T.J.H. 1990. Sedimentation in proglacial Ivory Lake, Southern Alps, New Zealand. *Arctic and Alpine Research* 22, 26-42.

Hillaire-Marcel, C., Occhiette, s. and Vincent, J.S. 1981. Sakami Moraine, Quebec; A 500-km-long moraine without climatic control. *Geology* 9, 210-214.

Hochstein, M.P., Claridge, D., Henrys, S.A., Pyne, A., Nobes, D. and Leary S.F. 1995. Downwasting of the Tasman Glacier, South Island, New Zealand: changes in the terminus region between 1971 and 1993. *New Zealand Journal of Geology and Geophysics* 38, 1-16.

Hochstein, M.P., Watson, M.I., Malengreau, B., Nobes, D.C. and Owens, I. 1998. Rapid melting of the terminal section of the Hooker Glacier (Mt. Cook National Park, New Zealand). *New Zealand Journal of Geology and Geophysics* 41, 203-218.

Holdsworth, G. 1973. Ice calving into the proglacial Generator Lake, Baffin Island, N.W.T., Canada. *Journal of Glaciology* 12, 235-250.

Holmlund, P. and Fuenzalida, H. et al. 1995. Anomalous glacier responses to 20th century climatic changes in Darwin Cordillera, southern Chile. *Journal of Glaciology* 41, 465-473.

Horne, E.P.W. 1985. Ice-induced vertical circulation in an Arctic fjord. *Journal of Geophysical Research* 90, 1078-1086.

Home, A.J. and Goldman, C.R. 1994. *Limnology*. McGraw-Hill International Editions. p. 48-69.

Hooke, R. LeB., Laumann, T. and Kennett, M.I. 1989. Austdalsbreen, Norway: expected reaction to a 40 m increase in water level in the lake into which the glacier calves. *Cold Regions Science and Technology* 17, 113-126.

Howarth, P.J. and Price, R.J. 1969. The proglacial lakes of Breiðamerkurjökull and Fjallsjökull, Iceland. *Geographical Journal* 135, 573-581.

Hughes, T.J. 1987. Ice dynamics and deglaciation models when ice sheets collapsed. In: Ruddiman, W.F. and Wright, H.E. (eds.) *North America and Adjacent Oceans*

during the Last Deglaciation. Geological Society of America, *The Geology of North America*, Vol. K-3, 183-220.

Hughes, T. 1992. Theoretical calving rates from glaciers along ice walls grounded in water of variable depths. *Journal of Glaciology* 38, 282-293.

Hughes, T. 2002. Calving Bays. *Quaternary Science Reviews*. 21, 267-282.

Hughes, T. and Nakagawa, M. 1989. Bending shear: the rate-controlling mechanism for calving ice walls. *Journal of Glaciology* 35, 260-66.

Hulton, N.R.J. and Sugden D.E. 1997. Dynamics of mountain ice caps during glacier cycles: the case of Patagonia. *Annals of Glaciology* 24, 81-89.

Hulton, N.R.J., Sugden, D.E., Payne, A.J. and Clapperton, C.M. 1994. Glacier modelling and the climate of Patagonia during the last glacial maximum. *Quaternary Research* 42, 1-19.

Hulton, N.R.J., Purves, R.S., McCulloch, R.D., Sugden, D.E. and Bentley, M.J. 2002. The last Glacial Maximum and deglaciation in southern South America. *Quaternary Science Reviews* 21, 233-241.

Hulton, N.R.J., Purves, R.S., McCulloch, R.D., Sugden, D.E. and Bentley, M.J. 2003. Author's response to the comments by G. Wenzens. *Quaternary Science Reviews* 22, 755-757.

Hunter, L.E. and Powell, R.D. 1998. Ice foot development at temperate tidewater margins in Alaska. *Geophysical Research Letters* 25, 1923-1926.

Hunter, L.E., Powell, R.D. and Lawson, D.E. 1996a. Morainal-bank sediment budgets and their influence on the stability of tidewater termini of valley glaciers entering Glacier Bay, Alaska, USA. *Annals of Glaciology* 22, 211-216.

Hunter, L.E., Powell, R.D. and Lawson, D.E. 1996b. Flux of debris transported by ice at three Alaskan tidewater glaciers. *Journal of Glaciology* 42, 123-135.

Huppert, H.E. 1980. The physical processes involved in the melting of icebergs. *Annals of Glaciology* 1, 97-101.

Huppert, H.E. and Josberger, E.G. 1980. The melting of ice in cold stratified water. *Journal of Physical Oceanography* 10, 953-960.

Huppert, H.E. and Turner, J.S. 1980. Ice blocks melting into a salinity gradient. *Journal of Fluid Mechanics* 100, 367-384.

Hutchinson, G.E. 1975. *A Treatise on Limnology. Volume 1, Part 1 – Geography and Physics of Lakes*. John Wiley & Sons. pp. 540.

Iken, A. 1977. Movement of a large ice mass before breaking off. *Journal of Glaciology* 19, 595-605.

International Glaciological Society, 1980. Proceedings of the Conference on Use of Icebergs: scientific and practical feasibility. *Annals of Glaciology* 1, 1-133.

Inoue, J., Kondo, H., Fujiyoshi, Y., Yamada, T., Fukami, H. and Nakajima, C. 1987. Summer climate of the Northern Patagonia Icefield. *Bulletin of Glacier Research* 4, 7-14.

Ivy-Ochs, S., Schlüchter, C., Kubik, P.W. and Denton, G.H. 1999. Moraine exposure dates imply synchronous Younger Dryas glacier advances in the European Alps and in the Southern alps of New Zealand. *Geografiska Annaler* 81, 313-323.

Iizuka, Y., Kobayashi, S. and Naruse, R. 2004. Water surface waves induced by calving events at Perito Moreno Glacier, southern Patagonia. *Bulletin of Glaciological Research* 21, 91-96.

Johannesson, T. and Sigurðsson, O. 1998. Interpretation of glacier variations in Iceland 1930-1995. *Jökull* 45, 27-34.

Johnson, P.G. 1997. Spatial and temporal variability of ice-dammed lake sediments in alpine environments. *Quaternary Science Reviews* 16, 635-647.

Josberger, E.G. 1978. A laboratory and field study of iceberg deterioration. In Husseiny, A.A. (ed.) Iceberg Utilisation. *Proceedings of the first International Conference, Ames, Iowa, 1977*. New York, Pergamon Press. p. 245-264.

Josberger, E.G. 1980. The effect of bubbles released from a melting ice wall on the melt-driven convection in salt water. *Journal of Physical Oceanography* 10, 474-477.

Josberger, E.G. 1983. Sea ice melting in the marginal ice zone. *Journal of Geophysical Research* 88, 2841-2844.

Josberger, E.G. and Neshyba, S. 1980. Iceberg melt-driven convection inferred from field measurements of temperature. *Annals of glaciology* 1, 113-117.

Josberger, E.G. and Martin, S. 1981. A laboratory and theoretical study of the boundary layer adjacent to a vertical melting ice wall in salt water. *Journal of Fluid Mechanics* 111, 439-473.

Kamb, B. 1990. Rheological nonlinearity and flow instability in the deforming-bed mechanism of ice-stream motion. *Journal of Geophysical Research* 98, 837-846.

Kamb, B., Engelhardt, H., Fahnestock, M.A., Humphrey, N., Meier, M. and Stone, D. 1994. Mechanical and hydrologic basis for the rapid motion of a large tidewater glacier, 2. Interpretation. *Journal of Geophysical Research* 80, 15231-15244.

Kennett, M., Laumann, T. and Kjøllmoen, B. 1997. Predicted response of the calving glacier Svartisheibreen, Norway, and outbursts from it, to future change in climate and lake level. *Annals of Glaciology* 24, 16-20.

Keys, J.R. and Williams, K.L. 1984. Rates and mechanisms of iceberg deterioration in the D'Urville Sea, Southern Ocean. *Journal of Glaciology* 30, 218-222.

Kerr, A. and Sugden, D.E. 1994. The sensitivity of the Chilean snow-line to climate change. *Climate Change* 28, 255-272.

Kim, J. and Sunder, S.S. 1997. Statistical effects on the evolution of compliance and compressive fracture stress of ice. *Cold Regions Science and Technology* 26, 137-152.

Kim, J., Schneider, R.R., Hebbeln, D., Muller, P.J. and Wefer, G. 2002. Last deglacial sea-surface temperature evolution in the Southeast Pacific compared to changes in the South American continent. *Quaternary Science Reviews* 21, 2085-2097.

Kirkbride, M.P. 1993. The temporal significance of transitions from melting to calving termini at glaciers in the central Southern Alps of New Zealand. *The Holocene* 3, 232-240.

Kirkbride, M.P. 2002. Icelandic climate and glacier fluctuations through the termination of the 'Little Ice Age'. *Polar Geography* 26, 116-133.

Kirkbride, M.P. and Warren, C.R. 1997. Calving processes at a grounded ice cliff. *Annals of Glaciology* 24, 116-121.

Kirkbride, M.P. and Warren, C.R. 1999. Tasman Glacier, New Zealand: Twentieth-century thinning and predicted calving retreat. *Global and Planetary Change* 22, 11-28.

Kirkbride, M.P. and Dugmore, A.J. 2003. Glaciological response to distal tephra fallout from the 1947 eruption of Hekla, south Iceland. *Journal of Glaciology* 49, 420-428.

Kobayashi, S., Naruse, R., Skvarca, P. and Sato, T. 2001. Calving activities of Perito Moreno Glacier, southern Patagonia, from water level measurements. In: Aniya,

M and Naruse, R. (eds.) *Glaciological and Geomorphological Studies in Patagonia, 1998 and 1999*. 145-152.

Koizumi, K. and Naruse, R. 1992. Measurements of meteorological conditions and ablation at Tyndall Glacier, southern Patagonia, in December 1990. *Bulletin of Glacier Research* 10, 79-82.

Kondo, H. and Inoue, J. 1988. Heat balance on the icefield of the San Rafael Glacier, the Northern Patagonia Icefield. *Bulletin of Glacier Research*. 6, 1-8.

Kondo, H. and Yamada, T. 1988. Some remarks on the mass balance and the terminal – lateral fluctuations of the San Rafael Glacier, the Northern Patagonia Icefield. *Bulletin of Glacier Research* 6, 55-64.

Krimmel, R.M. 1992. Photogrammetric determination of surface altitude, velocity and calving rate of Colombia Glacier, Alaska, 1983-1991. *U.S. Geol. Survey Open File Rep*. 92-194.

Krimmel, R.M. 1997. Documentation of the retreat of Columbia Glacier, Alaska. In: Van der Veen, C.J. 1997. (ed.) *Calving Glaciers: Report of a workshop, Feb. 28 - March 2, 1997. BPRC Report No. 15. Byrd Polar Research Centre, The Ohio State University, Columbus, Ohio*. 105-108.

Krimmel R.M. and Vaughn, B.H. 1987. Columbia glacier, Alaska: changes in velocity 1977-1986. *Journal of Geophysical Research* 92, 8961-8968.

Krinner, G., Mangerud, J. Jakobsson, M. Crucifix, M., Ritz, C. and Svendsen, J. I. 2004. Enhanced ice sheet growth in Eurasia owing to adjacent ice-dammed lakes. *Nature* 427, 429-432.

Landl, B., Björnsson, H. and Kuhn, M. 2003. The energy balance of calved ice in lake Jökulsárlón, Iceland. *Arctic, Antarctic and Alpine Research* 34, 475-481.

Laumann, T. and Wold, B. 1992. Reactions of a calving glacier to large changes in water level. *Annals of Glaciology* 16, 158-162.

Leiva, J.C. 2002. The Southern Patagonian Icefield mass balance. In: Casassa, G., Sepúlveda, F.V. and Sinclair, R.M. (eds.) *The Patagonian Icefields: a unique natural laboratory for environmental and climate change studies. Series of the Centro de Estudios Científicos*. Kluwer Academic. 85-88.

Licciardi, J.M., Teller, J.T. and Clark, P.U. 1999. Freshwater routing by the Laurentide Ice Sheet during the Last Deglaciation. In: Clark, P.U., Webb, R.S. and Keigwin,

L.D. (eds.) *Mechanisms of Global Climate Change at Millennial Timescales*. American Geophysical Union. Washington, USA

Lingle, C.S., Post, A., Herzfeld, U., Molnia, B., Krimmel, R.M. and Roush, J.J. 1993. Bering Glacier surge and iceberg-calving mechanism at Vitus Lake, Alaska, U.S.A. *Journal of Glaciology* 39, 722-77.

Liverman, D.G.E. 1987. Sedimentation in ice-dammed Hazard Lake, Yukon. *Canadian Journal of Earth Sciences* 24, 1797-1806.

Lliboutry, L. 1953. More about advancing and retreating glaciers in Patagonia. *Journal of Glaciology* 2, 168-172.

Lliboutry, L. 1956. *Nieves y Glaciares de Chile: Fundamentos de Glaciología*. Universidad de Chile, Santiago, 471 pp.

Lowell, R.V., Heusser, C.J., Anderson, B.G. *et al*. 1995. Interhemispheric correlation of the late Pleistocene glacial events. *Science* 269, 1541-1549.

MacAyeal. D.R. 1992. Irregular oscillations of the West Antarctic ice sheet. *Nature* 359, 29-32.

Mangerud, J., Astakhov, V. and Jakobsson, M. 2001a. Huge Ice-Age lakes in Russia. *Journal of Quaternary Science* 16, 773-777.

Mangerud, J., Astakhov, V., Murray, A. and Svendsen, J.I. 2001b. The chronology of a large ice-dammed lake and the Barents-Kara Ice Sheet advances, Northern Russia. *Global and Planetary Change* 31, 319-334.

Mangerud, J., Jakobsson, M., Alexanderson, H., Astakhov, V., Clarke, G.K.C., Henriksen, M., Murray, A., Nikolskaya, O., Saarnisto, M. and Svendsen, J.I. 2004. Ice-dammed lakes and rerouting of the drainage of northern Eurasia during the Last Glaciation. *Quaternary Science Reviews* 23, 1313-1332.

Mann, D.H. 1986. Reliability of a fjord glacier's fluctuations for palaeoclimatic reconstructions. *Quaternary Research* 25, 10-24.

Marden, C.J., and Clapperton, C.M. 1995. Fluctuations of the South Patagonian Ice-field during the last glaciation and the Holocene. *Journal of Quaternary Science* 10, 197-210.

Markgraf, V. 1991. Younger Dryas in southern South America? *Boreas* 20, 63-69.

Markgraf, V. 1993. Younger Dryas in southernmost South America – an update. *Quaternary Science Reviews* 12, 351-355.

Markgraf, V. (ed.) 2001. *Interhemispheric climate linkages*. Academic Press, San Diego 454pp.

Markgraf, V., Webb, R.S., Anderson, K.H. and Anderson, L. 2002. Modern pollen/climate calibration for southern South America. *Palaeogeography, Palaeoclimatology and Palaeoecology* 181, 375-397.

Martin, S. and Kauffman, P. 1977. An experimental and theoretical study of the turbulent and laminar convection generated under a horizontal ice sheet floating on warm, salty water. *Journal of Physical Oceanography* 7, 272-283.

Martin, S., Josberger, E.G. and Kauffman, P. 1978. Wave-induced heat transfer to an iceberg. . In Husseiny, A.A. (ed.) Iceberg Utilisation. Proceedings of the first International Conference, Ames, Iowa, 1977. New York, Pergamon Press, 260-263.

Matsuoka, K., Nishida, K. and Takeuchi, Y. 1995. Sinking of stones on glacier surface during the melting season. *Bulletin of Glacier Research* 13, 63-68.

Matthews, J.B and Quinlan, A.V. 1975. Seasonal characteristics of water masses in Muir Inlet, a fjord with tidewater glaciers. *Journal of Fish. Res. Board, Can.* 32, 1693-1703.

Mayo, L.R. 1988. Advance of Hubbard Glacier and closure of Russell Fjord, Alaska: environmental effects and hazards in the Yakutat area. *United States Geological Survey Circular* 1016.

McCulloch, R.D. and Bentley, M.J. 1988. Late glacial ice advances in the Strait of Magellan, southern Chile. *Quaternary Science Reviews* 17, 775-787.

McCulloch, R.D., Bentley, M.J., Purves, R.S., Sugden, D.E. and Clapperton, C.M. 2000. Climatic inferences from glacial and palaeoecological evidence at the last glacial termination, southern South America. *Journal of Quaternary Science* 15, 409-417.

McManus, J. & Duck, R.W. 1988. Localised enhanced sedimentation from icebergs in a proglacial lake in Briksdal, Norway. *Geografiska Annaler* 70A, 215-223.

Meier, M.F. 1989. Relation between water input, basal water pressure and sliding of Colombia Glacier, Alaska. *Journal of Glaciology* 23, 408.

Meier, M.F. 1994. Colombia Glacier during rapid retreat: interaction between glacier flow and iceberg calving dynamics. In: Reeh, N. (ed.) The Calving Rate of the West

Greenland Glaciers in Response to Climate Change. Workshop Rep., Copenhagen, 13-15 Sep. 1993. Danish Polar Center, Copenhagen, pp. 63-83.

Meier, M.F. 1997. The iceberg discharge process: observations and inferences drawn from the study of Columbia Glacier. In: Van der Veen, C.J. (ed.) *Calving Glaciers: Report of a Workshop, February 28-March 2, 1997*. BPRC Report No. 15, Byrd Polar Research Centre, The Ohio State University, Columbus, Ohio, 109-114.

Meier, M.F., Rasmussen, L.A. and Miller, D.S. 1985. Colombia Glacier in 1984: disintegration underway. *United States Geological Survey Open File Report* 85(81).

Meier, M.F. and Post, A. 1987. Fast Tidewater Glaciers. *Journal of Geophysical Research* 92(B9), 9051-9058.

Meier, M.F., Rasmussen, L.A., Post, A., Brown, C.S., Sikonia, W.G., Bindschadler, R.A., Mayo, L.R. and Trabant, D.C. 1980. Predicted timing of the disintegration of the lower reach of Colombia, Alaska. *United States Geological Survey, Open File* 80-582.

Meier, M.F., Lundsrom, Stone, D., Kamb, B., Engelhardt, H., Humphrey, N., Dunlap, W., Fahnestock, M., Krimmel, R. and Walters, R. 1994. Mechanical and hydrologic basis for the rapid motion of a large tidewater glacier. *Journal of Geophysical Research* (B8), 15244-15321.

Menzies, J. (ed.) 1995. *Modern Glacial Environments: Processes, dynamics and sediments*. Butterworth-Heinemann, Oxford. 621 pp.

Mercer, J.H. 1961. The response of fjord glaciers to changes in the firn limit. *Journal of Glaciology* 3, 850-858.

Mercer, J.H. 1964. Advance of a Patagonian glacier. *Journal of Glaciology* 5, 267-268.

Mercer, J.H. 1968. Variations of some Patagonian glaciers since the Late-Glacial. *American Journal of Science* 266, 91-109.

Mercer, J.H. 1970. Variations of some Patagonian glaciers since the Late-Glacial: II. *American Journal of Science* 269, 1-25.

Mercer, J.H. 1976. Glacial history of southernmost South America. *Quaternary Research* 6, 125-166.

Michel, R. and Rignot, E. 1999. Flow of Moreno Glacier, Argentina, from repeat-pass Shuttle Imaging Radar C images. *Journal of Glaciology* 45, 93-100.

Miller, A. 1976. The climate of Chile. In: Schwerdtfeger, W. (ed.) *World Survey in Climatology* 12, 113-145.

Moreno, P.I. 2002. Western Patagonia: A key area for understanding Quaternary palaeoclimate at southern mid-latitudes. In: Casassa, G., Sepúlveda, F.V. and Sinclair, R.M. (eds.) *The Patagonian Icefields: a unique natural laboratory for environmental and climate change studies. Series of the Centro de Estudios Científicos.* Kluwer Academic. 43-54.

Motyka, R.J. 1997. Taku Glacier, Alaska: advance and growth of a tidewater glacier. In: Van der Veen, C.J. (ed.) *Calving Glaciers: Report of a Workshop, February 28-March 2, 1997.* BPRC Report No. 15, Byrd Polar Research Centre, The Ohio State University, Columbus, Ohio, 119-120.

Motyka R.J. and Beget J.E. 1996. Taku Glacier, southeast Alaska, USA: late Holocene history of a tidewater glacier. *Arctic and Alpine Research* 28, 42-51.

Motyka, R.J., Hunter, L., Echelmeyer, K. and Connor, C. 2003a. Submarine melting at the terminus of a temperate tidewater glacier, LeConte Glacier, Alaska. *Annals of Glaciology* 36, 57-65.

Motyka, R.J., O'Neel, S., Connor, C.L. and Echelmeyer, K.A. 2003b. Twentieth century thinning of Mendenhall Glacier, Alaska, and its relationship to climate, lake calving and glacier runoff. *Global and Planetary Change* 35, 93-112.

Naruse, T., Skvarca, P., Satow, K., Takeuchi, Y. and Nishida, K. 1995a. Thickness changes and short-term flow variation of Moreno Glacier, Patagonia. *Bulletin of Glacier Research* 13, 21-28.

Naruse, R., Aniya, M., Skvarca, P. and Casassa, G. 1995b. Recent variations of calving glaciers in Patagonia, South America, revealed by ground surveys, satellite-data analyses and numerical experiments. *Annals of Glaciology* 21, 297-303.

Naruse, R., Skvarca, P. and Takeuchi, Y. 1997. Thinning and retreat of Glaciar Upsala, and an estimate of annual ablation changes in southern Patagonia. *Annals of Glaciology* 24, 38-42.

Naruse, R., Skvarca, P. and Kobayashi, S. 2001. Measurements of surface height and velocity at the calving terminus of Perito Moreno Glacier, southern Patagonia, in December 1999. In Aniya, M. and Naruse R. (eds.) *Glaciological and geomorphological studies in Patagonia, 1998 and 1999.* 141-144.

Neshyba, S. 1977. Upwelling by icebergs. *Nature* 267, 507-508.

Neshyba, S. and Josberger, E.G. 1980. On the estimation of Antarctic iceberg melt rate. *Journal of Physical Oceanography* 10, 1681-1685.

Nicholls, R.L. and Miller, M.M. 1951. Glacial geology of Ameghino valley, Lago Argentino, Patagonia. *Geographical Review* 41, 274-294.

Nishida, K., Satow, K, Aniya, M. Casassa, G. and Kadota, T. 1995. Thickness change and flow of Tyndall Glacier, Patagonia. *Bulletin of Glacier Research* 13, 29-34.

Oerlemans, J. 1993. Possible changes in the mass balance of the Greenland and Antarctic ice sheets and their effects on sea level. In: Warrick, R.A. (ed.) *Climate and sea level change*. Cambridge University Press. p. 144-161.

Oerlemans, J. and Fortuin, J.P.F. 1992. Sensitivity of glaciers and small ice caps to greenhouse warming. *Science* 258, 115-117.

Ohata, T., Kobayashi, S., Enomoto, H., Kondo, H., Saito, T. and Nakajima, C. 1985. The east-west contrast in meteorological conditions and its effect on glacier ablation. *Glaciological studies in Patagonia, Northern Icefield, 1983-1984.* Data Center for Glacier Research. JSSI 52-56.

O'Neel, S., Echelmeyer, K.A. and Motyka, R.J. 2001. Short-term flow dynamics of a retreating tidewater glacier: LeConte Glacier, Alaska, U.S.A. *Journal of Glaciology.* 47, 567-578.

Pálsson, F. and Björnsson, H. 1999. Icemass: Mass balance and meteorological observations on Vatnajökull 1999 (field report), RH-24-99

Paterson, W.S.B. 1994. *The Physics of Glaciers (3rd Edition).* Reed. Oxford, UK. pp480.

Pelto, M.S. and Warren, C.R. 1991. Relationship between tidewater glacier calving velocity and water depth at the calving front. *Annals of Glaciology* 15, 115-117.

Peña, H. and Escobar, F. 1987. Aspects of glacial hydrology in Patagonia. *Bulletin of Glacier Research* 4, 141-150.

Peña,H. and Gutierrez, R. 1992. Statistical analysis of precipitation and air temperature in the Southern Patagonian Icefield. In: Naruse, R. and Aniya, M. (eds.) *Glaciological Researches in Patagonia, 1990. Japanese Society of Snow and Ice*, 95-108.

Pendell, E., Markgraf, V., White, J.W.C., Dreier, M. and Kenny, R. 2001. Multiproxy Record of Late Pleistocene-Holocene Climate and Vegetation Changes from a Peat Bog in Patagonia. *Quaternary Research*. 55, 168-178.

Pfeffer, W.T., Cohn, J., Meier, M. and Krimmel, R.M. 2000. Alaskan Glacier Beats a Dramatic Retreat. *EOS, Transactions, American Geophysical Union* 577.

Philander, S.G.H. 1990. *El Niño, La Niña and the Southern Oscillation*. London, Academic, 293 pp.

Pickrill, R.A. and Irwin, J. 1993. Sedimentation in a deep glacier-fed lake – Lake Tekapo, New Zealand. *Sedimentology* 30, 63-75.

Pohjola, V. 2002. On the potential to retrieve climatic and environmental information from ice-core sites suffering periodical melt, with specific assessment of the Southern Patagonia Icefield. In: Casassa, G., Sepúlveda, F.V. and Sinclair, R.M. (eds.) *The Patagonian Icefields: a unique natural laboratory for environmental and climate change studies. Series of the Centro de Estudios Científicos*. Kluwer Academic. 125-138.

Pollard, D. 1984. Some Ice Age aspects of a calving ice sheet, model. In: Berger, A., Imbrie, J., Hays, J., Kukla, G. and Saltzman, N. (eds.) *Milankovitch and Climate, Part 2* (NATO ASI, Series C, Volume 126), Dordrecht: D. Reidel, 541-564.

Porter, S.C. 2000. Onset of Neoglaciation in the Southern Hemisphere. *Journal of Quaternary Science* 15, 395-408.

Post, A. 1975. Preliminary hydrography and historical terminal changes of Columbia Glacier, Alaska. *U.S. Geological Survey Hydr. Inv. Atlas,* HA-559.

Post. A. and Motyka, R.J. 1995. Taku and LeConte Glaciers, Alaska: calving speed control of late Holocene asynchronous advances and retreats. In: Nelson, F.E. (ed.) *Glaciers and Late Quaternary Environments of Alaska: I, Essays in Honour of William . Field. Physical Geography* 16, 59-82.

Powell, R.D. 1981. A model for sedimentation by tidewater glaciers. *Annals of Glaciology* 2, 129-134.

Powell, R.D. 1983. Glacial marine sedimentation processes and lithofacies of temperate tidewater glaciers, Glacier bay, Alaska. In: Molnia, B.F. (ed.) *Glacial-Marine Sedimentation*. Plenum Press, New York, 195-232.

Powell, R.D. 1990. Glacimarine processes at grounding-line fans and their growth to ice-contact deltas. In: Dowdeswell, J.A. and Scourse, J.D. (eds.) *Glacimarine Environments: Processes and Sediments*. Geological Society Special Publication 53, 53-73.

Powell, R.D. 1991. Grounding-line systems as second-order controls on fluctuations of tidewater termini of temperate glaciers. In: Anderson. J.B. and Ashley. G.M. (eds) *Glacial Marine Sedimentation: Palaeoclimatic Significance. Geological Society of America Special Paper* 261, 75-93.

Powell, R.D. and Domack, E. 1995. Modern Glaciomarine Environments. *In:* Menzies, J. (ed.), *Modern Glacial Environments - Processes, Dynamics and Sediments.* Butterworth-Heinemann, Oxford. pp. 445-459.

Powell, R.D. and Molnia, B.F. 1989. Glacimarine sedimentary processes, facies and morphology of the south-southeast Alaska Shelf and fjords. *Marine Geology* 85, 359-390.

Prinsenberg, S.J., Peterson, I.K. and Fowler, G.A. 1991. Estimates of ice-edge melt rates off Labrador and eastern Newfoundland, Canada. *Annals of Glaciology* 15, 163-170.

Pritchard, H., Murray, T., Strozzi, T., Barr, S. and Luckman, A. 2003. Surge-related topographic change of the glacier Sortebrae, East Greenland, derived from synthetic aperture radar interferometry. *Journal of Glaciology* 49, 381-390.

Provincial Airlines Ltd. Available at: http://www.provair.com/IcebergNet/index.html (22/06/04).

Purdie, J. and Fitzharris, B. 1999. Processes and rates of ice loss at the terminus of Tasman Glacier, New Zealand. *Global and Planetary Change* 22, 79-91.

Purves, R.S. and Hulton, N.R.J. 2000. Experiments in linking regional climate, ice-sheet models and topography. *Journal of Quaternary Science* 15, 369-375.

Qamar, A. 1988. Calving icebergs: a source of low-frequency seismic signals from Columbia Glacier, Alaska. *Journal of Geophysical Research* 93, 6615-6623.

Rabassa, J. and Clapperton, C.M. 1990. Quaternary glaciations of the southern Andes. *Quaternary Science Review*. 9, 153-174.

Rabus, B.T. and Lang, O. 2002. On the representation of ice-shelf grounding zones in SAR interferograms. *Journal of Glaciology* 48, 345-356.

Reeh, N. 1968. On the calving of ice from floating glaciers and ice shelves. *Journal of Glaciology* 7, 215-232.

Reeh, N. 1985. Long calving waves. *Proc. Int. Conf. Port and Ocean Eng. under Arctic Conditions, 8th (Narssarssuaq, Greenland, 7-14, September, 1985).* pp. 1310-1327.

Reeh, N. (ed.) 1994. Workshop on the calving rate of West Greenland glaciers in response to climate change, Sept. 13-15, 1993. Copenhagen, Denmark. Danish Polar Center.

Reeh, N., Christensen, E.L., Mayer, C. and Olesen, O.B. in press. Tidal bending of glaciers: a linear visco-elastic approach. *Annals of Glaciology*.

Reid, J.R. and Callender, E. 1965. Origin of debris-covered icebergs and mode of flow of ice into 'Miller Lake', Martin River Glacier, Alaska. *Journal of Glaciology* 5, 497-503.

Reynolds, J.M. 2000. On the formation of supraglacial lakes on debris-covered glaciers. *Debris-Covered Glaciers (Proceedings of a workshop held at Seattle, Washington, USA, September 2000). IAHS Publ.* 264, 153-164.

Richardson, S.D. and Reynolds, J.M. 2000. Degradation of ice-cored moraine dams: implications for hazard development. *Debris-Covered Glaciers (Proceedings of a workshop held at Seattle, Washington, USA, September 2000). IAHS Publ.* 264, 187-198.

Rignot, E. 1998. Hinge-line migration of Petermann Gletscher, north Greenland, detected using satellite-radar interferometry. *Journal of Glaciology* 44, 469-476.

Rignot, E., Forster, R.R. and Isacks, B.L. 1996a. Interferometric radar observations of Glaciar San Rafael, Chile. *Journal of Glaciology* 42, 279-291.

Rignot, E., Forster, R.R. and Isacks, B.L. 1996b. Mapping of glacial motion and surface topography of Hielo Patagónico Norte, Chile, using satellite SAR L-band interferometry data. *Annals of Glaciology* 23, 209-216.

Rignot, E., Padman, L., MacAyeal, D.R. and Schmeltz, M. 2000. Observation of ocean tides below the Filchner and Ronne Ice Shelves, Antarctica, using synthetic aperture radar interferometry: Comparison with tide model predictions. *Journal of Geophysical Research C: Oceans* 105, 19615-19630.

Rignot, E.J., Rivera, A. and Casassa, G. 2003. Contribution of the Patagonian Icefields of South America to sea level rise. *Science* 302, 434.

Rivera, A. and Casassa, G. 1999. Volume changes on Pio XI glacier, Patagonia: 1975-1995. *Global and Planetary Change* 22, 233-244.

Rivera, A., Lange, H., Aravena, J.C. and Casassa, G. 1997a. The 20th-century advance of Glaciar Pio XI, Chilean Patagonia. *Annals of Glaciology* 24, 66-71.

Rivera, A., Aravena, J.C. and Casassa, G. 1997b. Recent fluctuations of Glaciar Pio XI, Patagonia: discussion of a glacial surge hypothesis. *Mountain Research and Development* 17, 309-322.

Rivera, A., Acuña, C., Casassa, G., and Brown, F. in press. Use of remote sensing and field data to estimate the contribution of Chilean glaciers to eustatic sea level rise. *Annals of Glaciology* 34.

Robe, R.Q. 1978. Upwelling by icebergs. *Nature* 271, 687.

Roehl, K. 2003. Thermal regime of an ice-contact lake and its implication for glacier retreat. Ice in the Environment: Proceedings of the 16th IAHR International Symposium on Ice, Dunedin, New Zealand, 2-6th December 2002, 304-312.

Roehl, K. submitted. Thermal notch development at a freshwater-calving glacier.

Rose, J., Whiteman, C.A., Lee, J., Branch, N.P., Harkness, D.D. and Walden, J. 1997. Mid- and late-Holocene vegetation, surface weathering and glaciation, Fjallsjökull, southeast Iceland. *The Holocene* 7, 457-471.

Rosenblüth, B., Casassa, G. and Fuenzalida, H. 1995. Recent climate changes in western Patagonia. *Bulletin of Glacier Research* 13, 127-132.

Rosenblüth, B., Fuenzalida, H. and Aceituno, R. 1997. Recent temperature variations in southern South America. *International Journal of Climatology* 17, 67-85.

Rott, H., Stuefer, M. and Siegel, A. 1998. Mass fluxes and dynamics of Moreno Glacier, Southern Patagonian Icefield. *Geophysical Research Letters* 25, 1407-1410.

Russell-Head, D.S. 1980. The melting of free-drifting icebergs. *Annals of Glaciology* 1, 119-122.

Sakai, A., Chikita, K. and Yamada, T. 2000a. Expansion of a moraine-dammed glacier lake, Tsho Rolpa, in Rolwaling Himal, Nepal Himalaya. *Limnology and Oceanography* 45, 1401-1408.

Sakai, A., Takeuchi, N., Fujita, K. and Nakawo, M. 2000b. Role of supraglacial ponds in the ablation process of a debris-covered glacier in the Nepal Himalaya. *Debris*

Covered Glaciers (Proceedings of a workshop held at Seattle, Washington, USA, September 2000). IAHS Publication 265.

Sakai, A., Yamada, T. and Chikita, K. 2001. Thermal regime of a moraine-dammed glacial lake, Tsho Rolpa, in Rolwaling Himal, Nepal Himalaya. *Bulletin of Glaciological Research* 18, 37-44.

Sammakia, B. and Gebhart, B. 1983. Transport near a vertical ice surface melting in saline water. *International Journal of Heat and Mass Transfer* 26, 1439-1452.

Sassolas, C., Pfeffer, W.T. and Amadei, B. 1996. Stress interaction between multiple crevasses in glacier ice. *Cold Regions Science and Technology* 24, 107-116.

Satow, K. 1995. Chemical features of the precipitation in summer at Tyndall Glacier, Patagonia. *Bulletin of Glacier Research* 13, 57-62.

Savage, S.B., Crocker, G.B., Sayed, M. and Carrieres, T. 2000. Size distributions of small ice pieces calved from icebergs. *Cold Regions Science and Technology* 31, 163-172.

Shepherd, A. and Peacock, N.A. 2003. Ice shelf tidal motion derived from ERS altimetry. *Journal of Geophysical Research C: Oceans* 108, 29-1 - 29-9.

Shipton, E. 1959. Explorations in Patagonia. *Geographical Journal* 125, 312-325.

Sigurðsson, O. In press. Variations of termini of glaciers in Iceland in recent centuries and their connection with climate. In: Caseldine, C. *et al.* (eds.) *Iceland – Modern Processes and Past Environments*.

Sigurðsson, O. 1998. Glacier variations in Iceland 1930-1995 From the database of the Iceland Glaciological Society. *Jökull* 45, 3-26.

Sikonia, W.G. 1982. Finite-element glacier dynamics model applied to Columbia Glacier, Alaska. *U.S. Geological Survey Professional Paper 1258-B*, 74pp.

Skvarca, P. and Naruse, R. 1997. Dynamic behavior of Glaciar Perito Moreno, southern Patagonia. *Annals of Glaciology* 24, 268-271.

Skvarca, P. and De Angelis, H. 2002. Fifteen years of Southern Patagonia Icefield glaciers, Argentina-Chile, detected from Landsat TM mosaics. 29th International Symposium on Remote Sensing of Environment (29 ISRSE), Buenos Aires, Argentina.

Skvarca, P., Rott, H. and Nagler, T. 1995b. Drastic retreat of Upsala Glacier, southern Patagonia, revealed by ERS-1 images and field survey. *SELPER* 11, 51-55.

Skvarca, P., Steufer, M. and Rott, H. 1999. Temporal changes of Glaciar Mayo and Laguna Escondida, southern Patagonia, detected by remote sensing data. *Global and Planetary Change* 22, 245-253.

Skvarca, P., De Angelis, H., Naruse, R., Warren, C.R. and Aniya, M. 2002. Calving rates in freshwater: new data from southern Patagonia. *Annals of Glaciology* 34, 379-384.

Skvarca, P., Raup, B. and de Angelis, H. 2003. Recent behaviour of Glaciar Upsala, a fast-flowing calving glacier in Lago Argentino, southern Patagonia. *Annals of Glaciology* 36, 184-188.

Smith, N.D. 1978. Sedimentation processes and patterns in a glacier-fed lake with a low sediment input. *Canadian Journal of Earth Sciences* 15, 741-756.

Smith, S.D. 1993. Hindcasting iceberg drift using current profiles and winds. *Cold Regions Science and Technology* 22, 33-45.

Smith, N.D. and Ashley, G. 1996. A study of brash ice in the proximal marine zone of a sub-polar tidewater glacier. *Marine Geology* 133, 75-87.

Sugden, D.E., Hulton, N.R.J. and Purves, R.S. 2002. Modelling the inception of the Patagonian ice sheet. *Quaternary International* 95-96, 55-64.

Syvitski, J.P.M. 1989. On the deposition of sediment within glacier-influenced fjords: Oceanographic controls. *Marine Geology* 85, 301-329.

Takeuchi, Y., Naruse, R. and Satwo, K. 1995a. Characteristics of heat balance and ablation on Moreno and Tyndall glaciers, Patagonia, in the summer 1993/94. *Bulletin of Glacier Research* 13, 45-56.

Takeuchi, Y., Satwo, K., Naruse, R., Ibarzabel, T., Nishida, K. and Matsuoka, K. 1995b. Meteorological features at Moreno and Tyndall glaciers, Patagonia, in the summer 1993/94. *Bulletin of Glacier Research* 13, 35-44.

Takeuchi, Y., Naruse, R. and Skvarca, P. 1996. Annual air-temperature measurement and ablation estimate at Moreno, Patagonia. *Bulletin of Glacier Research* 14, 23-28.

Tangborn, W. 1997. Using low-altitude meteorological observations to calculate the mass balance of Alaska's Columbia Glacier and relate it to calving speed. In: Van der Veen, C.J. 1997. (ed.) *Calving Glaciers: Report of a workshop, Feb. 28 - March 2, 1997. BPRC Report No. 15. Byrd Polar Research Centre, The Ohio State University, Columbus, Ohio.* 141-162.

Teller, J.T. 1987. Proglacial lakes and the southern margin of the Laurentide ice sheet. In: Ruddimand, W.F., Wright Jr., H.E. (eds.) *North America and Adjacent Oceans during the Last Deglaciation* Vol. K-3, Geological Society of America, Geology of North America, Boulder, CO, pp. 39-69.

Theakstone, W.H. 1989. Further catastrophic break-up of a calving glacier: observations at Austerdalsisen, Svartisen, Norway. *Geografiska Annaler* 71A, 245-253.

Theakstone, W.H. and Knudsen, T.N. 1986. Recent changes on a calving glacier, Austerdalsisen, Svartisen, Norway. *Geografisker Annaler* 68A, 303-16.

Thomas, R.H. 1979. The dynamics of marine ice sheets. *Journal of Glaciology* 24, 167-177.

Thorarinsson, S. 1939. The ice dammed lakes of Iceland with particular reference to their values as indicators of glacier oscillation. *Geografiska Annaler* 21, 216-242.

Trabant, D.C., Krimmel, R.M. and Post, A. 1991. A preliminary forecast of the advance of Hubbard Glacier and its influence on Russell Fjord, Alaska. *U.S. Geological Survey Water-Resource Investment Report* pp 90-4172.

Trabant, D.C., Krimmel, R.M., Echelmeyer, K.A., Zirnheld, S.L. and Elsberg, D.H. 2003. The slow advance of a calving glacier: Hubbard Glacier, Alaska, U.S.A. *Annals of Glaciology* 36, 45-50.

Tulaczyk, S., Kamb, B., Scherer, R.P., and Engelhardt, H.F. 1998. Sedimentary processes at the base of a West Antarctic ice stream: Constraints from textural and compositional properties of sub-glacial debris. *Journal of Sedimentary Research* 68, 487-496.

Turner, K. 2003. *The Late Glacial history of the central Patagonian ice-dammed lakes.* Unpublished PhD thesis, University of Edinburgh.

Van der Veen, C.J. 1996. Tidewater calving. *Journal of Glaciology* 42(141), 375-385.

Van der Veen, C.J. 1997. (ed.) Calving Glaciers: Report of a workshop, Feb. 28 - March 2, 1997. BPRC Report No. 15. Byrd Polar Research Centre, The Ohio State University, Columbus, Ohio. 194 pp.

Van der Veen, C.J. 1998a. Fracture mechanics approach to penetration of bottom crevasses on glaciers. *Cold Regions Science and Technology* 27, 213-223.

Van der Veen, C.J. 1998b. Fracture mechanics approach to penetration of surface crevasses on glaciers. *Cold Regions Science and Technology* 27, 31-47.

Van der Veen, C.J. 1999. Crevasses on Glaciers. *Polar Geography* 23, 213-245.

Van der Veen, C.J. 2001. Greenland ice sheet response to external forcing. *Journal of Geophysical Research D: Atmospheres* 106, 34047-34058.

Van der Veen, C.J. 2002a. Calving Glaciers. *Progress in Physical Geography* 26, 97-122.

Van der Veen, C.J. 2002b. Polar ice sheets and global sea level: how well can we predict the future? *Global and Planetary Change* 32, 165-194.

Vaughan, D.G. 1993. Relating the occurrence of crevasses to surface strain rates. *Journal of Glaciology* 39, 255-266.

Vaughan, D.G. and Doake, C.S.M. 1996. Recent atmospheric warming and retreat of ice shelves on the Antarctic peninsula. *Nature*, 379, 328-331.

Ventakesh, S., El-Tahan, M. and Mitten, P.T. 1985. An Arctic iceberg deterioration field study and model simulations. *Annals of Glaciology* 6, 195-199.

Venteris, E.R. 1997. Evidence for bottom crevasse formation on Colombia Glacier Alaska, USA. In: Van der Veen, C.J. (ed.) *Calving Glaciers, Report of a Workshop, February 28 – March 2, 1997.* Byrd Polar Research Center, The Ohio State University, pp. 181-185, BPRC Report No. 15.

Venteris, E.R. 1999. Rapid tidewater glacier retreat: a comparison between Colombia Glacier, Alaska and Patagonian calving glaciers. *Global and Planetary Change* 22, 131-138.

Venteris, E.R., Whillans, I.M. and Van der Veen, C.J. 1997. Effect of extension rate on terminus position, Columbia Glacier, Alaska, U.S.A. *Annals of Glaciology* 24, 49-53.

Vischer, D., Funk, M. and Müller, D. 1991. Interaction between a reservoir and a partially flooded glacier: problems during the design stage. ETH, Switzerland, unpublished report.

Vieli, A., Funk, M. and Blatter, H. 2000. Tidewater glaciers: frontal flow acceleration and basal sliding. *Annals of Glaciology* 30, 217-221.

Vieli, A., Funk, M. and Blatter, H. 2001. Flow dynamics of tidewater glaciers: a numerical modelling approach. *Journal of Glaciology* 47, 595-606.

Vieli, A., Jania, J. and Kolondra, L. 2002. The retreat of a tidewater glacier: observations and model calculations on Hansbreen, Spitsbergen. *Journal of Glaciology* 48, 592-600.

Villalba, R. 1990. Climatic fluctuations in Northern Patagonia during the last 1000 years as inferred from tree-ring records. *Quaternary Research* 34, 17-24.

Villalba R., Cook E.R., Jacoby G.C., D'Arrigo R.D., Veblen T.T. and Jones P.D. 1998. Tree-ring based reconstructions of northern Patagonia since AD 1600. *Holocene* 8, 659-674.

Wada, Y. and Aniya, M. 1995. Glacier variation in the Northern Patagonia Icefield between 1990/91 and 1993/94. *Bulletin of Glacier Research* 13, 111-119.

Walters, R. 1989. Small-amplitude, short-period variations in the speed of a tidewater glacier in South-Central Alaska, U.S.A. *Annals of Glaciology* 12, 187-191.

Walters, R.A. and Dunlap, W.W. 1987. Analysis of time series of glacier speed: Columbia Glacier, Alaska. *Journal of Geophysical Research* 92B, 8969-8975.

Walters, R.A., Josberger, E.G. & Driedger, C.L. 1988. Columbia Bay, Alaska: an 'upside down' estuary. *Estuarine Coastal Shelf Science* 26, 607-617.

Warren, C.R. 1991. Terminal environment, trough geometry, and recent fluctuations of West Greenland glaciers. *Boreas* 20, 1-15.

Warren, C.R. 1992. Iceberg calving and the glacio-climatic record. *Progress in Physical Geography* 16, 253-282.

Warren, C.R. 1993. Rapid retreat fluctuations of the calving San Rafael Glacier, Chilean Patagonia: climatic or non-climatic? *Geografiska Annaler* 75A, 111-125.

Warren, C.R. 1994. Freshwater calving and anomalous glacier oscillations: Recent behaviour of Moreno and Ameghino glaciers, Patagonia. *The Holocene* 4(4), 422-429.

Warren, C.R. 1999. Calving speed in freshwater at Glacier Ameghino, Patagonia. *Zeitschrift für Gletscherkunde und Glazialgeologie* 35, 21-34.

Warren, C.R. and Hulton, N.R.J. 1990. Topographic and glaciological controls on Holocene ice-sheet margin dynamics, central west Greenland. *Annals of Glaciology* 14, 307-310.

Warren, C.R. and Sugden, D.E. 1993. The Patagonian Icefields: A Glaciological Review. *Arctic and Alpine Research* 25, 316-330.

Warren C.R. and Rivera, A. 1994. Non-linear climatic response of calving glaciers: a case study of Pio XI glacier, Chilean Patagonia. *Revista Chilena de Historia Natural Pura y Aplicada* 67, 385-394.

Warren, C.R. and Kirkbride, M.P. 1998. Temperature and bathymetry of ice-contact lakes in Mount Cook National Park, New Zealand. *New Zealand Journal of Geology and Geophysics* 41, 133-143.

Warren C.R. and Aniya, M. 1999. The calving glaciers of southern South America. *Global and Planetary Change* 22, 59-77.

Warren, C.R. and Kirkbride, M.P. 2003. Calving speed and climatic sensitivity of New Zealand lake-calving glaciers. *Annals of Glaciology* 36, 173-178.

Warren, C.R., Glasser, N.F., Harrison, S., Winchester, V., Kerr, A.R. and Rivera A. 1995a. Characteristics of tidewater calving at Glaciar San Rafael, Chile. *Journal of Glaciology* 41(138), 273-289.

Warren, C.R., Greene, D. and Glasser, N.F. 1995b. Glaciar Upsala, Patagonia: Rapid calving retreat in fresh water. *Annals of Glaciology* 21, 311-316.

Warren, C.R., Rivera, A. and Post, A. 1997. Greatest Holocene advance of Glacier Pio XI, Chilean Patagonian: possible causes. *Annals of Glaciology* 24, 11-15.

Warren, C.R., Benn, D.I., Winchester, V. and Harrison, S. 2001. Buoyancy-driven lacustrine calving, Glaciar Nef, Chilean Patagonia. *Journal of Glaciology* 47, 135-146.

Warrick, R.A. and Oerlemans, J. 1990. Sea level rise. In: Houghton, J.T., Jenkins, G.J. and Ephraums, J.J. (eds.) *Climate Change: The IPCC Scientific Assessment* Cambridge University Press pp. 257-281.

Watanabe, T., Kameyama, S. and Sato, T. 1995. Imja Glacier dead-ice melt rates and changes in a supraglacial lake, 1989-1994. *Mountain Research and Development* 15, 293-300.

Weeks, W.F. and Cambell, W.J. 1973. Icebergs as a freshwater source: an appraisal. *Journal of Glaciology* 12, 207-232.

Wenzens, G. 1999. Fluctuations of Outlet and Valley Glaciers in the Southern Andes (Argentina) during the Past 13000 years. *Quaternary Research* 51, 238-247.

Wenzens, G. 2003. Comment on: 'The Last Glacial Maximum and deglaciation in southern South America'. (Hulton *et al*, 2002). *Quaternary Science Reviews* 22, 751-754.

Wenzens, G. 2004. Comment on: "Modelling the inception of the Patagonian icesheet". (Sugden *et al.*, 2002). *Quaternary International* 112, 105-109.

Weertman, J. 1973. Position of ice divides and ice centers on ice sheets. *Journal of Glaciology* 12, 353-360.

Weertman, J. 1980. Bottom crevasses. *Journal of Glaciology* 25, 185-188. C2?

Whillans, I.M. and Venteris, E.R. 1997. Backstress on Columbia Glacier. In Van der Veen, C.J. 1997. (ed.) *Calving Glaciers: Report of a workshop, Feb. 28 - March 2, 1997. BPRC Report No. 15. Byrd Polar Research Centre, The Ohio State University, Columbus, Ohio.* 187-194.

White, F.M., Spaulding, M.L. and Gominho, L. 1980 Theoretical estimates of the various mechanisms involved in iceberg deterioration in the open ocean environment. *US Coast Guard Report No. CD-D-62-80,* 126pp.

Willis, I.C. 1995. Intra-annual variations in glacier motion: a review. *Progress in Physical Geography* 19, 61-106.

Williams, R.S. Jr., Hal, D.K., Sigurdsson, O. and Chien, J.Y.L. 1997. Comparison of satellite-derived with ground-based measurements of the fluctuations of the margins of Vatnajokull, Iceland, 1973-92. *Annals of Glaciology* 24, 72-80.

Wilson, N.W. and Sarma, T.S. 1980. Prediction of heat, mass, and momentum transfer during laminar forced convective melting of ice in saline water. In: Pritchard, R.S. (ed.) *Sea ice processes and models, Proc. AIDJEX/Int. Comm. Snow and Ice.* Univ. Wash. Press, Seattle, Wash., pp. 339-346.

Wilson, C.J.L., Zhang, Y. and Stüwe, K. 1996. The effects of localized deformation on melting processes in ice. *Cold Regions Science and Technology* 24, 177-189.

Winchester, V. and Harrison, S. 1996. Recent oscillations of the San Quintin and San Rafael glaciers, Patagonian Chile. *Geografiska Annaler* 78, 35-49.

Winchester, V., Harrison, S., Washington, R. and Warren, C.R. 1999. Austral summer of 1998: Observations on El Niño and the North Patagonian Icefield. *Weather* 54, 287-293.

Winchester, V. and Harrison, S. 2000. Dendrochronology and lichenometry, an investigation into colonization, growth rates and dating on the east side of the North Patagonian Icefield, Chile. *Geomorphology* 34, 181-194.

Winchester, V., Harrison, S., Warren C.R. 2001. Recent retreat Glaciar Nef, Chilean Patagonia, dated by lichenometry and dendrochronology. *Arctic, Antarctic and Alpine Research* 33, 266-273.

Wright, G.F. 1892. *Man and the glacial period*. Ohio, Werner Co.

Wiseman, S. 2004. The inception and evolution of supraglacial lakes on debris-covered glaciers in the Nepal Himalaya. Unpublished Ph.D. thesis, University of Aberdeen.

Xiao, J. and Jordan, I.J. 1996. Application of damage mechanics to ice failure in compression. *Cold Regions Science and Technology*. 24, 305-322.

Yamada, T. 1987. Glaciological characteristics revealed by 37.6-m deep core drilled at the accumulation area of the San Rafael Glacier, the Northern Patagonia Icefield. *Bulletin of Glacier Research* 4, 59-68.

Yamada, T. 1998. Glacier lake and its outburst flood in the Nepal Himalaya. *Monograph* 1. Data Center for Glacier Research, Japanese Society of Snow and Ice.

Yamada, T., Kondo, H. and Fukuzawa, T. 1987. Ice core drilling operations on the Northern Patagonia Icefield. *Bulletin of Glacier Research* 4, 151-156.

2001

	Serac	11/8	11/10	11/12	11/13	11/15	11/17
northern	6			158			
	D1				403		
	D2				268		
	D3			724			
	D4			270			
	D5				266		
	D6				508		
central	B2			1037			
	B3			912			
	4			974			
	A6		973				
south	7			739			
	8			927			
	9			958			
	10				819		
	12			351			
	VN			1050			
	VS1			545			
	VS2				474		

2002

Serac	10/17	10/18	10/20	10/24	10/26	11/4	11/5	11/8	11/10	11/11
1					815					
2				872						
3					235					
4			222							
D4								506		
5			492							
D5								699		
7			460							
E1								687		
G1									221	
15			1807							
17		1590								
18		1538								
19		2462								
20		2119								
21		2042								
21a		1659								
23		2638								
A1			2219							
8			934							
D8								463		
9							646			
10			1524							
D10								1311		
11			755							
D11								958		
13					1250					
14		2037								
25				405						
26				429						
A2				208						
B1				1570						
B2				335						
E6								949		
E7								410		

Appendix A Ice velocity (m a^{-1}) for each serac used in the ice velocity surveys in 2001 and 2002 at Glaciar León (4.2.2.ii). The shading indicates the duration of each serac in the survey.

APPENDIX B Water temperature data from Lago Leones, 2001 and 2002

DATE	TRANSECT	PROFILE	LATITUDE	LONGITUDE	WATER DEPTH (m)												
			dec. degrees	dec. degrees	0	5	10	15	20	30	40	50	60	70	80	90	100
14/10/01	LP	P1	46.72428	73.10818	6.33												
		P2	46.72873	73.11975	5.88		5.65		5.47	5.35	5.2	5.05	4.71	4.58	4.46	4.45	4.43
		P3	46.73380	73.13092	6.73		5.72		5.57	5.49	5.23	4.89	4.68	4.56	4.47	4.44	4.43
		P4	46.73893	73.14147	7.13		8.78		5.44	5.39	5.25	4.81	4.66	4.56	4.5	4.47	4.46
		P5	46.74357	73.15292	7.29		5.63		5.53	5.19	5.02	4.99	4.75	4.56	4.52	4.48	4.43
		P6	46.74827	73.16462	6.61		5.26		5.26	5.21	5.01	4.83	4.68	4.55	4.53	4.49	4.47
		P7	46.75233	73.17523	6.96		5.08		5.06	5.05	4.79	4.67	4.64	4.56	4.51	4.5	4.49
		P8	46.75492	73.18825	5.86		5.02		5.02	5.02	4.93	4.69	4.63	4.51	4.48	4.45	4.44
		P9	46.75945	73.20060	5.47		5		4.99	4.99	4.99	4.96	4.62	4.52	4.48	4.46	4.44
15/10/01	T2	P1	46.77097	73.21062	6.16	5.34	5.27	5.2	5.16	5	4.95	4.9	4.94	4.92	4.77	4.71	4.67
		P2	46.76825	73.21080	7.11	5.22	5.2	5.15	5.09	4.92	4.87	4.85	4.84	4.75	4.79	4.73	4.73
		P3	46.76532	73.21097	5.85	5.13	4.99	4.96	4.94	4.92	4.92	4.87	4.84	4.7	4.67	4.62	4.58
		P4	46.76262	73.21120	5.56	5.04	4.97	4.96	4.94	4.91	4.88	4.81	4.73	4.68	4.6	4.6	4.57
		P5	46.76022	73.21093	5.95	5.25	5.05	5.03	4.97	4.87	4.81	4.73	4.69	4.67	4.63	4.61	4.57
15/10/01	T3	P1	46.76927	73.18870	7.88	5.3	5.24	5.22	5.22	5.22	5.21	5.21	5.21	5.21	5.21	5.21	5.21
		P2	46.77090	73.19233	10.04	5.33	5.17	5.17	5.17	5.18	5.17	5.17	5.17	4.66	4.55	4.47	4.43
		P3	46.77257	73.19572	10.54	5.41	5.3	5.21	5.19	5.18	5.14	5.11	5.1	4.81	4.55	4.48	4.44
		P4	46.77353	73.19960	6.6	5.47	5.37	5.34	5.33	5.16	5.08	5.07	5.04	4.99	4.82	4.57	4.51
		P5	46.77408	73.20345	7.04	5.28	5.2	5.17	5.14	5.13	5.06	5.03	4.94	4.81	4.68	4.52	4.48
19/10/01	T4	P1	46.76810	73.18742	5.79	5.52	5.76	5.45	5.5	5.32	5.31	5.25	5	4.82	4.83	4.84	4.84
		P2	46.76462	73.19110	5.66	5.66	5.63	5.57	5.64	5.55	5.48	5.01	4.88	4.79	4.63	4.58	4.43
		P3	46.76272	73.19488	5.37	5.32	5.32	5.38	5.36	5.4	5.26	5.06	4.82	4.56	4.51	4.49	4.47
		P4	46.76017	73.19637	5.61	5.88	5.53	5.52	5.54	5.4	5.22	5.03	4.8	4.64	4.5	4.52	4.46
		P5	46.75817	73.19967	5.6	5.58	5.53	5.52	5.47	5.44	5.42	5.34	4.73	4.62	4.54	4.54	4.51
		P6	46.75658	73.20210	5.62	5.58	5.55	5.53	5.47	5.44	5.41	4.7	4.66	4.62	4.57	4.53	4.58
20/10/01	T5P1	P1	46.76403	73.18568	5.03	5.01	5	5.01	5.01	4.77	4.67	4.58	4.57	4.52	4.51	4.49	4.49
		P2	46.75963	73.18405	5.26	5.21	5.19	5.2	5.21	5.1	4.98	4.61	4.6	4.56	4.56	4.52	4.5
		P3	46.75490	73.18318	5.45	5.4	5.42	5.42	5.41	5.34	5.12	4.84	4.64	4.61	4.55	4.51	4.48
		P4	46.75080	73.17955	5.55	5.52	5.51	5.51	5.5	5.5	5.5	5.46	5.3	4.9	4.71	4.61	4.55
21/10/01	T6	P1	46.75630	73.19973	5.77	5.62	5.54	5.49	5.43	5.03	4.75	4.69	4.62	4.56	4.54	4.51	4.5
		P2	46.75568	73.19293	5.76	5.49	5.47	5.4	5.26	5.21	5.07	4.8	4.66	4.65	4.57	4.55	4.5
		P3	46.75570	73.18620	5.64	5.48	5.42	5.4	5.4	5.37	5.09	5.03	4.79	4.55	4.51	4.48	4.46
		P4	46.75603	73.17952	5.64	5.56	5.55	5.54	5.53	5.42	5.12	4.94	4.65	4.56	4.5	4.47	4.47
		P6	46.75612	73.16657	5.64	5.59	5.56	5.56	5.56	5.53	5.44	5	4.85	4.71	4.49	4.476	4.46

21/10/01	T7	P1	46.75267	73.17120	5.69	5.67	5.64	5.56	5.52	5.36	5.21	4.95	4.77	4.62	4.56	4.5	4.46
		P2	46.74913	73.17542	5.64	5.6	5.52	5.47	5.44	5.39	5.25	4.66	4.62	4.56	4.52	4.51	4.5
07/11/01	T2(2)	1	46.77145	73.21112	6.3	6.21	6.11	6.11	6.16	6.12	6.08	6.08					
		2	46.76867	73.21152	6.31	6.04	6	5.93	5.92	5.91	5.89	5.67	5.64	5.62	5.29	4.75	4.67
		3	46.76585	73.21127	6.1	5.88	5.87	5.85	5.82	5.74	5.67	5.52	5.38	5.17	5.05	4.93	4.81
		4	46.76310	73.21120	6.03	5.85	5.83	5.83	5.61	5.46	5.41	5.3	5.27	5.25	5.29	5.27	5.13
		5	46.76038	73.21143	6.22	6.08	6.03	5.93	5.67	5.49	5.49	5.48	5.42	5.39	5.36	5.14	4.93
06/11/01	T3(2)	1	46.76927	73.18885	6.18	5.98	5.75	5.53	5.68								
		2	46.77028	73.19253	6.8	6.5	6.37	5.86	5.73	5.01	4.94	4.95	4.9	4.76	4.63	4.6	4.59
		3	46.77065	73.19662	6.94	6.6	5.93	5.67	5.31	4.94	4.79	4.76	4.61	4.56	4.56	4.53	4.49
		4	46.77130	73.20020	6.72	6.18	5.6	5.34	5.17	4.8	4.79	4.7	4.58	4.64	4.65	4.59	4.55
		5	46.77173	73.20405	6.5	5.8	5.46	5.05	4.94	4.86	4.73	4.61	4.59	4.6	4.66	4.75	4.76
		6	46.77240	73.20790	6.55	5.37	5.12	5.02	5	4.73	4.65	4.62	4.59	4.59			
		7	46.77307	73.20953	6.64	5.15	5	4.95	4.87	4.83	4.83	4.86	4.87	4.87			
07/11/01	T3-4	1	46.76823	73.18883	6.73	6.33	6.18	6.15	6.13	6.18	5.78	5.28	5.19	5.06	5	4.78	4.78
		2	46.76638	73.19505	7.9	6.12	6.08	6.09	6.09	6.07	5.84	5.45	5.04	4.82	4.7	4.68	4.69
		3	46.76400	73.20073	6.97	6.15	5.98	5.96	5.94	5.76	5.5	5.44	5.41	4.82	4.68	4.58	4.52
		4	46.76128	73.20628	7.6	5.92	5.77	5.73	5.7	5.57	5.47	5.25	5.17	5.07	5	4.99	4.81
		5	46.75925	73.21048	7.09	5.09	5.79	5.8	5.78	5.77	5.74	5.77	5.72	5.63	5.58	5.57	5.59
12/11/01	T6(2)	1	46.75545	73.17002	6.51	6.39	6.39		6.38	6.11	5.92	5.58	5.41	5.19	4.88	4.78	4.83
		2	46.75605	73.17995	6.43	6.35	6.21		5.89	5.84	5.32	5.13	4.69	4.6	4.58	4.56	4.55
		3	46.75628	73.18982	6.47	6.36	6.3		5.81	5.42	5.08	4.76	4.68	4.62	4.57	4.55	4.51
		4	46.75627	73.19990	6.6	6.47	6.01		5.42	5.29	5.07	4.89	4.8	4.71	4.67	4.69	4.67
08/11/01	T9	1	46.75627	73.16608	7.09	6.92	6.79	6.4	6.25	5.85	5.62	5.17	4.71	4.61	4.6	4.6	4.6
		2	46.75353	73.16645	7.32	6.3	6.24	6.24	6.19	5.84	5.45	4.91	4.87	4.71	4.57	4.54	
		3	46.74920	73.16515	7.04	6.78	6.6	6.15	6.15	6.14	5.99	5.43	5	4.69	4.62	4.6	4.6
		5	46.74887	73.15953	6.48	6.44	6.43		6.42	6.42	6.35	5.7	5.22	5	4.74	4.71	4.7
		4	46.74258	73.15827	6.46	6.42	6.4		6.38	6.36	5.74	5.29	5.11	5.06	4.81	4.58	4.52
		3	46.73810	73.15787	6.51	6.48	6.46		6.42	6.14	5.37	5.1	4.8	4.7	4.67	4.59	4.54
		2	46.73357	73.15677	6.56	6.51	6.46		6.3	5.89	5.22	4.82	4.63	4.57	4.53	4.54	4.56
		1	46.72912	73.15545	6.65	6.59	6.53		6.32	5.22	5.19	5.29	5.34	5.34			
13/11/01	T10	1	46.73870	73.11870	6.83	6.8	6.77		6.71	6.59	6.34	5.45	5.42	5.42			
		2	46.74017	73.12528	6.78	6.75	6.74		6.64	6.5	5.28	4.83	4.62	4.52	4.52	4.52	4.51
		3	46.74172	73.13173	6.68	6.65	6.62		6.6	6.6	6.3	5.62	5.01	4.7	4.47	4.5	4.51
		4	46.74205	73.14007	6.68	6.65	6.6		6.55	5.96	5.62	5.32	5.12	4.77	4.66	4.61	4.52
		5	46.74350	73.14757	6.72	6.68	6.65		6.62	5.86	5.44	5.2	4.96	4.73	4.6	4.51	4.48
		6	46.74487	73.15482	6.65	6.6	6.6		6.54	5.82	5.67	5.26	5.01	4.72	4.65	4.51	4.59
		7	46.74603	73.16233	6.65	6.62	6.54		6.28	5.96	5.46	5.19	5.01	4.87	4.74	4.68	4.62
		8	46.74678	73.16968	6.68	6.56	6.55		6.38	5.95	5.65	5.46	5.15	5.1	4.92	4.76	4.62

09/11/01	T11	1	46.72488	73.10900	7.6	6.73	5.91	5.76	5.74	5.74	5.74					
		2	46.72925	73.11175	7.35	7.22	6.78	6.1	5.88	5.72	5.5	5.28	5.01	4.94	4.81	4.65
		3	46.73388	73.10853	7.2	6.99	6.71	6.6	6.02	5.36	5.2	4.94	4.79	4.73	4.7	4.62
09/11/01	T12	1	46.73640	73.11273	6.89	6.61	6.55	6.46	5.97	5.38	5.17	4.98	4.98	4.98		
		2	46.73540	73.11978	7.17	6.9	6.61	6.47	6.05	5.94	5.75	5	4.78	4.68	4.63	4.56
		3	46.73427	73.12628	7.11	6.63	6.55	6.42	6.31	6.01	5.41	5.07	4.85	4.66	4.56	4.53
		4	46.73322	73.13283	7.14	6.67	6.6	6.39	6.13	5.14	4.86	4.75	4.68	4.6	4.55	4.52
		5	46.73182	73.13923	7.12	6.75	6.6	6.32	5.85	5.22	4.85	4.7	4.6	4.49	4.48	4.47
		6	46.73060	73.14557	7.2	6.7	6.45	6.14	5.78	5.26	5.06	4.91	4.74	4.64	4.54	4.53
		7	46.72880	73.15243	7.28	6.7	6.65	6.43	6.03	5.73	5.45	5.33	5.27	5.27	5.27	
09/11/01	T13	1	46.73188	73.14782	7.23	6.62	6.44	6.28	5.98	5.54	5.18	4.84	4.74	4.67	4.59	4.51
		2	46.73515	73.14300	7.27	6.75	6.63	6.31	6.14	5.38	4.95	4.76	4.64	4.55	4.53	4.51
		3	46.73882	73.13918	7.5	6.72	6.55	6.42	6.25	5.83	4.98	4.7	4.55	4.53	4.5	4.48
		4	46.74258	73.13547	7.5	6.61	6.55	6.08	5.91	4.84	4.74	4.73	4.56	4.56	4.56	
09/11/01	T14	1	46.73843	73.13460	8.69	6.73	6.55	6.42	6.03	5.62	5.14	4.85	4.75	4.61	4.55	4.52
		2	46.73380	73.13513	8.08	6.63	6.53	6.4	6.16	5.35	4.87	4.75	4.67	4.52	4.5	4.45
		3	46.72918	73.13423	7.68	6.47	6.27	5.89	5.52	5.11	4.78	4.7	4.59	4.53	4.48	4.45
		4	46.72480	73.13242	7.54	6.49	6.23	5.9	5.3	5.12	5.03	4.96	4.86	4.61	4.57	4.53
		5	46.72058	73.14672	7.16	7.02	6.23	5.72	5.71	5.71	5.72	5.71				
09/11/01	T15	1	46.72427	73.12550	7.76	6.79	6.52	5.87	5.57	5.51	5.43	5.06	4.81	4.6	4.56	4.56
		2	46.72802	73.12082	7.65	6.69	6.48	6.04	5.74	5.44	5.43	5.22	4.97	4.69	4.63	4.49
		3	46.73215	73.11732	7.92	6.79	6.62	6.37	5.93	5.65	5.42	5.2	4.89	4.55	4.51	4.5
09/11/01	T16	1	46.73308	73.10363	8.1	6.97	6.77	6.32	5.97	5.74	5.39	5.29	5.29	5.18	5.16	5.08
		2	46.72960	73.09797	8.36	7.49	7.1	5.87	5.78	5.58	5.44	5.22	4.99	4.97	4.98	4.97
average at each depth					6.74	6.16	6.01	5.52	5.80	5.59	5.35	5.12	4.93	4.79	4.69	4.63	4.59
range					5.51	2.49	5.03		1.84	1.87	1.7	1.5	1.15	1.12	1.12	1.13	1.16

17/10/02	1	46.77139	73.20389	5.58	5.09	5.08	5.08	5.01	4.99	4.97	4.91	4.83	4.76	4.73	4.69
	2	46.76972	73.20361	5.4	5.1	5.09	5.08	5.07	4.96	4.92	4.88	4.81	4.74	4.71	4.69
	3	46.76694	73.20222	5.4	5.11	5.08	5.07	5.07	4.94	4.89	4.82	4.79	4.73	4.71	4.69
	4	46.76250	73.20528	5.37	5.1	5.08	5.07	5.05	4.78	4.75	4.73	4.7	4.69	4.65	4.65
	5	46.76167	73.21000	5.43	5.19	5.1	5.07	4.93	4.86	4.84	4.83	4.79	4.8	4.76	4.73
	7	46.77000	73.21222	4.95	5.01	5.01	4.94	4.87	4.84	4.84	4.82	4.78	4.78	4.78	4.78
18/10/02	1	46.76861	73.21139	5.1	5.01	4.99	4.92	4.89	4.87	4.87	4.86	4.85	4.84	4.8	4.77
	2	46.76500	73.21306	5.24	5.07	5.04	4.99	4.96	4.88	4.83	4.82	4.76	4.72	4.7	4.68
	3	46.76361	73.21500	5.5	5.06	5.03	4.97	4.89	4.86	4.8	4.8	4.8	4.8	4.8	4.8
	4	46.76278	73.21583	5.49	5.05	4.97	4.87	4.72	4.72	4.72	4.72	4.73	4.72	4.72	4.73
	5	46.76444	73.20028	5.12	5.09	5.01	4.96	4.9	4.78	4.77	4.75	4.73	4.69	4.67	4.65
	6	46.76500	73.20306	5.1	5.02	5.05	5.02	4.92	4.84	4.79	4.78	4.77	4.75	4.74	4.7
	7	46.76500	73.20639	5.05	4.99	4.97	4.94	4.91	4.86	4.82	4.81	4.79	4.71	4.67	4.65
	8	46.76500	73.21306	5.03	5.03	4.99	4.96	4.85	4.81	4.8	4.77	4.76	4.76	4.76	4.75
19/10/02	1	46.72222	73.10889	5.54	5.17	5.17	5.17	5.18							
	2	46.72722	73.11861	5.84	5.21	5.18	5.17	5.16	5.16	5.03	5.01	4.83	4.74	4.67	4.65
	3	46.73083	73.12806	5.58	5.13	5.11	5.1	5.09	5.09	5.09	5.05	4.8	4.72	4.69	4.64
	4	46.73306	73.13722	5.5	5.04	5.03	5.02	5.02	4.99	4.91	4.84	4.78	4.75	4.71	4.6
	5	46.73667	73.14667	5.49	5.09	4.98	4.96	4.93	4.74	4.69	4.67	4.64	4.63	4.63	4.62
	6	46.73944	73.15583	5.83	5.15	5.1	5.05	4.93	4.85	4.78	4.73	4.68	4.67	4.67	4.66
	7	46.74417	73.16556	6.17	5.2	5.17	5.16	5.11	4.94	4.83	4.8	4.75	4.73	4.7	4.68
	8	46.75028	73.17444	6.35	5.05	5.2	5.01	4.98	4.85	4.8	4.77	4.75	4.72	4.7	4.69
	9	46.75611	73.18417	6.45	5.05	5.01	4.98	4.96	4.77	4.72	4.68	4.67	4.64	4.62	4.61
	10	46.76028	73.19306	6.23	5.05	5.03	5.02	4.78	4.7	4.67	4.66	4.64	4.64	4.63	4.62
	11	46.76111	73.19500	6.34	5.04	5.03	5.01	4.96	4.7	4.69	4.66	4.63	4.63	4.62	4.62
	12	46.76139	73.19694	6.32	5.04	5.02	5.01	5	4.75	4.69	4.67	4.64	4.62	4.62	4.61
	13	46.76222	73.19889	6.07	5.37	5.01	5	4.96	4.73	4.7	4.67	4.67	4.67	4.65	4.63
	14	46.76278	73.20056	6.05	5.09	5.08	4.99	4.77	4.74	4.72	4.7	4.69	4.67	4.65	4.63
	15	46.76333	73.20250	6.01	5.08	5.06	4.93	4.8	4.76	4.73	4.72	4.68	4.66	4.65	4.64
	16	46.76444	73.20444	5.84	5.12	5.06	4.91	4.89	4.84	4.78	4.74	4.7	4.69	4.66	4.65
	17	46.76556	73.20639	5.73	5.14	4.99	4.99	4.93	4.85	4.78	4.74	4.72	4.69	4.67	4.65
	18	46.76722	73.20833	5.5	5.22	4.99	4.98	4.95	4.85	4.8	4.78	4.73	4.7	4.69	4.65
	19	46.76778	73.20889	5.5	5.14	4.98	4.98	4.97	4.82	4.79	4.77	4.74	4.71	4.7	4.68

24/10/02	5	46.76861	73.19778	6.1	5.33	5.04	4.97	4.94	4.94	4.96	4.96	4.94	4.92	4.87	4.82
	6	46.76861	73.19944	6.01	5.13	5.05	5	4.94	4.91	4.86	4.85	4.84	4.82	4.77	4.71
	7	46.76528	73.19944	5.4	5.14	5.01	4.09	4.83	4.8	4.78	4.76	4.74	4.71	4.68	4.62
	8	46.76639	73.20611	5.62	4.92	4.86	4.76	4.74	4.72	4.7	4.68	4.66	4.62	4.6	4.6
	9	46.75917	73.20167	6.44	4.85	4.81	4.8	4.8	4.79	4.78	4.77	4.77	4.76	4.73	4.65
	10	46.76028	73.20333	6	5.05	4.84	4.78	4.75	4.72	4.7	4.7	4.67	4.67	4.6	4.56
	11	46.76111	73.20222	6.25	4.89	4.85	4.79	4.76	4.76	4.72	4.69	4.68	4.66	4.6	4.58
	13	46.76167	73.20917	6.27	5	4.92	4.87	4.91	4.9	4.88	4.81	4.72	4.68	4.65	4.62
	14	46.76306	73.21083	6.42	5.03	4.94	4.91	4.9	4.89	4.83	4.81	4.76	4.71	4.68	4.66
25/10/02	1	46.76833	73.21167	5.98	5.57	5.37	5.28	5.17	5.1	5.07	4.99	4.99	5	5	5
	2	46.76917	73.21167	6.2	5.5	5.42	5.25	5.11	5.07	5.05	5.02	5.01	5.02	4.92	6.85
	3	46.76917	73.21194	6.32	5.4	5.38	5.15	5.1	5.05	5.03	4.95	4.93	4.73	4.74	4.74
	4	46.76694	73.21250	6.42	5.35	5.28	5.12	5.08	5.04	5.01	4.99	4.97	4.88	4.85	4.61
	5	46.76556	73.21194	6.15	5.33	5.09	4.97	4.97	4.97	4.97	4.97	4.96	4.92	4.89	4.91
25/10/02	A1	46.77139	73.19361	6.3	5.49	5.43	5.29	5.22	5.18	5.12	5.08	5.04	4.79	4.68	4.63
	A2	46.77250	73.19583	6.45	5.53	5.46	5.35	5.26	5.13	5.11	5.08	5.07	4.87	4.74	4.76
	A3	46.77389	73.19833	6.67	5.6	5.43	5.35	5.31	5.16	5.12	5.08	5.06	5.02	4.71	4.62
	A4	46.77500	73.20056	6.4	5.76	5.48	5.4	5.25	5.08	5.05	5	4.77	4.96		
25/10/02	B1	46.77333	73.20417	6.27	5.51	5.46	5.35	5.2	5.15	5.14	5.12	5.08	5.02	4.63	4.62
	B2	46.77250	73.20306	5.9	5.56	5.52	5.3	5.27	5.21	5.13	5.11	5.07	5.03	4.82	4.6
	B3	46.77194	73.20167	6.55	5.58	5.52	5.25	5.2	5.18	5.12	5.07	5.04	4.96	4.75	4.66
	B4	46.77083	73.19972	6.65	5.63	5.49	5.23	5.2	5.16	5.1	5.06	5.04	4.9	4.73	4.66
04/11/02	A1	46.76494	73.21067	6.52	5.75	5.51	5.37	5.25	5.11	5.01	5	4.96	4.91	4.89	4.88
	A2	46.76572	73.20931	7.08	5.55	5.49	5.37	5.28	5.12	4.81	4.95	4.9	4.87	4.86	4.86
	A3	46.76769	73.20822	7.01	5.64	5.53	5.52	5.26	5.18	5.12	5.05	4.93	4.87	4.84	4.86
	A4	46.76836	73.20750	7.42	5.35	5.65	5.52	5.33	5.26	5.19	5.12	4.95	4.87	4.83	4.83
	A5	46.76983	73.20611	6.75	5.93	5.87	5.61	5.51	5.33	5.23	5.04	4.95	4.86	4.81	4.82
04/11/02	B1	46.77033	73.21128	6.16	6.01	5.92	5.69	5.42	5.33	5.22	5.09	5.07	5.07	5.06	5.07
	B2	46.76894	73.21169	6.21	6.03	5.67	5.61	5.31	5.31	5.28	5.22	5.05	4.89	4.77	4.77
	B3	46.76700	73.21214	6.52	6.08	5.62	5.52	5.3	5.27	5.2	5.2	5.17	5.09	5.09	5.09
	B4	46.76522	73.21211	6.38	6.09	5.6	5.53	5.36	5.26	5.16	5.16	5.16	5.14	5.07	4.96
	B5	46.76364	73.21253	6.06	5.71	5.52	5.26	5.23	5.25	5.2	5.11	5.05	5.04	4.86	4.87
05/11/02	C1	46.76794	73.20861	6.43	6.24	5.99	5.92	5.87	5.83	5.81	5.63	5.53	5.47	5.42	5.4
	C2	46.76847	73.20933	6.15	6.02	5.82	5.72	5.68	5.64	5.57	5.41	5.31	5.23	5.19	5.07
05/11/02	D1	46.76447	73.20981	6.19	6.12	5.75	5.54	5.41	5.36	5.25	5.18	5.07	4.97	4.95	4.94
	D2	46.76483	73.21031	6.22	5.99	5.77	5.5	5.4	5.33	5.24	5.17	5.06	4.97	4.9	4.86
	D3	46.76519	73.21122	6.16	5.88	5.62	5.47	5.43	5.39	5.24	5.19	5.11	5.02	4.92	4.86
	D4	46.76525	73.21211	6.18	5.93	5.71	5.46	5.44	5.36	5.2	5.25	5.15	5.06	5.06	5.1
	D5	46.76542	73.21231	6.29	5.99	5.88	5.7	5.7	5.53	5.54	5.19	5.13	5.06	5.14	4.88

06/11/02	1	46.72572	73.11453	7.01	6.87	6.32	5.69	5.43	5.23	5.04	4.99	4.97	4.88	4.83	4.79
	2	46.73417	73.13128	7.12	7.02	6.5	5.76	5.57	5.19	4.96	4.87	4.85	4.8	4.77	4.77
	3	46.73564	73.14150	6.69		6.52	6.41	5.2	5.02	4.95	4.85	4.83	4.82	4.79	4.78
	4	46.74161	73.15189	6.84	6.74	6.68	6.49	5.78	5.56	5.51	4.87	4.82	4.78	4.75	4.73
	5	46.74758	73.16039	6.54	6.4	6.29	5.95	5.71	5.52	5.41	5.26	5.02	4.88	4.84	4.9
	6	46.75250	73.17228	6.37	6.11	5.94	5.47	5.3	5.2	5.17	5.14	5.02	4.95	4.93	4.94
	7	46.75742	73.18217	6.36	6.07	5.98	5.68	5.18	5.03	5.02	4.99	4.94	4.9	4.84	4.88
	8	46.76211	73.19158	7.06	5.89	5.72	5.54	5.15	4.98	4.88	4.85	4.83	4.83	4.81	4.79
	9	46.76325	73.19344	7.02	6.01	5.81	5.32	5.13	4.99	4.91	4.92	4.87	4.82	4.8	4.77
	10	46.76394	73.19664	6.72	6.05	5.67	5.25	5.18	5.01	4.99	4.95	4.92	4.85	4.82	4.82
	11	46.76425	73.20025	6.69	5.76	5.48	5.44	5.33	5.17	5.06	5.02	4.96	4.9	4.88	4.84
	12	46.76533	73.20344	6.69	5.87	5.59	5.5	5.46	5.42	5.14	5.12	5.01	4.96	4.87	4.88
	13	46.76558	73.20611	6.52	5.77	5.63	5.54	5.41	5.31	5.23	5.14	5.05	5.06	5.01	5.07
	14	46.76656	73.20819	6.95	5.72	5.62	5.57	5.45	5.34	5.29	5.2	5.14	5.07	5.02	5.12
08/11/02	1	46.76911	73.21167	7.7	6.97	6.57	6.1	5.65	5.25	5.05	4.97	4.97	4.89	4.82	4.82
	2	46.76706	73.21197	6.97	6.91	6.12	5.84	5.53	5.36	5.08	4.94	4.87	4.87	4.87	4.87
	3	46.76842	73.21178	7.05	6.86	6.14	5.75	5.48	5.27	5.05	4.94	4.91	4.84	4.84	4.84
	4	46.76861	73.19778	8.67	7.01	6.39	6.02	5.5	5.22	5.06	5.01	4.89	4.89	4.85	4.83
	7	46.76500	73.19944	8.41	6.82	6.29	5.85	5.52	5.34	5.18	4.96	4.91	4.84	4.82	4.76
	8	46.76639	73.19528	9.22	7.16	6.19	5.6	5.31	5.1	4.92	4.87	4.84	4.84	4.77	4.76
10/11/02	1	46.76517	73.21056	7.88	5.97	6.32	6.01	5.84	5.52	5.44	5.23	5.13	5.07	4.99	5.02
	2	46.76542	73.20914	8.15	7.44	6.37	6.02	5.85	5.49	5.37	5.06	5.04	4.91	4.9	4.87
	3	46.76750	73.20886	8.22	7.62	7.09	6.24	5.75	5.56	5.39	5.23	5	4.94	4.93	4.86
	4	46.76833	73.20731	7.96	7.41	6.67	6.11	5.67	5.61	5.35	5.2	5.05	4.95	4.87	4.86
10/11/02	1	46.77036	73.21108	7.91	7.36	7.26	6.31	5.81	5.74	5.24	5.07	5.07	4.95	4.94	4.95
	2	46.76867	73.21158	7.99	7.3	6.75	6.36	6.32	5.69	5.17	5.12	4.99	4.94	4.93	4.99
	3	46.76697	73.21211	8.29	7.36	6.74	6.23	6.01	5.53	5.2	4.98	5.04	5.05	5.05	5.09
	4	46.76494	73.21250	7.2	6.8	6.39	6.33	6.29	6.02	5.59	5.16	5.12	5.02	5.03	5.14
	5	46.76389	73.21258	8.07	7.19	6.74	6.34	5.98	5.6	5.36	5.13	5.03	4.98	4.92	4.92
11/11/02	9	46.76758	73.20906	7.63	7.51	7.38	7.1	6.97	6.76	6.01	5.65	5.32	5.13	5.04	4.96
	8	46.76583	73.20028	7.81	7.36	7.27	6.15	6.55	6.11	5.57	5.39	5.18	5.11	4.97	4.86
	7	46.76536	73.19550	7.67	7.24	7.08	6.36	6.3	5.96	5.31	5.14	4.92	4.89	4.86	4.85
	6	46.76281	73.19164	7.52	7.08	6.66	6.15	5.37	5.95	5.98	5.14	5.17	5.12	4.88	4.86
	5a	46.75975	73.18856	7.65	7.41	6.62	6.23	5.55	5.35	5.09	5.04	5.02	4.98	4.92	4.86
	4	46.75197	73.17492	8.02	7.27	6.85	6.03	5.78	5.63	5.48	5.29	5.06	4.91	4.87	4.84
	3	46.74636	73.16592	7.71	6.95	6.39	5.84	5.52	5.34	5.25	5.08	4.94	4.92	4.93	4.86
	2	46.74333	73.15778	7.61	6.43	5.99	5.81	5.38	4.93	4.88	4.85	4.81	4.78	4.77	4.74
	1	46.74036	73.14994	7.29	6.9	5.71	5.28	5.1	5.01	4.92	4.88	4.84	4.79	4.75	4.73

12/11/02	A1	46.76275	73.18408	7.06	6.83	6.26	5.64	5.54	5.36	5.26	5.13	5.01	4.94	4.9	4.86
	A2	46.76406	73.18653	6.9	6.75	6.61	5.81	5.5	5.37	5.27	6.13	4.93	4.2	4.9	4.81
	A3	46.76508	73.18867	7.5	6.63	6.59	6	5.88	5.4	5.28	5.12	4.95	4.91	4.87	4.85
	A4	46.76611	73.19094	7.46	6.72	6.48	6.27	5.63	5.35	5.25	5.09	4.96	4.91	4.86	4.85
	A5	46.76708	73.19308	7.66	6.85	6.59	6.42	5.75	5.3	5.19	5.11	5.02	4.97	4.9	4.86
12/11/02	B1	46.76117	73.18597	7.27	7	6.4	5.66	5.37	5.24	5.2	5.02	4.92	4.88	4.84	4.81
	B2	46.76189	73.18739	7.17	7	6.52	5.59	5.34	5.26	5.18	5.11	4.94	4.88	4.85	4.84
	B3	46.76225	73.18917	7.35	6.97	6.77	5.74	5.41	5.26	5.19	5.09	4.96	4.9	4.87	4.83
	B4	46.76317	73.19175	7.54	6.83	6.7	6	5.45	5.25	5.13	5.13	5.04	5	4.88	4.8
	B5	46.76356	73.19442	7.5	6.74	6.6	6.31	5.7	5.3	5.16	5.09	5.05	4.87	4.85	4.85
12/11/02	C1	46.75825	73.18794	7.57	7.29	6.3	5.54	5.41	5.26	5.14	5.02	4.91	4.9	4.85	4.8
	C2	46.75911	73.19014	7.68	7.13	6.16	5.54	5.34	5.15	5.05	5.02	4.97	5.93	4.85	4.83
	C3	46.75992	73.19231	7.49	6.93	6.7	6.68	5.74	5.41	5.29	5.1	5.04	4.97	4.86	4.86
	C4	46.76089	73.19453	7.56	7.14	6.59	5.9	5.45	5.15	5.07	5.01	4.88	4.89	4.81	4.81
	C5	46.76156	73.19708	7.27	6.74	6.72	6.52	6.02	5.6	5.33	5.07	5.06	4.96	4.92	4.92
12/11/02	D1	46.75472	73.18967	7.43	7.25	6.92	5.95	5.5	5.33	5.2	5.04	4.99	4.9	4.82	4.8
	D2	46.75506	73.19178	7.39	7.28	6.92	6.07	5.77	5.19	5.07	5	4.97	4.88	4.87	4.87
	D3	46.75556	73.19406	7.35	6.25	6.94	6.17	5.9	5.38	5.1	5.05	4.59	4.56	4.5	4.84
	D4	46.75592	73.19617	7.33	7.28	6.75	6.49	6.23	5.83	5.76	5.17	5.07	4.98	4.87	4.85
	D5	46.75664	73.19844	7.28	7.21	7.19	6.94	6.25	5.78	5.45	5.48	5.27	5.2	5.12	5
average at each depth				6.64	6.01	5.79	5.52	5.34	5.19	5.08	5.00	4.92	4.87	4.82	4.81
range				3.64	2.77	2.57	3.01	2.25	2.06	1.34	1.47	0.94	1.73	0.82	0.84

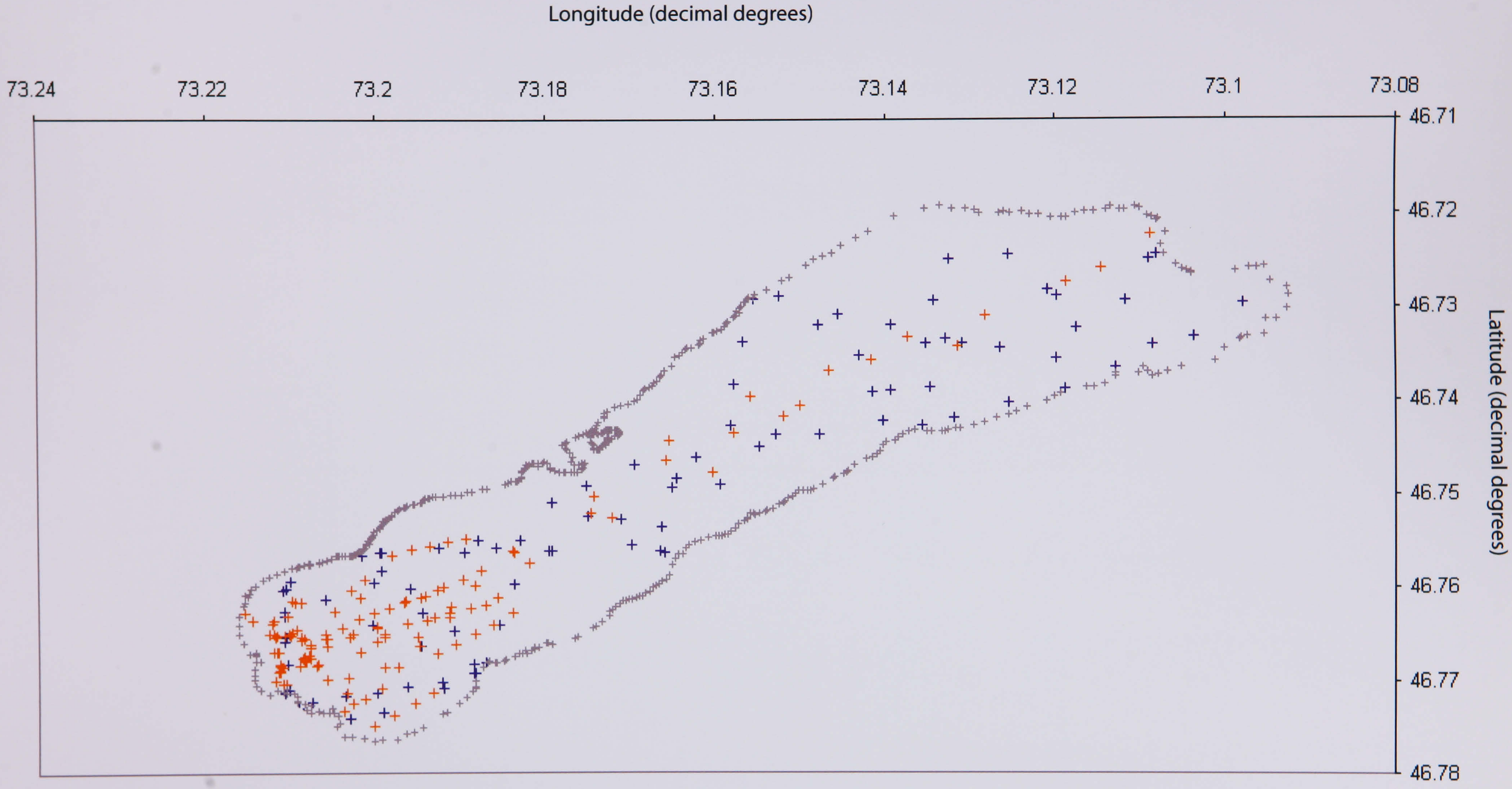

Appendix B (map) Map of Lago Leones to show the locations of temperature profiles (2001 - blue; 2002 - orange). (Not to scale).

Date Aug-03	Time (hh:mm)	Event size (cm)	Av. size/ day (cm)	Time between events (hrs)	Rain mm/hr	General lake trend	Trend immed. before	Water level post event
7th	12:10	10.3			0.5	falling	falling	higher
	17:57	13.1		5	0.5	rising	falling	lower
	19:11	4.6		1	0.5	rising	falling	higher
	19:19	18.2		0	0.5	falling	falling	lower
	19:37	8.3	10.9	0	0.5	falling	falling	lower
8th	02:25	8.1		7	0.5	falling	falling	lower
	11:32	6		8	0	rising	falling	higher
	19:41	9.8	8.0	8	1.9	falling	falling	lower
9th	14:58	10.5		9	1	falling	falling	lower
	16:02	30.4		1	1	falling	falling	higher
	16:05	26.3		0	1	falling	rising	higher
	17:01	6		1	1	rising	rising	same
	23:51	5.9	15.8	7	1	falling	falling	higher
10th	11:24	24.3		12	0	falling	falling	lower
	22:49	4.1	14.2	11	0.9	falling	falling	lower
11th	03:38	5.8		5	0.9	level	falling	lower
	09:26	5		6	0	falling	falling	higher
	11:22	33.5		1	1.8	falling	falling	higher
	11:32	5.9		0	1.8	level	falling	higher
	14:54	18.3		3	1.8	falling	falling	higher
	15:46	29.2	16.3	0	1.8	rising	falling	higher
12th	09:11	20.9		18	1.4	falling	falling	lower
	10:31	36.2		1	1.4	falling	falling	lower
	15:02	22.3		5	0	rising	falling	higher
	15:10	12.1		0	0	rising	falling	higher
	17:44	12.3		2	0	falling	falling	higher
	21:40	12.1		4	0	rising	rising	higher
	21:50	5.76		0	0	rising	rising	same
	23:04	15.9	17.2	2	0	falling	falling	lower
13th	08:10	11.9		9	0	rising	rising	higher
	08:15	13.5		0	0	falling	falling	lower
	08:25	40.8		0	0	falling	falling	higher
	08:47	28.1		0	0	rising	falling	higher
	09:09	8.2		0	0	rising	falling	higher
	09:17	37.4		0	0	rising	falling	higher
	09:49	18.24		0	0	falling	falling	lower
	12:07	12.6		3	0	rising	falling	higher
	12:15	17.1		0	0	falling	falling	higher
	17:34	10.4		5	0	falling	falling	lower
	17:38	11.6		0	0	rising	falling	higher
	17:59	25.4		0	0	rising	falling	higher
	18:12	42.9	21.4	0	0	falling	falling	lower
14th	05:38	8.6		11	0	rising	falling	higher
	06:52	6.1		1	0	falling	falling	higher
	07:04	84.8		0	0	rising	falling	higher
	07:21	7.4		0	0	falling	falling	lower
	07:25	7.3		0	0	falling	falling	lower
	09:16	11.7		0	0	rising	falling	lower
	09:32	10.8		0	0	falling	falling	higher
	09:50	19.3		0	0	rising	falling	higher
	17:57	16.2		9	0	falling	falling	higher
	19:35	21.6		1	0	falling	falling	lower
	21:12	6.7		1	2.1	falling	falling	lower
	21:42	23.6		0	2.1	rising	rising	higher
	21:58	4.7		0	2.1	rising	falling	same
	22:05	6.9		0	2.1	falling	falling	higher
	22:53	5.1	16.1	0	2.1	rising	falling	higher
15th	02:31	7.2		4	2.1	rising	falling	same
	05:13	16.8		3	0	falling	falling	higher
	05:28	8.9		0	0	falling	falling	higher
	06:34	4.2		1	0	falling	falling	higher
	13:26	20	11.4	7	0	falling	falling	higher
16th	00:39	19.6		12	0	rising	rising	higher
	05:53	8.8	14.2	6	0	falling	falling	higher

Av. interval 3.0h

Av. event size (cm)	16.0
Median size (cm)	12
Modal size (cm)	6

60% events during falling stage
90% events experienced a fall in stage immediately before an event
60% events were followed by a higher stage

Gemini Data Sheet

Tinytag Aquatic
TG-3100

Issue 10: 31st Sept 2003
E&OE

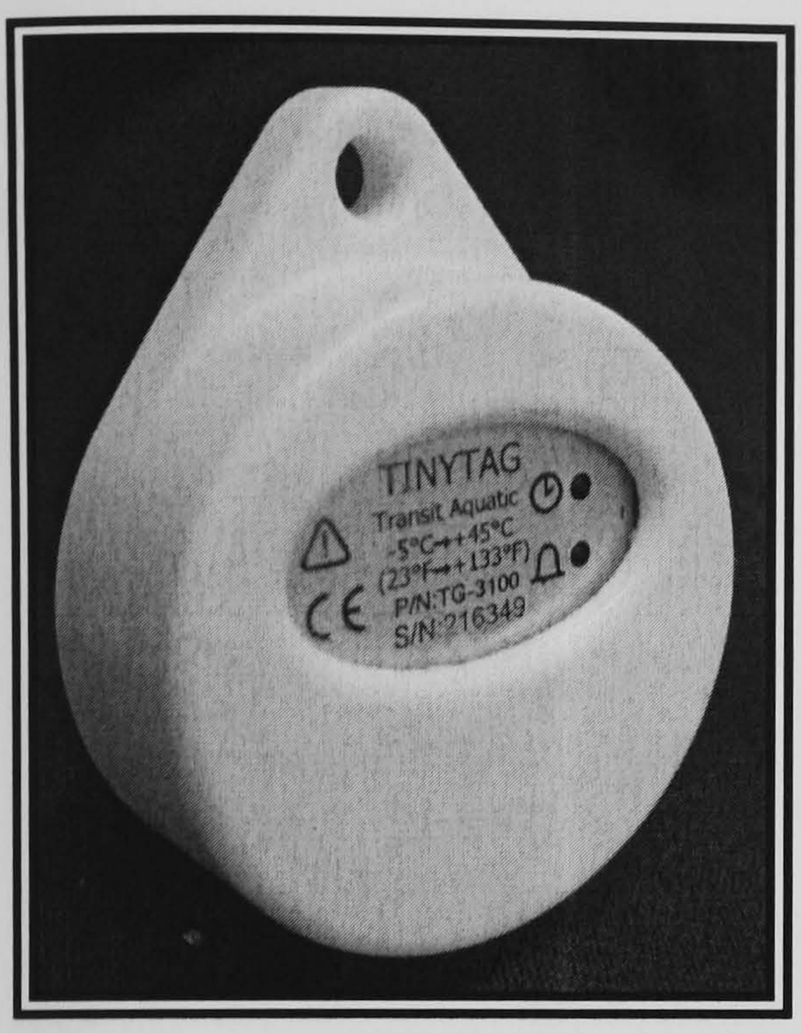

Features

Memory Size :	16k (Non-volatile)
No. of Readings :	8,000 approx
Resolution :	10 bit
Trigger Start :	Reed Relay
Delayed Start :	Relative / Actual up to 45 days
Stop Options :	When Full After n Readings Never (Wrap around)
Reading Types :	Actual, Min, Max.
Logging Interval :	1 sec to 10 days
Offload :	While stopped or when logging in minute multiples
Alarms :	Two, fully Programmable
Functional Range[1] :	-40°C → +85°C / -40°F → +185°F
IP Rating :	IP68
Battery Life[2] :	Up to 2 years
Offload Speed :	Approx 20 Seconds
Offload Method :	Close proximity

Notes:
[1] Functional Range describes the range over which the logger will function, **not** the sensor range over which it will record

[2] The battery is not replaceable.

Sensor Details

Range :	-5°C → +45°C / 23°F → +113°F
Sensor Type :	10k NTC Thermistor (Encapsulated)
Sensor location :	Internally mounted
Response Time :	10 min to 90% typ. (in water) 15 min to 90% typ. (in air)
Sensor accuracy :	± 0.2°C / ± 0.36°F From -5°C → 45°C / 23°F → 113°F
Resolution :	<0.2°, -5° → +45°C <0.1°, 2° → 20°C

Mechanical Data

Case Style : Fully encapsulated

Case Dimensions

Diameter :	48.5mm / 1.9"
Thickness :	18mm / 0.7"
Hanging tab :	extra 12mm / 0.47"
Mounting hole :	6mm / 0.24" diameter

Weight : 100g / 4oz approx.

Approvals

This equipment complies with part 15 of the FCC Rules. Operation is subject to the following two conditions: (1) this device may not cause any harmful interference, and (2) this device must accept any interference received, including interference that may cause undesired operation.

This product is manufactured by Gemini Data Loggers (UK) Ltd to BS EN ISO 9001:2000 (Certificate No. 6134), and is CE approved to EN50081 part 1:1992 and EN50082 part 1 and 2:1992/95 with any standard leads or probes supplied.

UKAS traceable calibration certificates are available on individual units.

Special Notes

The battery is not replaceable in this fully encapsulated unit.

Interface Information and Related Products

To use your Tinytag Data Logger you will require:

Transit base station (ACS-3010) or Tinytag Pad base station (ACS-3020), PC with GLM (SWCD-0009) or Easyview (SW-0500)

Gemini Data Loggers Pty
Australia

Gemini Data Loggers UK Ltd
UK

Gemini Data Loggers Inc
USA

http://www.geminidataloggers.com **e-mail: sales@geminidataloggers.com**